U.S. DEPARTMENT OF COMMERCE
National Technical Information Service

PB-273 828

Environmental Protection Agency (EPA) 2nd Fine Particle Scrubber Symposium Held in New Orleans, LA on May 2-3, 1977

Air Pollution Technology, Inc, San Diego, Calif

Prepared for

Industrial Environmental Research Lab, Research Triangle Park, N C

Sep 77

PB 273 828

EPA-600/2-77-193
September 1977

Environmental Protection Technology Series

UNITED STATES · ENVIRONMENTAL PROTECTION AGENCY

REPRODUCED BY
NATIONAL TECHNICAL
INFORMATION SERVICE
U. S. DEPARTMENT OF COMMERCE
SPRINGFIELD, VA. 22161

RESEARCH REPORTING SERIES

Research reports of the Office of Research and Development, U.S. Environmental Protection Agency, have been grouped into five series. These five broad categories were established to facilitate further development and application of environmental technology. Elimination of traditional grouping was consciously planned to foster technology transfer and a maximum interface in related fields. The five series are:

1. Environmental Health Effects Research
2. Environmental Protection Technology
3. Ecological Research
4. Environmental Monitoring
5. Socioeconomic Environmental Studies

This report has been assigned to the ENVIRONMENTAL PROTECTION TECHNOLOGY series. This series describes research performed to develop and demonstrate instrumentation, equipment, and methodology to repair or prevent environmental degradation from point and non-point sources of pollution. This work provides the new or improved technology required for the control and treatment of pollution sources to meet environmental quality standards.

EPA REVIEW NOTICE

This report has been reviewed by the U.S. Environmental Protection Agency, and approved for publication. Approval does not signify that the contents necessarily reflect the views and policy of the Agency, nor does mention of trade names or commercial products constitute endorsement or recommendation for use.

This document is available to the public through the National Technical Information Service, Springfield, Virginia 22161.

TECHNICAL REPORT DATA
(Please read Instructions on the reverse before completing)

1. REPORT NO. EPA-600/2-77-193	2.	3. RECIPIENT'S ACCESSION NO. PB273828
4. TITLE AND SUBTITLE Second EPA Fine Particle Scrubber Symposium		5. REPORT DATE September 1977
		6. PERFORMING ORGANIZATION CODE
7. AUTHOR(S) Richard Parker and Seymour Calvert		8. PERFORMING ORGANIZATION REPORT NO.
9. PERFORMING ORGANIZATION NAME AND ADDRESS Air Pollution Technology, Inc. 4901 Morena Boulevard, Suite 402 San Diego, California 92117		10. PROGRAM ELEMENT NO. 1AB012; ROAP 21ADL-029
		11. CONTRACT/GRANT NO. 68-02-2190
12. SPONSORING AGENCY NAME AND ADDRESS EPA, Office of Research and Development Industrial Environmental Research Laboratory Research Triangle Park, NC 27711		13. TYPE OF REPORT AND PERIOD COVERED Proceedings; 9/76-7/77
		14. SPONSORING AGENCY CODE EPA/600/13

15. SUPPLEMENTARY NOTES IERL-RTP project officer for this report is Dennis C. Drehmel, Mail Drop 61, 919/541-2925.

16. ABSTRACT The report presents the proceedings, including introductory remarks and 16 technical papers, of the Second Fine Particle Scrubber Symposium, held May 2-3, 1977, in New Orleans. Sponsored by the U.S. Environmental Protection Agency, the symposium was held to stimulate and generate new ideas for fine particle control using wet scrubbers, and to promote the transfer of technology to users. Subject matter concerned the collection of fine particles in any type of wet collector with emphasis on scrubber performance data in industrial applications.

17. KEY WORDS AND DOCUMENT ANALYSIS

a. DESCRIPTORS	b. IDENTIFIERS/OPEN ENDED TERMS	c. COSATI Field/Group
Air Pollution Dust Scrubbers Industrial Processes	Air Pollution Control Stationary Sources Particulate	13B 11G 07A 13H

18. DISTRIBUTION STATEMENT Unlimited	19. SECURITY CLASS *(This Report)* Unclassified	21. NO. OF PAGES 356
	20. SECURITY CLASS *(This page)* Unclassified	22. PRICE A16 - A01

EPA Form 2220-1 (9-73)

EPA-600/2-77-193
September 1977

SECOND EPA FINE PARTICLE SCRUBBER SYMPOSIUM

by

Richard Parker and Seymour Calvert

Air Pollution Technology, Inc.
4901 Morena Boulevard, Suite 402
San Diego, California 92117

Contract No. 68-02-2190
ROAP No. 21ADL-029
Program Element No. 1AB012

EPA Project Officer: Dennis C. Drehmel

Industrial Environmental Research Laboratory
Office of Energy, Minerals, and Industry
Research Triangle Park, N.C. 27711

Prepared for

U.S. ENVIRONMENTAL PROTECTION AGENCY
Office of Research and Development
Washington, D.C. 20460

ABSTRACT

The Second Fine Particle Scrubber Symposium was held on May 2-3, 1977 in New Orleans, Louisiana. The symposium was sponsored by the U.S. EPA and was organized and hosted by A.P.T., Inc.

The conference was intended to stimulate and generate new ideas for fine particle control using wet scrubbers, and to promote the transfer of technology to users. The subject matter was concerned with the collection of fine particles in any type of wet collector with emphasis on scrubber performance data in industrial applications.

This report presents the symposium proceedings, including introductory remarks and the sixteen technical papers.

ACKNOWLEDGEMENT

A.P.T., Inc. wishes to express its appreciation for excellent coordination and assistance in organizing and conducting this symposium to Dr. Dennis Drehmel, EPA Project Officer.

TABLE OF CONTENTS

Page

Abstract. iii
Acknowledgement iv
List of Figures vi
List of Tables. xiv
Introductory Remarks. 1
Paper 1 - Wet Scrubbing Experiences for Steel Mill Applications. 5
Paper 2 - Wet Scrubbing Experience with Fine Borax Dust . . 25
Paper 3 - F/C Scrubber Demonstration on a Secondary Metals Recovery Furnace 35
Paper 4 - Fine Particulate Scrubbing - New Problems and Solutions 61
Paper 5 - Entrainment Separators for Scrubbers. 75
Paper 6 - Relationships of Collection Efficiency and Energy Dissipation in Particulate Scrubbers. 97
Paper 7 - Diffusiophoretic Particle Collection under Turbulent Conditions. 115
Paper 8 - Improved Design Method for F/C Scrubbing. 141
Paper 9 - Interfacial Surface Effects on Particle Collection. 163
Paper 10A- EPA Mobile Particulate Collectors - Program Intentions. 187
Paper 10B- Cupola Foundry Particle Control with Venturi and Sieve Tray Scrubbers. 195
Paper 11 - Field Test of a Venturi Scrubber in Russia. . . . 209
Paper 12 - A.P.T. Field Evaluation of Fine Particle Scrubbers 221
Paper 13 - Results of Flue Gas Characterization Testing at the EPA Alkali Wet-Scrubbing Test Facility . . 255
Paper 14 - The Waterloo Scrubber 279
Paper 15 - Fine Particle Control with UW Electrostatic Scrubber. 303
Paper 16 - Fine Particle Scrubbing with Lone Star Steel Hydro-Sonic Cleaners "The Coalescer". 319
List of Attendees 339

LIST OF FIGURES

Figure Page

PAPER 1

1 No. 1 Boiler House, Middletown Works Scrubber System Flow Diagram. 21

2 Sinter Plant, Houston Works Scrubber System Flow Diagram 22

3 No. 2 Open Hearth, Middletown Works Scrubber System Flow Diagram. 23

4 Recycle Plant, Middletown Works Scrubber System Flow Diagram. 24

PAPER 2

1 Modified Scrubber. 33

2 Emission Rate vs. Scrubber Pressure Drop for Triple Scrubber. 34

PAPER 3

1 F/C Scrubber Demonstration Plant 51

2 Flow Diagram of F/C Scrubbing System 52

3 Quencher Unit of F/C Demonstration Scrubber. 53

4 Scrubber Unit of F/C Demonstration Plant 54

5 Cooling Tower of F/C Demonstration Scrubber System 55

6 F/C Demonstration Scrubber Performance 56

7 Particle Penetration Versus Aerodynamic Diameter for Run 64. 57

8 Particle Penetration Versus Aerodynamic Diameter for Run 74. 58

9 Particle Penetration Versus Aerodynamic Diameter for Run 69. 59

PAPER 4

1 Competing Devices (Non-Scrubber) 67

2 Comparison of New Scrubber Devices 68

3 New Scrubber Applications. 69

4 Manufacturers. 70

5 Useful Addresses of Information Sources. 72

Figure Page

PAPER 5

1 Tube Bank Configuration. 85
2 Baffle Configuration 86
3 Inclined Baffle Configuration. 87
4 Experimental Penetration through Mesh, Upward Flow. 88
5 Experimental Penetration through Packed Bed, Upward Flow 89
6 Experimental Penetration through Tube Bank, Upward Flow. 90
7 Experimental Penetration through Horizontal Baffles, Upward Flow 91
8 Experimental Penetration through 30° Inclined Baffles, Upward Flow 92
9 Experimental Penetration through 45° Inclined Baffles, Upward Flow 93
10 Entrainment Separator Performance Cut Diameters. . . 94

PAPER 6

1 Flowsheet of Experimental Scrubber System. 107
2 Multiple-Orifice Series Gas/Liquid Contactor 107
3 Spray Gas/Liquid Contactors. 108
4 Miniscrubber Signature Curves for Aerosols D, E, F, and G 109
5 Orifice Scrubber Performance Curve for Aerosol D . . 109
6 Orifice Scrubber Performance Curve for Aerosol E . . 110
7 Orifice Scrubber Performance Curve for Aerosol G . . 110
8 Multiple-Orifice Series Scrubber Performance on Aerosol D 111
9 Multiple-Orifice Series Scrubber Performance on Aerosol E 111
10 Multiple-Orifice Series Scrubber Performance on Aerosol G 112
11 Performance of Spray Scrubbers on Aerosol D at Values of f=0 - 0.39 112
12 Performance of Spray Scrubbers on Aerosol D at Values of f=0.90 - 0.99. 113
13 Performance of Spray Scrubbers of Ejector Configuration of Aerosol D 113

Figure **Page**

PAPER 7

1 Schematic Diagram of Experimental Equipment. 132
2 Results for Helium-Ammonia Mixtures with 0.79 Micron Diameter Particles. 133
3 Results for Methane-Ammonia Mixtures with 0.79 Micron Diameter Particles. 134
4 Results for Nitrogen-Ammonia Mixtures with Particles of Various Diameters 135
5 Results for Argon-Ammonia Mixtures with 0.79 Micron Diameter Particles. 136
6 Results for Freon 12 (dichlorodifluoromethane)-Ammonia Mixtures with Particles of Various Diameters. 137
7 Results for Nitrogen-Trimethylamine Mixtures with Particles of Various Diameters. 138

PAPER 8

1 Generalized F/C Scrubber System. 153
2 Multiple Plate F/C Scrubber System 154
3 Effect of Particle Diameter on Condensation Ratio. . 155
4 Effect of Liquid Bulk Temperature on Condensation Ratio 156
5 Effect of Gas Inlet Temperature on Condensation Ratio. 157
6 Effect of Particle Number Concentration on Condensation Ratio 158
7 Effect of Liquid Heat Transfer Coefficient on Condensation Ratio. 159
8 Particle Size Distribution Before and After Condensation 160
9 Particle Penetration vs Aerodynamic Dia.- Run 64 . . 161
10 Particle Penetration vs Aerodynamic Dia.- Run 69 . . 162

PAPER 9

1 Model for Collision of Particle and Liquid Droplet . 172
2 Models for Surface Deformation 173
3 High Speed Cine Microscope Equipment used for Experimental Evaluation of Coalescence Mechanisms. . 174

Figure Page

PAPER 9 (Continued)

4 Glass Rod with Simulated Fly Ash Particle Mounted on Traversing Mechanism. 175

5 Traversing Mechanism for Impacting Particles into Water Droplets. 176

6 Coalescence of 2800 μm Diameter Glass Particle with Water Droplet, 1200 μsec Delay (10,000 pps) . . 177

7 Coalescence of 2800 μm Diameter Glass Particle with Water Droplet, 2067 μsec Delay. 178

8 Coalescence of 1700 μm Diameter Glass Particle with Water Droplet, 585 μsec Delay 180

9 Coalescence of 1000 μm Diameter Glass Particle with Water Droplet, 780 μsec Delay 181

10 Coalescence of 725 μm Diameter Glass Particle with Water Droplet, 468 μsec Delay 182

11 Coalescence of 275 μm Diameter Glass Particle with Water Droplet, 351 μsec Delay 183

12 Coalescence of 100 μm Diameter Glass Particle with Water Droplet, 156 μsec Delay 184

13 Comparison of Theoretical Predictions and Experimental Measurements of Coalescence Delay Time 185

PAPER 10-A

1 Scrubber Flow Schematic. 192

2 Plan View of Mobile ESP Facility 193

PAPER 10-B

1 Scrubber Flow Schematic. 200

2 Effect of L/G Ratio on Venturi Scrubber. 201

3 Effect of Throat Velocity on Venturi Scrubber. . . . 202

4 Effect of Pressure Drop on Venturi Scrubber. 203

5 Effect of Presaturation on Venturi Scrubber. 204

6 Fractional Removal Efficiency for Venturi Scrubber 205

7 Effect of L/G Ratio on Sieve Tray Scrubber 206

8 Fractional Efficiency of Sieve Tray Scrubber 207

Figure Page

PAPER 11

1 NIKOPOL Scrubbing Apparatus. 217
2 NIKOPOL Scrubber Sampling Port Locations 218

PAPER 12

1 Predicted and Experimental Penetrations for Koch Flexitray 237
2 Predicted and Experimental Penetrations for Ducon Multivane Scrubber 238
3 Predicted and Experimental Penetration for Mobile Bed Scrubber. 239
4 Predicted and Experimental Penetrations for Chemico Venturi. 240
5 Predicted and Experimental Penetrations for Encott Wetted Fiber Scrubber 241
6 Predicted and Experimental Penetration for Sly Impinjet 242
7 Predicted and Experimental Grade Penetration Curves for Venturi Rod Scrubber. 243
8 Predicted and Experimental Penetrations for AAF Kinepactor 32. 244
9 Predicted and Experimental Grade Penetration Curves for AAF Kinepactor 56 245
10 Predicted and Experimental Penetrations for Variable Rod Scrubber. 246
11 Theoretical and Experimental Cut Diameters as a Function of Pressure Drop for Several Scrubber Types. 247
12 Efficiency of Single Drop Versus Inertia Parameter at $N_{Red}=9.6$ with N_{FD} as Parameter. 248
13 Experimental and Predicted Particle Penetration Versus Particle Diameter 249
14 Experimental Grade Penetration Curve for CHEAF . . . 250
15 Cut Diameter Versus Pressure Drop for Fibrous Bed. 251
16 Experimental Penetration Curve for Charged Droplet Scrubber 252

Figure Page

PAPER 13

1 Mean Differential Mass Loading Versus Aerodynamic Particle Size for All Venturi/Spray Tower System High Fly Ash Loading Runs. 269
2 Mean Differential Mass Loading Versus Aerodynamic Particle Size for the Venturi/Spray Tower System Low Fly Ash Loading Run. 270
3 Mass Percent Penetration Versus Aerodynamic Particle Diameter for All Venturi/Spray Tower High Fly Ash Loading Runs. 271
4 Mass Percent Penetration Versus Aerodynamic Particle Diameter for Venturi Spray Tower Low Fly Ash Loading Run VFG-1B 272
5 Particulate on Third Stage of Outlet Impactor During Venturi/Spray Tower Run VFG-1A, Magnification 2000X. 273
6 Particulate on Sixth Stage of Outlet Impactor During Venturi/Spray Tower Run VFG-1A, Magnification 5000X. 273
7 Mean Differential Mass Loading Versus Aerodynamic Particle Size for All TCA System High Fly Ash Loading Runs 274
8 Mean Differential Mass Loading Versus Aerodynamic Particle Size for All TCA System Low Fly Ash Loading Runs 275
9 Mass Percent Penetration Versus Aerodynamic Particle Size for All TCA High Fly Ash Loading Runs 276
10 Mass Percent Penetration Versus Aerodynamic Particle Size for All TCA Low Fly Ash Loading Runs 277

PAPER 14

1 Waterloo Scrubber - Laboratory Installation. 289
2 Cross-Section Details of Waterloo Scrubber 290
3 Dust Feeding Equipment 291
4 Typical Particle Size Distributions (not normalized) in Inlet and Outlet Duct Samples on the Waterloo Scrubber 292
5 Fine Particulate Removal Efficiency as Related to Fan Speed 293

Figure Page

PAPER 14 (Continued)

6 Water Droplet Size vs. Air Pressure for Spraying Systems Air Atomizing Nozzle 294

7 Number of Water Droplets Produced per Minute with the Spraying Systems Air Atomizing Nozzle . . . 295

8 Histogram Showing Droplet Size Distribution from a Spraying Systems Air Atomizing Nozzle. 296

9 Fine Particulate Removal Efficiency as a Function of Dust Loading and Amount of Fine Water Spray Used 297

10 Schematic Drawing of the Revised Consolidated Bathurst Installation. 298

11 Semrau Plot for the Recovery Boiler on a Kraft Pulp Mill. 299

12 Relationship Between Fan Speed and Capacity at Constant Residence Time 300

PAPER 15

1 UW Electrostatic Scrubber. 305

2 General Layout of Electrostatic Scrubber Pilot Plant (Mark 2P Model). 306

3 UW Electrostatic Scrubber Pilot Plant at Steel Plant. 307

4 Influence of Gas Residence Time on Particle Collection Efficiency. 311

5 Influence of Aerosol and Droplet Charging on Particle Collection Efficiency 312

6 Influence of Water Droplet Charging Voltage on Particle Collection Efficiency 313

7 Influence of Water to Gas Flow Rate Ratio on Particle Collection Efficiency 313

8 Influence of SCA and L/G on Particle Collection Efficiencies 315

9 Collection Efficiencies at an Electric Arc Steel Furnace. 316

Figure Page

PAPER 16

1 Hydro-Sonic Cleaners 330
2 Energy Utilization Region. 330
3 Fan Coalescer. 331
4 Ejector Coalescer. 331
5 Shaped Droplets - Subsonic Nozzle. 332
6 Shaped Droplets - Supersonic Nozzle. 332
7 Droplet Growth 332
8 Supersonic Ejector Drive 333
9 Coalescer - Energy vs Cleaning 333
10 Fan Coalescer - Energy vs Outlet Grain Loading . . . 334
11 Paper Recovery Boiler. 335
12 Energy vs Particle Size. 336

LIST OF TABLES

Table | Page

PAPER 1

1 No. 1 Boiler House Scrubber Performance. 15
2 Houston Sinter Plant Steam-Hydro Performance 16
3 Houston Sinter Plant Scrubber System Wastewater Characteristics. 17
4 Middletown Open Hearth Scrubber System Wastewater Characteristics 18
5 Middletown Recycle Plant Scrubber System Wastewater Characteristics 19
6 Middletown Recycle Plant Scrubber System Performance. 20

PAPER 3

1 F/C Scrubbing Studies by A.P.T. for EPA. 45
2 Process Streams for F/C Scrubber System at Metals Recovery Furnace. 46
3 F/C Scrubber Demonstration Plant Operating Modes . . . 47
4 Chemical Analysis of Particulates at Secondary Metals Recovery Furnace. 48
5 Chemical Analysis of Impinger Solution at Secondary Metals Recovery Furnace. 49
6 Cost Comparison for Premium Wire Recovery. 50

PAPER 6

1 Test Aerosol Characteristics 106

PAPER 10-A

1 Mobile Particulate Collector Capabilities. 191

PAPER 10-B

1 Range of Conditions. 197
2 Sieve Tray Testing Conditions. 198

Table Page

PAPER 11

1 Properties of Nikopol Electric Arc Flue Gas 214
2 Results of Concentrations Measurements at Inlet and Outlet of Nikopol Scrubber. 215
3 Nikopol Scrubber Fractional Efficiency. 216

PAPER 12

1 Summary of Scrubbers Tested 235
2 Design Equations for Various Scrubber Types 236

PAPER 13

1 Flue Gas Characterization Program Results for the Venturi/Spray Tower System. 266
2 Flue Gas Characterization Program Results for the TCA System. 267
3 Selected Venturi/Spray Tower Outlet Mass Loading Solids Analysis and Resulting Calculated Reaction Products Emission 268

PAPER 15

1 Source Test Parameters and Measurement Techniques . . 308
2 DOP Test Results. 309
3 Results of Tests at Coal-Fired Boiler 309
4 Results of Tests at Electric Arc Steel Furnace. . . . 310

PAPER 16

1 Scrubber Inlet Loading by Size Interval 327
2 Scrubber Outlet Loading by Size Interval. 328
3 Inlet Particle Size Distribution. 329

INTRODUCTORY REMARKS

by

Steven Reznek

Office of Energy, Minerals and Industry
United Stated Environmental Protection Agency
Washington, D.C. 20460

INTRODUCTORY REMARKS

Good morning.

I would like to welcome you all to the second Fine Particle Scrubber Symposium. The first was three years ago in San Diego, It is appropriate that I give this talk today, since I represented EPA at the first (and perhaps only) symposium on fabric filters. So under the equal time rule -- let me now support scrubbers. In keeping with the tradition of conferences let me encourage everyone to exaggerate the attributes of wet scrubbers, refrain from mentioning their shortcomings and ignore competing control technologies.

I want to address first the subject -- why fine particulate? As you all know, nature designed your respiratory systems with a "wet contact" scrubber. Surface contact scrubbers are, of course, much more efficient on large particles. And your respiratory system is not efficient at removing fine particles -- those that are small enough to behave as gases and follow gas flow, but are too large to be subject to molecular diffusion.

Because all particle control measures have similar limitations, the particle sizes in controlled exhaust gases are likely to be at just that diameter -- about one or two microns -- where they can most effectively penetrate deep into the respiratory system.

A fundamental question has long been whether control measures for stationary sources are solving the less important problem of dust and failing to affect the important problem of the particulate that actually reaches the lungs.

The problems of establishing the relationship between human health and specific size and chemical fractions of particulate in the urban atmosphere are enormously difficult and complex. Because of this complexity it is very unlikely that air quality managers will soon feel that particulate control technologies are fully available or completely adequate.

Therefore, we meet here today with shared interest both in increasing the ultimate capability of control devices and in lowering the cost of achieving a specified level of control. So whether interest in improved methods stems from the fear that we have not yet addressed the most important health problem or from the conviction that while we can control 80 to 95% of the problem we would still like to reduce the remaining emission, especially when particulates may be toxic or hazardous. The focus of research and development now is on particles a few microns in diameter.

My second question is why wet scrubbers? Several forces are at work which will result in a reexamination of wet scrubbers as the particulate control device of choice, other than the impetus toward controlling smaller, more toxic particles. Principally these relate to the required control of both gaseous and particulate components in exhaust gases. While the primary focus of this conference is industrial applications, I can best illustrate the point by referring to electric utility uses. The desire to control SO_2 and particulates has produced a technology - stack gas desulfurization. This technology, by proper design, can be optimized to reduce the cost of SO_2 and particulate control.

Another approach to meeting SO_2 standards is the use of low sulfur coal. The increased resistivity of the fly-ash, from low sulfur coal reduces the efficiency of electrostatic precipitators. For high resistivity particulates, scrubbers may present a viable alternative. At present, over 47,000 megawatts in electric generating capacity is committed to scrubbers -- principally for SO_2 control.

The president's Energy Message strongly endorses increased coal use -- over 1 billion tons/year by 1990. Because of the desire to assure the transfer from an oil and gas based energy system will not entail a cost in public health, EPA's energy program will support R&D on fine particulate control. Part of that effort will be devoted to scrubbers. While the final program events await White House Staff approval to determine exact amounts, fine particle scrubber research effects will be substantial.

EPA PROGRAM

EPA initiated the Wet Scrubber Systems Study in 1970. At that time the state-of-the-art was largely empirical. Each application was considered to be a special case. Engineering design was based on primitive, try and see approaches. Very little scrubber performance information was available. Often over-design increased the costs of operating units.

In EPA's Wet Scrubber Systems Study all available information concerning scrubber theory and practice was collected and evaluated. Engineering design methods were evaluated and, where necessary, new methods were developed to provide as sound a basis as possible for predicting performance. The result of this study was the 1972 publication of the "Scrubber Handbook", now widely recognized as the most extensive engineering text on the subject.

Two recommendations for improved scrubber technology were developed in the Wet Scrubber Systems Study:

1. Study new phenomena which can enhance the ability to separate particles from gas streams and;
2. Study entrainment separators (or "mist eliminators") and develop improved design methods and equipment.

Acting on the first, EPA began its effort for developing and demonstrating Flux/Condensation scrubbers. In a Flux/Condensation scrubber water is condensed on the particles increasing their mass and thus making separation easier.

A series of condensation scrubbing studies have progressed from theory, through experiment, and into industrial demonstration. They have produced a useful body of engineering knowledge. It is now possible to make reliable process designs and cost estimates for condensation scrubbers following inexpensive, small scale sampling studies. For certain emissions, condensation scrubbers can be economically superior to conventional techniques.

EPA has measured the fine particle scrubber performance for a number of industrial sources. These measurements are now the most detailed and precise body of information available on collection efficiency as a function of particle size. All of EPA's scrubber performance studies include a comparison of the measured efficiency with that predicted by theory. One very useful engineering design tool developed through the EPA program is the relationship between particle cut diameter and required scrubber pressure drop. This relationship now allows reasonably accurate estimates of the power required to achieve specified collection efficiencies.

The second recommendation concerned re-entrainment. The problem of entrainment has placed serious constraints in the overall efficiency of scrubber operation, particularly for lime/limestone slurry systems. A portion of EPA's efforts have been aimed at this problem. The results have been knowledge of the efficiency, capacity and pressure drops of entrainment separators, and of the size distribution of the entrained mist. Here again, the EPA program has expanded the rational basis for the engineering design of better, more reliable and more economical equipment.

Some of the research problems remain for wet scrubbers. Principal among these are re-entrainment and reduced overall removal efficiency, the energy penalties of scrubbers including stack gas reheating and the overall environmental impact of scrubber blow down, its handling and disposal. However, scrubbers are perhaps the only technology applicable to corrosive or dangerous stack gases. Another obvious advantage of scrubbers is their ability to be used for both particulate and gaseous pollutant removal.

This symposium is intended to stimulate and generate new ideas for fine particulate control by bringing together experts in the development and use of wet scrubbers.

I want to wish you well in your efforts both here and out there in the French Quarter.

WET SCRUBBING EXPERIENCES FOR STEEL MILL APPLICATIONS

B. A. Steiner
R. J. Thompson

Armco Steel Corporation
Middletown, Ohio

ABSTRACT

This paper will discuss wet scrubbing experiences at a variety of steel mill applications including sinter plant, blast furnace, open hearth, and industrial boiler installations. A number of case studies will be examined. For each, the process, emission characteristics, and wet scrubber system design will be described. Actual performance will be compared with design values, and particular emphasis will be placed on water chemistry control and related problems.

WET SCRUBBING EXPERIENCES FOR STEEL MILL APPLICATIONS

Discharges from air pollution sources in the steel industry are often characterized by high concentrations of finely divided particles, high gas temperatures, moisture, and the presence of certain troublesome gaseous pollutants. Some process discharges also contain sub-micron condensed hydrocarbons, sublimates, or carbon particles which make gas cleaning more difficult. When these characteristics are complicated further by wide variations and fluctuations associated with the cyclic nature of many steelmaking processes, it is easy to comprehend why wet scrubbers, which are well-suited to cope with many of these design requirements, have been so widely used in the steel industry. Virtually every major type of air pollution source in the industry has been controlled by a wet scrubber application at one plant or another.

Among all major types of air pollution control equipment, the wet scrubber represents the smallest investment as a proportion of the total pollution control system cost. For example, the installed cost of the wet scrubber and mist eliminator portion of a scrubbing system may represent only 5-10% of the total system cost. In contrast, a fabric filter or electrostatic precipitator may represent 25-30% of the total system cost. Although auxiliary equipment is important for all pollution control applications, the proportionately greater emphasis on auxiliary systems for wet scrubbing systems substantially increases their significance and the dependence on proper design and operation. The interface with water pollution control requirements inherent with wet scrubbing systems also results in a greater emphasis on the waste treatment aspects of a wet system. Therefore, it comes as no surprise that many of the unfavorable experiences with wet scrubbing systems are related to the auxiliary systems and in particular the water and waste treatment aspects of the system.

Armco Steel Corporation has installed over 40 major scrubber systems in the past 10 years, including blast furnace, basic oxygen furnace, open hearth, electric furnace, scarfer, coal dryer, sinter plant, coke plant, and boiler applications. Several of these systems have been plagued with problems of varying magnitude which will be discussed as case histories below.

Middletown Coal-Fired Boilers

The No. 15 and No. 16 boilers at the Middletown (Ohio) No. 1 Boiler House are multi-retort, underfeed stoker, coal-fired units, each with a capacity of 100,000 pounds of steam per hour. Although not an application unique to the steel industry, this source typifies many of Armco's scrubber installations. The coal burned is typically 0.7-0.9% sulfur and 8-10% ash. This boiler house is normally operated in the winter months only.

A scrubber was selected for this application to provide removal of sulfur dioxide as well as particulate matter to allow burning of high sulfur coals if necessary. A single scrubber was installed in 1975 to serve both boilers. Gases are extracted from the existing stacks and passed successively through a fan, scrubber, mist eliminator, and stack (Figure 1).

The scrubber consists of a variable throat, orifice venturi scrubber with a pressure drop-controlled adjustable plug. The 17' diameter mist eliminator is equipped with three gas scrubbing trays, and "S" type chevron separator, and an 8'-10" diameter stub stack. The system is designed for 140,000 acfm @ 425°F and 15" w.c. with an outlet loading of 0.02 gr/dscf.

With the present design, fresh water is supplied from a clarified river water system at a rate of 1600 gpm to both the top tray of the demister and to the venturi throat. Water from the mist eliminator flows into a 10,000 gallon recycle tank where lime slurry is added to maintain an approximate pH of 6. Water from the tank is recirculated to the bottom two trays of the demister. Waste water from the tank is pumped to an abandoned hot strip mill flume and scale pit for settling of solids.

The largest problem affecting scrubber performance has been control of excess air on the boilers. Without control, excess air in the range of 100-250% was experienced, resulting in 1½-3 times the scrubber design flow rate. At this flow the scrubber and fan were unable to maintain the 15" w.c. pressure drop while providing proper boiler stack draft. These high excess air rates also resulted in the presence of unburned carbon which could not be wetted and compounded the poor performance. By controlling excess air in the range of 60-80%, gas volume was kept within reasonable limits, permitting the plug to adjust to the proper location, thereby providing acceptable scrubber efficiency (Table 1); however, the design outlet grain loading has yet to be obtained.

The originally installed mist eliminator chevrons were constructed of Norel plastic rated at 225°F continuous duty, which was well above the temperature at that location in the system. However, overlooked was the fact that Norel is creep sensitive at 20°F above ambient and the chevrons failed within a few months. New chevrons of the same material are also being damaged. Either stainless steel or fiberglass reinforced plastic (FRP) is a preferable material for this application.

The original water system was designed to apply fresh water to the demister trays, and to use recirculated water with a suspended solids concentration of 40-50,000 mg/l at the venturi. All piping under this service was mild steel and was severely abraded, causing numerous leaks. The piping was replaced with the same material, but was modified so that the water to the venturi is now once-through, and the abrasion has ceased.

A similar leakage problem was caused by abrasion of the 12" steel pipe carrying dirty water from the scrubber trays to the recycle tank. Partial flow in this pipe, which caused a wet-dry line, was also a contributing factor. This line was replaced with a rubber-lined flanged elbow and rubber hose, which have held up very well to date.

Abrasion also caused leaks in the pumps which deliver sludge from the recycle tank to the waste treatment system. Lowering pump speed from 1780 to 1180 rpm helped greatly to reduce abrasion. In addition, rubber lined, standard flanged "T" sections were installed on the suction side of the sludge pumps and recirculation pumps and have withstood abrasion better than any other material tried.

Generally speaking, it is believed that all flyash slurry lines should be rubber-lined and assembled in lengths of ten feet or less for ease of handling.

One problem which was anticipated but has not occurred was lime buildup in the demister trays during low gas flow rates. A pH of 4-6 was thought necessary to minimize this problem. However, at sustained pH levels of 6-6.5 there has been no significant lime accumulation on the trays.

The lime slurry system has also presented problems. Clogging of the lime slurry line is attributed to its excessive length. Control of the lime addition rate is also a problem, but can be resolved with the installation of a proportional feed lime slaker.

Houston Sinter Plant

The Armco Houston Works Sinter Plant produces a sized agglomerate for blast furnace feed from finely divided iron bearing material. Coke breeze is used as a fuel and limestone as a flux. These materials are mixed together with a blend of iron ore fines, blast furnace flue dust, blast furnace filter cake, and mill scale, and are placed in a 10-12 inch layer on a traveling grate. The surface of the bed is ignited with natural gas and progressively burns downward as combustion air is drawn through the bed from top to bottom through a series of windboxes and an induced draft fan. The fused material is sinter which is subsequently crushed, screened, cooled, and screened again prior to use in the blast furnace. The plant produces 1500 tons per day of sinter at a base/acid ratio of 1.0 to 1.5.

The plant was originally installed with cyclonic separators for removal of particulate matter ahead of the fan. The resultant discharge was about 0.3 gr/scf dry, which was in excess of Texas process weight limitations, as well as opacity restrictions of 30%. About 45% of the particulate matter was determined to be chloroform-extractable hydrocarbon, which was driven from oily feed material and condensed. These hydrocarbons were a primary contributing factor to stack opacity and represented a major consideration in selection of a control system. Also present in the stack discharge were sulfur dioxide, chlorides, and fluorides.

Five different control systems were investigated, including dry and wet electrostatic precipitators, fabric filters, wet scrubbers, and Lone Star Steel's Steam-Hydro scrubber. Both high energy venturi scrubbers and the Steam-Hydro scrubbers were pilot tested. Both were found to satisfactorily remove particulate and, to a lesser extent, hydrocarbons; however, the Steam-Hydro was considerably more efficient on hydrocarbons. Because of the concern for opacity, the high hydrocarbon efficiency gave an edge to the Steam-Hydro system, which also had a slight economic advantage, but only due to the availability of steam generating capacity and low cost fuel to generate the steam.

The Steam-Hydro system was installed in 1975 as six parallel units, five operating and one spare. Each unit consists of (1) a combination steam-water nozzle where the steam atomizes the water droplets, (2) a mixing tube where the particles and droplets contact, and (3) twin cyclone separators where the particle-laden droplets are removed and the clean gas is discharged through stub stacks. The original induced draft fan supplies the dirty gas to the units, and the motive force of the steam forces the gas through the gas cleaning system. Results of performance tests on the system are shown in Table 2 . Opacity problems still exist periodically due to high oil content of sinter feed materials.

Waste water from the Steam-Hydro cyclones is neutralized and clarified in two parallel systems, each capable of treating the entire flow. Each system consists of a lime neutralization unit, flocculator, clarifier, and sludge pump (Figure 2). Hydrated lime is fed from a storage bin and volumetric feeder into a mechanical mix tank. The neutralized waste flows to a Lamella separator equipped with an integral flash mixer and flocculator. Polymer additions are capable of being made but have not been necessary. The Lamella underflow is pumped to the blast furnace gas cleaning water system for ultimate disposal. The Lamella effluent is recirculated to the Steam-Hydro units at a rate of 370 gpm.

The principal problem with the system since start-up has been weld failures in the 304 stainless steel components. These failures were corrected in the field and have continued to occur, but at a much slower rate. Fabrication practices and corrosion may be contributing factors.

Also, steam expansion at the steam-water nozzles results in considerable noise. Measurements near the units indicate levels of 110 dB on the A scale. However, the noise is very localized, and because no operator is required in the immediate area, no corrective action has been necessary to date.

Several problems have been encountered in the water system, primarily in the lime handling and sludge handling areas. Self-cleaning pH probes were originally installed in the neutralization tanks for automatic control of lime feed. At this location the probes were rapidly coated with calcium sulfate scale and malfunctioned. This problem was solved by relocating the probes to the effluent end of the Lamella separators, but frequent cleaning is still required.

The lime storage and feeding equipment is located above the neutralization tank. Dry hydrated lime falls from the feeder through a vertical 2-inch pipe directly into the tank. Because of the high humidity in the area, the lime feed pipe plugged frequently. Although plugging has not been eliminated completely, it has been reduced to an acceptable frequency by (1) adjusting the pH control system so that lime feeding is nearly continuous, and (2) blowing dry air through the lime feed pipe to minimize the amount of moisture entering the pipe.

Air operated diaphragm pumps were initially installed to transfer Lamella underflow slurry to the blast furnace water system. Numerous diaphragm failures were encountered with these pumps. After a year of unsuccessful attempts to find a reliable diaphragm material, these pumps were replaced with centrifugal pumps. No problems have yet been experienced with the new pumps.

Shortly after the system was started up, corrosion coupons were installed. The first test indicated a corrosion rate of 68 mils per year (mpy) on carbon steel and no corrosion on 304 stainless steel. Although the entire gas cleaning system is constructed of 304 stainless steel, the entire water system is carbon steel construction. The high corrosion rate was attributed to chlorides and sulfates in the waste water and poor pH control due to the problems previously discussed. After a more stable pH control operation was achieved, a second test indicated corrosion rates of 10 to 20 mpy on carbon steel. Further refinements in the pH control system have been made, and a third corrosion rate test is now being conducted. If the results of this test continue to indicate excessive corrosion, chemical corrosion inhibitors will be investigated.

It should be noted that neither the slurry conveyed to the blast furnace water system nor the Lamella effluent is acceptable for direct discharge to a stream. The treatment facilities described are designed for making the water amenable to recirculation only. Table 3 compares the characteristics of the recirculated water, a portion of which might ordinarily be blown down to a stream, with tentative EPA Effluent Guidelines. The differences represent the required removal of pollutants before direct discharge can occur. These additional facilities are likely to experience similar, perhaps more complex, difficulties in operation and maintenance.

Middletown No. 2 Open Hearth

The Middletown No. 2 Open Hearth Shop consists of six 300-ton furnaces, each with a maximum firing rate of 170 MMBTU/Hr. Oxygen is normally used at rates of 60,000 scf/hr with a maximum of 100,000 scf/hr. Checker blowing is conducted on a 4-hour cycle. The furnaces were designed to be fueled by 75% natural gas and 25% tar. However, since 1974 with severe gas curtailments, they have been fired primarily with tar and fuel oil. These furnaces are now normally on a 100% scrap charge which results in average heat duration of about 12 hours. Depending upon availability of molten pig iron, the furnaces can also be charged with hot metal which significantly reduces heat time.

Scrubbers were installed at this facility in 1970. Scrubbers were selected because of greater expected reliability and flexibility over electrostatic precipitators. There was also a decided cost edge because precipitators would have required the added expense of installing waste heat boilers.

The scrubbers are orifice type, adjustable throat, venturi scrubbers of the flooded disc design. Each furnace has an individual scrubber system consisting of venturi scrubber, flooded elbow, cyclonic separator, fan, and a sound-attenuated stack (Figure 3). The open hearth stack gases have a maximum flow rate of 225,000 acfm @ 1350°F with an average dust concentration of 5 gr/scfd. During oxygen lancing, the dust concentration is about 6 gr/scfd, and during checker blowing concentrations as high as 25 gr/scfd may be present. Depending on the fuel being used, sulfur dioxide concentrations may range from negligible to 650 ppm. The guaranteed outlet dust concentration is 0.03 gr/scfd. A series of 19 performance tests in 1971 at a scrubber pressure drop of 47" w.c. showed an average outlet particulate concentration of 0.0127 gr/scfd.

Scrubber water is supplied from and returned to a single water treatment plant. Within each scrubber system, water is recirculated to the flooded disc from a pump tank at a rate of 1000 gpm. An additional 500 gpm of makeup water is supplied from the treatment plant to the wetted inlet of each scrubber. With approximately 200 gpm of evaporation, the remaining 300 gpm is returned to the treatment plant for pH adjustment and clarification. At the treatment plant, a blowdown of about 100 gpm is made to control dissolved solids, and fresh makeup is added.

The system was originally intended to be operated without pH control, and all components were constructed either of 316L stainless steel or of fiberglass reinforced plastic (FRP). Because of the presence of sulfur, chlorides, and fluorides and the resulting formation of acidic solutions, the system initially operated with recirculated water with a pH of 2 to 3. Several problems were encountered. Mist carryover from the stack was acidic and fallout in the area was of concern. Stress corrosion cracking of some stainless components and total corrosion of some mistakenly installed non-stainless hardware was occurring. Also, pH adjustment of the final blowdown was causing precipitation of large quantities of solids which were soluble at the lower operating pH levels. These solids were creating severe plugging problems in equipment.

To circumvent these problems, a lime neutralization system was installed to maintain a scrubber water pH of 8 to 8.5. Experience under this mode of operation also was unfavorable due to widespread scaling of calcium sulfate, especially when higher sulfur fuels were used for firing the furnace. Increased iron precipitation was also occurring in the system. Due to the presence of chlorides and fluorides, acute acidic attack was occurring in some areas while the severe scaling was occurring in other areas. More recently, caustic has replaced lime for neutralization, a pH of 5.5 to 6 is maintained, and the scaling problem is mitigated to some degree.

Corrosion was worst in the 316L stainless steel clarifiers. The clarifier sludge rakes were patch-welded and the interiors of the clarifiers were sand blasted to remove scales, then coated with a coal tar epoxy.

All water piping in the system is FRP. Proper design allowances were not made for the high thermal expansion rates of FRP piping, and it was necessary to install additional expansion joints. Plugging of the piping was also a problem and was attributed to the failure to use large radius elbows.

At the scrubbers, mist eliminator water was intended to be discharged to a screw classifier to remove large particles before recirculating or returning the water to the treatment plant. These classifiers were largely ineffective because of the small particle size of the solids and were removed.

The positioning mechanism for the scrubber malfunctioned due to the accumulation of sludge in the packing box as a result of leakage of dirty water around the top seal of the box, causing the shaft to bind. To alleviate this, the bottom seal was removed to allow the sludge to drain from the packing box, and wear plates were added to the shaft.

Numerous cracks appeared in the welds and blades of all the fans shortly after start-up. These problems were extremely critical at the time and after many tests, were attributed to a marginal stress application for 316L stainless steel, which had not previously been used for this size and type of fan. The fans were redesigned and modified in the field and have since experienced no problems of that nature.

One other water problem has been the occasional occurrence of a foam in the treatment plant. Although still largely unexplained, it has been suggested that, because of a high concentration of zinc oxide (63%) in the foam, the zinc is causing a change in surface tension of the water. The sporadic nature of the problem may be due to the fluctuations in zinc scrap additions in the open hearth furnace.

Table 4 shows the present treatment plant discharge in comparison to tentative EPA Effluent Guidelines. Modifications to the plant are now underway to achieve the BPCTCA limits.

Middletown Recycle Plant

In 1974, a new plant was built in Middletown for the recycling of iron-bearing waste materials. The facility is referred to as the Recycle Plant because it is intended to convert exclusively in-plant iron-bearing waste fines into blast furnace feed material. The process is very similar to the Houston operation but is designed to produce 2640 tons/day of sinter at a base/acid ratio of 3.0 to 3.5.

Based upon wet scrubber pilot plant testing at two existing sinter plants and concern for hydrocarbon emissions, a high energy, variable throat, orifice venturi scrubber with an adjustable plug was selected. The gas cleaning system consists of, in sequence, dry primary and secondary cyclones, two induced draft fans in series, a wet scrubber, and a cyclonic mist eliminator with a stub stack (Figure 4). The system is designed for 304,500 acfm @ 300°F with a venturi pressure drop of 45" w.c. with an outlet loading of 0.02 gr/scfd.

Water is supplied to the scrubber throat and inlet at 1800 gpm recirculated from the mist eliminator tank. Make-up water is supplied to the mist eliminator at the rate of 400 gpm from other sinter plant noncontact cooling water sources. From the bottom of the mist eliminator tank, a blowdown of 325 gpm is pumped to blast furnace sludge settling ponds and becomes part of the blast furnace scrubber water system blowdown. A hydrated lime neutralization system is provided for pH control of the recirculated water, but the system has been operated in the acid mode without problems, and no neutralizing has been necessary. The wastewater characteristics of the blowdown are shown in Table 5.

The major problem with this installation has been the design of the scrubber itself. The initial design exhibited a pressure drop of 80" w.c. Following some field alterations, including leveling of the weir which supplies water to the inlet, proper alignment of the bull nozzle which supplies water to the plug, and widening of throat opening, the scrubber drop still could not be lowered below 55" w.c. Even at this pressure drop, the outlet grain loading was reduced only to .07-.09 gr/scfd. As a result, the scrubber manufacturer supplied a second scrubber design with a modified throat profile. Although the second design resulted in better performance, an operating pressure drop of 68" w.c. was required. Mechanical difficulties, inability to properly control pressure drop, and an inadequate throat opening all plagued this second design. A third design with yet a larger opening and a modified throat profile was furnished by the manufacturer in early 1976, and performance and pressure drop are now in accordance with design criteria (Table 6). These problems were all believed to be attributed to the scrubber manufacturer's basic unfamiliarity with the capabilities of its own scrubber designs.

Some performance difficulties were experienced even with the third scrubber design with respect to removal of condensed hydrocarbons. Initial tests revealed grain loadings in excess of .07 gr/scfd and excessive stack opacities. Pilot testing had previously shown scrubbers to be capable of some removal of hydrocarbons but with certain inlet loading limitations. Only after selective elimination of certain excessively oily feed materials were the results in Table VI able to be achieved.

A number of mechanical problems were also experienced but all were attributed to marginal mechanical design rather than corrosion or abrasion problems characteristic of the other case histories discussed previously. These problems included failure of shaft bushings, cracked expansion joints, collapsed water hoses, failure of mist eliminator core buster supports, and peeling of mist eliminator protective lining. Bushings were replaced, shaft diameter was increased, hoses were replaced with a stronger material, expansion joint designs were modified, and the mist eliminator lining was patched with a better material.

The water system has been generally free of problems for the following reasons: (1) proper material selection based on other system experiences, (2) lack of need for chemical additions, (3) lesser quantities of acid gases, (4) greater blowdown percentage, (5) fan placement upstream of the scrubber, and (6) greater mechanical collector efficiency ahead of the scrubber.

Conclusions

These four case histories illustrate some of the types of problems experienced by Armco Steel Corporation with wet scrubbing installations. These experiences have aided Armco with subsequent system designs, and it is hoped others will also benefit from the descriptions of these problems. Although most problems have been resolved or corrected, one of the basic reasons for these difficulties persists.

USEPA Effluent Guidelines place emphasis on minimization of waste water discharge flows and attainment of best available technology. To achieve these standards, maximum recirculation is required. As recirculation rates are increased, many of the types of problems discussed come into play. Chemical treatment and solids removal processes and equipment become more sophisticated. The accumulation of dissolved solids and acidic solutions and the attendant fluctuations in pH lead to scaling and/or corrosion problems. Suspended solids buildups cause abrasion and erosion.

More importantly, however, only the very basic of the water treatment needs have been addressed to date. As efforts to remove such pollutants as fluorides, cyanides, phenol, ammonia, and heavy metals are required by BATEA water standards, the air pollution control technology of scrubbers is likely to be overshadowed by water pollution control technology for the scrubber water. Although there are several reasons that scrubbers are losing favor for steel mill applications, energy considerations and competition with other more efficient control devices among the most important, the concern for water and waste treatment standards also looms as a significant factor. When New Source Performance Standards are proposed with scrubbers considered to be best available control technology, the water treatment aspects cannot be casually dismissed as an engineering detail. Development of waste water treatment technology must simultaneously accompany scrubber technology if scrubbers are to remain as an influence in the air pollution control field.

TABLE I

No. 1 Boiler House Scrubber Performance

No. Tests	3	
Ave. Steam Output	191,571	lb/hr
Ave. Heat Input	252	MMBTU/hr
Ave. Excess Air	71	% (V)
Ave. Moisture Content	5.3	% (V)
Ave. Temperature	71	°F
Ave. Flow Rate	83,233	SCFM dry
Ave. Particulate Loading	0.0465	gr/SCF dry
	0.130	lb/MMBTU
Allowable Particulate Loading	0.152	lb/MMBTU

TABLE II

Houston Sinter Plant Steam-Hydro Performance

No. Tests	4	
Sinter Production	58.8	Tons/Hour
Average Inlet Conditions		
Volume	134,350	SCFM
Temperature	167	°F
Moisture	4.7	% (V)
Particulate*	0.5011	gr/scf
Average Outlet Conditions		
Volume	134,250	SCFM
Temperature	147	°F
Moisture	20.8	% (V)
Particulate*	0.0301	gr/scf
	38.5	lb/hr
Allowable Discharge*	90.6	lb/hr
Average Inlet SO_2 (3 Tests)	66.8	ppm
Average Outlet SO_2 (3 Tests)	10.0	ppm

*Total Particulate, including filter and impinger catch, State of Texas Compliance Sampling Manual

TABLE III

Houston Sinter Plant Scrubber System
Wastewater Characteristics

Parameter	Recirculated Water	USEPA Effluent Guidelines	
		BPCTCA	BATEA
Discharge, gal/ton	44*	50	50
pH	8.5	6-9	6-9
Suspended Solids, mg/1	350	50	25
Oil & Grease, mg/1	—	10	10
Fluoride, mg/1	—	—	20
Sulfide, mg/1	—	—	0.3
Dissolved Solids, mg/1	4300	—	—
Chloride, mg/1	720	—	—
Sulfate, mg/1	1900	—	—
Ammonia (N), mg/1	144	125**	10**
Cyanide (CN), mg/1	<0.1	15**	0.25**
Phenol, mg/1	3.0	4**	0.5**

*Assumed discharge flow, equivalent to the present slurry flow.
**Blast Furnace guidelines, all others are Sinter Plant.

TABLE IV

Middletown Open Hearth Scrubber System Wastewater Characteristics

Parameter	Existing Blowdown	Water Quality-Based NPDES Limit	USEPA Effluent Guidelines BPCTCA	USEPA Effluent Guidelines BATEA
Flow, gal/ton	44	—	50	50
pH	6.5	6-9	6-9	6-9
Suspended Solids, mg/1	95	34	50	25
Fluoride, mg/1	400	22	—	20
Nitrate, mg/1	28	—	—	45
Zinc (Total), mg/1	1940	10	—	5
Lead (Total), mg/1	12	1	—	—
Iron (Total), mg/1	44	—	—	—
Iron (Diss.), mg/1	—	2	—	—
Sulfate, mg/1	3200	—	—	—

TABLE V

Middletown Recycle Plant Scrubber System
Wastewater Characteristics

Parameter	Recycle Plant Blowdown	USEPA Effluent Guidelines BPCTCA	BATEA
Flow, gal/ton	177	50	50
pH	4.5	6-9	6-9
Suspended Solids, mg/1	440	50	25
Oil & Grease, mg/1	135	10	10
Fluoride, mg/1	55	—	20
Sulfide, mg/1	2	—	0.3
Sulfate, mg/1	520	—	—
Ammonia (N), mg/1	14	125*	10*
Cyanide (CN), mg/1	0.13	15*	0.25*
Phenol, mg/1	2.2	4*	0.5*
Zinc, mg/1	0.3	—	5**

*Blast Furnace Effluent Guidelines
**Steelmaking Effluent Guidelines

TABLE VI

Middletown Recycle Plant
Scrubber System Performance

No. Tests	3	
Ave. Sinter Production	101.6	T/Hr
Ave. Process Weight Rate	159.3	T/Hr
Ave. Gas Flow	200,000	SCFMD
Ave. Temperature	130	ºF
Ave. Moisture	12.5	% (V)
Ave. Particulate Emission*	0.0173	gr/SCFD
	0.29	lb/T sinter
	0.19	lb/T feed
	29.58	lb/Hr
Allowable Emission	50.00	lb/Hr

*USEPA Method 5, front half only

FIGURE 1

No. 1 Boiler House, Middletown Works

Scrubber System Flow Diagram

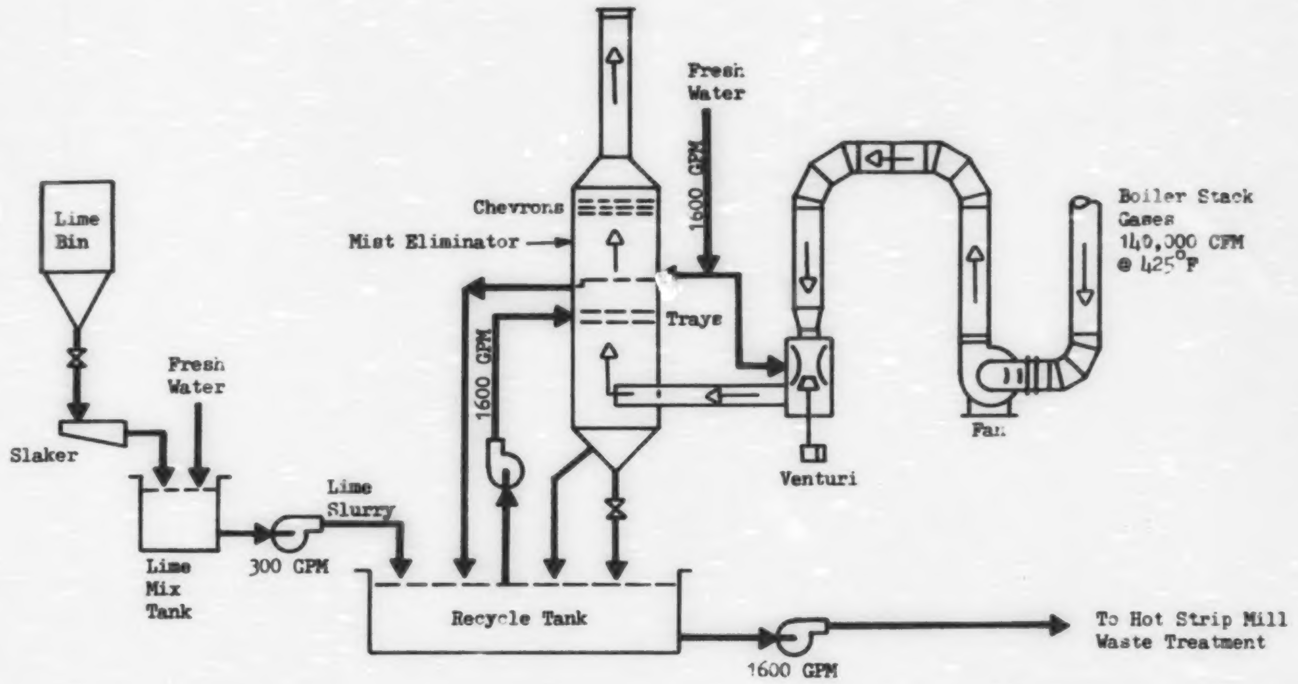
Lime Bin
Slaker
Fresh Water
Lime Mix Tank
300 GPM
Lime Slurry
Recycle Tank
1600 GPM
Mist Eliminator
Chevrons
1600 GPM
Fresh Water
Trays
Venturi
Fan
Boiler Stack Gases 140,000 CFM @ 425°F
1600 GPM
To Hot Strip Mill Waste Treatment

FIGURE 2

Sinter Plant, Houston Works
Scrubber System Flow Diagram

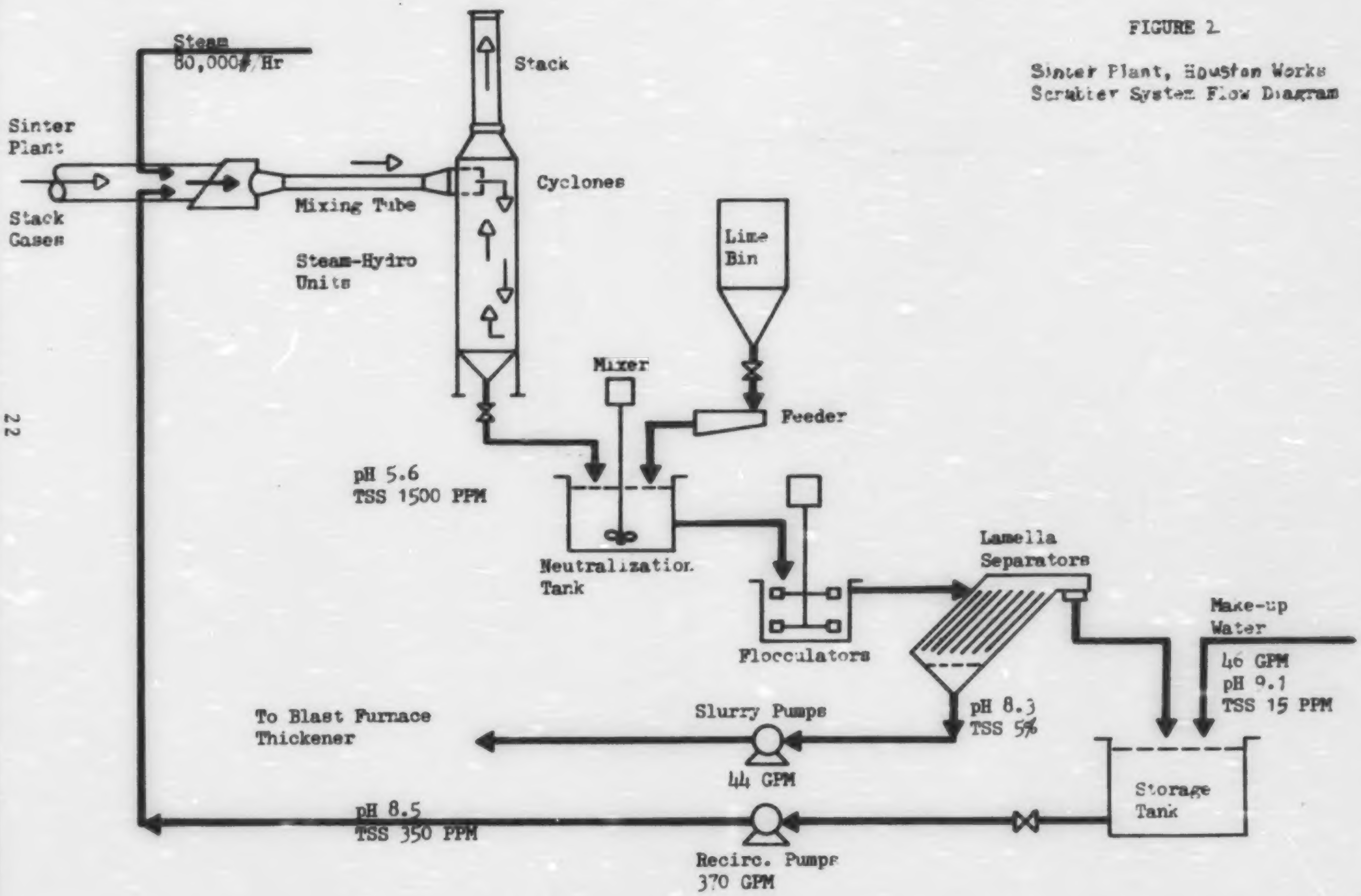
Steam
80,000#/Hr
Stack
Sinter
Plant
Stack
Gases
Cyclones
Mixing Tube
Steam-Hydro
Units
Lime
Bin
Mixer
Feeder
pH 5.6
TSS 1500 PPM
Neutralization
Tank
Flocculators
Lamella
Separators
Make-up
Water
46 GPM
pH 9.1
TSS 15 PPM
To Blast Furnace
Thickener
Slurry Pumps
44 GPM
pH 8.3
TSS 5%
Storage
Tank
pH 8.5
TSS 350 PPM
Recirc. Pumps
370 GPM

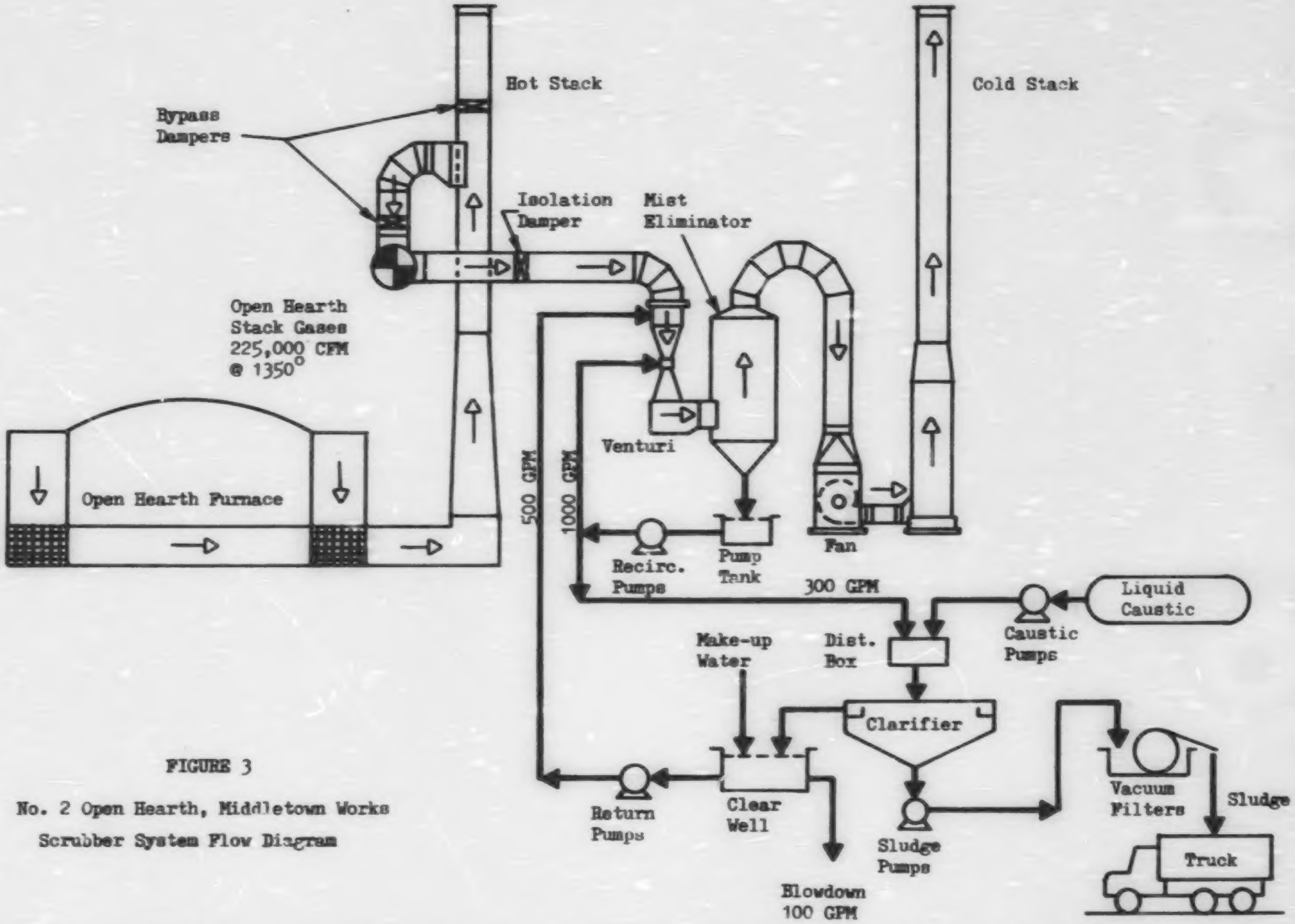
Hot Stack
Cold Stack
Bypass Dampers
Isolation Damper
Mist Eliminator
Open Hearth Stack Gases 225,000 CFM @ 1350°
Open Hearth Furnace
Venturi
500 GPM
1000 GPM
Recirc. Pumps
Pump Tank
Fan
300 GPM
Liquid Caustic
Caustic Pumps
Make-up Water
Dist. Box
Clarifier
Clear Well
Return Pumps
Sludge Pumps
Vacuum Filters
Sludge
Truck
Blowdown 100 GPM

FIGURE 3

No. 2 Open Hearth, Middletown Works
Scrubber System Flow Diagram

FIGURE 4

Recycle Plant, Middletown Works

Scrubber System Flow Diagram

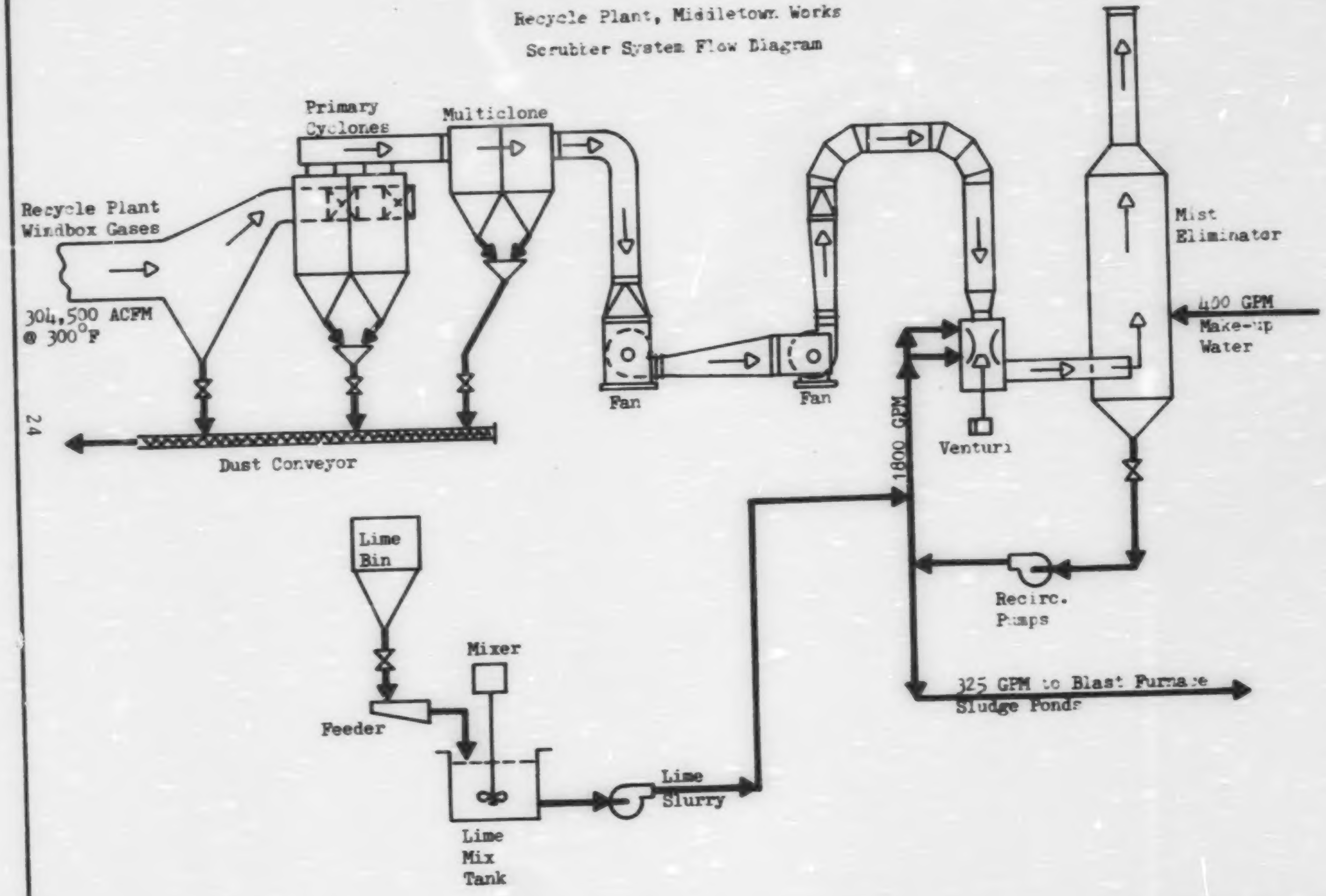
Recycle Plant
Windbox Gases
304,500 ACFM
@ 300°F
Primary
Cyclones
Multiclone
Dust Conveyor
Fan
Fan
Venturi
Mist
Eliminator
400 GPM
Make-up
Water
1800 GPM
Recirc.
Pumps
325 GPM to Blast Furnace
Sludge Ponds
Lime
Bin
Feeder
Mixer
Lime
Mix
Tank
Lime
Slurry

WET SCRUBBING EXPERIENCE WITH FINE BORAX DUST

E. Dean Lemon
U.S. Borax and Chemical Co.
Boron, California

ABSTRACT

Borax dust emissions from borax fusion furnaces and calciners can be controlled by a moderate pressure drop scrubbing system designed to fit the particle characteristics. A case history is given for the upgrading of an inadequate scrubber system to a successful one by modification of existing equipment. Power requirement for the upgraded scrubber is 400 H.P., as compared to 700 H.P. for the alternative high energy scrubber which had been successfully used on other furnace lines. Capital cost for the modified system was much less than that of a new replacement.

WET SCRUBBING EXPERIENCE WITH FINE BORAX DUST

Many of us have been confronted in recent years with the problem of what to do in the face of increasingly stringent emission requirements with emission control equipment giving marginal or inadequate performance for the revised standards. In many cases, we have been required to go to new equipment, or new technology and have had to rip out equipment still capable of performing but not at the level required. This paper is primarily a description of a solution to this problem by modification of existing equipment and it indicates that, given the time and with application of ingenuity and effort, it may be possible to devise a better and cheaper approach through modification or retrofit.

In 1958, our Company completely changed its mode of operation from underground to open pit mining and, in connection with that change, revised its primary processing from dry concentration to a wet solution and recrystallization process. A secondary process for manufacture of Anhydrous Borax was incorporated in the change with a method and production capacity different and larger than anything we had attempted previously. This process, which is referred to as fusing, generated a serious emission problem.

In the late 1960's, when it became necessary to add to original capacity, it also became necessary to install additional control equipment. For various reasons, wet scrubbers were selected. After a look at the requirements of the then young Los Angeles Air Pollution Control District, which covered the next adjacent county, particulate emission standards of 0.3 gr/SCF were set as an objective and impingement type, comparatively low energy scrubbers were installed to attain it. Our presumption that future regulations for a remote, unpopulated desert area would never be more demanding than those for the urban area proved incorrect. In the early 1970's the plant was faced with 0.2 gr/SCF standards for existing equipment and 0.1 gr/SCF for new equipment and, most critical, a process weight rule (the so-called 40# rule) that set particulate emission standards for the current operating conditions at a maximum of 18 pounds per hour. The previously installed scrubbers met the 0.2 gr/SCF requirement but produced emissions at 34 to 62 pounds per hour.

Further capacity increases in the early 1970's successfully incorporated high energy (high pressure drop) scrubbers so it was known that this technology could be used.

The borates primarily used in commerce are the sodium salts of boric oxide with varying degrees of hydration spanning the range from zero (or anhydrous) to 10 mol (or 47% water). Sodium borates occur naturally in two forms, both of which are found in the open pit mine at Boron, Calif. They are Tincal, the 10 mol hydrate, and Kernite, a 4 mol hydrate. Processing of these ores consists of dissolving the borate portions, separating the insoluble gangue and recrystallizing the borates. Application of the phase rule and temperature controls causes crystals to form as sodium borate decahydrate, $Na_2B_4O_7 \cdot 10H_2O$, which is 47% water, and as sodium borate pentahydrate, $Na_2B_4O_7 \cdot 5H_2O$, 31% water. A third sodium borate, anhydrous borax, is produced by fusing one of the hydrated forms, that is, heating it above the melting point of sodium borate, which is 742°C (1,360°F).

The hydrated borate crystals are subject to intumescence, that is, swelling on rapid or severe heating. This is caused by the rise in vapor pressure inside the crystal to a point where the crystal is ruptured and the water escapes. The ruptured crystal takes on the appearance of popcorn and is very light and easily friable, breaking down readily into fine, light particles. This material can have an apparent bulk density as low as one pound per cubic foot and will run 20 to 30% sub-micron particle size if it has been subjected to much handling. These particles are white and even the finest particles diffuse and scatter light so that visibility of this material as a particulate emission is very high.

The process for manufacture of Anhydrous Borax has been the source of our worst dust problem. Beginning with 10 mol borax, the material is put through rotary kilns where it is heated by the off gasses from the fusing furnace and calcined to about 3 or 4 mols of water content. It is then introduced to the fusing furnace where it is melted under temperatures of 1,800° to 2,000°F.

There are five furnace lines using the process. Furnace capacities vary from 80 tons per day to 100 tons per day. Air quantities required average 45,000 ACFM. Flue gas introduced to the kiln is discharged from the furnace at 1,800°F, is diluted with outside air in a mixing chamber, and the flow rate through the kiln is approximately 10,000 ACFM at 800°F. The gas stream arrives at the dust control equipment at a temperature of 350°F to 500°F. Heating in the kiln is rapid and the vapor pressure within the pieces of borax becomes extreme. Intumescence is, therefore, severe and the potential for creation of fine particulates is extremely high. Temperatures in the fusion furnace are so high that there is vaporization and condensation leading to fume formation.

Control Efforts

In connection with a fusing furnace much smaller but otherwise similar to those presently used, we successfully installed a fabric type dust collector, using glass fiber material for the bags because of the high temperatures. After some difficulty in obtaining satisfactory operation due primarily to maintenance problems, this collector has been made to work satisfactorily from an emission control standpoint. However, the size of collector required for the larger furnaces has obviated this approach for the new installations.

In 1958 the first four of the large furnaces were built and operated using only cyclone type dust collectors. This proved to be highly unsatisfactory and within two years efforts were begun to install additional control equipment. After some test work, it was decided that wet scrubbers would be the most practical for this installation due primarily to the proximity of plentiful supply of process water and because area limitations would not allow construction of amply-sized baghouses. As stated earlier, a particulate standard of 0.3 grains was selected as the objective. A fifth furnace was built in the early 1960s and the low energy scrubbers were installed on all five. These scrubbers were an impingement type operated at a 14" w.c. pressure drop and handled an average 45,000 ACFM with 200 H.P. fans. These fans had to be run wet to minimize buildup of borax deposits on the fan blades. By contrast, three high energy scrubbers installed later with larger furnaces operated at 35" and 40" w.c. pressure drop, handled 70,000 ACFM to 100,000 ACFM and used between 1,000 connected horse power and 1,500 connected horse power.

After an Air Pollution Control District was established for the local area a process weight rule was adopted and the five oldest furnace lines were in violation so we investigated possible solutions to the problem. An obvious approach was to install the same type scrubber with 40" w.c. pressure drop as had been successfully used on the latest installations. At that time, the first rumblings of energy shortage were being heard and it was decided that something less energy-demanding than the 1,000 to 1,500 H.P. fan motors should be sought.

A first attempt was the installation of knitted-mesh mist eliminators. Experimental work had indicated that some of the escaping particulate material was dissolved in mists escaping from the stacks. This proved to be effective at times but was not reliable and had to be rejected.

Several alternatives were then considered, among which was a further modification of the impact type scrubbers. A.P.T. Inc. was retained to study the problem and to determine whether or not scrubber performance could be improved to give satisfactory results with lower energy requirements than the high pressure drop scrubbers and less capital investment than other total replacement methods.

The process gas streams were sampled at various locations to determine particle size, particle concentration, gas flow rates, and other parameters. Particle mass growth due to the condensation of water vapor to form drops of borax solution was measured in special experiments. On the basis of these studies and other system data and parameters, it was concluded that the scrubbers could indeed be modified to achieve the desired result. The inlet particle size distribution to the scrubber had a mass median diameter of 14 microns aerodynamic and a geometric standard deviation of 5.5. The particulate loading was 550 lbs./hour and the minimum acceptable scrubber efficiency based on the emission rate limit was 97%.

Preliminary design and cost estimates were made and on the basis of these figures, it was decided to build a small scale pilot plant for further study and confirmation of the design predictions. The pilot model was completed and with the data obtained, more detailed designs and cost estimates were made. The results indicated a 20" pressure drop and 400 horse power fan motor would be effective. This seemed attractive enough for a go-ahead and U.S. Borax decided to proceed with the modification that is now called the A.P.T. Triple Scrubber.

It should be noted that the local control agency cooperated with this program and granted the necessary variances for continued operation while the test work and design was going on.

The existing scrubber was a high velocity impingement-entrainment type in which four annular gas jets impinged on the surface of a liquid pool within the scrubber body. The gas then passed through a baffled passage which caused several changes of gas flow direction in order to disengage entrained liquid. It was possible to utilize the existing scrubber body and most of the piping and ducting in the modification.

Figure 1 illustrates the components of the Triple Scrubber. First, the process gas stream goes through a saturator and precleaner section which were added upstream of the existing scrubber body and where quenching and temperature reduction occur. Note that the walls of the circular section are wetted to prevent material buildup, which is a continual problem when dealing with near-saturated solutions. In addition, sprays bring the gas up to saturated humidity and wet the particles to foster the particle growth that is important to the success of the process.

Second, the gases are conducted through a low velocity impingement section where larger particles are removed. Experience with scrubber systems handling borax solutions and/or hard water has shown that large deposits of precipitate can form at various points and can then break loose and deposit downstream, where blocking or plugging of apertures can occur.

Third, the gases enter a high velocity impingement section and are diverted downward through a group of high velocity nozzles at the bottom of which are adjustable throats. These nozzles impart the high velocity that gives the impingement efficiency necessary to remove the finer particles and attain 97+% efficiency. The original annular orifices were replaced with a set of adjustable throats, which were placed within the old scrubber body.

Leaving the high velocity section, the gases travel over a baffle arrangement and through a mist eliminator (entrainment separator) that is a series of vertical zigzag vanes set within the scrubber body. The mist eliminator was designed so that it could be removed through an access door for inspection and cleaning.

One scrubber was modified as described above to permit full-scale prototype testing before modifying the scrubbers on the other furnace lines. In addition to the internal changes, the scrubber body was stiffened by welding on steel angles so that it could withstand the increased negative pressure. An old fan which was on hand at the plant was suitable for the prototype test and it was installed to handle the increased pressure drop.

Performance

After construction and start up the modified scrubber was tested over a range of pressure drop. The results of this test series are shown in Figure 2, which shows the relationship between the emission rate and pressure drop. It also shows the upper limit for emissions based on the process weight rule as a horizontal line at 15# per hour. The curve shown represents the prediction by A.P.T. on the basis of results from the small scale pilot plant test. The points outlined by squares were determined by the A.P.T. sampling team shortly after start-up of the full scale test unit and indicate some degree of instability in the operation resulting in some erratic results at mid-range pressure drop. The triangles indicate data collected over a longer period of time by the U.S. Borax stack sampling team and show remarkable correlation with the predicted operating results. These data points are all obtained by E.P.A. method 5 particle emission tests.

On the basis of these successful tests on the full scale prototype, the Company is proceeding to modify its other scrubbers and has finished the second. The modified scrubbers are being operated at between 20" and 24" w.c. and are reducing emissions to approximately 9 pounds per hour, as indicated on Figure 2.

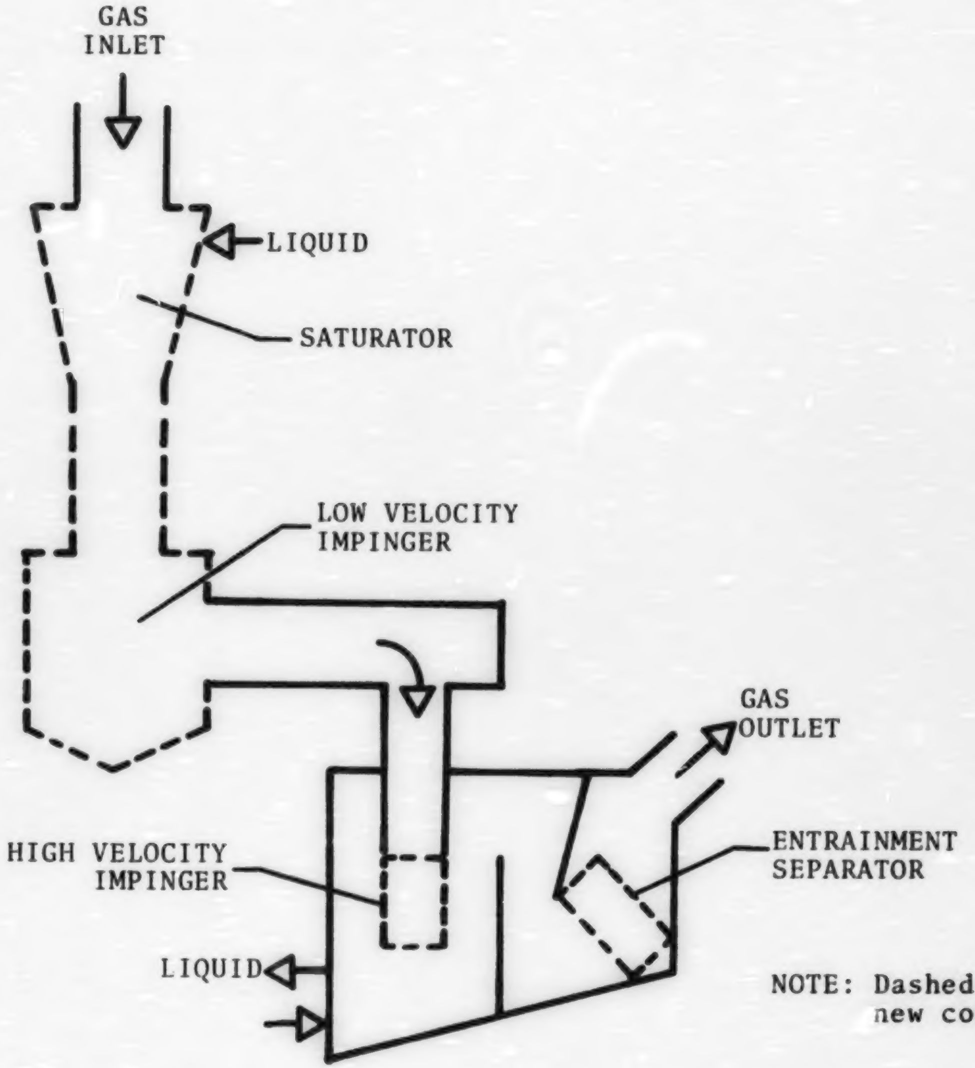
GAS
INLET
LIQUID
SATURATOR
LOW VELOCITY
IMPINGER
GAS
OUTLET
HIGH VELOCITY
IMPINGER
ENTRAINMENT
SEPARATOR
LIQUID

NOTE: Dashed lines outline new components.

Figure 1. Modified scrubber.

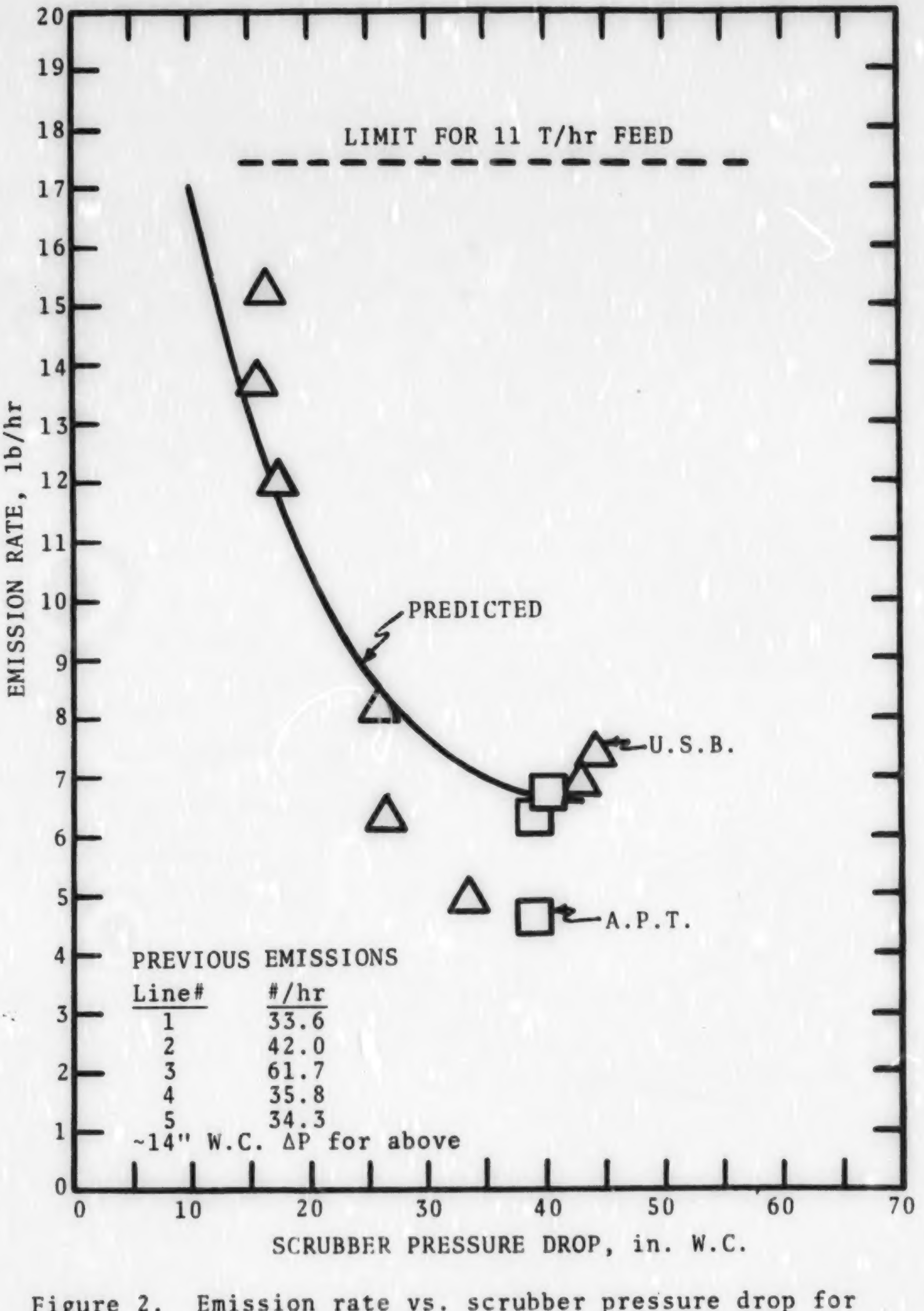

Figure 2. Emission rate vs. scrubber pressure drop for Triple Scrubber.

F/C SCRUBBER DEMONSTRATION ON A SECONDARY METALS RECOVERY FURNACE

by

Seymour Calvert
Shamim Gandhi

Air Pollution Technology, Inc.
San Diego, California 92117

Dale Harmon
Leslie Sparks

U.S. Environmental Protection Agency
Research Triangle Park
North Carolina 27711

ABSTRACT

A flux/force condensation scrubbing system was built to control particulate emissions from a secondary metals recovery furnace. Total mass penetration and fractional penetration measurements were made under several different operating modes. The performance of the demonstration scrubber was consistent with the results of previous studies on F/C scrubbing. The system was generally capable of 90% to 95% efficiency on particles with a mass median aerodynamic diameter of 0.75 μmA. This efficiency was achieved with a 68 cm (27") W.C. gas phase pressure drop.

F/C SCRUBBER DEMONSTRATION ON A SECONDARY METALS RECOVERY FURNACE

INTRODUCTION

Flux force/condensation (F/C) scrubbing can achieve high efficiency fine particle collection at lower power input than the conventional high-energy scrubbing systems. F/C scrubbing effects are generally caused by contacting hot humid gas with colder liquid and/or by injecting steam into saturated gas. First, the transfer of water vapor toward the cold surface sweeps particles with it and this effect is referred to as diffusiophoresis. In addition, the condensation of water on the suspended particles causes the particle size to increase. The resultant particles are easier to collect by inertial impaction after growth has occurred by condensation.

The demonstration scrubber described in this paper was part of an R&D sequence supported by EPA contracts (see Table 1). The basic theory and potential applications of F/C scrubbing were treated in the scrubber systems study and reported in the "Scrubber Handbook." The feasibility of F/C scrubbing was evaluated in the next contract program which covered the development of mathematical models for predicting the efficiency and bench scale laboratory work for experimental verification. This was followed by two pilot plant studies. The first study was a 14 m^3/min (500 CFM) multiple sieve plate column with provisions for steam addition and water cooling. The second study was a 28 m^3/min (1,000 CFM) horizontal spray scrubber with water cooling. The object of the demonstration program as described in this paper was to test an F/C scrubbing system on an actual industrial source.

SOURCE INFORMATION

A secondary metal recovery furnace was selected for control in the demonstration. The source operation, which was ranked among the top 15 particulate sources in the Midwest Research Institute particulate system study, involved the burning of insulation from scrap copper wire.

The operator loaded metal pallets covered with randomly coiled scrap wire into a preheated gas-fired furnace. The charging door was closed, and as the insulation became hot, it melted and burned. Dense black smoke containing hydrochloric acid, metal chlorides, and other components was emitted through a breeching into the first of two gas-fired afterburners. Because of the batch loading and the variable emissions as the insulation burned away, the particulate emission rate was very cyclic. Opacity was high during the first several minutes and gradually decreased over the 30-minute operating cycle.

F/C SCRUBBER SYSTEM

The scrubbing system was composed principally of a crossover duct from the furnace stack, a spray type quencher, a sieve plate column scrubber, and a spray type cooling tower. The plant as built is shown in Figure 1, while the F/C scrubber system is shown schematically in Figure 2.

F/C Process Description. A maximum flow of 200 Am^3/min (7,000 ACFM) of flue gas flowed from the afterburner stack through a 9.1 m (30') long crossover duct to a spray quencher. The gases were preconditioned in the crossover duct and the quencher by circulating water sprays to reduce the volume and to saturate the gases with moisture. From the quencher the gas flowed to a multiple plate column, where it was contacted with a cooled solution of Na_2CO_3, and the particles were grown and collected by a combination of diffusiophoresis and inertial impaction. The gas flowed from the scrubber through an entrainment separator into the induced draft fan, and then to the exhaust stack.

Mechanical Design. A 9.1 m (30') long crossover duct and associated supporting truss were built from the furnace stack to the F/C scrubbing system. Because of the high temperature and the need to conserve gas enthalpy, the duct had to be insulated. During the program the carbon steel duct deteriorated due to corrosion, and it was replaced with a type 316 S.S.

Several spray nozzles were also installed to introduce a Na_2CO_3 solution for cooling and corrosion abatement.

The quencher included a 1.52 m (5') diameter and 3.7 m (12') long vertical spray chamber with cocurrent gas-liquid contact (see Figure 3). The quencher had a type 316 S.S. shell and also type 316 S.S. spray nozzles and heater piping. The external piping of the quench unit was CPVC (chlorinated polyvinyl chloride), and the gas duct to the scrubber was fiberglass reinforced plastic. The FRP duct held up well during the program. A bed of 2.54 cm (1") polypropylene pall rings was used as an entrainment separator and placed at the bottom of the quencher upstream of the outlet to minimize entrainment to the plate scrubber. While only a few percent of the rings were heat deformed during the four months of operation, this design would not be satisfactory without positive means for keeping the packing wet.

The F/C scrubber consisted of a cylindrical 2.3 m (7'6") and 3.0 m (10') high, five plate structure with provision for locating a sixth plate in a split tower design (see Figure 4). The plate scrubber was a hybrid design which offered flexibility in the mixing of sprays and plates, in the number of plates, and in the points of liquid introduction. The design was desirable for the pilot study, but it was much larger and more complex than would be required for ordinary use. As tested, the scrubber unit incorporated several combinations of plates with 0.48 cm (3/16") and 0.32 cm (1/8") diameter perforations. The scrubber entrainment separator was a tube bank with ten rows of 1.3 cm (½") diameter tubes in a series.

Scrubber liquid cooling was done by spraying into the upper part of a forced draft tower (see Figure 5). A spray type tower was used rather than a packed (or filled) tower because of the concern with solid deposition. Air was drawn upward through the tower by a propeller fan, which was located above an entrainment separator. Special attention was given to the design and provision for a high efficiency entrainment separator which was required because of the fine spray developed in the tower. The unit consisted of three rows of wave plate baffles with spacing of 1.3 cm (½") and a wave amplitude of 2.2 cm (7/8"). Baffle rows were offset 0.65 cm (¼") and baffle direction in each row was also reversed. The cooling tower piping was PVC, the spray nozzles were 316 S.S., and the sump tank was polyethylene.

The induced draft fan for the scrubbing system was a 25 HP, belt driven blade type, which was capable of 142 m^3/min (5,000 SCFM) at 56 cm (22") water column pressure. In some of the experimental runs the fan capacity was augmented to give 69 cm (27") W.C. pressure.

Instrumentation was provided to measure the parameters listed below:

1. Flow rates
2. Temperatures
3. Pressures
4. Humidities
5. Particulate mass loadings
6. Particle size distributions
7. Gas compositions

The parameters were included to measure both the performance and the process conditions at different locations of the scrubber system during the test program.

Liquor System. Water from the quencher was drained to a holding tank and recirculated to the quencher inlet. Liquor from the scrubber was collected in another tank and sprayed in the cooling tower. The cold outlet liquid from the cooling tower was then recirculated to the scrubber. Liquid disposal requirements were obtained from the local authorities and the demonstration plant was operated in compliance. The major requirements were that the liquid discharge to the sewer be neutralized and that it not interfere with the sewage treatment plant processes. The liquor was treated periodically and the pH was controlled by the addition of soda ash.

EXPERIMENTAL RESULTS AND DISCUSSION

The scrubber system was operated for about four months under several different modes. The purpose of the testing phase of the program was to obtain the overall mass efficiency of the system, the particle collection efficiency across the F/C scrubber, the operational reliability of the demonstration plant, and the economics of F/C scrubbing.

Results. The F/C demonstration plant was evaluated at six operating modes as listed in Table 3. A major division of the experimental measurements can be made by grouping the runs before the crossover duct corroded out (Modes A-E) and those after the new duct was installed (Modes F-J). This is because not only was the duct replaced but additional sprays were installed in the duct, an additional plate was added in the scrubber unit, and fan pressure capacity was augmented by the addition of a booster blower.

The chemical nature of the effluent was determined via atomic absorption. The particulate filter catch was largely composed of metals and halogens while the impinger catch showed a high concentration of hydrochloric acid (see Tables 4 and 5). In some runs where fluorinated polymer insulation was present in the scrap, hydrofluoric acid was encountered. Because of the very high halogen acid concentration, we used a basic addition to the scrubber liquor and corrosion resistant materials. For some particle size distribution sampling, cascade impactors were machined from Teflon.

Total mass penetration measurements were made for all runs and fractional penetration measurements were made for selected runs. Fractional penetration is penetration related to particle diameter and it was computed from cascade impactor inlet and outlet particle size distribution data.

Overall penetration in an F/C scrubber depends on particle size distribution, scrubber design, pressure drop, particle number concentration, particle composition, and the mechanism by which condensation occurs. Consequently Figure 6, which is a plot of penetration versus condensation ratio, is subject to many qualifications. The condensation ratio is the ratio of grams of water condensed per gram of dry gas. In Figure 6, the two solid curves show the penetration versus condensation results from a previous pilot plant study on F/C scrubbing, while the data points show some of the overall penetration data from the demonstration scrubber. The penetration decreases with condensation ratio, and the system performance was better after the new duct and other modifications were made. The data points represented by the triangles were taken while the old duct was in place, and the data points represented by the circles were taken after the new duct was installed.

Fractional penetration characteristics are shown in Figures 7 to 9. It is important to note that these are for a given scrubber design, pressure drop, condensation ratio, and particle number concentration. The figures show the experimental penetration curves and that predicted by means of a design model. Figure 7 shows a case where the fit between experiment and prediction is excellent, while Figure 8 shows a case where the fit was not so good. Figure 9 shows an average case where the match between performance and prediction is good and definitely adequate for design purposes.

Performance. The system was generally capable of about 90% to 95% efficiency on particles with a mass median aerodynamic diameter of 0.75 μmA (about 0.3 μm physical diameter for particles with a density of 4.0 g/cm^3). This efficiency was achieved with a 68 cm (27") W.C. gas phase pressure drop. A conventional high energy scrubber without F/C effects would require a pressure drop of roughly 250 cm (98") W.C. for 90% particle collection efficiency (σ_g=2.5).

Economics. In order to compare an F/C scrubber system with a conventional high energy scrubber, the knowledge from the demonstration study was used to refine the F/C scrubber design. A cost estimate was made for this design and compared to a parallel design and cost estimate for a conventional high energy system. It is important to note that the high concentration of acid gases required both mass transfer and particle collection capability.

The refined F/C system design includes the factors listed below:

1. Scrap - premium #1 wire
2. Efficiency required - 88% by mass
3. Inlet particle size distribution
   a. mass median diameter = 0.75 μmA
   b. standard deviation = 2.5
4. Pressure drop required - 70 cm (28") W.C.
5. Equipment
   a. saturator
   b. condenser
   c. venturi
   d. entrainment separator
   e. cooling tower

The control of furnace emissions from the incineration of premium no. 1 wire would require 88% collection efficiency and a scrubber pressure drop of about 70 cm (28") of W.C. High mass transfer efficiency is required to control the acid gases, so the total combination of saturator, condenser, scrubber, and entrainment separator must be included in the design. A venturi scrubber appears to be the best choice for particle collection after condensation and growth have occurred in the condenser. Because the mass transfer capability of a venturi and entrainment separator is limited, the saturator and condenser must be efficient for gas absorption.

The high energy scrubber system design features are outlined as follows:

1. Scrap - premium #1 wire
2. Efficiency required - 88% by mass

3. Inlet particle size
    a. mass median diameter = 0.75 μmA
    b. standard deviation = 2.5
4. Pressure drop required - 238 cm (94") W.C.
5. Equipment
    a. saturator
    b. condenser
    c. venturi
    d. entrainment separator

The conventional high energy system without any F/C effects would also require 88% collection efficiency but a pressure drop of 238 cm (94") W.C. for collection of particles with a mass median aerodynamic diameter of 0.75 μmA and standard deviation of 2.5 The high energy scrubber would have to include the same mass transfer capability as the F/C system and would have the same components as the F/C system except for the cooling tower and associated apparatus.

A cost comparison between the F/C scrubber and the high energy scrubber is given in Table 6. The initial capital investment is lower for the F/C system, and the annual power cost is also less than the conventional system. After accounting for depreciation and all operating costs including power, the total annual cost of the F/C system is about $10,000 less than the conventional high energy system at this particular source. The cost of electric power used was 0.045¢/kWh.

CONCLUSIONS

The following conclusions can be drawn from the results of this study:

1. The demonstration plant performance was consistent with the results of previous studies on F/C scrubbing.
2. A conventional high energy scrubbing system without any F/C effects would require a pressure drop of about 250 cm (98") W.C. to give the same efficiency as the demonstration plant did at 68 cm (27") W.C. pressure drop.

3. Particle number concentration and grown particle sizes are very important in F/C scrubbing.
4. An improved and simplified design procedure gave performance predictions which were in good agreement with experimental results.
5. An F/C scrubber capable of controlling no. 1 premium wire incineration from this source would cost \$103,000 to install and would have a total annual cost of about \$21,000 based on a ten-year life depreciation and all operating charges.

ACKNOWLEDGEMENT

The work described in this publication was performed under Contract No. 68-02-1801 with the U.S. Environmental Protection Agency.

ABBREVIATIONS AND SYMBOLS

C' = Cunningham correction factor, dimensionless

d_p = particle diameter, μm

n_p = particle number concentration, #/cm³

S.S. = stainless steel

σ_g = geometric standard deviation of particle size distribution

ρ_p = particle density, g/cm³

μm = micrometer (micron)

μmA = aerodynamic diameter, $d_p(C'\rho_p)^{1/2}$, $\mu m(g/cm^3)^{1/2}$

Table 1. F/C SCRUBBING STUDIES BY A.P.T. FOR EPA

Title	Contract	Report No. & Date	Subject
Wet Scrubber System Study - Scrubber Handbook (Vol. 1) Final Report (Vol. 2)	CPA-70-95	NTIS #PB 213-016 (1972)	F/C scrubbing principles and potential discussed.
Feasibility of Flux Force/ Condensation Scrubbing for Fine Particulate Control	68-02-0256	EPA 650/2-73-036 NTIS #PB 227-307 (1973)	Theoretical analysis, mathematical modeling, computer predictions, experimental data from bench-scale F/C scrubbers.
Study of Flux Force/ Condensation Scrubbing of Fine Particles	68-02-1082	EPA 600/2-75-018 (1975)	Laboratory pilot-plant study of F/C scrubbing in sieve plate and spray apparatus.
Study of Horizontal Spray Flux Force/Condensation Scrubber	68-02-1328 Task #10	EPA 600/2-76-200 (1976)	Laboratory pilot-plant study of F/C scrubbing in horizontal spray apparatus.

Table 2. PROCESS STREAMS FOR F/C SCRUBBER SYSTEM AT METALS RECOVERY FURNACE (see Figure 2)

STREAM NO.	COMPOSITION	TEMP °C	VOL.FLOW Am /min(G) or ℓ/min(L)	MASS FLOW kg/hr	ENTHALPY (0°C BASE) kcal/kg	y $\frac{\text{g water}}{\text{g d.gas}}$
1	Flue Gas	649	198	4,400	226 (d.g.)	0.07
2	Gas Mixture	71.7	100	5,384	211 (d.g.)	0.31
3	Gas Mixture	50.6	71.8	4,480	67.5(d.g.)	0.09
4	Water	59.4	59.0	3,540	59.4	--
5	Water	40.6	568	34,100	40.6	--
6	Water	59.4	568	34,100	59.4	--
7	Water	59.4	568	34,100	59.4	--

Table 3. F/C SCRUBBER DEMONSTRATION PLANT OPERATING MODES

Mode No.	Description of System
A	5 plates in scrubber, 0.48 cm hole diameter, cold water on pass A of scrubber.
B	5 plates in scrubber, 0.48 cm hole diameter, cold water on pass B of scrubber.
C	6 plates in scrubber, 4 plates with 0.48 cm hole diameter, 2 plates with 0.32 cm hole diameter, cold water on pass B of scrubber.
D	5 plates in scrubber, 3 plates with 0.48 cm hole diameter, 2 plates with 0.32 cm hole diameter, cold water on pass B of scrubber.
E	5 plates in scrubber, 3 plates with 0.48 cm hole diameter, 2 plates with 0.32 cm hole diameter, cold water on pass A of scrubber.
F	5 plates in scrubber, 3 plates with 0.48 cm hole diameter, 2 plates with 0.32 cm hole diameter, cold water on pass B of scrubber, sodium carbonate solution spray in crossover duct, charge wetted with water.
G	Sampling at peak of emissions only, 5 plates in scrubber, 3 plates with 0.48 cm hole diameter, 2 plates with 0.32 cm hole diameter, cold water on pass B of scrubber, sodium carbonate solution spray in crossover duct, charge wetted with water.
H	Sampling at peak of emissions only, 5 plates in scrubber, 3 plates with 0.48 cm hole diameter, 2 plates with 0.32 cm hole diameter, cold water on pass B of scrubber, sodium carbonate solution spray in crossover duct, charge wetted with water, water spray in crossover duct.
I	Sampling at peak of emissions only, 6 plates in scrubber, 4 plates with 0.48 cm hole diameter, 2 plates with 0.32 cm hole diameter, cold water on pass B of scrubber, sodium carbonate solution spray in crossover duct, charge wetted with water, water spray in crossover duct.
J	6 plates in scrubber, 4 plates with 0.48 cm hole diameter, 2 plates with 0.32 cm hole diameter, cold water on pass B of scrubber, sodium carbonate solution spray in crossover duct, charge wetted with water, water spray in cross over duct.

Table 4. CHEMICAL ANALYSIS OF PARTICULATES AT SECONDARY METALS RECOVERY FURNACE

ATOMIC ABSORPTION ANALYSIS	
Cu	11.2%
Fe	8.3%
Na	6.3%
Pb	22.6%
Zn	1.8%

Table 5. CHEMICAL ANALYSIS OF IMPINGER SOLUTION AT SECONDARY METALS RECOVERY FURNACE

COMPONENT	mg/ℓ	WT %
Cl^-	6,370	85.3
$SO_4^=$	136	1.8
NO_3^-	93	1.2
Zn	390	5.2
Fe	240	3.2
Cu	85	1.1
Pb	60	0.8
Si	73	1.0
Ca	17	0.2

Table 6. COST COMPARISON FOR PREMIUM WIRE RECOVERY

COST ITEM*	COST FOR F/C	COST FOR CONVENTIONAL
Total Capital Investment	$103,120	$111,240
Depreciation**	10,310	11,125
Maintenance	6,185	6,675
Water	180	180
Raw Materials	1,650	1,650
Power***	2,370	11,530
Total Annual Cost	$ 20,695	$ 31,160

* Cost based on 4th quarter 1976

** Based on 10 years straight line depreciation

*** Electric power @ 0.045¢/kWh

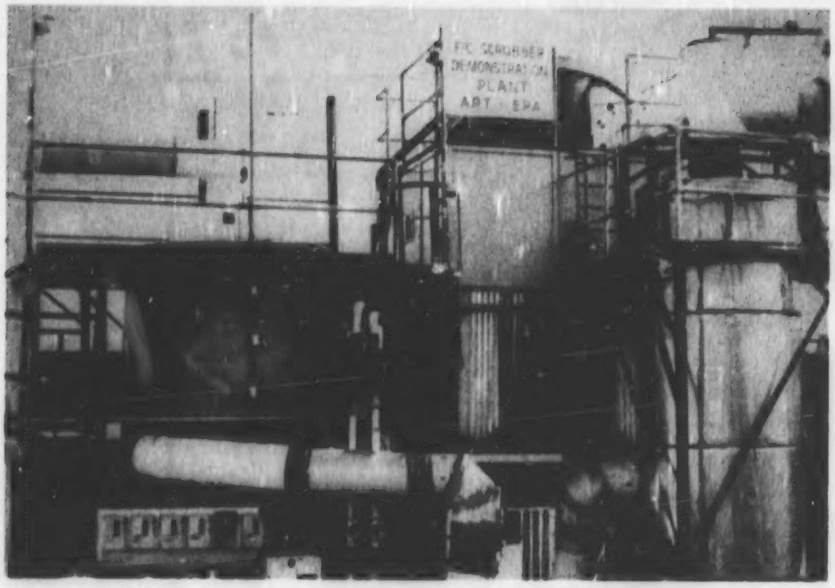
F/C SCRUBBER
DEMONSTRATION
PLANT
ART - EPA

Figure 1. Front view of F/C demonstration scrubber.

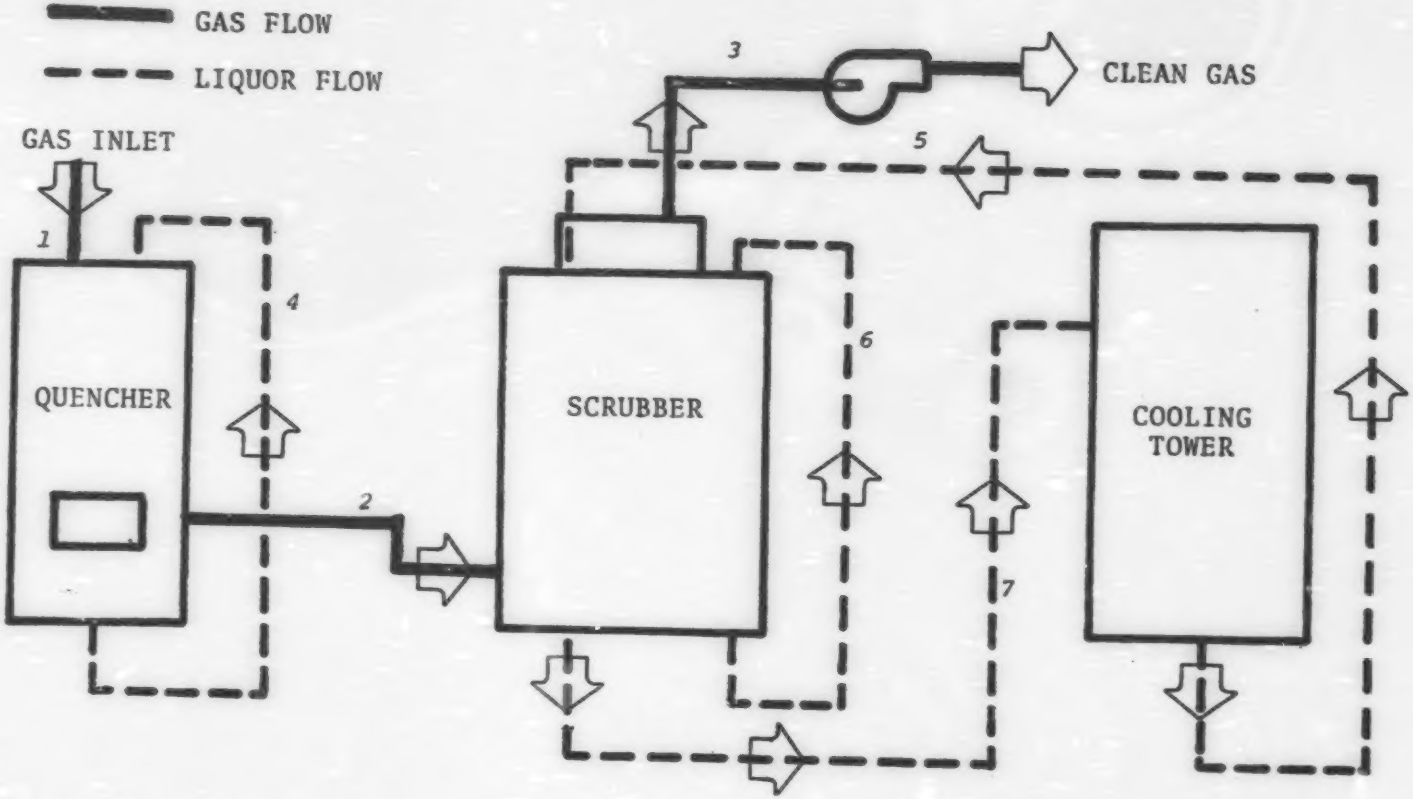
GAS FLOW
LIQUOR FLOW
GAS INLET
1
QUENCHER
4
2
3
SCRUBBER
5
6
7
CLEAN GAS
COOLING TOWER

Figure 2. Flow diagram of F/C scrubbing system. (see Table 2 for description of process streams)

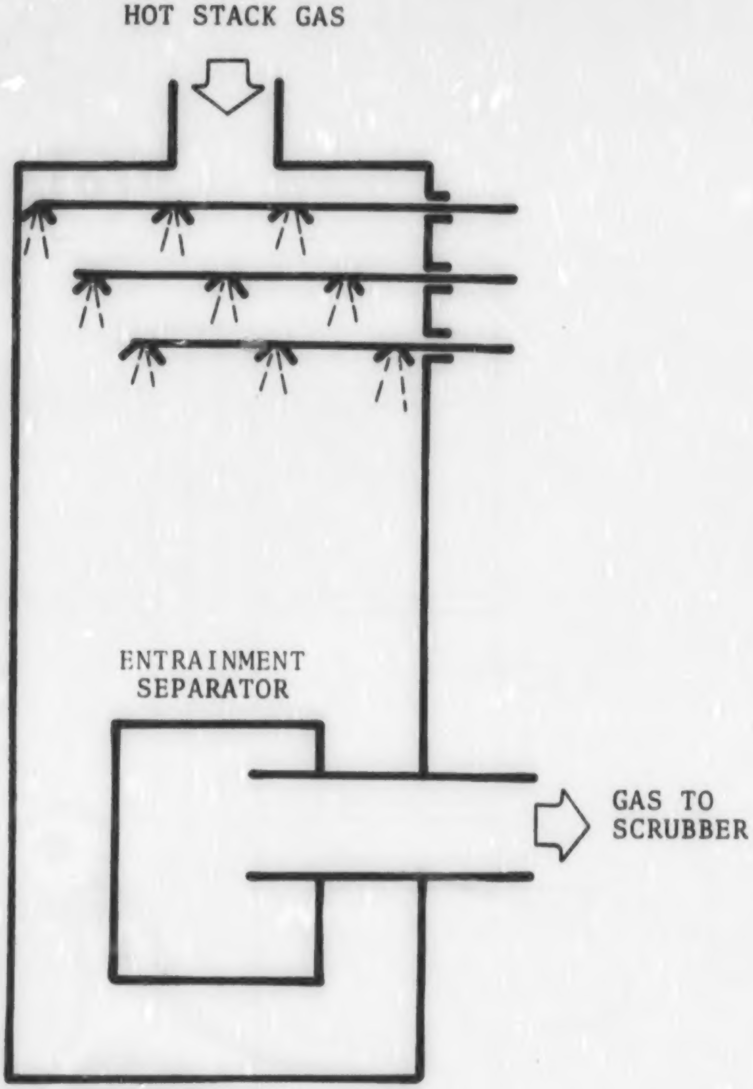
HOT STACK GAS
ENTRAINMENT SEPARATOR
GAS TO SCRUBBER

Figure 3. Quencher unit of F/C demonstration scrubber.

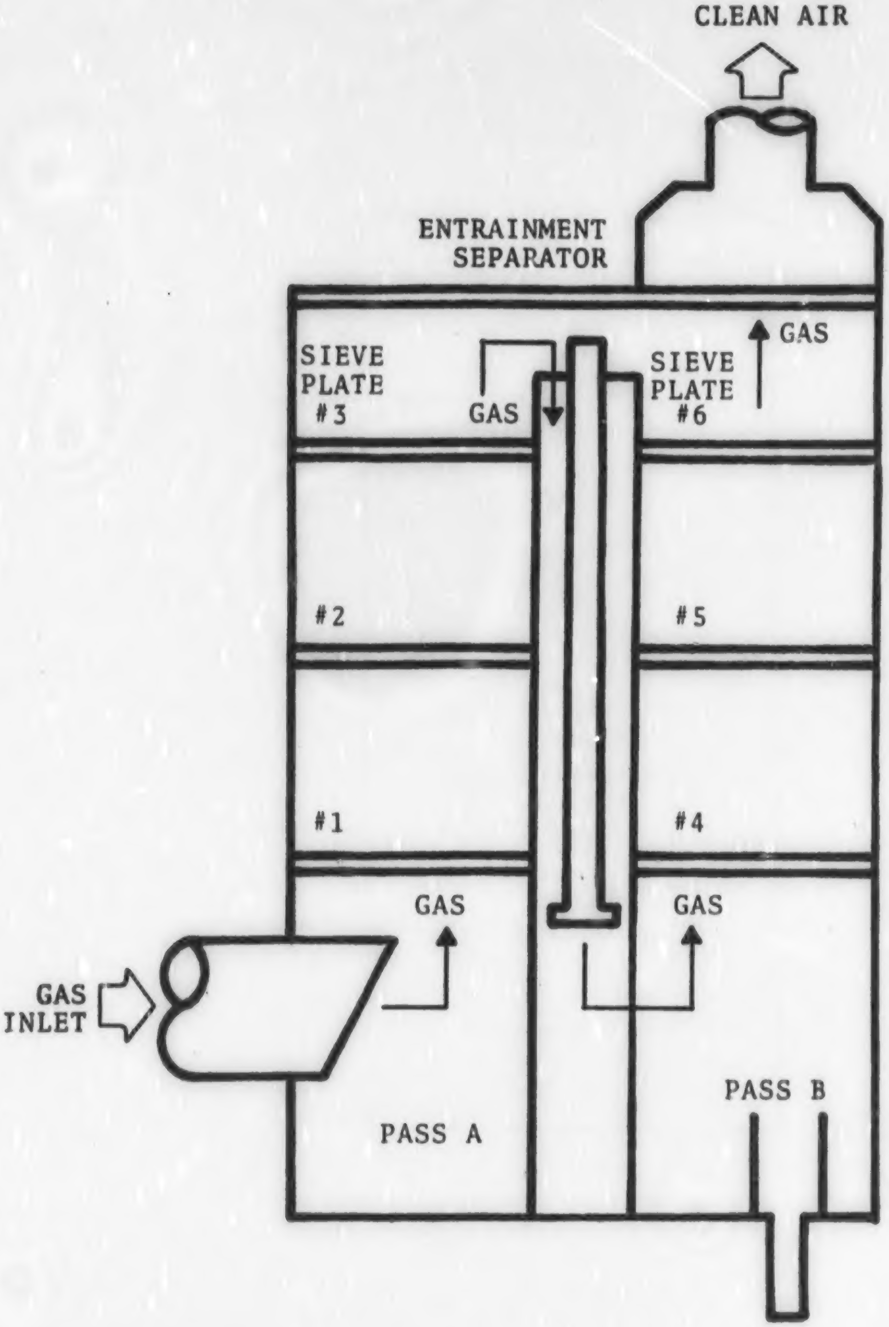
CLEAN AIR
ENTRAINMENT SEPARATOR
GAS
SIEVE PLATE #3
GAS
SIEVE PLATE #6
#2
#5
#1
#4
GAS
GAS
GAS INLET
PASS A
PASS B

Figure 4. Scrubber unit of F/C demonstration plant.

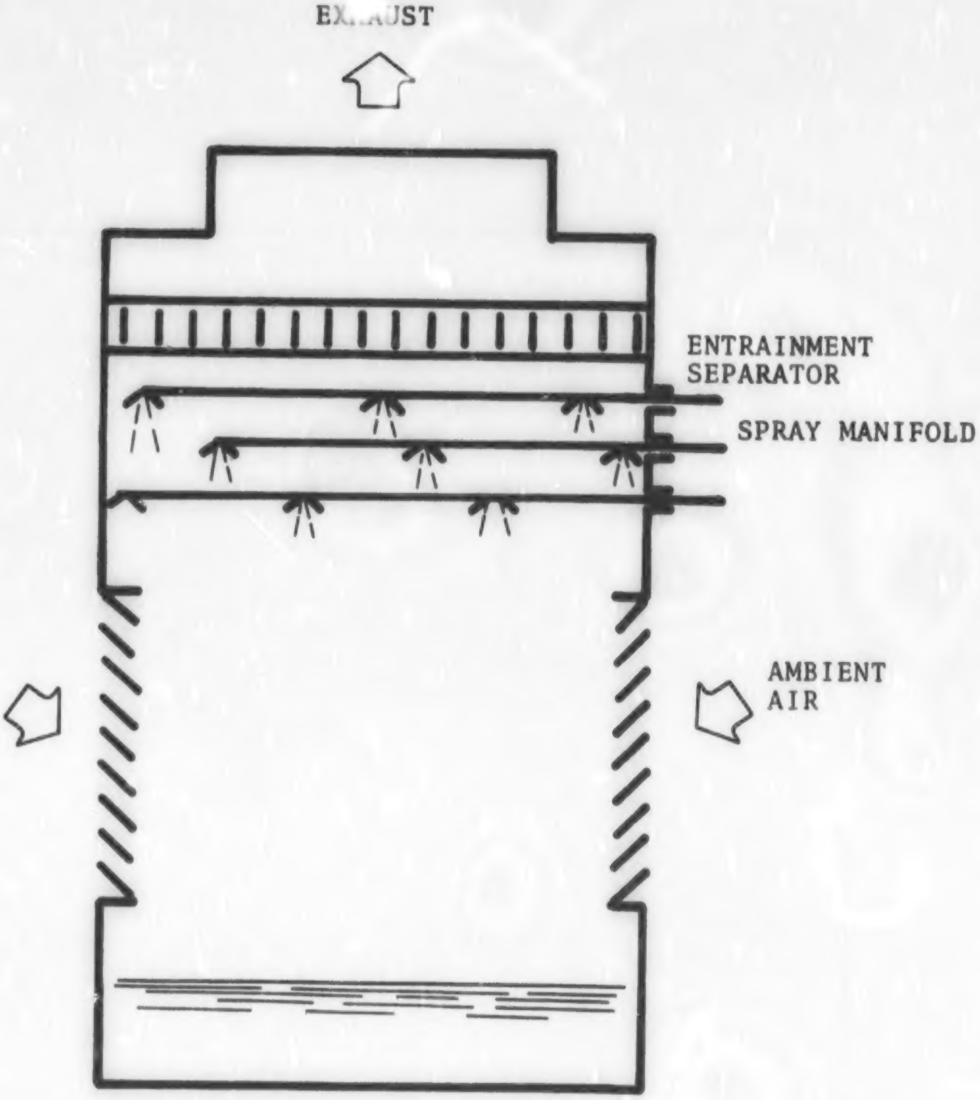
EXHAUST
ENTRAINMENT SEPARATOR
SPRAY MANIFOLD
AMBIENT AIR

Figure 5. Cooling tower of F/C demonstration scrubber system.

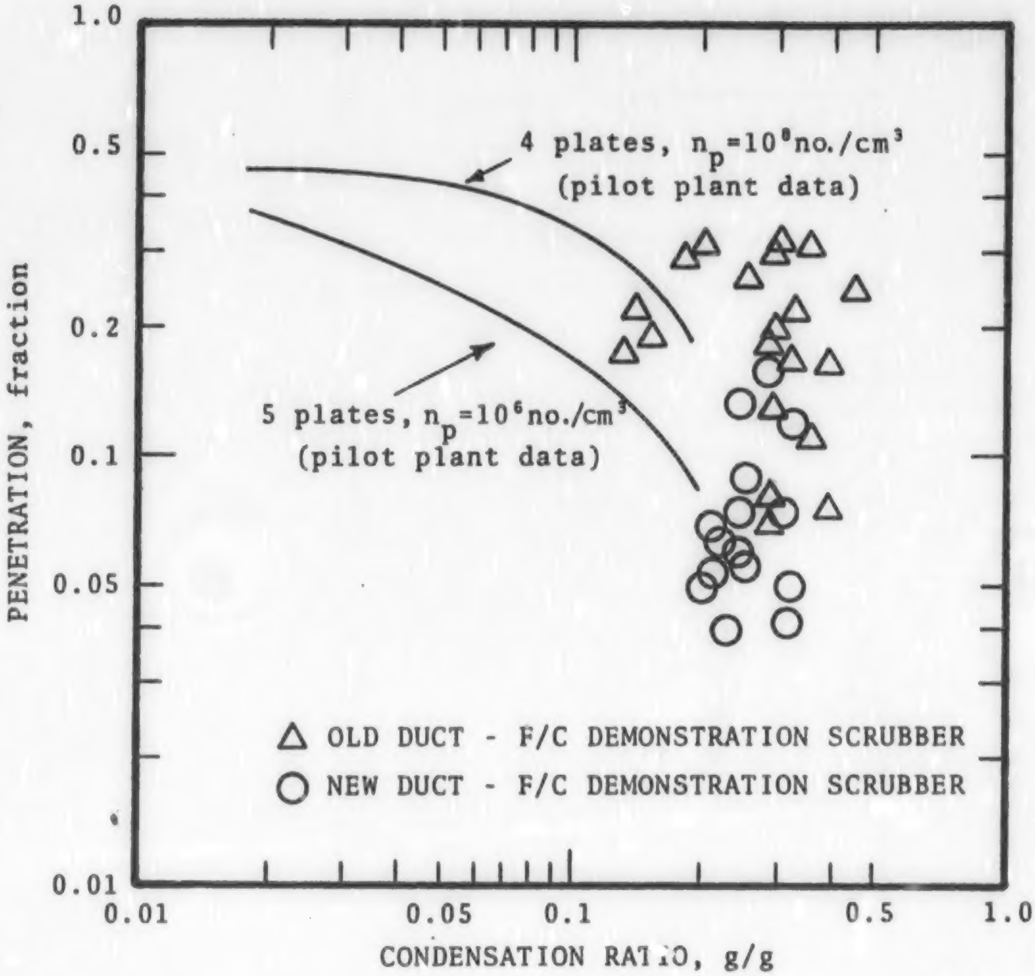

Figure 6. F/C demonstration scrubber performance.

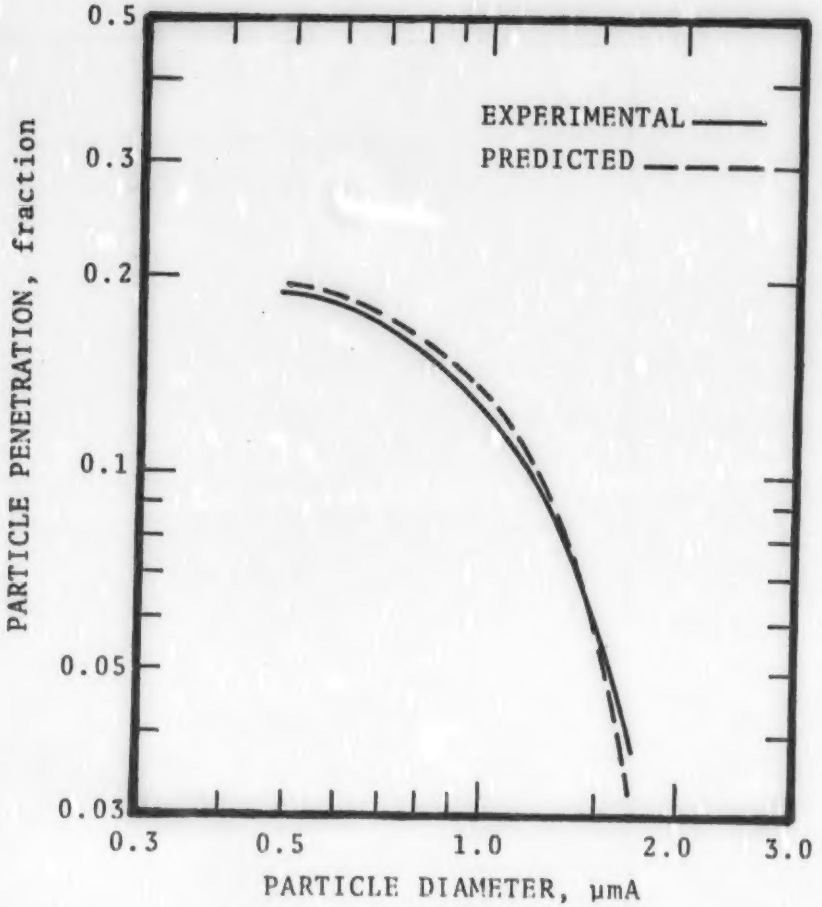

Figure 7. Particle penetration versus aerodynamic diameter for Run 64.

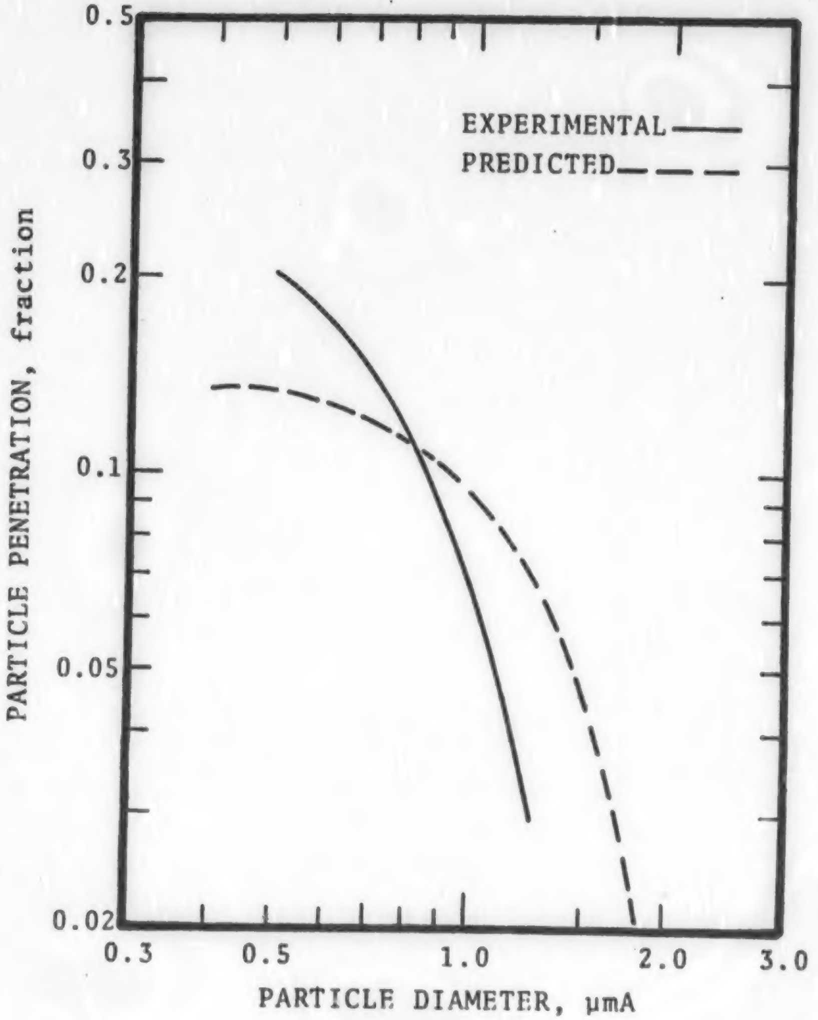

Figure 8. Particle penetration versus aerodynamic diameter for Run 74.

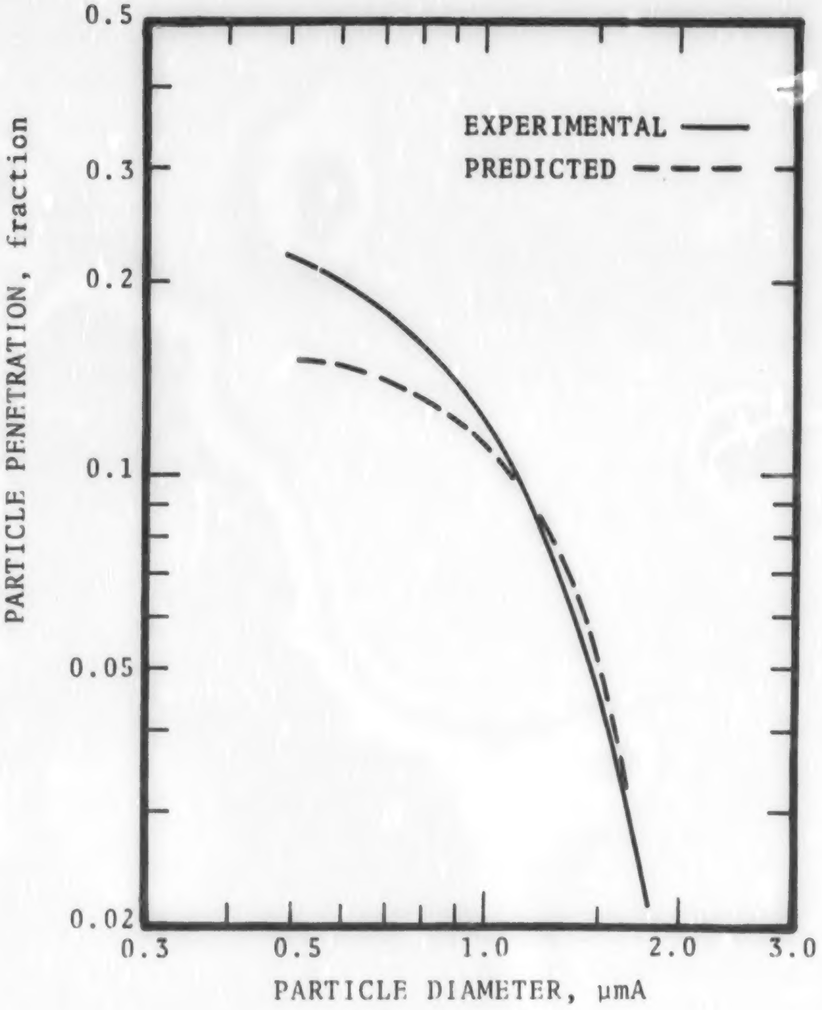

Figure 9. Particle penetration versus aerodynamic diameter for Run 69.

REFERENCES

1. Calvert, S., J. Goldshmid, D. Leith, and D. Mehta. Scrubber Handbook. A.P.T., Inc., EPA Contract No. CPA-70-95. NTIS No. PB 213-016. August, 1972.
2. Calvert, S., J. Goldshmid, D. Leith, and N. Jhaveri. Feasibility of Flux Force/Condensation Scrubbing for Fine Particulate Collection. A.P.T., Inc., EPA Contract No. 68-02-0256. NTIS No. PB 227-307. October, 1973.
3. Calvert, S., and N. Jhaveri. Flux Force/Condensation Scrubbing. J. Air Pollution Control Association. 24 (10): 947-951. October, 1974.
4. Calvert, S., N. Jhaveri, and T. Huisking. Study of Flux Force/Condensation Scrubbing of Fine Particles. A.P.T., Inc. EPA Contract No. 68-02-1082. August, 1975.
5. Calvert, S., and S. Yung. Study of Horizontal Spray Flux Force/Condensation Scrubber. A.P.T., Inc., EPA Contract No. 68-02-1328, Task No. 10. July, 1976.
6. Handbook of Emissions, Effluents and Control Practices for Stationary Particulate Pollution Source. Midwest Research Institute. Report to NAPCA. Contract No. CPA 22-69-104. 1970.
7. Peters, M.S., and K.D. Timmerhaus. Plant Design and Economics for Chemical Engineers. New York. McGraw Hill. 1968.

FINE PARTICULATE SCRUBBING - NEW PROBLEMS AND SOLUTIONS

Robert W. McIlvaine
The McIlvaine Company
Northbrook, Illinois 60062

ABSTRACT

Because of new processes and legislation, new problems have arisen that cannot easily be solved by conventional precipitation, fabric filtration or scrubbing. A need for new, high efficiency scrubbing techniques is indicated.

Several of these problems are described in this paper, and proposed or actual solutions are discussed. For example, a foundry shakeout scrubber in Tennessee is in violation because of a visible blue haze. The emission is less than .005 gr/SCF. Adding a wet precipitator is ridiculously expensive, while a fabric filter replacement is hazardous because of the moisture content. Some improved scrubbing technique is warranted. Evaluation of alternatives is now under way, with the addition of an ionizing section prior to the scrubber and a wet filter being considered.

Sinter plants in steel mills produce condensables that are not captured by fabric filters and precipitators. Considerable energy is required with venturi scrubbers to solve this problem. Results of pilot and full-scale scrubbers are discussed, along with other metallurgical problems.

FINE PARTICULATE SCRUBBING - NEW PROBLEMS AND SOLUTIONS

Many new scrubbing techniques for fine particles are being considered. A number of manufacturers have developed unique devices for applications where other devices have proved inadequate or economically unfeasible. The Environmental Protection Agency has undertaken a substantial investigation of new scrubbing devices for removing particles of less than 1 micron because of their detrimental effect on health.

As a publisher of technical information on the scrubber industry, we have not yet come across any data that has attempted to summarize the various applications to which the new scrubber designs may be applied and to match them to the various designs available. It is the intent of this paper to provide such a summary.

Why the need for new scrubbing techniques?

We will not attempt to discuss in this paper the health effects of fine particulate. We are starting with the assumption that a number of companies will be required to remove fine particulate from their exhausts in the future. If more thorough cleaning of the air is required and many other types of collectors exist, why not use something other than scrubbers? Various alternatives are presented in Figure 1. These are dry electrostatic precipitators, wet electrostatic precipitators, fabric filters, and incinerators. There are some applications to which these pieces of equipment cannot be successfully applied. By successful we mean that they are neither economical nor reliable.

Four conditions which increase the cost and/or decrease the reliability of existing equipment are humidity, corrosion, high temperature, and high ash resistivity. Fabric filters do not function well in highly humid atmospheres. Corrosion can be a substantial problem for fabric filters, wet electrostatics and dry electrostatics. High temperature creates a particular problem for fabric filters. High resistivity ash makes collection difficult in dry precipitators and is one reason they are not widely used in industrial applications. Wet electrostatic precipitators function well because of the presence of water and are not affected by ash resistivity. Of course, fabric filters are not affected by ash resistivity.

Again with reference to Figure 1, these devices vary in efficiency versatility. For example, incineration works well only on combustible particles and is not applicable to the majority of particulate emission problems. Fabric filters and wet electrostatics are versatile in that they will obtain high efficiency on the large majority of applications whereas dry electrostatics are more limited.

Many of these aspects affect cost. We must differentiate between small and large units because the economics are entirely different for a 10,000 CFM unit than for a 1,000,000 CFM unit. Dry electrostatics are relatively uneconomical at low volumes. Incineration is ruled out in many cases because of the high operating cost, especially when natural gas is used. In addition there are applications where incinerators do not have the required efficiency. Fabric filters are unpredictable depending on the humidity, temperature and other physical conditions. Wet electrostatic precipitators are extremely costly when handling corrosive gases. Dry electrostatic precipitators have a limited number of applications where they can produce high efficiency and are not economical for very small installations. Thus, it is evident that there are a number of instances when this equipment is not satisfactory and scrubbers should be considered.

What new scrubber types are available for fine particulate removal?

Before we eliminate the venturi scrubber entirely, we should note that venturis are being used at ever-increasing pressure loss. For example, there are venturi scrubbers on an iron foundry cupola operating at 120 inches pressure drop with an outlet emission of less than .01 grains/SCF. However, there are also applications where even at 200 inches pressure drop, venturis do not have acceptable efficiency.

Four types of scrubbers that do have high efficiency potential are foam scrubbers, electrostatically augmented scrubbers, steam-assisted scrubbers, and fiber scrubbers. Figure 2 compares the general performance of each of these types to venturi scrubbers and conventional low-energy scrubbers. All of the new types achieve high efficiency on fine particulate, at least under some conditions. The foam scrubber, specifically, can combine absorption along with particulate collection. In fact, one pilot foam scrubber appeared to have the absorption efficiency of a packed tower of nearly 1000 feet high. The other types are neither designed for nor do they have high absorption efficiency. At present the obvious drawback of these designs is their relatively high initial cost compared to either the venturi scrubber or the impingement plate scrubber, although this initial cost differential can be offset by their lower energy consumption and operating cost. The foam scrubber should be capable of removal of even the very finest particles with less than twenty inches pressure drop, most of which would be in the foam breaker. Operating cost should be relatively low if foam is recycled.

On commercial installations, electrostatic augmentation has proved to have achieved both low energy consumption and operating cost. Steam-assisted scrubbers use a considerable amount of energy; but when used on hot applications, can use waste heat, thus greatly reducing the net energy consumption and total operating costs.

Fiber-type scrubbers do require a considerable amount of energy compared to electrostatically augmented scrubbers, but require less energy than venturis. They are incapable of handling certain particulate and are therefore potentially unreliable on a number of applications. It is really too early to evaluate the reliability of foam scrubbers, although there is no indication that they cannot be made to operate quite reliably.

As for liquid requirements, we have not compared liquid-to-air ratios for the various devices since such a comparison is meaningless. Liquid is always recycled to some degree, so the more important issue is how clear the water has to be when it is introduced to the scrubber and how expensive will the water clarification system be. Both steam-assisted scrubbers and fiber scrubbers require a high degree of clarity. In the case of the steam-assisted scrubber the water must pass through a heat exchanger. Adaptability to corrosion-resistant construction is a positive feature of all scrubber types with the exception of the fiber scrubber and electrostatically-augmented scrubbers. However, this statement must be qualified by the fact that certain manufacturers, such as Ceilcote, have designed an all plastic scrubber which does have good corrosion resistance.

With the exception of the foam scrubber, there is considerable operating experience with all the new designs.

What are the specific applications to which new scrubbers are and will be applied?

This question is a difficult one for two reasons. First, there are numerous individual applications, particularly in the chemical industry upon which one cannot generalize. Second, unusual problems arise requiring more elaborate equipment in applications normally handled by conventional means. For example, thousands of scrubbers function adequately on foundry shakeouts. Emissions are generally less than 0.02 grains/SCF and the stacks are frequently clear. However, in at least five U.S. foundries, there is a substantial visible blue or gray haze being emitted from the scrubber discharge, and in all five cases local authorities have demanded that equipment be improved.

There are particular coal dryers, sinter plants and foundry cupolas which are not typical and produce very fine fumes impossible to control with conventional venturis. Therefore, one substantial area of application of new scrubbers is in industries and on processes that were ordinarily handled by other devices.

In addition, there are a number of processes for which there is no satisfactory alternative. Those applications which are in this category are quickly determined by examining the various columns in Figure 3. Federal S.I.C. numbers (Standard Industrial Classification) for the various applications have been used for easy reference. The equivalent venturi pressure drop requirement tells us immediately whether or not the new scrubber types can compete economically. On refractory kilns, for example, a pressure drop of over 100 inches may be required with a venturi to produce an acceptable plume, so this becomes a natural application for a new scrubber type. Some ferroalloy applications require pressure drop considerably in excess of others. A Fluid-Ionic scrubber has just been applied to a mineral wool furnace where the pressure drop requirement for the venturi pilot scrubber was over 100 inches water gauge.

Municipal incinerators are also good applications because of the high pressure requirements for venturis. In fact, there have been a number of unsatisfactory venturi scrubber installations on municipal incinerators.

The market size for the various applications in millions of dollars per year is based on complete installed cost of equipment. There are at least nine categories which offer a potential in excess of $5 million per year on an installed basis. We have not attempted to include coal-fired boilers on the assumption that the only way this market would even lend itself to the new scrubbers would be if standards were issued which require exceptional control on fine particulate.

The last three columns in Figure 3 indicate the physical aspects of the processes described which are most important in determining whether scrubbers are more attractive than fabric filtration, precipitators, etc. Obviously, for an application such as liquid waste incineration where high temperature, high corrosion, and high humidity are all involved, some form of scrubber will almost always be used. In contrast, electric arc furnaces in the steel industry can be economically controlled by fabric filters or electrostatic precipitators.

High, fair, and low penetration estimates are based on total market share percentage calculations. In liquid waste incineration where very high pressure venturis are required and high temperature, corrosion, and humidity are involved, the potential penetration of new devices is very high. On coal dryers where the pressure requirement on venturis is relatively low, there is not much likelihood of a substantial penetration of new devices. For certain applications, such as black liquor recovery boilers, there is likely to be some penetration, but other control devices are well established.

Which companies are involved in development and commercialization of these new devices?

In addition to the companies listed in Figure 4, several universities and research organizations are participating through EPA-sponsored projects. Our survey includes Asian and European companies; but because our news-gathering network is more efficient here in the U.S., we may have missed some of the foreign companies active in this field.

As shown in Figure 4, at least twelve of these companies have equipment that is now commercially available and at least thirteen have conducted pilot tests. Monsanto probably has the largest number of commercial installations of any in this group, with over 1500 installations on SO_2 mist removal and other similar applications. The foam scrubber lags the farthest behind with no known commercial installations. However, there have been some pilot operations which show a great deal of promise.

Electrostatically augmented scrubbers have been installed in a number of different applications. Both the Ceilcote and TRW units have been used on installations as large as 200,000 CFM. Fluid-Ionic Systems has installed several large units. Heat Systems-Ultrasonics has specialized in small units often with soluble fumes. Chemico has concentrated on coke oven pushing exhaust and has a complete coke oven pushing car system revolving around the Aronetics scrubber. The initial success with the Lone Star Steel scrubber was on open hearth furnaces so that steam-assisted scrubbers are now commercially well-established, but only for a limited number of applications. For the convenience of readers, names and addresses of companies that are potential information sources in this field have been included in Figure 5.

In summary, there is a great deal of pilot work that will need to be done in order to make the new scrubber designs more universally applicable. However, for certain applications, a number of commercial devices have been established as both economical and reliable, and it is expected that an increasing market share will be captured by these devices in the next few years.

FIGURE 1

COMPETING DEVICES (NON-SCRUBBER)

Device	How well does it cope with				High Efficiency Versatility	Initial Cost of Unit		Operating Costs
	Humidity	Corrosion	Temperature	High Resistivity Dust		Small	Large	
Dry electrostatic	Well[1]	Poorly	Well	Poorly	Low	High	Low	Low
Wet electrostatic	Well	Poorly	Well	Well	High	High	High	Low
Fabric Filter	Poorly	Poorly	Poorly	Well	High	Low	Medium	Medium
Incineration	Well	Well	Well	-	Low	Low	Low	High

---

[1] Except acid dewpoint corrosion

FIGURE 2

COMPARISON OF NEW SCRUBBER DEVICES

METHOD	PARTICULATE EFFICIENCY	ABSORPTION EFFICIENCY	INITIAL COST	ENERGY CONSUMPTION	OPERATING COST	RELIABILITY	LIQUID CLARITY REQUIREMENT	ADAPTABILITY TO CORROSION RESISTANT CONST	OPERATING FULL SCALE EXPERIENCE
Foam	H	H	H	L	U	U	L	H	L
Electrostatic Augment	H	L	H	L	L	M	M	L	M
Steam Assist	H	L	H	H/L[1]	M	M	H	H	M
Fiber	H	L	H	M	M	L	H	L	H
Venturi 50" ΔP	M	L	M	H	H	H	L	H	H
Impingement Plate 6" ΔP	L	M	L	L	L	H	L	H	H

(U) Undetermined
(H) High
(M) Medium
(L) Low
1 Net energy requirement is low if waste energy used

FIGURE 3

NEW SCRUBBER APPLICATIONS

SIC NO.	DESCRIPTION	EQUIV.* VENTURI ΔP REQ.	MARKET SIZE $ MILLIONS/YR <1	1-5	>5	TEMPERATURE	CORROSION	HUMIDITY	POTENTIAL PENETRATION
0020	Bark & Mixed Fuel Boilers	7-30		x		H	H/L	L	Low
1000	Coal Dryers	10-40		x		M	H	H	Low
1010	Iron Ore Size Reduction	5-30		x		L	L	L	Low
1010	Pellet Furnaces	10+			x	H	M	L	Fair
2040	Grain Dryers	40+		x		M	M	H	Fair
2600	Black Liquor Recovery Boilers	30+			x	H	H	H	Fair
2800	Acid Mist	30+			x	L	H	H	Fair
2800	Sublimation	60+		x		H	H/L	H/L	High
2871	Prilling Towers	60+		x		L	H	H	Fair
2871	Phosphate Processing	5-40		x		M	H	H	Low
2895	Carbon Black Pellet Dryers	30+			x	M	H	H	Fair
2990	Coal Gasification	20+			x	H	H	L	High
3200	Glass Furnaces	40+		x		H	H	L	Fair
3251	Refractory Kilns	100+		x		H	H	L	High
3290	Mineral Wool Furnace	25-100		x		H	?	L	Fair
3312	BOF	40+			x	H	L	L	Low
3312	Sinter Plants	20-60		x		M	H/L	L	Fair
3312	Coke Oven Off Gas	20+		x		H	H	L	Fair
3312	Coke Oven Pushing	20-60			x	L	L	H	Good
3312	Electric Furnaces	40+			x	H	L	L	Low
3312	Scarfing	30+		x		L	M	L	Fair
3313	Ferroalloys	60+		x		H	H	L	Fair
3320	Foundry Cupolas	40-120		x		H	L	L	Low
3320	Foundry Shakeouts	4-100+		x		L	L	H	Fair
3340	Secondary Smelting	40+		x		H	H	L	Fair
4953	Municipal Incinerators	50+			x	H	H	L	Fair
4953	Liquid Waste Incinerators	50+		x		H	H	H	High

* inches w.g.
L low
M medium
H high

FIGURE 4 MANUFACTURERS

	IS UNIT COMMERCIALLY AVAILABLE?	HAVE FIELD PILOT PLANT TESTS BEEN CONDUCTED?	NUMBER OF FULL-SCALE INSTALLATIONS	APPLICATIONS
FOAM				
Monsanto Res-EPA	No	Yes	0	Laboratory tests show high efficiency potential
Alfa-Laval	Yes	Yes	Several	Metallic mining, foundries
Riley-Envir	No	Yes	0	Absorption as well as particulate
Miura Engr	?	?	?	Japanese patent issued in 1972
ELECTROSTATIC AUGMENTATION				
Ceilcote	Yes	Yes	Many	Refractory kilns, incinerators, petroleum, coke, calcining kiln
TRW	Yes	Yes	Several	Hot grinding, coke oven, scarfing, sludge incinerator
Fluid-Ionic	Yes	Yes	Several	Aluminum, steel, pulp & paper, glass, meat smoking, mineral wool cupola
Chemico	?	?	?	(Recent license arrangement with Soc. Lab)
Fyltis	Yes	Yes	-	Aluminum prebake & Soderberg pots, iron & steel, detarring, chemical industries
RP Ind	Yes	Yes	-	PVC textile oven exhaust, foundry cupola
APS	Yes	Yes	-	EPA tests conducted, pilot on hog-fuel boiler
WET FILTRATION				
Air Industrie	Yes	Yes	Many	Phosphoric & sulfuric acid mist in the chemical industry
Andersen 2000	Yes	Yes	Many	Phosphorous furnaces, coal dust, acid mist, glass furnaces, galvanizing
Cabeco	Yes	Yes	Many	Ammonium chloride
Monsanto	Yes	Yes	1000's	Acid mist from sulfuric acid plants, fertilizer prill towers, textile driers
Heat Systems-Ultrasonic	Yes	Yes	Many	Aluminum chloride, fertilizer ammoniator, paint fume, oil mist, engine exhaust

FIGURE 4 MANUFACTURERS

	IS UNIT COMMERCIALLY AVAILABLE?	HAVE FIELD PILOT PLANT TESTS BEEN CONDUCTED?	NUMBER OF FULL-SCALE INSTALLATIONS	APPLICATIONS
STEAM ASSISTANCE				
Chemico	Yes	Yes	Several	Ferroalloy furnace, coke oven pushing, carbon black pellet driers
Lone Star Steel	Yes	Yes	Several	Black liquor recovery boilers, open hearth furnaces
Roskel	Yes	Yes	-	Asphalt plants, incinerators

FIGURE 5

USEFUL ADDRESSES OF INFORMATION SOURCES

COMPANY NAME AND ADDRESS	ACTIVITY
Air Industrie 19-21 av. Dubonnet Courbevoie 92, France	Manufacturer of wet sleeve filter
Air Pollution Systems 1114 Andover Park West Tukwila, Washington 98188	Manufacturer of electrostatic ionizers and scrubbers
Air Pollution Technology, Inc. 4901 Morena Boulevard, Suite 402 San Diego, California 92117	Designer of scrubber systems and mist eliminators. R&D contractor for E.P.A. and other clients.
Alfa-Laval AB Fack S-147 00 Tumba, Sweden	Commercial manufacturer of foam scrubbers
Andersen 2000, Inc. 2000 Sullivan Road College Park, Georgia 30337	Manufacturer of CHEAF unit
Cebeco Manufacturing Company 1300 North 9th Street Philadelphia, Pennsylvania 19122	Manufacturer of wet filter
Ceilcote Company 140 Sheldon Road Berea, Ohio 44017	Manufacturer of Ionizing Wet Scrubber
Chemico Air Pollution Control Company One Penn Plaza New York, New York 10001	Recent licensee of Societe Lab; Aronetics wet scrubber
Environmental Protection Agency Industrial Environmental Research Lab. Research Triangle Park North Carolina 27711	Active in the investigation of novel new devices
Fluid-Ionic Systems Div. of Dart Industries Inc. P.O. Box 20684 2525 East Magnolia Phoenix, Arizona	Manufacturer of Hydro-Precipitrol
Fyltis/Tissmetal Lionel-Dupont 138 Boulevard de La Croix-Rousse 69283 Lyon Cedex 1, France	Manufacturer of electrostatic liquid spray precipitator
Heat Systems-Ultrasonics, Inc. 38 East Mall Plainview, New York 11803	Manufacturer of Mystaire scrubber
Lone Star Steel Company 2200 West Mockingbird Lane Dallas, Texas 75235	Steam-Hydro Scrubber

FIGURE 5 (Continued)

COMPANY NAME AND ADDRESS	ACTIVITY
The McIlvaine Company 2970 Maria Avenue Northbrook, Illinois 60062	Publisher of manuals, newsletters, abstracts and search services on all aspects of scrubbing
Monsanto Enviro-Chem Systems, Inc. 800 North Lindbergh Boulevard St. Louis, Missouri 63166	Manufacturer of Brink Mist Eliminator
Monsanto Research Corporation Station B, Box 8 Dayton, Ohio 45407	Conducting foam scrubbing tests under contract to EPA
RP Industries 15 Kane Industrial Drive Hudson, Massachusetts 01749	Manufacturer of Electro-Dynactor
Riley Environeering, Inc. 7401 N. Hamlin Avenue Skokie, Illinois 60076	Foam scrubber development
Roskel Air Pollution Control, Inc. 503 Idaho Building Boise, Idaho 83706	Steam assisted scrubber
TRW Inc. One Space Park Redondo Beach, California 90278	Manufacturer of charged droplet scrubber
University of Washington Seattle, Washington 98105	Under EPA contract investigating electrostatic augmentation

ENTRAINMENT SEPARATORS FOR SCRUBBERS

Seymour Calvert
Shui-Chow Yung
Harry F. Barbarika
Air Pollution Technology, Inc.
San Diego, California

Leslie E. Sparks
U.S. Environmental Protection Agency
Industrial Environmental Research Laboratory
Research Triangle Park, North Carolina

ABSTRACT

Experimental results of research and development on entrainment separators by Air Pollution Technology, Inc. is presented. Performance tests were made of four types of entrainment separators, oriented so that the gas flow was vertically upward. The tests showed that re-entrainment occurred at lower superficial gas velocities in this configuration than when the gas flow was horizontal. Studies of solids deposition in entrainment separators were made and an experimental correlation is presented. Finally, a design method is described which uses the "cut diameter" versus pressure drop relationship for entrainment separators.

Preceding page blank

ENTRAINMENT SEPARATORS FOR SCRUBBERS

Gas scrubbers create mist while collecting particles. This mist is entrained by the gas to an extent depending on the type of scrubber and the operating conditions. The entrained drops carry dissolved and suspended solids which will constitute a particulate emission if they are carried out of the stack. It is always important and sometimes of overwhelming importance to separate this entrainment from the gas before it is emitted to the atmosphere.

Air Pollution Technology, Inc. (A.P.T.) has performed research and development on entrainment separators under several Environmental Protection Agency (EPA) contracts. The work has been reported in the "Scrubber Handbook," Calvert, et al. (1972) and in contract reports by Calvert et al. (1974a) and (1975). A review has also been given in the literature by Calvert et al. (1974b). In this paper results of further work concerning entrainment separators are presented. Three topics will be covered:

1. Results of performance tests of four types of entrainment separators oriented so that the gas flow is vertically upward in all cases.
2. Studies of solids deposition in entrainment separators.
3. A design method for entrainment separators.

PERFORMANCE TESTS

Four types of entrainment separators were studied experimentally. These are described below:

1. Knitted Mesh - ACS Model 4CA, 10 cm (4 in.) thick; 0.028 cm (0.011 in.) diameter wires arranged in layers; 98.2% porosity; and specific surface area of 2.8 cm^2/cm^3 (85.4 ft^2/ft^3).

2. Packed Bed - Polypropylene pall rings, 2.5 cm (1 in.) in diameter; packed to a 30 cm (1 ft) height ; and with specific surface area of 1.9 cm^2/cm^3 (58 ft^2/ft^3).
3. Tube Bank - Six rows of 1.9 cm (0.75 in.) diameter tubes, as shown in Figure 1; center-to-center spacing within a row of 3.8 cm (1.5 in.); and center-to-center spacing between rows of 2.13 cm (0.84 in.).
4. Zigzag Baffles -
    a) Horizontal - Six rows of discontinuous baffles, as shown in Figure 2; baffle width of 7.6 cm (3 in.); baffle thickness of 0.16 cm (0.063 in.); space between baffles within a row of 7.6 cm (3 in.); space between rows of 2.5 cm (1 in.); and angle to flow of 30°.
    b) Inclined - Same baffle size, spacing and angle to flow, as the horizontal. The baffles were inclined from the horizontal. Two inclination configurations were tested: 30° and 45°. Figure 3 shows the 45° inclined baffles.

All these entrainment separators and a cyclone separator had previously been tested in an arrangement with horizontal gas flow, as reported by Calvert et al. (1974a,b). For the latest series of experiments they were put in a tower with vertically upward gas flow. Vertical flow was expected to decrease the capacity as measured by the reentrainment velocity for a given liquid flow rate and not affect primary collection efficiencies. The entrainment was generated by spray nozzles arranged below the test section. Room temperature air and water were used.

The test section was about 76 cm (2.5 ft) square and the fan was capable of moving about 1.42 m^3/s (3,000 CFM). The performance efficiency was determined from a water balance over the gas and liquid streams. The entrainment drop diameters were averages for specific nozzles operated at a given pressure. Entrainment liquid flow rate to the spray section was measured by a calibrated water meter and checked by supply tank level measurements. The air flow rate was determined by a standard pitot tube located at the air inlet.

Performance Parameters

There are three basic performance parameters. The first is the primary efficiency, which is the efficiency at which the entrainment separator first collects the drops entering it. When the velocity in the separator becomes so great that the liquid which collects on surfaces is sheared off, or the liquid clogs air passages, reentrainment of the collected drops begins The velocity at which reentrainment first noticeably occurs is the second parameter. The final parameter is the pressure drop through the separator, which will not be discussed here because flow orientation did not have any effect on the previously reported (Calvert et al. (1974a,b) pressure drop data.

Performance of Knitted Mesh

The efficiency of the wire mesh as a function of superficial gas velocity is shown in Figure 4. Penetration in percentage is 100 minus the efficiency and is used rather than efficiency for convenience. Two different liquid flow rates, which correspond to different entrainment fluxes, were parameters. Dividing the entrainment flux by the gas velocity will provide the entrainment liquid to gas (L/G) volume ratio. Entrainment L/G's around 1 or 2 ℓ/m^3 are in a range which could be expected from scrubbers. A set of nozzles providing a drop diameter of 84 μm was used. Theoretically, a mesh should be 100 percent efficient once a small minimum velocity is reached; the break in the curve must represent the onset of reentrainment.

The onset of reentrainment is related to flooding. The predicted flooding velocity, based on correlation by Poppelle (1958) for an air-water system, is shown in the Figure 4 for the two entrainment fluxes. The predicted flooding velocity is lower than our observed reentrainment velocity. This is because the onset of flooding does not mean that heavy reentrainment will immediately occur, since flooding begins at the bottom of the mesh or packing while reentrainment comes mainly from the top of the mesh or packing.

Performance of Packed Bed

Penetration data for the packed bed are shown for similar entrainment fluxes in Figure 5. Here the penetration is not zero, but 1 or 2 percent at the lower velocities. Heavy reentrainment begins at about 6 m/s, which is higher than the flooding velocity for these liquid flow rates. The flooding velocity prediction is based on Sherwood's correlation for dumped packing (reported in Perry and Chilton, 1973). As with the mesh, the flooding correlation underpredicts the reentrainment velocity.

Performance of Tube Bank

Penetration through the tube bank is shown in Figure 6. The 2.5 ℓ/m^2-s flux represents a very heavy inlet entrainment, such as would come from a venturi. The dashed line is a prediction of the primary penetration for 90 μm diameter drops. The onset of reentrainment prediction is based on streamlined strut data which were independent of entrainment flux, depending only on the gas and liquid properties. It was much higher than observed. The experimental onset of reentrainment of 3 m/s (10 ft/s) is the lowest so far shown, but it occurred at a very high entrainment flux.

Performance of Horizontal Baffles

Penetration of the zigzag baffles in the horizontal configuration is shown in Figure 7. Here all the entrainment rates are moderate. The primary efficiency prediction for 90 μm diameter drops is shown as a dashed line. The onset of reentrainment was predicted, based on the tearing of drops from the baffle surface, as being between 5 and 6 m/s. The prediction is independent of the entrainment flux. The data, however, do show such a dependence.

Performance of Inclined Baffles

Inclined baffles were used in experiments with large drops and very heavy entrainment as shown in Figures 8 and 9. For the 30° inclined baffles reentrainment was noticed at about 6 m/s gas superficial velocity. The onset of reentrainment for 45°

inclined baffles was not reached. Figures 7, 8, and 9 graphically show the effect orientation has on the velocity of the onset of reentrainment. The more vertical, in this case the baffles inclined 45°, are better draining and have definitely higher reentrainment velocity characteristics.

Performance Test Conclusions

Primary efficiency can be predicted based on equations given in the literature and the contract reports. The present study showed that orientation of the entrainment separator did not affect the primary efficiency. Reentrainment was not that predictable and predictions based on flooding were too conservative. Orientation definitely had an effect. Unlike that used in the present experiments, the configuration with the gas flowing horizontal has better reentrainment characteristics.

SOLIDS DEPOSITION STUDIES

Possible deposition and removal mechanism studies, experiments for verification, and correlations have been made. All the deposition mechanisms involve transfer of solid particles from slurry drops or streams to a solid surface in the separator.

The possible mechanisms are:

1. Gravity settling to non-vertical surfaces.
2. Inertial impaction due to liquid flow direction changes, whether caused by the separator surface curvature or by the turbulence of the gas stream.
3. Diffusion.
4. Electrophoresis.
5. Liquid loss from the slurry due to:
   a) Liquid drops falling away from the concentrated solids interface.
   b) Evaporation.
   c) Sorption by a dry surface.

Chemical reactions and precipitation were not included as part of this study.

Once the solid particles deposit on a surface they will adhere to it for any number of reasons. Wetting of the surfaces seems to be the most important mechanism in overcoming the adhesion. Wetting the surfaces is commonly performed by washing. Theoretically, the liquid film thickness must be greater than the slurry particle diameter to provide washing.

A series of auxiliary experiments was conducted using a calcium carbonate slurry to provide information on solids deposition characteristics. The apparatus for this study consisted of a baffle plate upon which a slurry stream impinged after being atomized by an air jet. The major factors affecting deposition and washing were slurry flux, slurry drop size, and collection surface orientation.

Based on the auxiliary experiments and a few runs using slurry in the pilot scale system, the following conclusions were drawn:

1. Deposition rate decreases as the slurry flux on the surface is increased.
2. Deposition rate decreases as the liquid film thickness is increased.
3. Deposition rate is higher on an inclined baffle than on a vertical baffle due to the increase in settling rate of solids suspensions.
4. Small drops are more susceptible to being caught in eddies which would bring them to the back surfaces of the baffles.
5. Small drops which do hit the baffle surface have a higher deposition rate than larger drops because of their lower localized slurry flux.

The deposition data were correlated by the following empirical equation:

$$R_S = W\phi \exp\left[-(0.13 + 0.53\phi)\delta\right] \qquad (1)$$

where R_S = deposition rate of $CaCO_3$ on a vertical flat surface, mg/cm^2-s

W = weight fraction of solids in the slurry

ϕ = slurry flux, mg/cm^2-s

δ = liquid film thickness, μm

Although slurry flux, "ϕ", applies as a multiplicative factor, the exponential term predominates so that deposition rate decreases as "ϕ" increases. This equation can be used for similar slurries and conditions if the slurry flux and the liquid film thickness are known. Slurry flux in rows of baffles can be estimated using the efficiency equations. A prediction method for liquid film thickness is also available in the report by Calvert et al. (1975). The maximum thickness occurs where "δ" is zero, such as at a leading edge. The row at which "R_S" first becomes significant would be the one where washing would be most effective.

DESIGN METHOD

Three steps must be followed to properly select and design an entrainment separator. The first step is the determination of the performance requirements, including collection efficiency, maximum outlet loading, behavior of emitted entrainment, capacity, physical or process limitations, and cost. The second step requires gathering of information about the nature of the liquid entrainment and carrier gas, especially the liquid drop size distribution. The final step is the selection of candidate designs and prediction of the characteristics of these designs. For most of the types collection efficiency is very good as long as the reentrainment velocity is not exceeded.

For cases where drop collection efficiency requirements are stringent, such as when a significant amount of the drops have diameters 10 μm or smaller, the prediction of efficiency must be precise. The "cut diameter method" described by Calvert (1974) provides a convenient approach to the definition of separator efficiency. For most inertial collection devices, including entrainment separators, the cut diameter is a power law function of the energy consumed (or pressure drop). The "cut diameter" is defined as the diameter of drops collected at 50% efficiency.

Figure 10 is a plot of performance cut diameter versus gas pressure drop. This figure was drawn based on design equations and experimental correlations. Shown in Figure 10 are curves for: baffles at two angles of attack to the flow direction (not inclinations to the horizontal), tube banks with two different spacings between tubes within a row, packing of one particular size, and knitted mesh with a specific wire diameter. The curves would be different for entrainment separators of other collection element dimensions but are not much affected by the number of separator elements. For instance, while wire diameter changes move the lines, changing the thickness of the knitted mesh pad does not (over a reasonable range).

In any design, one must try to minimize reentrainment by keeping the superficial gas velocity below the reentrainment velocity. Trade-offs on capital and operating costs are needed to determine the size and gas velocity or pressure drop of the entrainment separator. Since pressure drops are usually low, capital costs predominate and suggest that a high velocity be used so that equipment size is kept as small as possible.

Primary efficiency data, such as presented here for a few drop sizes, are also available in the literature for other drop sizes and conditions. Predictions can be made based on the models presented in these reports. Finally, consideration of plugging characteristics of the design is needed since solids will be present on most entrainment separators for scrubbers. One would probably not choose the mesh or packing designs, which Figure 10 shows are most power efficient. This is because designs which have mostly vertical surfaces that are easily washed will be the best to use.

In general, it is possible to design entrainment separators of the types studied so that their performance and pressure drop are predictable. It is likely to be more difficult to specify the entrainment drop size and loading which must be treated. Reliable measurements of entrainment parameters are required if one is to make a rational design of an entrainment separator.

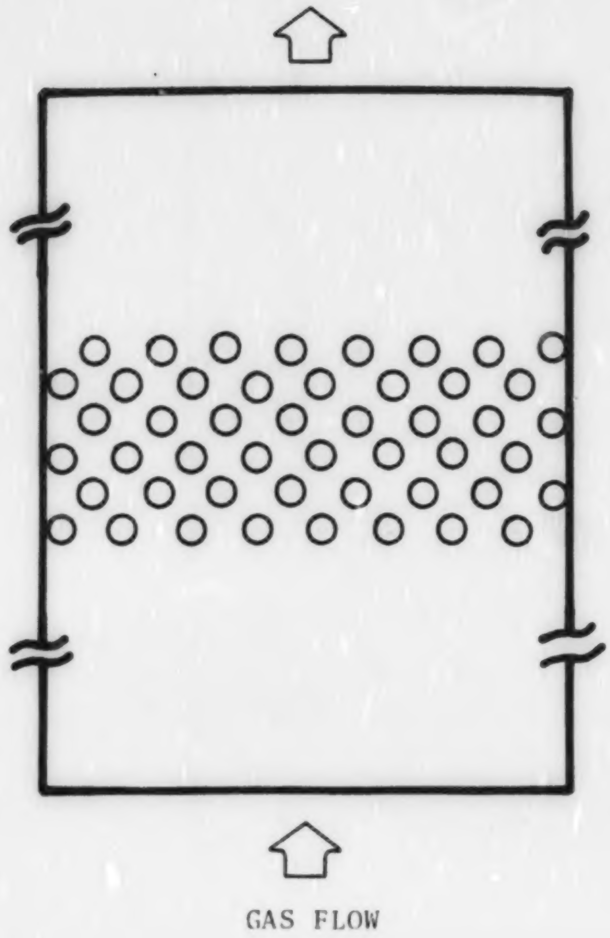

Figure 1. Tube bank configuration.

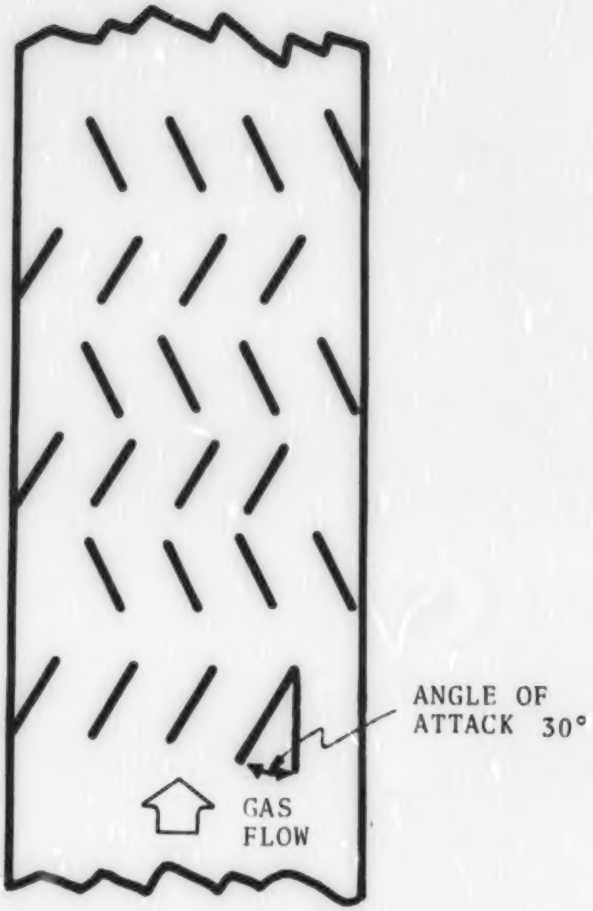
ANGLE OF
ATTACK 30°
GAS
FLOW

Figure 2. Horizontal baffle configuration.

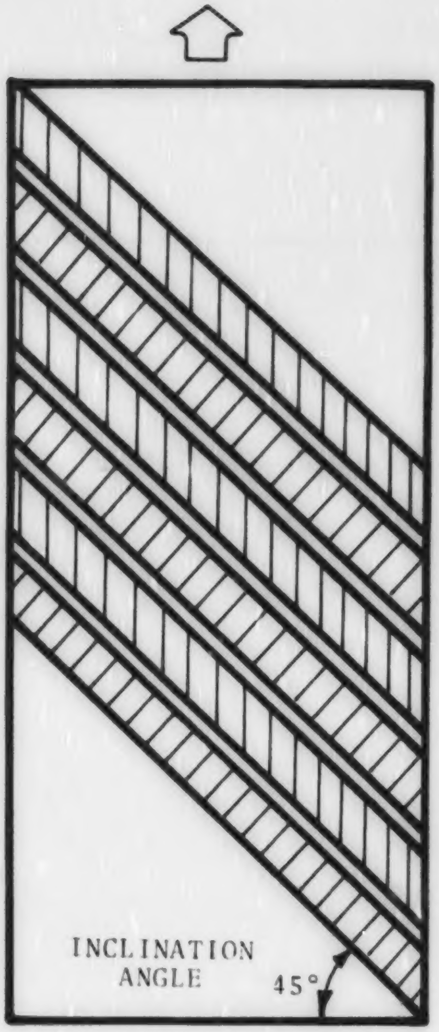
INCLINATION
ANGLE
45°

Figure 3. Inclined baffle configuration.

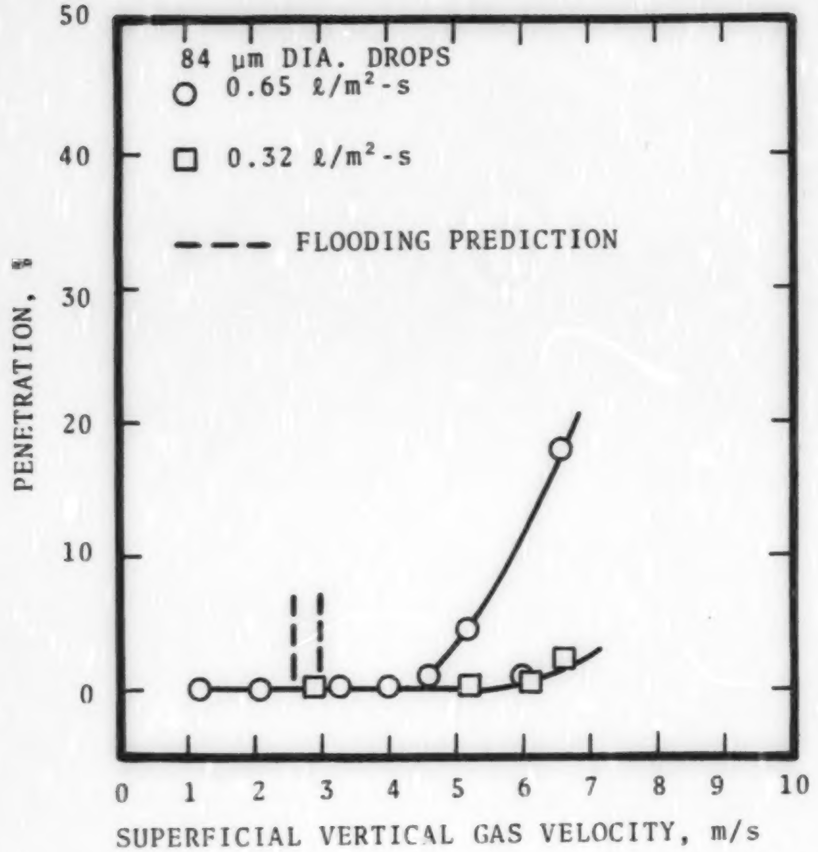

Figure 4. Experimental penetration through mesh, upward flow.

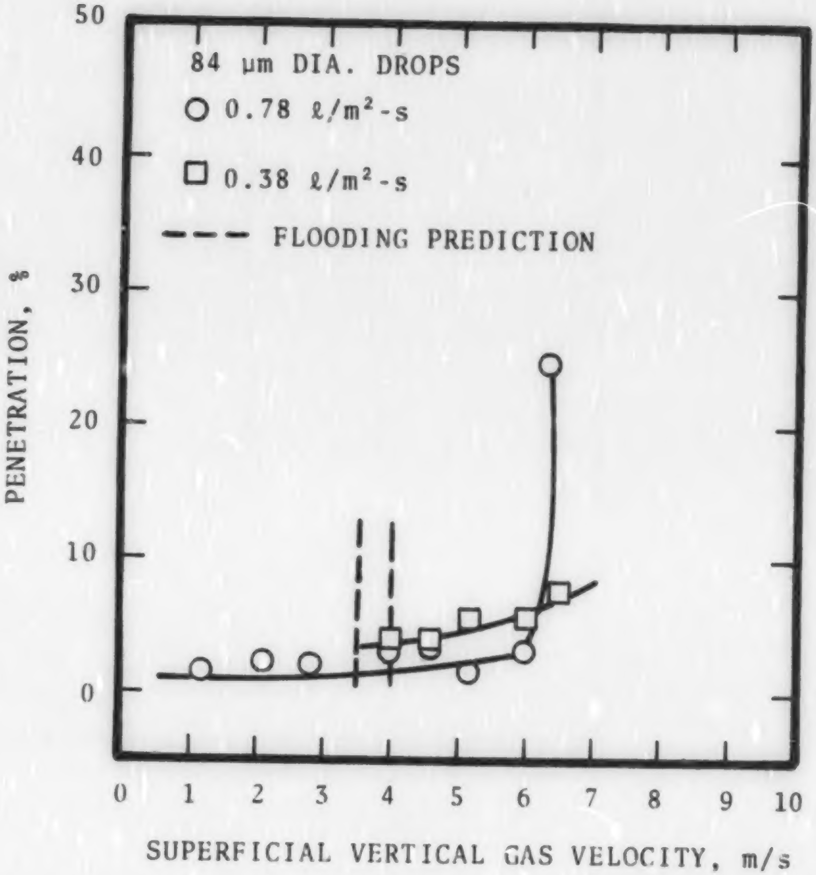

Figure 5. Experimental penetration through packed bed, upward flow.

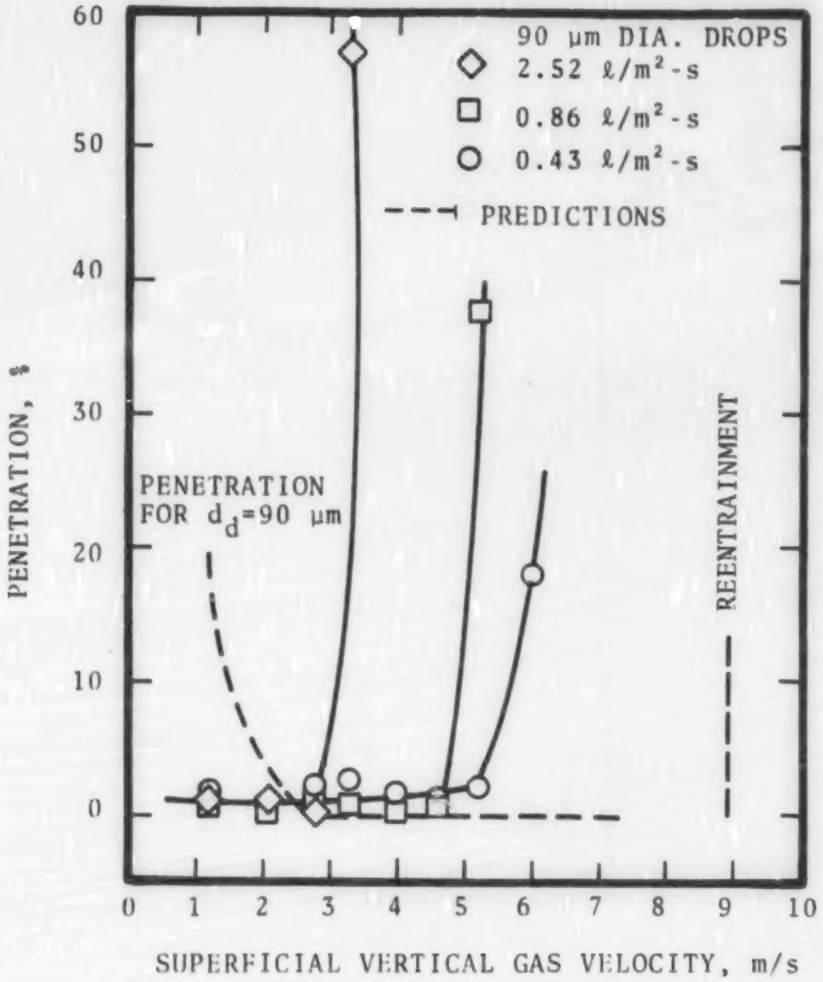

Figure 6. Experimental penetration through tube bank, upward flow.

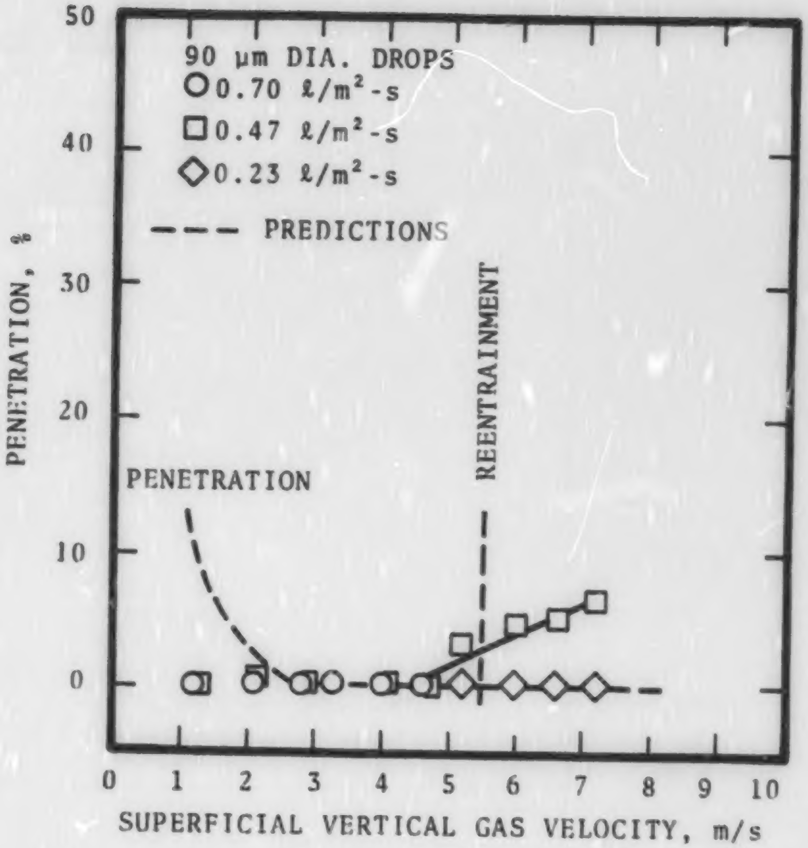

Figure 7. Experimental penetration through horizontal baffles, upward flow.

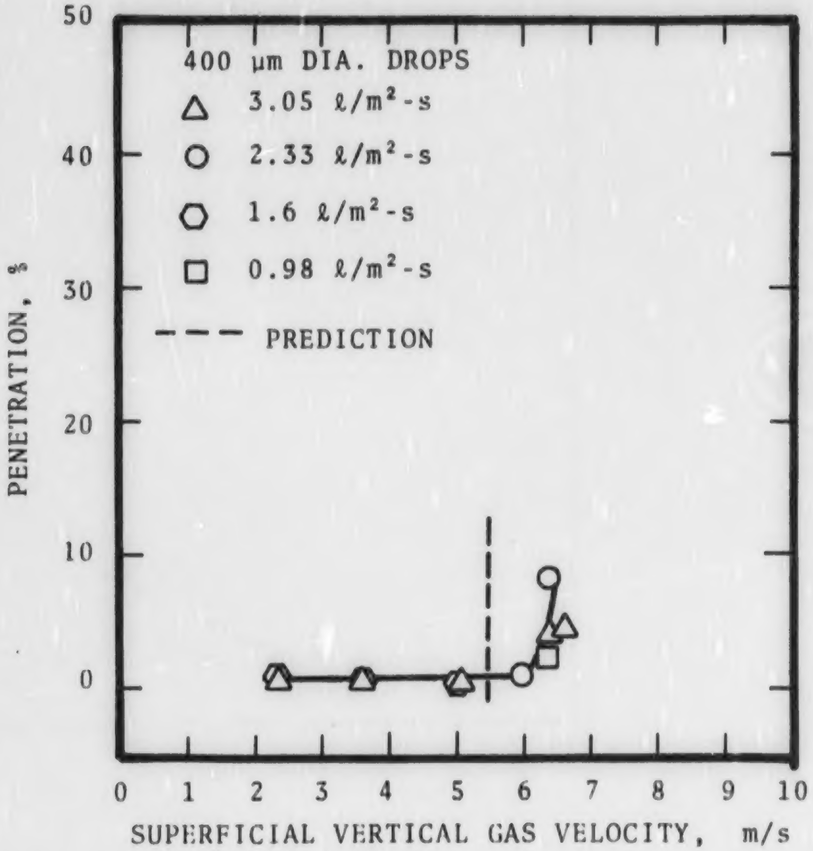

Figure 8. Experimental penetration through 30° inclined baffles, upward flow.

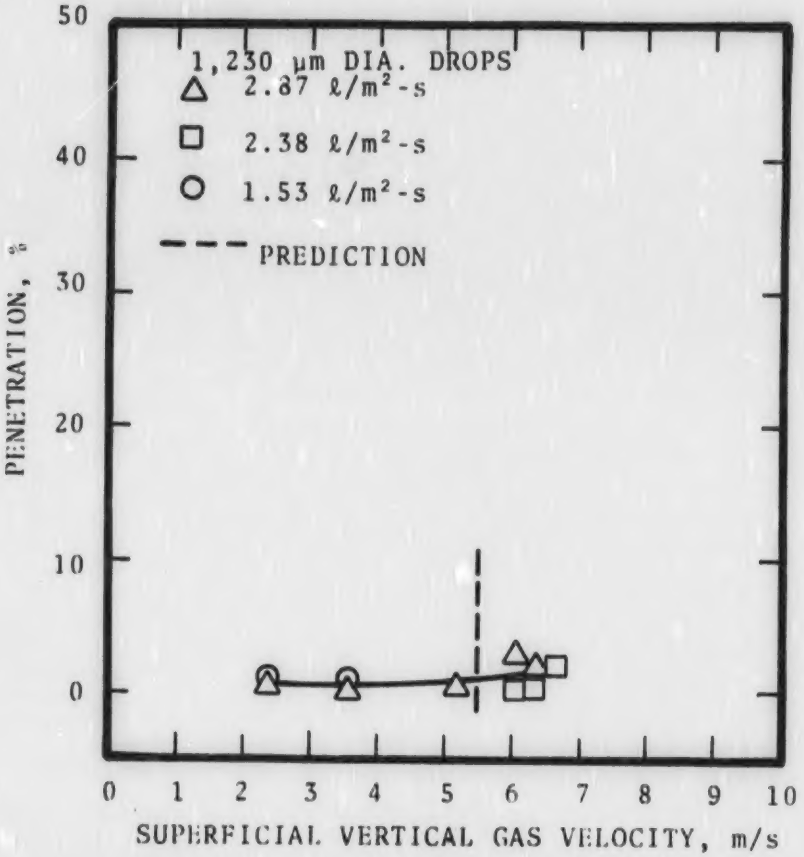

Figure 9. Experimental penetration through 45° inclined baffles, upward flow.

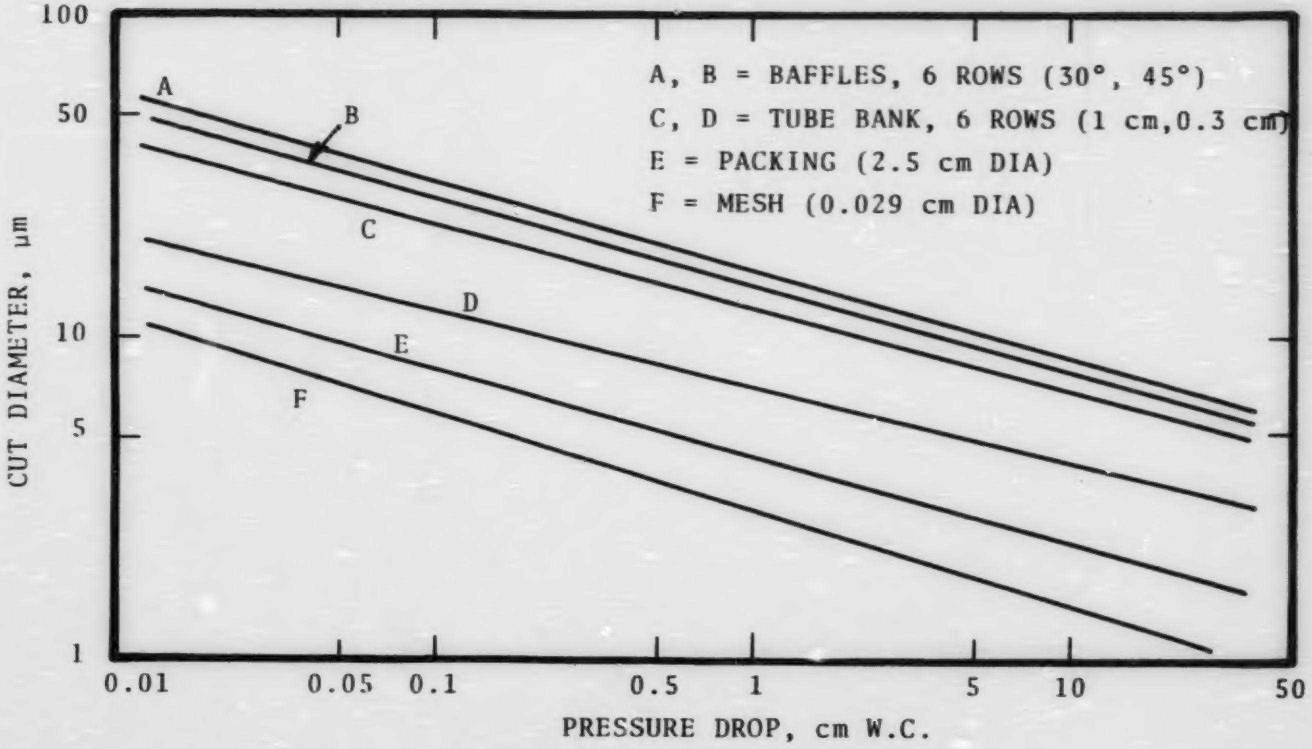

Figure 10. Entrainment separator performance cut diameters.

REFERENCES

Calvert, S., J. Goldshmid, D. Leith, and D. Mehta, "Scrubber Handbook," EPA-R2-72-118a, NTIS No. PB 213-016, August 1972.

Calvert, S., "Engineering Design of Fine Particulate Scrubbers J. Air Pollution Control Assoc. 24: 929 (1974).

Calvert, S., I.L. Jashnani, S. Yung, and S. Stahlberg, "Entrainment Separators for Scrubbers--Initial Report, EPA-650/2-74-119a, NTIS No. PB 241-189, October 1974a.

Calvert, S., I.L. Jashnani, and S. Yung, "Entrainment Separators for Scrubbers", J. Air Pollution Control Association 24: 971 (1974b).

Calvert, S., S. Yung, and J. Leung, "Entrainment Separators for Scrubbers--Final Report", EPA-650/2-74-119b, NTIS No. PB 248-050, August 1975.

Houghton, H.G., and W.H. Radford, "Measurements on Eliminators and the Development of a New Type for Use at High Gas Velocities", Trans. American Inst. of Ch.E. 35: 427, (1939).

Perry, R.H., and C.H. Chilton, "Chemical Engineer's Handbook", 5th edition, McGraw-Hill, New York, 1973.

Poppelle, E.W., Master's Thesis, Newark College of Engineering, 1958.

RELATIONSHIPS OF COLLECTION EFFICIENCY AND ENERGY DISSIPATION IN PARTICULATE SCRUBBERS

by

Konrad T. Semrau, Clyde L. Witham, and
William W. Kerlin
Stanford Research Institute
Menlo Park, California 94025

ABSTRACT

A pilot-plant-scale investigation was made of how the collection efficiency of a particulate scrubber is affected by the way that energy (contacting power) is applied to the gas/liquid contacting process. The tests were made with standardized, polydisperse synthetic aerosols of three different particle sizes. The performance of a conventional orifice contactor was taken as the reference for comparison of the other contactors, which included a contactor with multiple orifices in series, a variety of pressure spray nozzles, and a combination of an orifice with a pressure spray nozzle. Efficiencies were determined over a wide range of operating conditions with each contactor. The multiple-orifice series contactor gave the same performance as the orifice contactor at high contacting power, but poorer performance in lower ranges of contacting power. Contacting power derived from the liquid stream by use of spray nozzles gave lower efficiencies than were obtained with contacting power derived from the gas stream in the orifice scrubber. The deviation between the two levels of performance became relatively greater with decrease in the aerosol particle size. With one exception, the different spray nozzles gave nearly the same performance at a given contacting power.

Preceding page blank

RELATIONSHIPS OF COLLECTION EFFICIENCY AND POWER DISSIPATION IN PARTICULATE SCRUBBERS

The "contacting power" method for correlation of scrubber efficiency data was originally developed in a series of four papers(1-4) in which it was shown that the performance of a scrubber on a given aerosol could be represented by an expression of the form

$$N_t = \alpha P_T^{\gamma} \tag{1}$$

where N_t is the number of transfer units, P_T is the contacting power, and α and γ are empirical constants characteristic of the aerosol entering the scrubber. This is the equation of the "performance curve" for the scrubber and aerosol. The contacting power is that which is dissipated in fluid turbulence, and ultimately as heat, during gas/liquid contacting in a scrubber. It may be supplied from the gas stream, the liquid stream, or a mechanically driven rotor.

In scrubbers in which all the contacting power is obtained from the gas stream, the contacting power is essentially equivalent to the gas pressure drop or (more precisely) to the "effective friction loss" through the wetted equipment. An accumulation of data from various sources (1-7) as well as a large body of experience have established that, for scrubbers in this category, the collection efficiency on a given aerosol is almost wholly dependent on the contacting power and is little affected by the design or geometry of the scrubber. In other words, the constants α and γ of Equation (1) are characteristic of the aerosol, not the scrubber. Occasional devices or operating modes deviating from this generality have been ones yielding inferior performance. Other data (2-4) indicated strongly that contacting power derived from the liquid stream or from a mechanical rotor was probably equivalent to gas-phase contacting power, but no data obtained under closely controlled conditions have been available to clearly confirm or disprove this hypothesis.

In the present investigation, a critical comparison was made of gas-phase and liquid-phase contacting power. In addition, the performance of a multiple-orifice series contactor was studied. The technique used was to compare all the gas/liquid contactors over wide ranges of operating variables, using standardized synthetic test aerosols of three different sizes. The different devices were compared by reference to the baseline performance curves established with a conventional orifice contactor. All tests were made using air and water at ambient temperature.

Experimental System

The flowsheet of the experimental scrubber system is shown in Figure 1. The system could handle up to about 250 m^3/hr (150 ft^3/min) of air at ambient temperature and pressure, and gas pressure drops across the scrubber up to about 320 cm WC (125 inches WC). The scrubber consisted of a gas/liquid contactor section followed by a cyclone entrainment separator. The contactor section consisted of a straight, vertical section of tubing that could accommodate different types of gas/liquid contactors.

The air stream was drawn from the room and through the scrubber by a positive-displacement blower of the Roots type. The entering air was metered with an orifice meter, mixed with the test aerosol, and then drawn through the scrubber. The reference gas/liquid contactor consisted of an orifice located in the vertical contacting line, through which the air and scrubbing water passed downward; this unit was studied in a previous investigation.(5) The scrubbing water was fed through a single sidewall tap located two pipe diameters above the orifice. The air and water leaving the contactor were separated in the cyclone, and the air then passed to the blower.

The multiple-orifice series contactor (Figure 2) consisted of half-discs mounted in a staggered array within a tube flanged at one end. The assembly was held in position by the orifice flanges that normally held the orifice plate used as the reference contactor.

The spray gas/liquid contactors (Figure 3) consisted of five pressure spray nozzles (Configurations SS1 through SS5) and one combination of a pressure spray nozzle and an orifice (spray-orifice contactor SO). The SS1 nozzle was a specially fabricated concentric tube with multiple perforations that discharged solid radial streams of water at right angles to the direction of air flow. All the other spray nozzles were commercial products. The SS2 nozzle delivered a flat, fan-shaped spray. Nozzle SS4 produced a hollow-cone spray pattern deflected to a spray angle of 180°. The SS3, SS5, and SO spray nozzles were all of the solid-cone type, having nominal spray angles of 100°, 30°, and 60°, respectively. The water was supplied to the nozzles at pressures of up to about 13.6 atm gauge (200 lb/in^2 gauge).

Gas flow through the scrubber system was regulated by bypassing air from the room directly to the blower inlet. With spray configurations SS5 and SO, the water jets developed sufficient draft that the scrubber could be operated without the blower if desired. In these cases the air flow through the scrubber was controlled by restricting the discharge of the air to the atmosphere downstream of the scrubber.

The scrubber efficiency was determined by sampling the aerosol at the inlet and outlet of the scrubber. At the outlet, the aerosol was collected on a Nuclepore membrane filter. At the inlet, the sample was collected in a miniscrubber composed of four Greenburg-Smith inpingers in series followed by a Nuclepore filter; this unit both characterized the aerosol and determined its quantity.

Aerosol Generation

The aerosol generation system, shown schematically in Figure 1, was similar to that used in a previous investigation.(5) A cloud of droplets of the solution of aerosol material (ammonium fluorescein) was swept out of the aerosol generator by a small metered flow of saturated cold air, then dried by mixing with an additional metered flow of dry air. The resulting dry aerosol particles were then mixed with the main air stream passing to the scrubber.

The aerosol generator(8) was a greatly improved development of a generator used in the previous investigation.(5) The basic element was a commercial Mist-O_2-Gen ultrasonic nebulizer, but this was combined with other components designed to aid production of a stable and consistent aerosol. The particle size of the solid aerosol was determined by the initial droplet size and by the concentration of ammonium fluorescein in the solution. The ammonium fluorescein aerosols were spherical, nonhygroscopic, and only very slightly soluble in water; small samples could be determined precisely by fluorometric analysis. Three polydisperse aerosols of similar character but different particle sizes were produced by varying the solution concentrations; their size characteristics are presented in Table I.

The aerosol concentrations at the inlet ranged from about 0.02 to 20 mg/std m^3, depending on the air flow rate and the aerosol being generated. This low aerosol concentration range was beneficial in limiting the tendency of the particles to flocculate.

Results and Discussion

Although the aerosol generator was reasonably stable, the particle-size characteristics of the aerosols sometimes underwent substantial variations, and the possibilities of greater variations could not be ignored. An accurate, rapid, and simple method was needed to determine the variability of the aerosol, both for initial study of the generator itself and for monitoring the aerosol during scrubber testing. The miniscrubber was used for this purpose as well as for determining the inlet concentration to the scrubber. It was always operated at the same conditions, with a total pressure drop across the four impingers of 200 cm WC. The quantities of aerosol collected by each impinger and the final filter were determined individually, permitting determination of the efficiency of each stage and of the complete train of impingers. Plotting the cumulative number of transfer units against the corresponding cumulative pressure drop produced a performance curve for each miniscrubber run (Figure 4). Since the miniscrubber was always operated in an identical manner, this performance curve was characteristic of a given aerosol and was therefore termed the "signature curve" or "signature" of the aerosol. Although the signature gave no absolute measurement of the aerosol particle size, it was a very sensitive indicator of changes in the particle size and/or size distribution. If the signature of the inlet aerosol for a given scrubber test varied from the norm by an unreasonable margin, the test could be discounted. Figure 4 shows the average signature curves for Aerosols D, E, and G as well as that for Aerosol F, which was originally intended to serve as the finest of the aerosols but was found unsatisfactory because of contamination of the solution. The contaminant was apparently silica dissolved in the ammonium hydroxide used to prepare the solution. Its effect was to cause formation of nonspherical particles.

Performance curves for the orifice scrubber were determined for each of the three aerosols (Figures 5, 6, and 7). For convenience, the contacting power was expressed as effective friction loss. In each case, a two-branched performance curve was clearly defined, with the lower branch having a slope greater than 1.0. These phenomena were first observed, but much less clearly, in the earlier study with a similar ammonium fluorescein aerosol.(5) It is speculated that this type of behavior may be associated with a transition between controlling mechanisms in the collection of the particle.

The performance of the multiple-orifice series contactor on these aerosols is shown in Figures 8, 9, and 10, in which the baseline performance curves for the orifice scrubber are shown for reference. With Aerosols D and E, the data fitted the correlations for the orifice scrubber in the upper range of effective friction loss, but fell below the orifice scrubber curves in the lower ranges (Figures 8 and 9). With Aerosol G, the performance of the multiple-orifice series contactor was inferior to that of the orifice contactor except at the highest levels of effective friction loss that were attainable with the experimental system (Figure 10). The trends of performance with the three aerosols show that the deviation of the multiple-orifice contactor performance from that of the orifice scrubber increased with a decrease in aerosol particle size. There is no obvious explanation for the performance deviation and, indeed, no reason to assume that such a deviation should necessarily be characteristic of all forms of series contactors or scrubbers in series.

In the tests with spray contactors, there was always a gas pressure drop (or friction loss) across the scrubber, so that there were no cases in which all the contacting power was derived from the liquid stream. The gas-phase and liquid-phase contacting powers and the total contacting power were computed in units of kWh/1000 m^3 from the following equations:

$$P_G = 0.02724\ F_E \tag{2}$$

$$P_L = 0.02815\ p_f\ (L/G) \tag{3}$$

$$P_T = P_G + P_L \tag{4}$$

where

F_E = effective friction loss, cm WC

p_f = liquid feed pressure, atm gauge

G = gas flow rate, m^3/min

L = liquid flow rate, liters/min.

Some of the tests of the SS5 spray configuration and the spray-orifice contactor were made without use of the blower, but with the draft supplied by the water jets. The operating mode was thus the same as that of the ejector venturi scrubbers that are in wide use. In all these cases, there was a net gas pressure rise, rather than a pressure drop, across the scrubber, so that the nominal P_G value was negative. The nominal P_G value did not, in fact, constitute contacting power since it represented energy that was converted to gas pressure instead of dissipated in turbulence. The energy of the liquid jet was used in two ways, partly as contacting power and partly to pump the gas through the scrubber. Furthermore, a portion of the part of the energy that was used to pump the gas was eventually converted to gas-phase contacting power. Of the total gas pressure head developed by the liquid jet, part was lost by friction in passage through the scrubber; neither of these two quantities was measured explicitly in the experiments, but only the difference between them, which was the net pressure rise across the scrubber.

The tests of the spray scrubbers covered wide ranges of gas pressure drops, liquid and gas rates, and feed water pressures. When the efficiency data were correlated as functions of the total contacting power, the performance varied widely but was always definitely inferior to the performance of the orifice scrubber when a substantial fraction of the total contacting power was derived from the liquid. However, the deviation between the performances of the orifice scrubber and the spray scrubbers was found to be correlated with a simple parameter _f_, the ratio of the liquid-phase contacting power to the total contacting power. These correlations for tests with Aerosol D are illustrated in Figures 11, 12, and 13. Complete data are presented in the final project report.(8)

Since efficiency data were not determined for precisely equal values of _f_, they were grouped according to _f_ values lying in short ranges. For _f_ values in the range 0-0.39, the data points fell on or close to the orifice scrubber performance curve (Figure 11). At least part of the scatter in the data was due to the wide range of _f_ values. At _f_ values in the range 0.90-0.99, three correlation curves appeared, one for configurations SS5 and SO, one for SS1, SS2, and SS3, and one for SS4. The performance of SS4 was much inferior to that of the other configurations, for undetermined reasons. However, at least part of the difference between the performance of SS5 and SO and that of SS1, SS2, and SS3 has an apparent explanation. Because the liquid jets of the SS5 and SO contactors supplied part of the propulsion for the gas stream, part of the contacting power nominally calculated as liquid-phase was actually gas-phase, as expained above. Consequently, the actual value of _f_ was lower than indicated. If this factor could be determined quantitatively, the performances of the SS5 and SO contactors and of the SS1, SS2, and SS3 contactors would certainly be in closer agreement.

The performances of the SS5 and SO contactors were identical within the precision of measurement (Figures 12 and 13). Adding the orifice as a gas-phase turbulence promoter in conjunction with the spray nozzle afforded no interaction increasing the effectiveness of the liquid-phase contacting power. The performance of the two contactors when operated in the "ejector mode" (Figure 13) was nearly the same as that obtained at _f_ = 0.90-0.99 with the blower in operation (Figure 12).

In Figures 12 and 13, the performance curves for the spray scrubbers were arbitrarily drawn parallel to the branches of the reference performance curves of the orifice scrubber, since inspection of all such data obtained (8) made this procedure seem as reasonable as any other.

Additional tests of spray scrubbers were made using Aerosol G.(8) The efficiency data showed the same trends as were found with Aerosol D, but the relative deviation between the performances of the orifice and the spray scrubbers was greater.(8) Thus, the relative inferiority of the spray scrubbers was a function of the aerosol particle size and increased with decrease in the particle size. If the deviation in performance consistently decreases with increase in particle size, then for collection of particulates larger than perhaps 2-3 µm, liquid-phase contacting power may not be substantially less effective than gas-phase contacting power. If so, this phenomenon would explain earlier observations (2-4) that liquid-phase and gas-phase contacting power appeared to be fully equivalent. Most of these early observations were made in relation to collection of dusts that contained substantial fractions of relatively coarse particles.

At least part of the apparent systematic inferiority of liquid-phase contacting power may result from an unavoidable approximation in the calculation of P_L from Equation (3). The calculated value of P_L is equivalent to the theoretical kinetic energy of the liquid spray emerging from the nozzle. It is assumed that all this energy is effective in gas/liquid contacting and hence can be considered as contacting power. In fact, the energy delivered in the spray is reduced by friction in the nozzle, which is not known and would be difficult to determine. The internal construction of the SS4 nozzle indicates that the friction loss should have been greater than that in the other nozzles, which may explain at least some of the relative inferiority of the SS4 performance.

Once the spray has been discharged from the nozzle, some of the kinetic energy may be lost by dissipation in ways that do not contribute to gas/liquid contacting. It has been speculated that inelastic impact of spray on the pipe walls might be sufficient to account for the apparent relative inferiority of liquid-phase contacting power. However, this conjecture does not appear to be entirely consistent with the relative performance of spray nozzle arrangements that differed widely with respect to spray impact on the walls.

It is notable that all the spray contactors except SS4 gave about the same performance at a given contacting power despite radical differences in the nozzle designs and arrangements. Certainly, the various nozzles delivered sprays with different drop sizes as well as different configurations. Yet, such differences in the nature of the sprays evidently had little or no influence, independent of the contacting power, on the collection efficiency.

Nomenclature

$\underline{f}$ = ratio P_L/P_T

F_E = effective friction loss, cm WC

G = volumetric gas flow rate, m^3/min

L = volumetric liquid flow rate, liters/min

N_t = number of transfer units, dimensionless

= $\ln[1/(1 - \eta)]$

p_f = liquid feed pressure, atm gauge

P_G = gas-phase contacting power, kWh/1000 m^3

P_L = liquid-phase contacting power, kWh/1000 m^3

P_T = total contacting power, kWh/1000 m^3

α = coefficient of P_T in Equation (1), $[\text{kWh}/1000\ \text{m}^3]^{-\gamma}$

γ = exponent of P_T in Equation (1), dimensionless

η = fractional collection efficiency, dimensionless

Table I Test aerosol characteristics

Code designation	Particle-size range[a] (μm)	Mass-median diameter[b] (μm)	Geometric standard deviation[c]
D	0.2 -5	1.05	1.58
E	0.15-2.6	0.68	1.69
G	0.07-1.3	0.42	--

[a] Observed from electron micrographs.

[b] Aerodynamic diameter determined by cascade impactor.

[c] Particle-size distribution taken as log-normal.

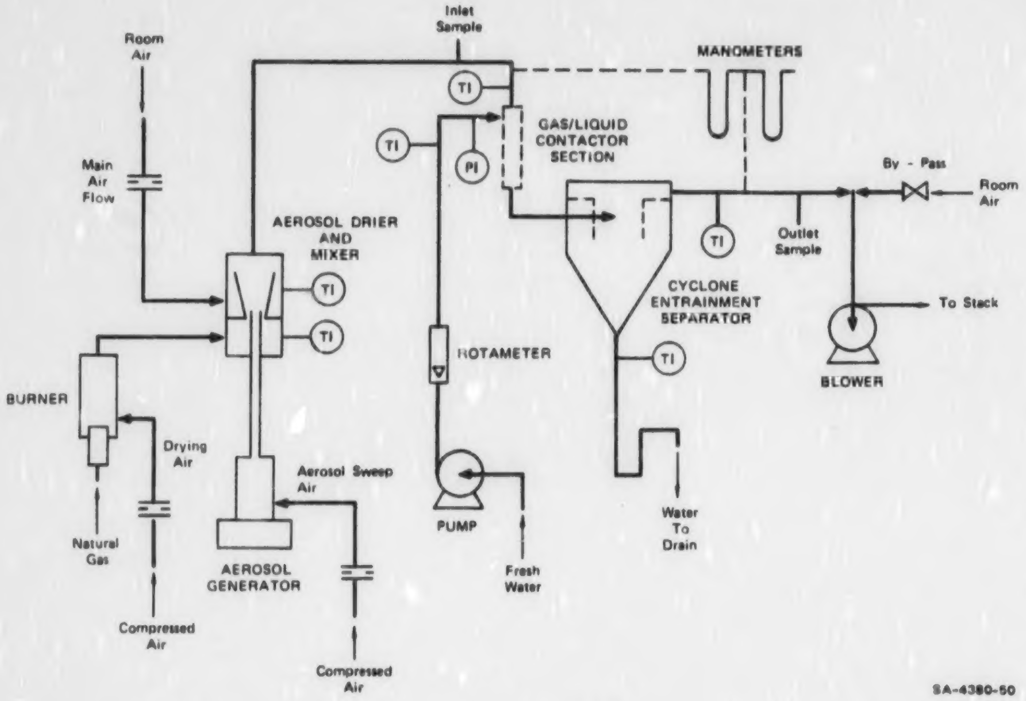
Inlet Sample
Room Air
MANOMETERS
TI
GAS/LIQUID CONTACTOR SECTION
TI
PI
Main Air Flow
By - Pass
Room Air
AEROSOL DRIER AND MIXER
TI
Outlet Sample
TI
CYCLONE ENTRAINMENT SEPARATOR
To Stack
TI
ROTAMETER
TI
BLOWER
BURNER
Drying Air
Aerosol Sweep Air
PUMP
Water To Drain
Natural Gas
AEROSOL GENERATOR
Fresh Water
Compressed Air
Compressed Air
SA-4380-50

Figure 1 Flowsheet of experimental scrubber system

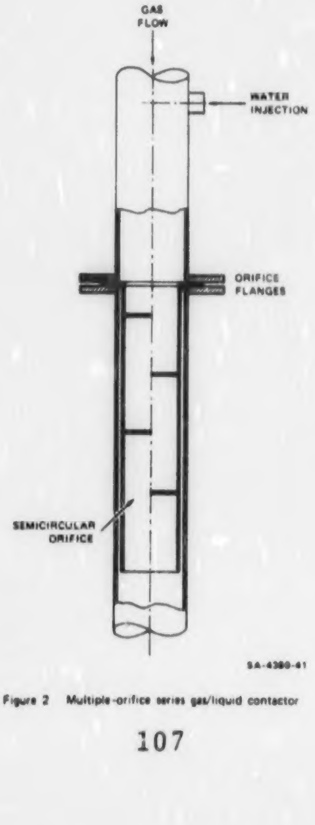
GAS FLOW
WATER INJECTION
ORIFICE FLANGES
SEMICIRCULAR ORIFICE
SA-4380-41

Figure 2 Multiple-orifice series gas/liquid contactor

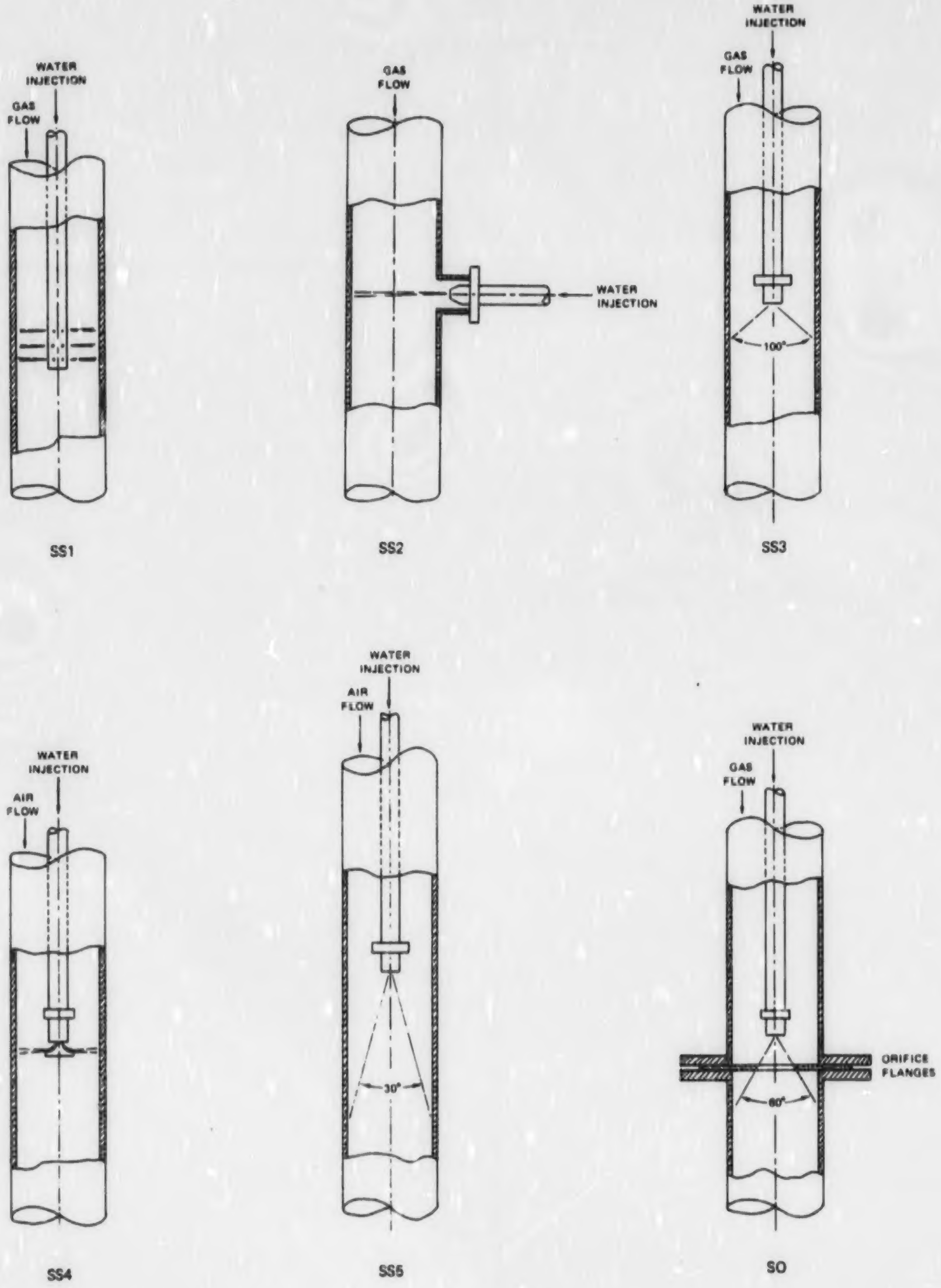
WATER INJECTION
GAS FLOW
WATER INJECTION
100°
AIR FLOW
30°
60°
ORIFICE FLANGES

SS1 SS2 SS3

SS4 SS5 SO

Figure 3 Spray gas/liquid contactors

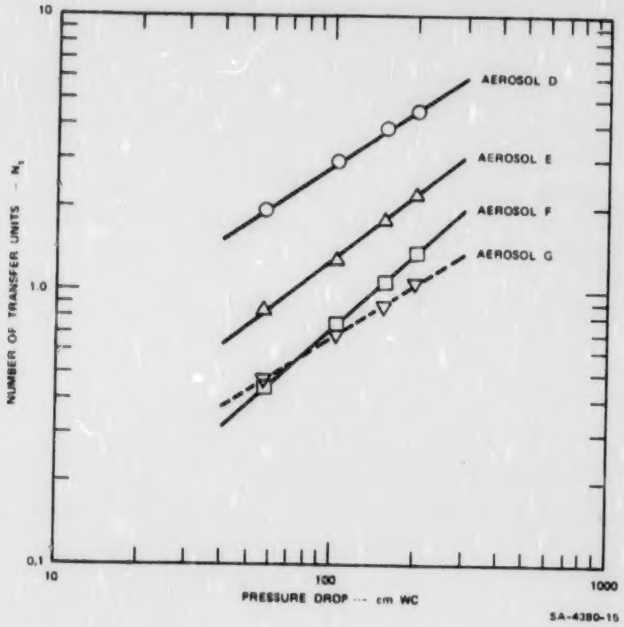

Figure 4 Miniscrubber signature curves for aerosols D, E, F, and G

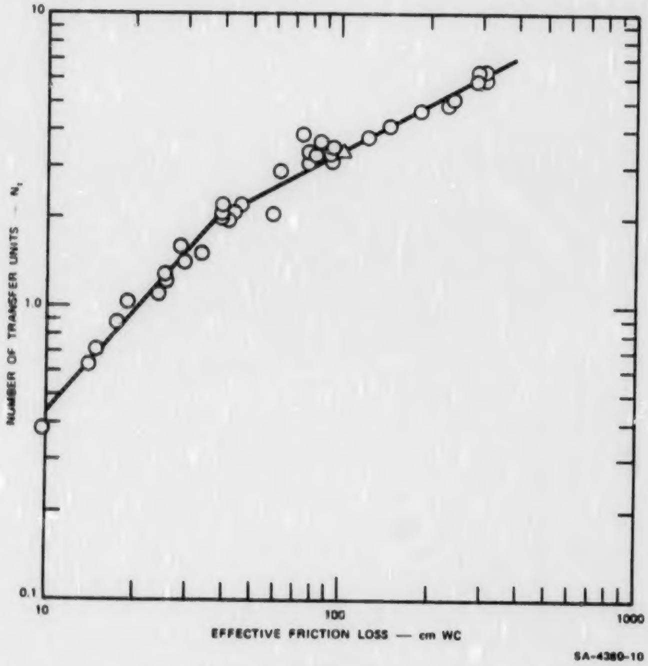

Figure 5 Orifice scrubber performance curve for aerosol D

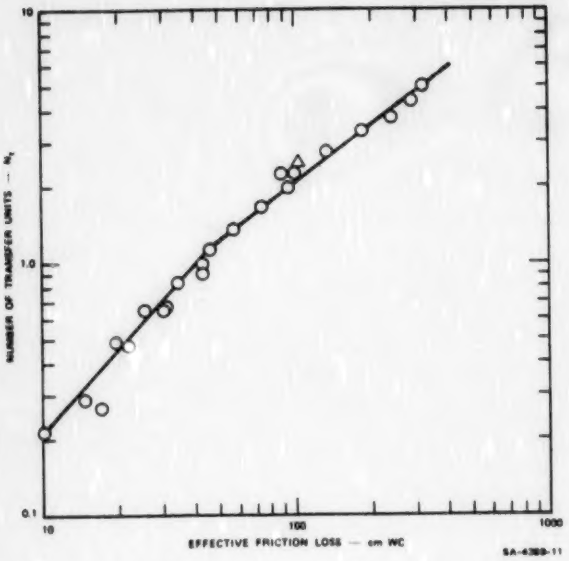

Figure 6 Orifice scrubber performance curve for aerosol E

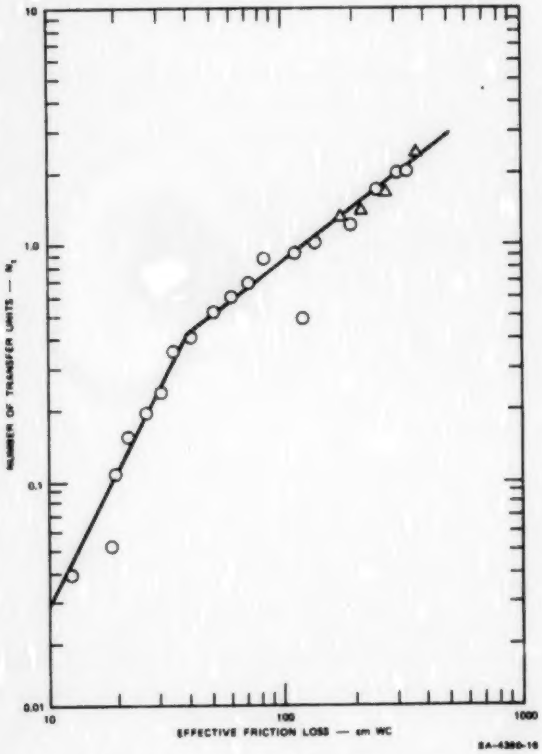

Figure 7 Orifice scrubber performance curve for aerosol G

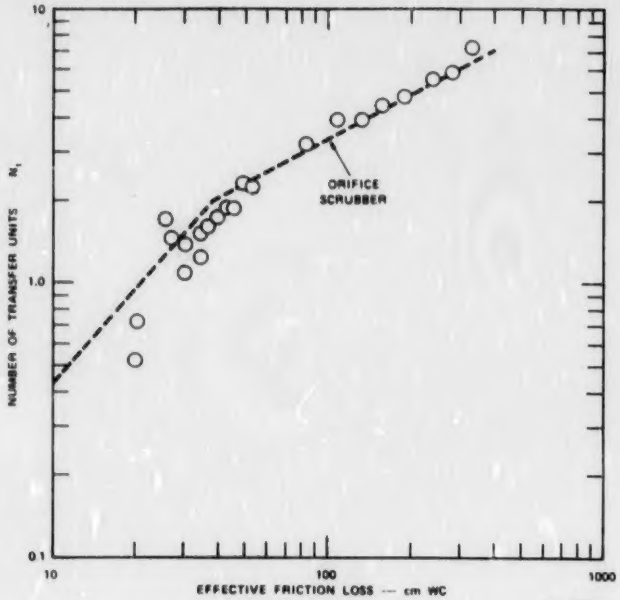

SA-4380-17

Figure 8 Multiple-orifice series scrubber performance on aerosol D

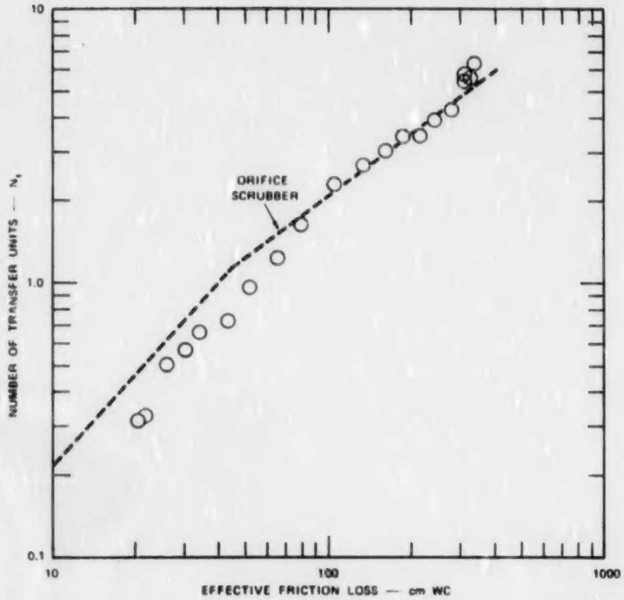

SA-4380-18

Figure 9 Multiple-orifice series scrubber performance on aerosol E

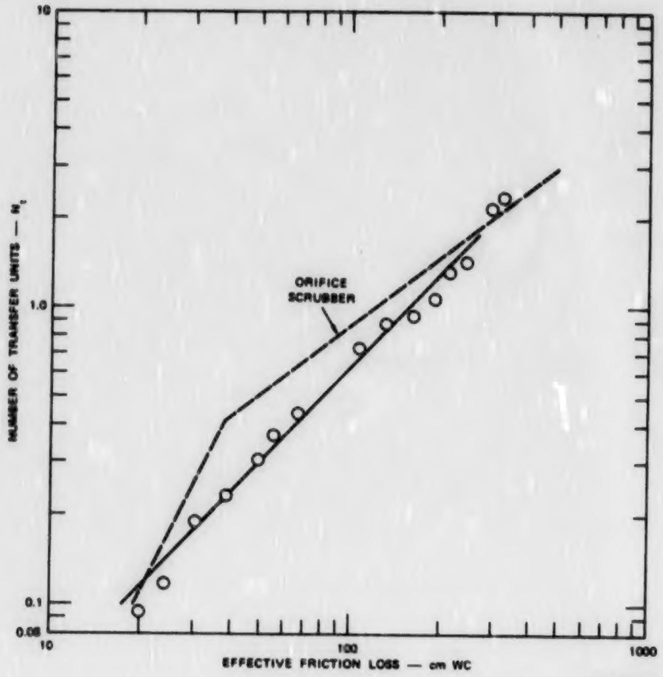

SA-4380-20

Figure 10 Multiple-orifice series scrubber performance on aerosol G

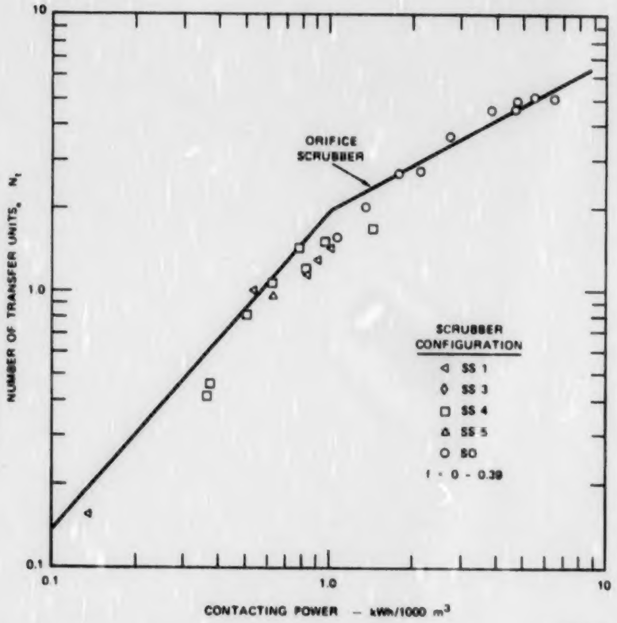

SA-4380-33

Figure 11 Performance of spray scrubbers on aerosol D at values of f = 0 - 0.39

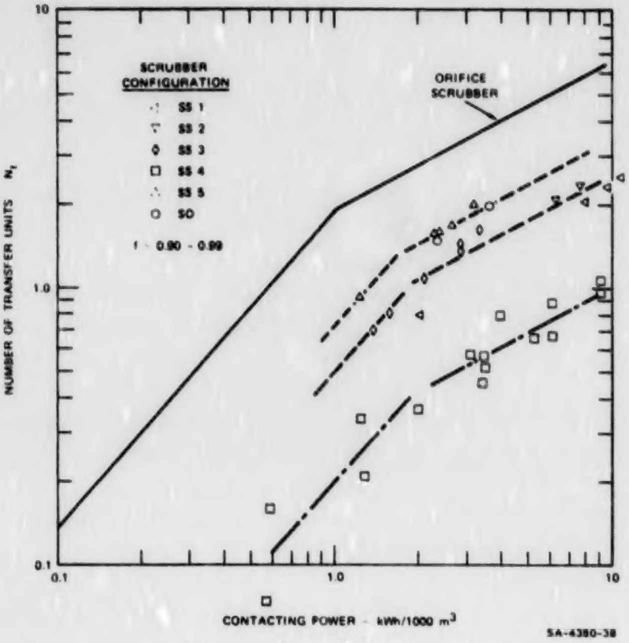

Figure 12 Performance of spray scrubbers on aerosol D at values of f = 0.90 - 0.99

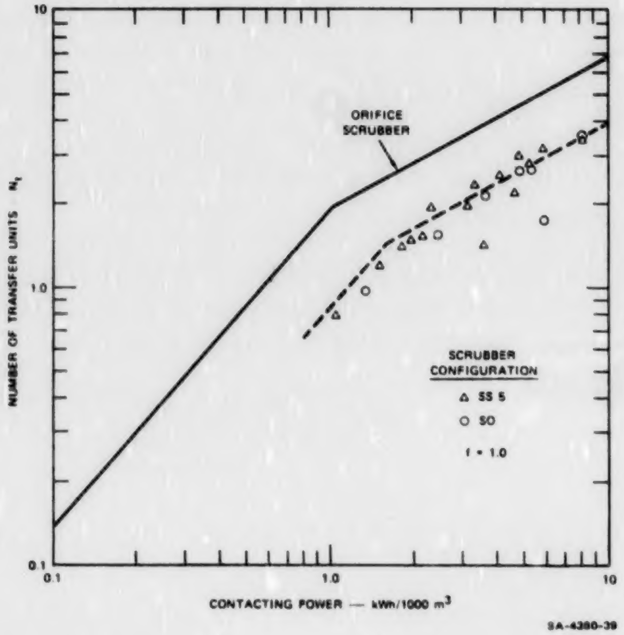

Figure 13 Performance of spray scrubbers of ejector configuration of aerosol D

References

1. C. E. Lapple and H. J. Kamack, "Performance of wet dust scrubbers," *Chem. Eng. Progr*. **51** (3):110 (1955).

2. K. T. Semrau, C. W. Marynowski, K. E. Lunde, and C. E. Lapple, "Influence of power input on efficiency of dust scrubbers," *Ind. Eng. Chem.* **50** (11):1615 (1958).

3. K. T. Semrau, "Correlation of dust scrubber efficiency," *J. Air Pollut. Contr. Assn.* **10** (3):200 (June 1960).

4. K. T. Semrau, "Dust scrubber design--a critique on the state of the art," *J. Air Pollut. Contr. Assn.* **13** (12):587 (1963).

5. K. T. Semrau and C. L. Witham, "Wet scrubber liquid utilization," EPA-650/2-74-108, U.S. Environmental Protection Agency, Washington, D.C. (October 1974).

6. A. B. Walker, "Enhanced scrubbing of black liquor boiler fume by electrostatic preagglomeration: A pilot plant study," *J. Air Pollut. Contr. Assn.* **13** (12):622 (December 1963).

7. A. B. Walker and R. M. Hall, "Operating experience with a flooded-disc scrubber--a new variable throat orifice contactor," *J. Air Pollut. Contr. Assn.* **18** (5):319 (May 1968).

8. K. T. Semrau, C. L. Witham, and W. W. Kerlin, "Energy utilization by wet scrubbers," Final report, Contract No. 68-02-2103, U.S. Environmental Protection Agency, Washington, D.C. (Draft in review, March 1977).

DIFFUSIOPHORETIC PARTICLE COLLECTION UNDER TURBULENT CONDITIONS

Peter J. Whitmore and Axel Meisen
Department of Chemical Engineering
The University of British Columbia
Vancouver, B.C., Canada V6T 1W5.

ABSTRACT

Diffusiophoresis, which is the movement of aerosol particles induced by diffusing gases, was studied under conditions of turbulent flow. A novel theory for diffusiophoretic particle removal is presented which depends solely on the non-steady-state forms of the continuity equations for the particles and gas mixture. It is therefore independent of equipment geometry and patterns of mass transfer or gas flow. Collection efficiencies are predicted for particles moving with the Schmitt and Waldmann velocity (or small particle velocity) as well as the local mean mass and local mean molar velocities of the gas mixture. It is shown that, in the latter two cases, the particle collection efficiency equals the fractional mass and molar removal of gas, respectively.

Experimental studies were performed by passing a binary gas mixture containing aerosol particles up through a wetted wall column (0.0254 m I.D. and 0.77 m in length), countercurrent to a flow of water. One component was inert, while the other was partially absorbed. The resulting particle removal was determined by measuring the inlet and outlet aerosol number concentrations in the gas. The soluble gases tested were ammonia and trimethylamine, while the insoluble gases were helium, methane, nitrogen, argon and freon 12 (dichlorodifluoromethane). Uniform latex particles of 0.50, 0.79, 1.011, 2.02, and 5.7 microns in diameter were used. The experimental results were in satisfactory agreement with theoretical predictions.

DIFFUSIOPHORETIC PARTICLE COLLECTION UNDER TURBULENT CONDITIONS

INTRODUCTION

Small particles suspended in diffusing fluid mixtures experience a force and move in a preferred direction. Although this phenomenon, called diffusiophoresis, was first reported by Aitken (1) last century it did not receive much attention until recently. The diffusiophoretic velocity was found to be almost independent of particle size, which is in marked contrast to Brownian diffusion and inertial deposition; diffusiophoresis can therefore provide a useful technique for separating micron-size particles from gases[†]. One simple way of achieving particle collection by diffusiophoresis is to add a gaseous component to a particle bearing gas and then remove the component in an absorber. Transfer of the gaseous component causes the simultaneous deposition of particles by diffusiophoresis in the absorption medium. If the gaseous component is a vapour, such as steam, and its removal is effected by condensation, the particle collection can also be enhanced by thermophoresis and particle growth (3, 4). All of these effects usually occur in conjunction with Brownian motion and inertial deposition.

The diffusiophoretic velocity depends on whether the particles are "small", "similar" or "large" compared with the mean free path of the surrounding molecules. The corresponding particles are usually classified as belonging to the "free molecule", "transition" and "continuum regimes". Basic theories describing diffusiophoresis in gases at rest have been extensively reviewed elsewhere (5-7) and need not be repeated here.

A model for diffusiophoretic removal of particles from turbulent gases was first proposed by us (8) and a similar, but less accurate, model was later published by Azarniouch et al. (9). A brief critique of the latter paper as well as an extension of our original work to diffusio- and thermophoretic collection of particles of all sizes will appear shortly (2). Our model was based on the assumption that mass and particle transfer take place from a turbulent fluid core across a laminar film adjacent to the transfer surface. This approach is not quite correct since disturbances from the turbulent core prevent the establishment of a laminar, steady-state film. In spite of this shortcoming the film model was expected to yield good approximations since it has proven to be very successful in classical heat and mass transfer studies. Although attempts have been made to predict diffusiophoretic particle removal from laminar gas streams (eg., by Meisen et al. (10)), no general models have so far been developed.

[†] Diffusiophoresis also occurs in liquid systems but very little is presently known about it (2).

The theory which we present in this paper is of a different genre from all previous ones. It is based on the particle and fluid continuity equations, written in special forms, and it does not depend on the assumption of a laminar, steady-state film.

The efficacy of diffusiophoresis for removing micron-size particles from gas streams in laminar flow was demonstrated experimentally by Schmitt (11), Goldsmith and May (12), Stinchcombe and Goldsmith (13), and Meisen et al. (10). In order to minimize equipment size (or cost), industrial applications usually require that particle collectors operate under turbulent conditions. The first experimental study of diffusiophoresis under turbulent conditions was performed by Whitmore and Meisen (7) who dealt with the removal of 0.79 μm latex particles from nitrogen-ammonia mixtures in a wetted wall column. Water was used as the absorption medium. The results gave satisfactory agreement with the predictions of the film theory derived for the case where the particles adopt the local mean mass velocity of the gas mixture. The experiments were later repeated in more detail using improved techniques (2) but the results were essentially the same.

Azarniouch et al.(9) have also published data on diffusiophoresis under turbulent conditions. However, since diffusiophoresis was not the only, and in many cases not even the dominant, mechanism for particle removal, their results are hard to interpret. Similar difficulties arise with the papers of Calvert et al.(3, 4) who studied diffusiophoresis in the presence of condensation effects which led to particle enlargement.

THEORY

We consider the situation where a particle-bearing gas mixture† is passed through a device which removes at least one of the mixture components partially or completely by contact with a separate phase. This process is accompanied by particle transport towards the interface which arises from bulk fluid flow as well as diffusiophoretic particle motion relative to the bulk flow. (The existence of bulk flow towards the interface is most obvious in the case of a single component, absorbable gas). The present theory is applicable to situations with and without bulk flow towards the interface and the following main assumptions are made:

---

† Our theory also holds for suspensions of particles in liquids, and might have application in problems such as particle transfer during liquid-liquid extraction.

1. Particles move relative to the surrounding gas mixture only by diffusiophoresis.
2. The volume fraction of particles in the gas mixture is small.
3. Particles which reach the interface are not re-entrained.

The first assumption excludes the possibility of significant particle collection by Brownian motion, inertial mechanisms as other effects. The second assumption is needed since the particle and fluid continuity equations, on which our theory is based, are only valid for systems with low particle concentrations. Many industrial aerosols fall into this category.

The particle continuity equation may be written as

$$\frac{\partial n}{\partial t} + \underline{\nabla} \cdot n \, \underline{v}_p = 0 \qquad (1)$$

where n is the particle number concentration, t is time and $\underline{v}_p$ is the particle velocity due to diffusiophoresis as well as bulk fluid flow. The general continuity equation for the fluid is given by

$$\frac{\partial c'}{\partial t} + \underline{\nabla} \cdot c' \, \underline{v}' = 0 \qquad (2)$$

where c' denotes the fluid concentration expressed in some units (as yet unspecified) and $\underline{v}'$ is the appropriate related fluid velocity.

Equations (1) and (2) are quite similar and they may be combined by *choosing* a fluid velocity, $\underline{v}'$, which is identical to the particle velocity, $\underline{v}_p$. This is, however, only possible if an appropriate fluid concentration, c', exists. Assuming this to be the case gives

$$\frac{\partial(n/c')}{\partial t} + \underline{v}' \bullet \underline{\nabla} \; (n/c') = 0 \tag{3}$$

for $c' \neq 0$. Equation (3) can be written as

$$\frac{D(n/c')}{Dt} = 0 \tag{4}$$

where

$$\frac{D}{Dt} = \frac{\partial}{\partial t} + \underline{v}' \bullet \underline{\nabla} \tag{5}$$

The quantity D/Dt denotes the time derivative for an element following the fluid as it moves with velocity $\underline{v}'$. When $\underline{v}'$ is the mean mass velocity, $\underline{v}$, equation (6) defines the well-known substantive derivative. It follows from equation (4) that n/c', the number of particles per unit of fluid, is constant along the path of the element.

The particle collection efficiency for an arbitrary piece of equipment operating at steady-state is defined in the usual way.

$$\varepsilon_p = [\int_{A_{in}} n \; v' \; dA - \int_{A_{out}} n \; v' \; dA] \; / \; \int_{A_{in}} n \; v' \; dA \tag{6}$$

where A_{in} and A_{out} denote the inlet and outlet cross-sectional areas, respectively

The component of $\underline{v}'$ perpendicular to the elemental area dA is represented by v'. Similarly, the fraction of fluid removed (in appropriate units) is given by

$$\varepsilon_f = [\int_{A_{in}} c'\, v'\, dA - \int_{A_{out}} c'\, v'\, dA] / \int_{A_{in}} c'\, v'\, dA \qquad (7)$$

Since we are now dealing with steady-state conditions, the variables on the right hand side of equations (6) and (7) must be interpreted as time-averaged rather than instantaneous values.

If n/c' is constant throughout the inlet fluid, i.e. the entering gas is well mixed, then n/c' must also be constant everywhere in the equipment. It follows immediately that

$$\varepsilon_p = \varepsilon_f \qquad (8)$$

Thus, *when the inlet fluid is well mixed*, the fractional particle collection equals the fraction of incoming fluid removed, measured in the appropriate units. This is the primary result of our theory.

In many practical situations, one component of the fluid is essentially inert, and passes through the equipment unchanged. In this case the previous result can be readily expressed in terms of inlet and outlet fluid concentrations. Rewriting the expression for particle removal efficiency by using appropriate average values of c' and v' for the terminal conditions, yields

$$\varepsilon_p = 1 - [c'\, v'\, A]_{out} / [c'\, v'\, A]_{in} \qquad (9)$$

Also, if component 1 is inert, it follows that

$$[\ c_1' \ v' \ A]_{in} = [c_1' \ v' \ A]_{out} \tag{10}$$

where c_1' is the concentration of component 1 in the mixture. Substitution of equation (10) into (9) gives :

$$\varepsilon_p = 1 - [\ c'/c_1']_{out} \ / \ [\ c'/c_1']_{in} \tag{11}$$

We can now obtain specific results for various particle velocity expressions. Four different cases will be considered.

1. *Large Particles Adopting the Fluid Mean Mass Velocity*

As discussed previously, we consider this to be the most likely velocity adopted by large particles, i.e. particles falling into the continuum regime. (This is also the probable result for particles in liquids). Equations (1) and (2) can be combined by putting

$$\underline{v}_p = \underline{v}' = \underline{v}',$$

$$c' = \rho \text{ and } c_1' = \rho_1$$

where ρ_1 denotes the mass of component 1 per unit volume of mixture. From equations (7) and (8) it follows that *the fraction of particles removed equals the fraction of fluid mass transferred.* If component 1 passes through the equipment unaffected, equation (11) gives

$$\varepsilon_p = 1 - \ [\rho/\rho_1]_{out} \ / \ [\rho/\rho_1]_{in} \tag{12}$$

For gas mixtures it is often more convenient to work in terms of molar units and equation (12) can be re-written as

$$\varepsilon_p = 1 - [M/\gamma_1]_{out} / [M/\gamma_1]_{in} \tag{13}$$

where the mean molecular weight is given by

$$M = \sum_{i=1}^{k} \gamma_i M_i \tag{14}$$

The mole fraction and molecular weight of component i are denoted by γ_i and M_i, respectively.

2. *Particles Adopting the Fluid Mean Molar Velocity*

Derjaguin et al. (6, 14) obtained this result theoretically for the velocity of large particles in gases. Although we have criticized their work elsewhere (7) and the agreement with experimental measurements is not very good as shown later in this paper, the mean molar velocity may nevertheless constitute a useful limiting case for the diffusiophoretic particle velocity. As before, equations (1) and (2) can be combined by putting

$$\underline{v}_p = \underline{v}^* = \underline{v}' ,$$

$$c' = c \quad \text{and} \quad c_1' = c_1$$

where $\underline{v}^*$ denotes the mean molar velocity. The molar concentration and partial molar concentration of component 1 are represented by c and c_1, respectively. Equations (7) and (8) therefore indicate that the *fractional particle removal is equal to the fraction of fluid moles transferred.* When component 1 is inert, equation (11) gives

$$\epsilon_p = 1 - [c/c_1]_{out} / [c/c_1]_{in} \tag{15}$$

or

$$\epsilon_p = 1 - [\gamma_1]_{in} / [\gamma_1]_{out} \tag{16}$$

3. *Small Particles*

Derjaguin and Bakanov (15) first derived an expression for small particles in gases by using methods of molecular mechanics. Employing similar techniques, but allowing for more complex interactions between the gas molecules and particle surface, Waldmann independently obtained a comparable equation. Later derivations by Bakanov and Derjaguin (16), Mason and Chapman (17), Derjaguin and Yalamov (6) and Annis et al.(18) suggested the presence of small second-order terms and other minor changes in Waldmann's expression. However, none of these modifications affect the particle velocity significantly in most practical situations.

Although previous workers mainly considered diffusiophoresis in binary gases, the general velocity expression for systems consisting of k components can be deduced:

$$\underline{v}_p = \sum_{i=1}^{k} a_i \sqrt{M_i}\ \underline{N}_i \Big/ c \sum_{i=1}^{k} a_i \sqrt{M_i}\ \gamma_i \tag{17}$$

where $\underline{N}_i$ denotes the molar flux of component i and a_i is a coefficient depending on the interaction between component i and the particle surface.

There is no standard form of the fluid continuity equation written in terms of this velocity but such an equation can be constructed. In order to do this we define a new unit of concentration which may be called the "root mass concentration".

$$c_i^r = a_i \sqrt{M_i}\, c_i \tag{18}$$

Other related variables can then be defined to form a compatible system

$$\underline{N}_i^r = a_i \sqrt{M_i}\, \underline{N}_i \tag{19a}$$

$$c^r = \sum_{i=1}^{k} c_i^r \tag{19b}$$

$$\underline{v}^r = \sum_{i=1}^{k} \underline{N}_i^r \Big/ c^r = \sum_{i=1}^{k} a_i \sqrt{M_i}\, \underline{N}_i \Big/ c \sum_{i=1}^{k} a_i \sqrt{M_i}\, \gamma_i \tag{20}$$

The velocities given by equations (17) and (20) are now identical. The fluid continuity equation in terms of root mass units can be derived from the standard continuity equation for component i:

$$\frac{\partial c_i}{\partial t} + \underline{\nabla} \cdot \underline{N}_i = 0 \tag{21}$$

Multiplying this equation by $a_i \sqrt{M_i}$ and summing over all component yields

$$\frac{\partial}{\partial t} \sum_{i=1}^{k} a_i \sqrt{M_i}\, c_i + \underline{\nabla} \cdot \sum_{i=1}^{k} a_i \sqrt{M_i}\, \underline{N}_i = 0 \tag{22}$$

or, upon using the definitions (18) to (20),

$$\frac{\partial c^r}{\partial t} + \underline{\nabla} \cdot c^r \underline{v}^r = 0 \tag{23}$$

By putting

$$\underline{v}_p = \underline{v}^r = \underline{v}' ,$$

$$c' = c^r \text{ and } c_i' = c_i^r$$

the conditions for equations (7) and (8) are satisfied. Hence, *the fraction of particles collected equals the fraction of root mass units of gas transferred from the fluid.* If one component in the gas mixture is inert, equation (11) becomes

$$\varepsilon_p = 1 - \left[\sum_{i=1}^{k} a_i \sqrt{M_i}\, \gamma_i / \gamma_1 \right]_{out} / \left[\sum_{i=1}^{k} a_i \sqrt{M_i}\, \gamma_i / \gamma_1 \right]_{in} \tag{24}$$

The coefficients a_i are usually of similar magnitude and can therefore be cancelled from equation (24) without great loss of accuracy. Under these conditions the particle collection efficiency falls between the mass and molar fraction of gas removed.

4. *Particles of Intermediate Size*

There is no satisfactory theoretical expression for the velocity of particles in the transition regime. However, some experimental evidence suggests that the velocity falls between that for small and large particles(5). The following approximation therefore suggests itself for the transition regime

$$\underline{v}_{p,\,\mathrm{trans}} = f\;\underline{v}_{p,\,\mathrm{small}} + (1-f)\;\underline{v}_{p,\,\mathrm{large}} \tag{25}$$

where f is a constant of order 1 or smaller. Although the particle collection efficiency can be developed for this expression by the earlier film model (8), we are unable to make the same derivation using the continuity equations. Indeed, the only type of expression which seems to permit the latter approach is

$$\underline{v}_p = \sum_{i=1}^{k} a_i\, M_i^{\alpha}\, \underline{N}_i \,/\, c \sum_{i=1}^{k} a_i\, M_i^{\alpha}\, \gamma_i \tag{26}$$

where α is an exponent probably lying between 0.5 and 1. However, equation (26) has no theoretical basis. By defining the concentration of component i as $a_i\, M_i^{\alpha}\, c_i$, it is easy to find the particle collection efficiency. If component 1 is inert, the result is

$$\epsilon_p = 1 - \Big[\sum_{i=1}^{k} a_i\, M_i^{\alpha}\, \gamma_i \,/\, \gamma_1 \Big]_{\mathrm{out}} \,/\, \Big[\sum_{i=1}^{k} a_i\, M_i^{\alpha}\, \gamma_i/\gamma_1 \Big]_{\mathrm{in}} \tag{27}$$

EXPERIMENTAL WORK

A simplified diagram of the experimental equipment is shown in Fig. 1. The apparatus and procedure were essentially those described earlier (8).

However, the Royco Optical counter (Model 225) and sampling technique were improved to further reduce errors in particle count. These modifications are fully described by Whitmore (19).

Most of the experiments were performed with a wetted wall column 0.77 m in length and 25.4 mm in diameter. Latex particles 0.50, 0.79, 1.011, 2.02 and 5.7 μm in diameter were used and the following gas systems were investigated: helium-ammonia, methane-ammonia, nitrogen-ammonia, argon-ammonia, freon 12 (dichlorodifluoromethane) - ammonia, nitrogen-trimethylamine. Water was the absorption medium in all cases.

The Reynolds number for the gas phase ranged from 2000 to 8000 with respect to the column wall and, as in previous experiments, no particle removal by mechanisms other than diffusiophoresis could be detected. A check was also made for possible end-effects by performing some runs with a column of identical design except for its shorter length. As expected from the theory, there were no end effects.

RESULTS

The main experimental data are shown in Figs. 2 to 7. Three theoretical values for the particle removal efficiency are also given in each figure. These were calculated from the expressions developed in the Theory section and correspond to the assumptions that the particles travel respectively with the local gas mean mass velocity, the mean molar velocity, or the velocity predicted for small particles. For some gas mixtures experiments were made with particles of different sizes. In these cases (Figs. 4, 6, 7) only the average particle removal efficiency is shown for each particle size and set of experimental conditions. Where particles of just one size were used (Figs. 2, 3, 5) all results are plotted.

The experiments for each gas mixture, except helium-ammonia, were conducted with a constant flow rate of inert gas and a range of inlet flow rates of transferred gas. The former flow was chosen so that all results fell into the turbulent regime. In the helium-ammonia experiments helium useage was minimized by operating with a constant inlet flow rate of ammonia and varying the helium flow rate.

The figures show that the experimental data tend to lie within the envelope formed by the efficiency predictions of the mean mass and mean molar velocity models. Furthermore, the trend exhibited by the set of data for each specific gas system, particle size, and type of experiment, is very similar to the trends of the three theoretical predictions. Since the experiments cover such a wide range of mass transfer conditions and gas physical properties, such agreement provides strong evidence that the theory of particle deposition presented in the previous section is correct, at least as a first order approximation.

At the same time, the position of the data relative to the three models varies with both gas system and particle size, and the data as a whole do not correlate well around the predictions of any specific model. As discussed by Whitmore(19), the possible systematic errors alone *could* account for the lack of correlation with the mean mass velocity model. This does not mean, however, that the position of the data relative to the various models is without significance. It is unlikely that the variation in data position is caused primarily by systematic errors, as these would tend to nullify the observed similarity between the trends shown by each set of data and the corresponding model predictions.

The only obvious remaining explanation for the experimental results is that the particles were exhibiting transition regime behaviour. According to our theory(7) large particles move with the mean mass velocity of the fluid, while small particles travel at essentially the Schmitt and Waldmann (or small particle) velocity. The latter falls generally between the mean mass and mean molar velocities and the removal efficiencies in the transition regime should therefore lie between the same limits. Furthermore, for a given gas system and particle size, these efficiencies should show the same trend as the model predictions, when experimental conditions are systematically varied. Since the outlined behaviour is identical to that exhibited by the experimental results obtained in the present study, it is concluded that the particles generally fell within the transition regime. The Knudsen number, i.e. the ratio of the mean free path of the gas molecules to the particle radius, ranged from 0.015 to 0.30.

Previous work(5) on phoretic effects indicates that transition behaviour is to be expected for such Knudsen numbers.

The transition regime behaviour precludes definite confirmation that large particles move at the mean mass velocity. There is, however, an indication that they do, since for small Knudsen numbers the data tend to correlate around the corresponding model predictions. In contrast, only a small fraction of the data agree with the predictions of the mean molar velocity model. This suggests that the theories of Derjaguin et al. (6, 14), which predicted this velocity for large particles, may be incorrect.

Practical and cost aspects were considered by Whitmore(19) and will be published separately.

CONCLUSIONS

A new theory has been presented for predicting diffusiophoretic particle collection in mass transfer equipment operating under turbulent conditions. The theory is general and depends primarily on the particle and fluid continuity equations as well as the fundamental diffusiophoretic particle velocity. The experimental results, which agree quite well with the theoretical predictions, generally fall between the limits given by particles adopting the mean mass and mean molar velocity of the fluid. This suggests that the particles used in this study exhibited transition regime behaviour.

ACKNOWLEDGEMENTS

The financial support provided by the National Research Council of Canada, the Government of the Province of British Columbia and the University of British Columbia are gratefully acknowledged.

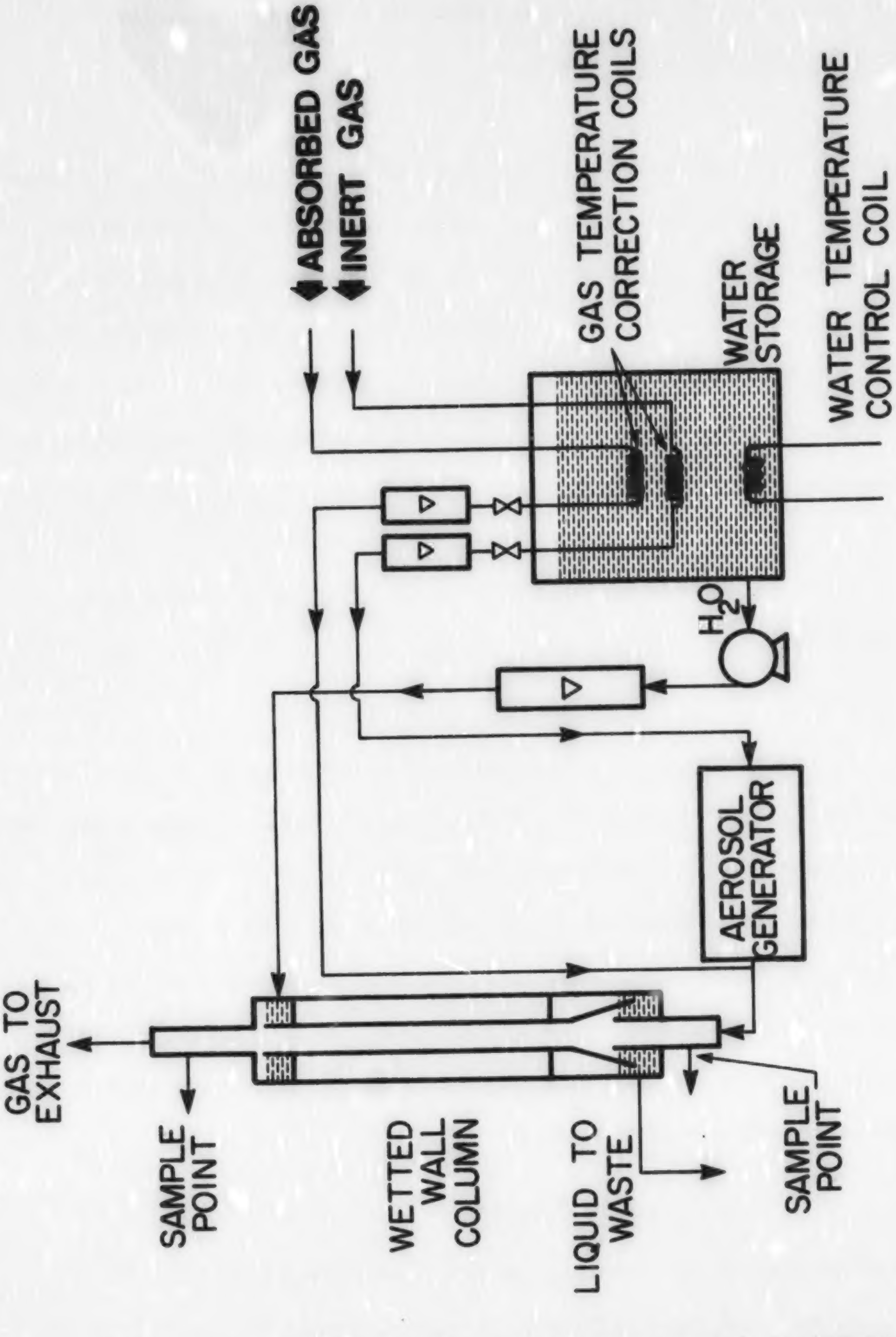
ABSORBED GAS
INERT GAS
GAS TEMPERATURE CORRECTION COILS
WATER STORAGE
WATER TEMPERATURE CONTROL COIL
H_2O
AEROSOL GENERATOR
GAS TO EXHAUST
SAMPLE POINT
WETTED WALL COLUMN
LIQUID TO WASTE
SAMPLE POINT

Figure 1. Schematic diagram of experimental equipment.

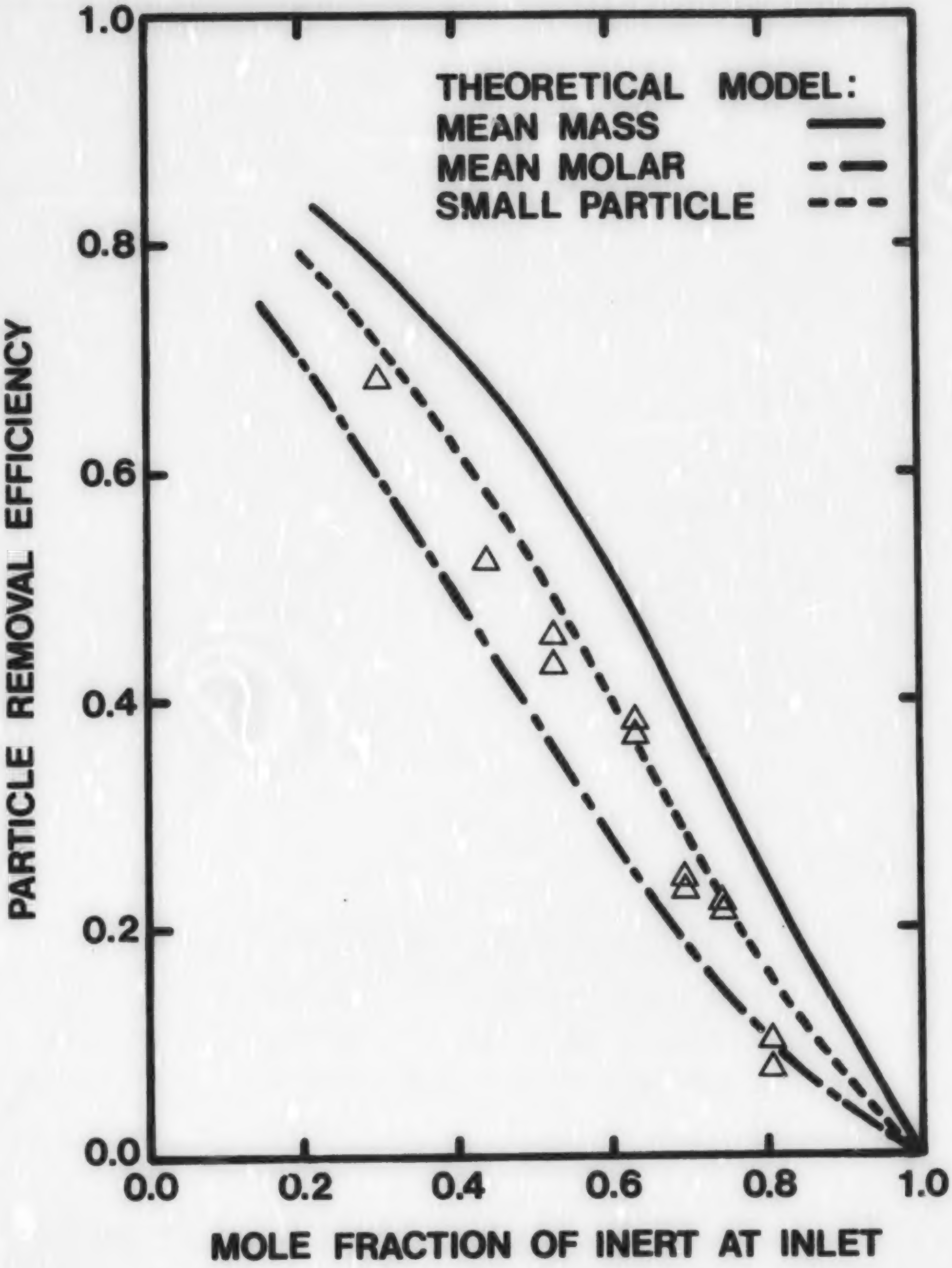

Figure 2. Results for helium-ammonia mixtures with 0.79 micron diameter particles. Inlet flow rate of ammonia held constant at $6.0 \times 10^{-4}\,m^3/sec$.

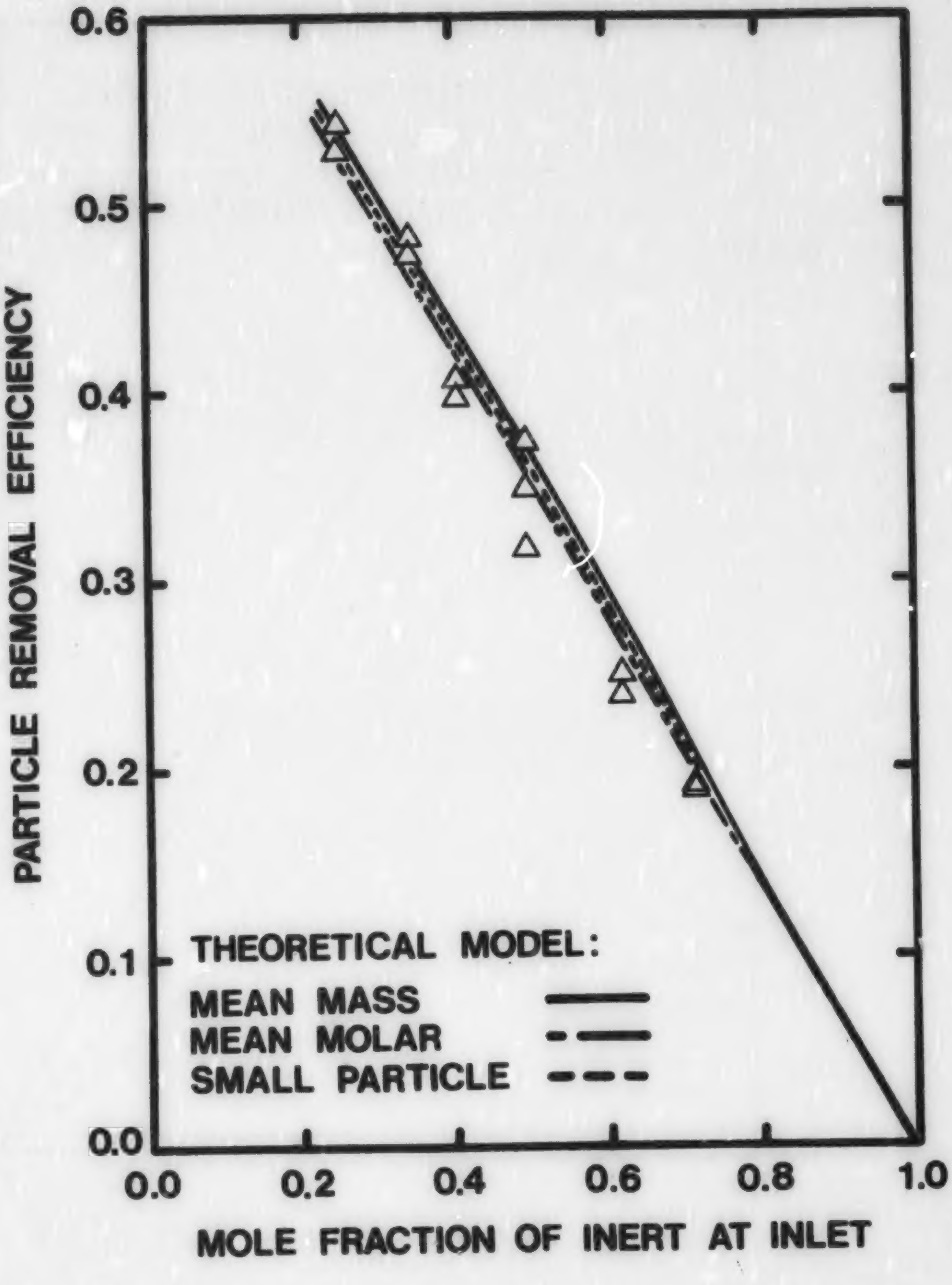

Figure 3. Results for methane-ammonia mixtures with 0.79 micron diameter particles. Flow rate of methane held constant at 5.98 x 10^{-4} m^3/sec.

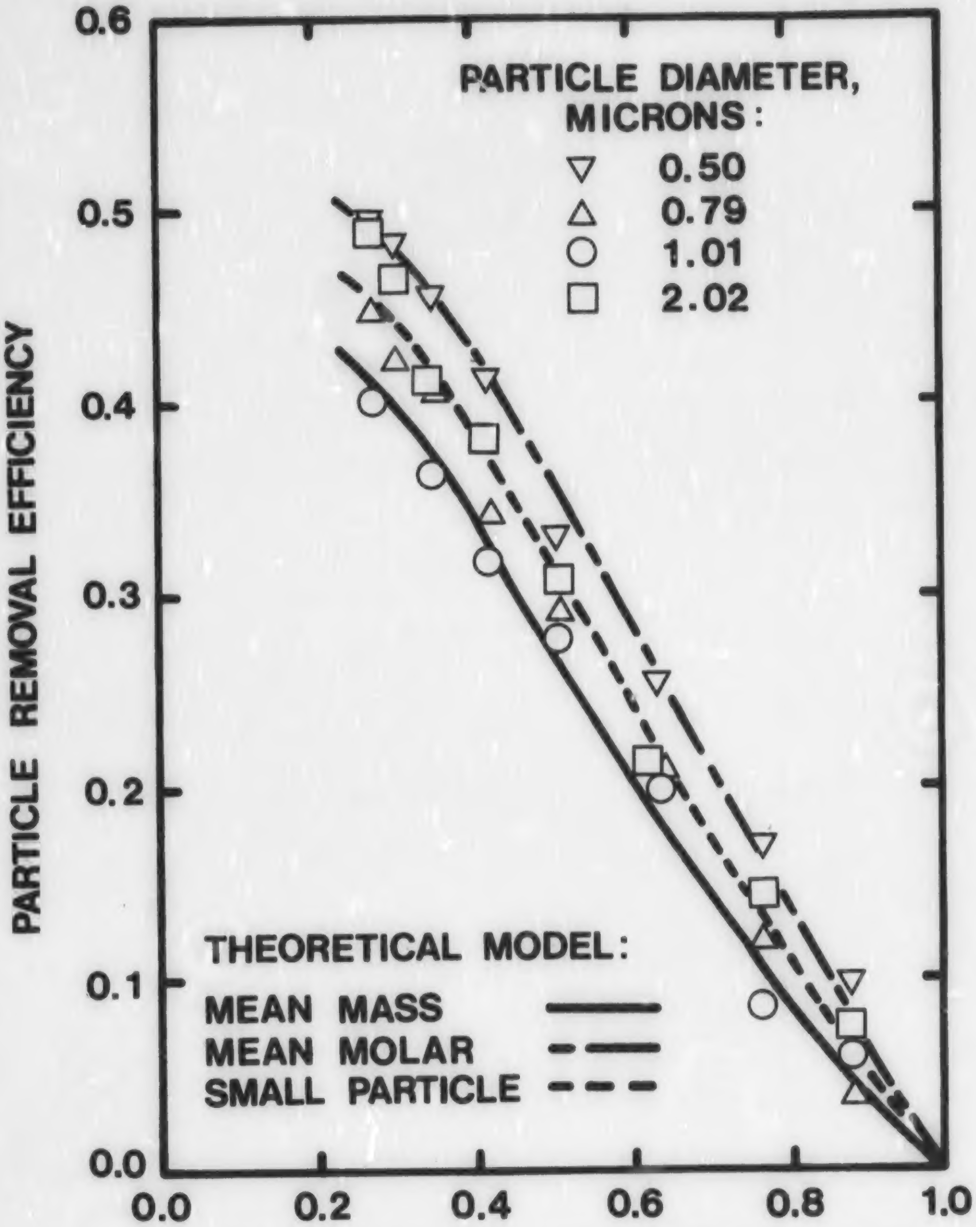

Figure 4. Results for nitrogen-ammonia mixtures with particles of various diameters. Flow rate of nitrogen held constant at 6.0×10^{-4} m^3/sec.

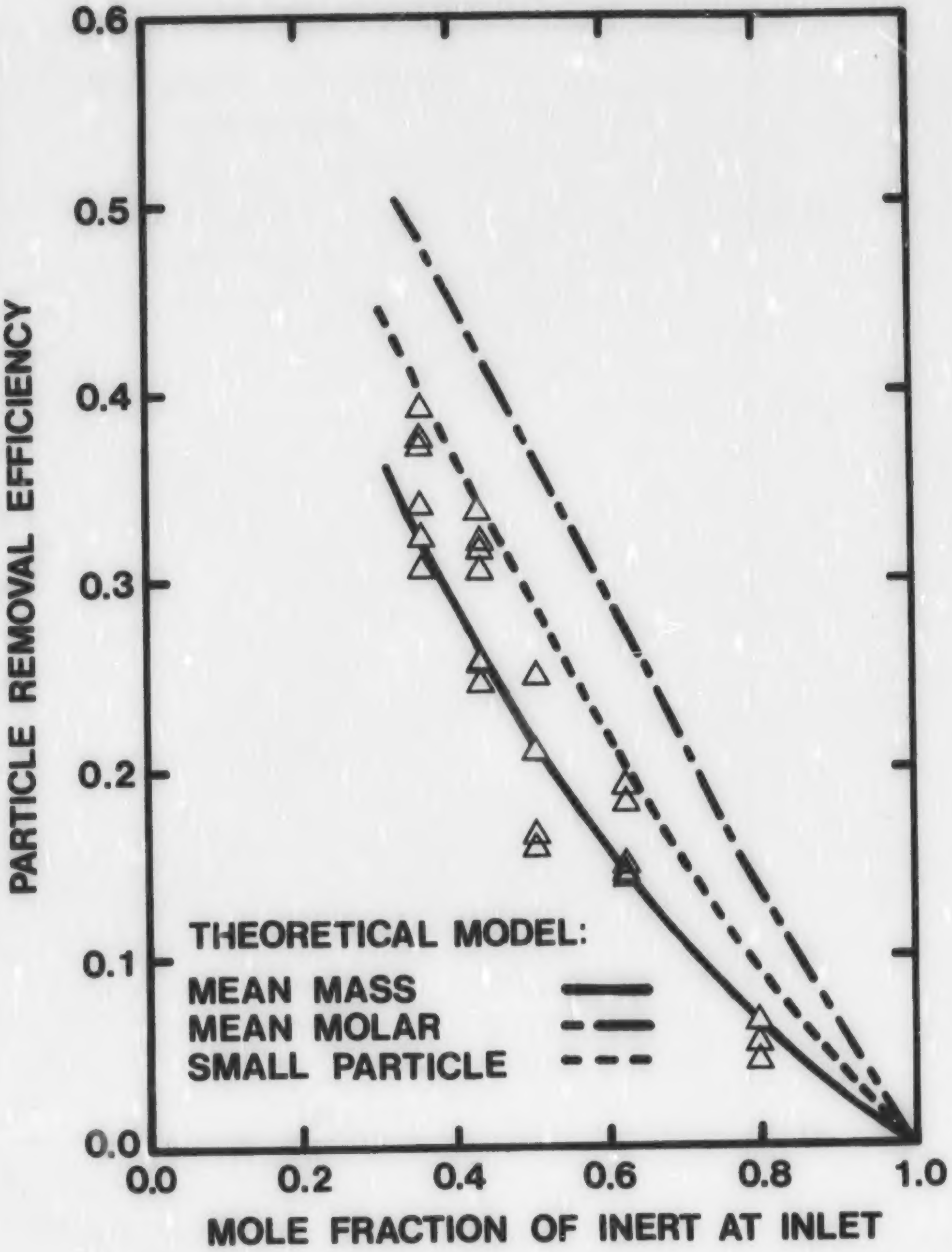

Figure 5. Results for argon-ammonia mixtures with 0.79 micron diameter particles. Flow rate of argon held constant at 5.6×10^{-4} m^3/sec.

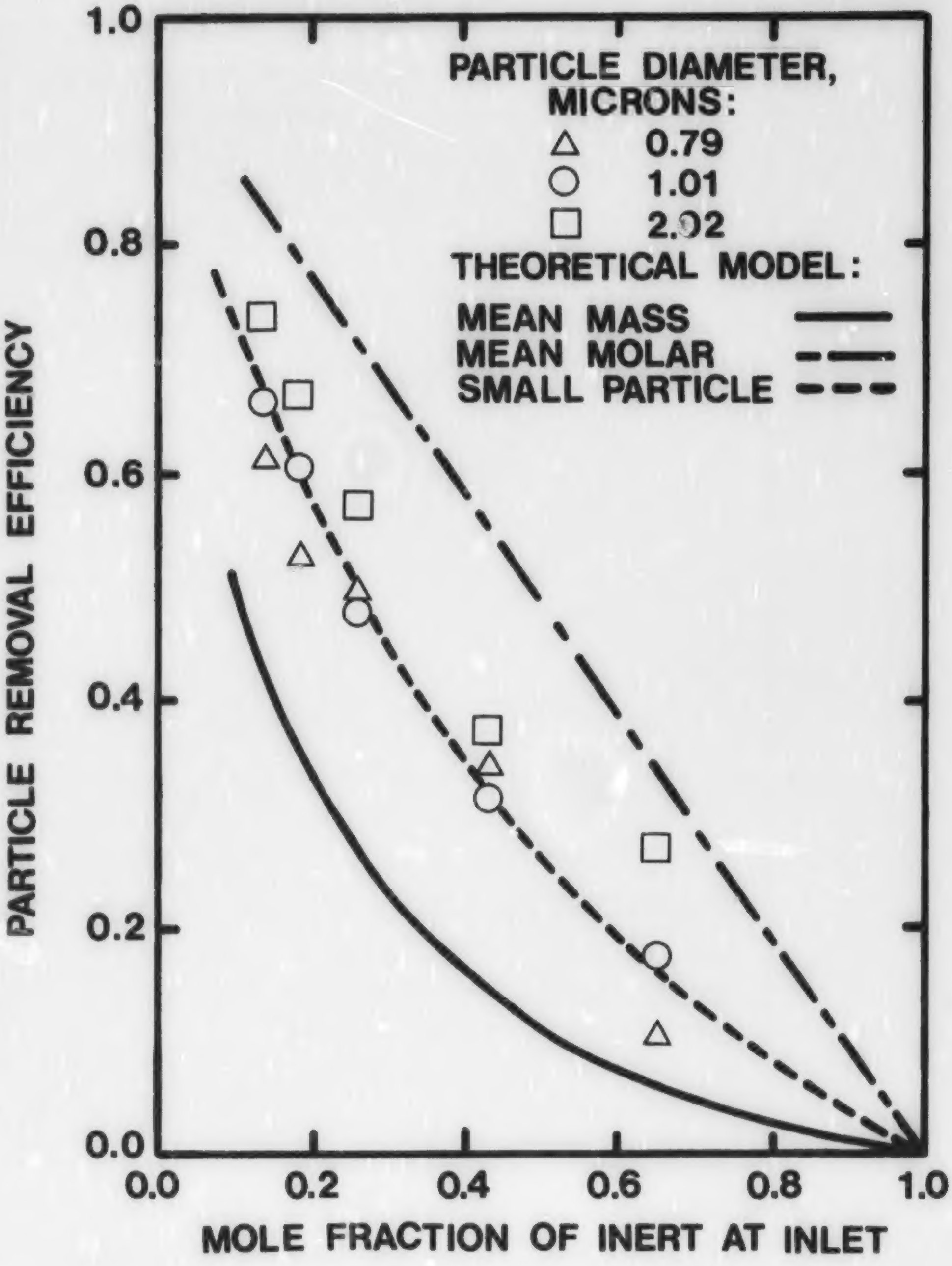

Figure 6. Results for freon 12 (dichlorodifluoromethane) - ammonia mixtures with particles of various diameters. Flow rate of freon 12 held constant at $0.98 \times 10^{-4} m^3/sec$.

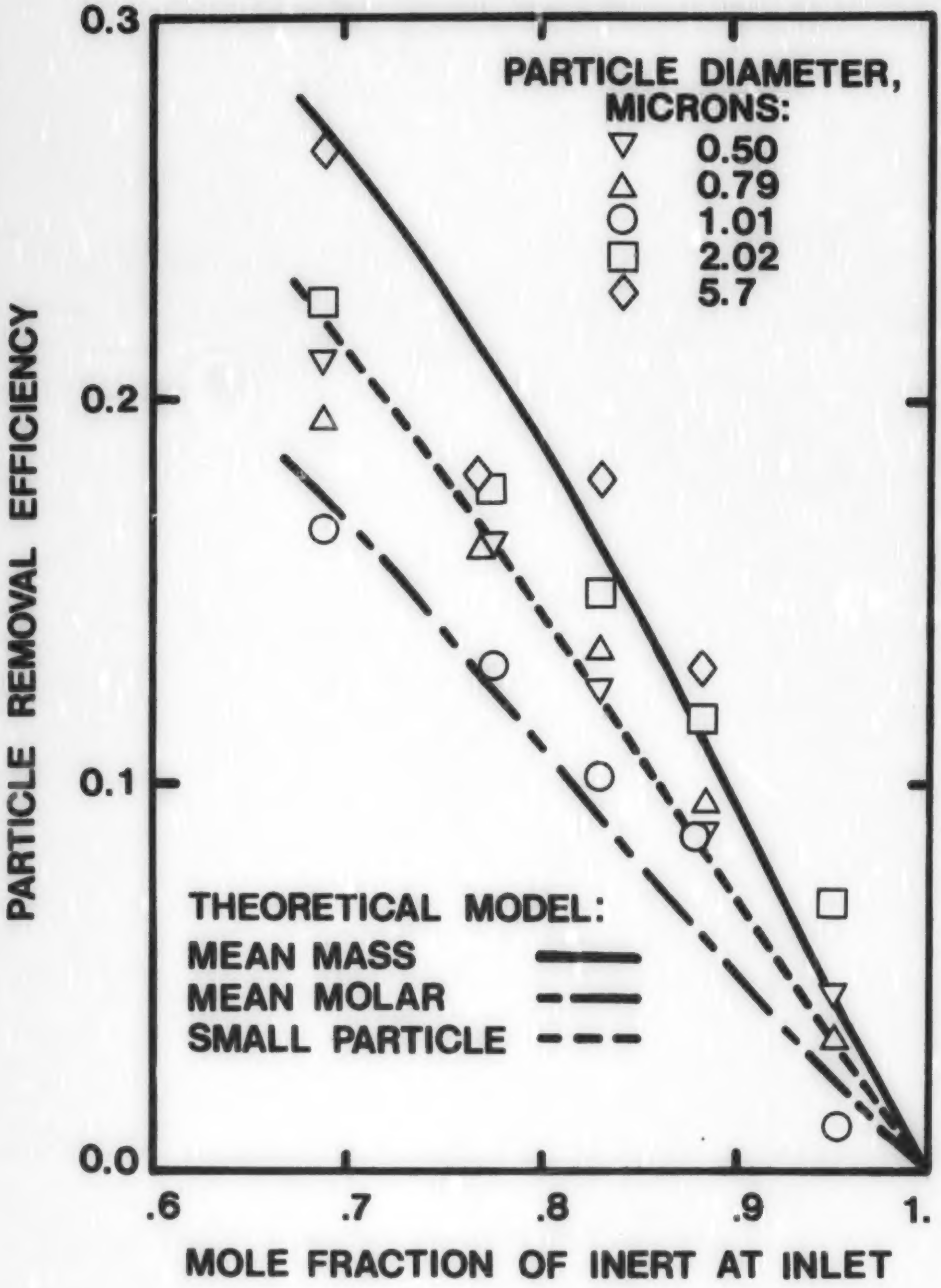

Figure 7. Results for nitrogen-trimethylamine mixtures with particles of various diameters. Flow rate of nitrogen held constant at $6.0 \times 10^{-4} m^3/sec$.

REFERENCES

1. J. Aitken, "On the Formation of Small Clear Spaces in Dusty Air". Trans. Roy. Soc. Edin., 32: 239, 1883.

2. P.J. Whitmore and A. Meisen, "Estimation of Thermo - and Diffusiophoretic Particle Deposition". To be published in Can. J. Chem. Eng.

3. S. Calvert and N.C. Jhaveri, "Flux Force/Condensation Scrubbing". J. Air Poll. Control Assoc., 24: 946, 1974.

4. S. Calvert, J. Goldshmid, D. Leith and N.C. Jhaveri, Feasibility of Flux Force/Condensation Scrubbing for Fine Particulate Collection, E.P.A. - 650/2-73-036, Oct. 1973.

5. L. Waldmann and K.H. Schmitt, "Thermophoresis and Diffusiophoresis of Aerosols" in Aerosol Science, C.N. Davies (ed), Academic Press, London, 1966, p. 137.

6. B.V. Derjaguin and Yu. I. Yalamov, "The Theory of Thermophoresis and Diffusiophoresis of Aerosol Particles and their Experimental Testing" in Topics in Current Aerosol Research (Part 2), G.M. Hidy and J.R. Brock (eds), Pergamon Press, Oxford, 1972, p. 1.

7. P.J. Whitmore and A. Meisen, "The Theory of Diffusiophoresis for Large Aerosol Particles". J. Aeros. Sci., 7: 297, 1976.

8. P.J. Whitmore and A. Meisen, "Diffusiophoresis under Turbulent Conditions". J. Aeros. Sci., 4: 435, 1973.

9. M.K. Azarniouch, E.J. Farkas, N.E. Cooke and A.J. Bobkowicz, "Removal of Micron-Size Particles from Gases by Turbulent Deposition and Diffusiophoresis". Can. J. Chem. Eng., 53: 278, 1975.

10. A. Meisen, A.J. Bobkowicz, N.E. Cooke and E.J. Farkas, "The Separation of Micron-Size Particles from Air by Diffusiophoresis". Can. J. Chem. Eng., 49: 449, 1971.

11. K.H. Schmitt, "Quantitative Untersuchungen zur Staubabscheidung in Diffundierendem Wasserdampf". Staub, 21: 173, 1961.

12. P. Goldsmith and F.G. May, "Diffusiophoresis and Thermophoresis in Water Vapour Systems" in Aerosol Science, C.N. Davies (ed), Academic Press, London, 1966, p. 163.

13. R.A. Stinchcombe and P. Goldsmith, "Removal of Iodine from the Atmosphere by Condensing Steam". J. Nucl. Eng. 20: 261, 1966.

14. B.V. Derjaguin, Yu. I. Yalamov and A.I. Storozhilova, "Diffusiophoresis of Large Aerosol Particles". J. Coll. and Interf. Sci., 22: 117, 1966.

15. B.V. Derjaguin and S.P. Bakanov, "The Theory of the Motion of Small Aerosol Particles in a Diffusion Field". Dokl. Akad. Nauk. SSSR, 117: 959, 1957.

16. S.P. Bakanov and B.V. Derjaguin, "The Motion of a Small Particle in a Non-Uniform Gas Mixture". Disc. Farad. Soc., 30: 130, 1960.

17. E.A. Mason and S. Chapman, "Motion of Small Suspended Particles in Non-uniform Gases". J. Chem. Phys., 36: 627, 1962.

18. B.K. Annis, A.P. Malinauskas and E.A. Mason, "Theory of Diffusiophoresis of Spherical Aerosol Particles and of Drag in a Gas Mixture". J. Aeros. Sci., 4: 271, 1973.

19. P.J. Whitmore, "Diffusiophoresis under Turbulent Conditions". Ph.D. thesis, Dept. of Chem. Eng., Univ. of British Columbia, Vancouver, Canada, 1976.

IMPROVED DESIGN METHOD FOR F/C SCRUBBING

Seymour Calvert
Shamim A. Gandhi

Air Pollution Technology, Inc.
San Diego, California 92117

ABSTRACT

A new design method for predicting the efficiency of a flux force/condensation (F/C) scrubber is presented. This method uses mathematical models which define the particle collection due to diffusiophoresis, the amount of particle growth due to water vapor condensation, and the collection efficiency for the grown particles. Predictions for a sieve-plate column are confirmed by pilot demonstration plant data.

IMPROVED DESIGN METHOD FOR F/C SCRUBBING

Flux force/condensation (F/C) scrubbing provides a means for the enhancement of fine particle collection efficiency through the effects of condensing water vapor. Several phenomena are simultaneously involved and a detailed mathematical model is complex. In a series of previous studies [1,2,3,4] we have developed a design method (i.e., performance prediction) based on a model which required the simultaneous solution of several differental equations. While it produced useful results, it was a time-consuming procedure, even with the aid of an electronic computer.

In the course of refining our design method we arrived at the conclusion that the flux force effects could be treated separately from the condensation effects in many scrubber situations. While the condensation-induced improvement in inertial impaction efficiency could be handled conveniently, the flux force deposition prediction remained cumbersome. Recently the senior author became aware of a concept developed by Whitmore[5] which provided the key to simplifying the prediction of the flux force effects in F/C scrubbing. By incorporating Whitmore's concept into our model we have developed a much simpler design method which is convenient to use. This revised model will be described below.

BASIC CONCEPTS - Before proceeding to the details of the mathematical model the basic concepts and outline of the approach will be discussed. If we consider a typical F/C scrubbing system, it might have the features shown in Figure 1. The gas leaving the source is hot and has a water vapor content which depends on the source process. The first step is to saturate the gas by quenching it with water. This will cause no condensation if the particles are insoluble, but will if they are soluble. There will be a diffusiophoretic force directed away from the liquid surface.

Condensation is required in order to have diffusiophoretic deposition, any growth on insoluble particles, and extensive growth on soluble particles. Contacting with cold water or a cold solid surface is done next to cause condensation. While condensation occurs there will be diffusiophoretic and thermophoretic deposition as well as some inertial impaction (and, perhaps, Brownian diffusion). The particles in the gas leaving the condenser will have grown in mass due to the layer of water they carry.

Subsequent scrubbing of the gas will result in more particle collection by inertial impaction. This will be more efficient than impaction before particle growth because of the greater inertia of the particles. There may be additional condensation, depending on water and gas temperatures, and its effects can be accounted for as discussed above.

One can apply this general outline of F/C scrubbing to a variety of scrubber types and Figure 2 shows a multi-plate F/C scrubber system. It can be seen that the gas is saturated before entering the plate column, although this is not always necessary. The first plate can serve as the saturator and partial condenser. Generally, the efficiency of heat and mass transfer is so high (say, 80%+) on a well designed plate that most of the condensation occurs on the first plate.

In subsequent plates the gas is scrubbed by inertial impaction and there will be a minor amount of additional condensation. We have shown a simple counter-current column but other variations are possible.

The mathematical model is based on the process just described for a plate-type F/C scrubber. It is outlined on the following page.

I. Saturate the gas before plate 1
  A. Particles are collected at size "d_{p_1}".
  B. No condensation occurs on the particles (they are assumed insoluble).

II. Contact on plate 1
  A. Particles are collected by impaction in the bubble formation zone, still at size "d_{p_1}".
  B. Condensation occurs and particles grow to "d_{p_2}".
  C. Diffusiophoretic deposition removes some particles from the gas in the froth layer on the plate. Thermophoresis and centrifugal deposition are neglected.

III. Contact on plate 2
  A. Particles are collected by impaction in the bubble formation zone at size "d_{p_2}".
  B. Negligible condensation occurs.

IV. Contact on subsequent plates has same characteristics as plate 2.

Although the model is somewhat idealized, it is well within the bounds of engineering accuracy and the precision of experimental measurements. One can always revise any stage of the model with a closer approximation of parameters if he wishes to examine the sensitivity of the method to parametric values. In our evaluations of the model we found that further refinements did not produce significant changes in predictions.

DIFFUSIOPHORETIC DEPOSITION

Particle deposition by diffusiophoresis was described by the following equation in our previous models [2,3,4]:

$$u_{pD} = \frac{\sqrt{M_1}\ D_G}{\left[y\sqrt{M_1} + (1-y)\sqrt{M_2}\right](1-y)} \left(\frac{dy}{dr}\right), \text{cm/s} \tag{1}$$

or,

$$u_{pD} = C_1\ D_G \left(\frac{1}{1-y}\right) \frac{dy}{dr} \tag{2}$$

where D_G = diffusivity of water vapor in carrier gas, cm^2/s
M_1 = molecular weight of water, g/mol
M_2 = molecular weight of non-transferring gas, g/mol
y = mole fraction water vapor, dimensionless
r = distance in the direction of diffusion, cm

The molecular weight and composition function represented by "C_1". describes the effect of molecular weight gradient on the deposition velocity corresponding to the net motion of the gas due to diffusion (the "sweep velocity"). For water mole fraction in air ranging from 0.1 to 0.5, "C_1", varies from 0.8 to 0.88. We used a rough average of 0.85 for "C_1", for computing "u_{pD}" and consequent particle collection efficiency by integrating over the period of condensation.

Whitmore[5] concludes that the fraction of particles removed from the gas by diffusiophoresis is equal to either the mass fraction or the mole fraction condensing, depending on what theory is used for deposition velocity. In other words, it is not necessary to follow the detailed course of the condensation process, computing instantaneous values of deposition velocity, and integrating over the entire time to compute the fraction of particles collected. One can simply observe that if some fraction of the gas is transferred to the liquid phase it will carry along its load of suspended particles.

We have used Whitmore's general concept but with two modifications. First, one can see from equation (1) that Whitmore's theory would be comparable to assuming that the particles move with the same velocity as the gas phase. We have chosen to retain the correction for molecular weight gradient, which means that we will compute the particle collection efficiency as 85% of the volume fraction of gas condensing on the cold surface.

The second modification concerns how to compute the proper value of the volume fraction of gas condensing. The problem is that not all of the condensate goes to the heat transfer surface; some of it goes to the suspended particles. As will be shown in detail later, the fraction of the condensate which causes particle growth depends on several factors and ranged from about 0.1 to 0.4 of the total condensate for the range of parameters we explored.

If one is concerned only with diffusiophoretic deposition the particle collection efficiency would, therefore, be 60% to 90% of that computed without accounting for condensation on particles. In the case of a scrubber which also employs inertial impaction the particles would be agglomerated to some extent by the diffusional sweep, so they would have higher mass and be easier to collect.

Without going into a detailed model of this phenomenon one could use either of two simplifying assumptions:

1. Assume that the condensation on particles causes no agglomeration.
2. Assume that the condensation on particles causes agglomeration and that the inertial impaction efficiency is sufficiently high that all of the particles swept to other particles will be collected by impaction.

The first assumption will lead to too low an efficiency and the second to too high an efficiency. However, the maximum difference between the two for a representative case of 25% of the volume condensing and 25% of that going to the particles would be 5.3% (i.e., 0.25 x 0.85 x 0.25 x 100). This is a relatively small effect compared to the other uncertainties.

PARTICLE GROWTH

Particle growth is dependent on how well the particles can compete with the cold surface for the condensing water. There are several transport processes at work simultaneously in the condenser section of an F/C scrubber:

1. Heat transfer
    a. From the gas to the cold surface
    b. From the particles to the gas
2. Mass transfer
    a. From the gas to the cold surface
    b. From the gas to the particles

A mathematical model which accounted for these transport processes in addition to particle deposition has been described in EPA reports [2,3,4]. The portions of that model relating to particle deposition were deleted to provide a model which would describe particle growth in the absence of deposition. The basic relationships involved are as follow:

The rate of change of particle radius is given by a mass balance,

$$\frac{dr_p}{dt} = \frac{k'_{pG} \, (p_G - p_{pi})}{\rho_M}, \text{ cm/s} \tag{3}$$

where:

$$k'_{pG} = \frac{2 \, D_G \, P}{RT_G \, d_p \, p_{BM}}$$ = particle to gas mass transfer coefficient, gmol/cm²-s-atm (4)

pG = water vapor partial pressure in bulk of gas bubble, atm

p_{BM} = mean partial pressure to non-transferring gas, atm

r_p = particle radius, cm

T_G = gas bulk temperature, °K

ρ_M = molar density of water, gmol/cm³

p_{pi} = water vapor partial pressure at vapor-liquid interface, atm

Particle temperature can be computed from an energy balance:

$$h_{pG}\,(T_{pi} - T_G) + \left(\frac{\rho_p\, C_{pp}\, r_p}{3}\right)\frac{d\,T_{pi}}{dt} = k'_{pG}\, L_M\,(P_G - p_{pi}) \tag{5}$$

where:

$$h_{pG} = \frac{2k}{d_p} = \text{particle to gas heat transfer coefficient, cal/cm}^2\text{-s-°K} \tag{6}$$

where C_{pp} = heat capacity of particle, cal/g-°K
k = thermal conductivity of gas, cal/cm²-s-°K/cm
L_M = latent heat of vaporization for water, cal/gmol
t = time, s

The overall energy balance for the gas-liquid interface is given by:

$$k'_G\;a_t\,L_M\,(p_G - p_{Li})\,A_p\,dZ =$$

$$h_L\,a_t\,(T_{Li} - T_L)\,A_p\,dZ + h_G\,a_t\,(T_{Li} - T_G)\,A_p\,dZ \tag{7}$$

where k'_G = mass transfer coefficient, gas to liquid, gmol/cm²-s-atm
a_t = interfacial area for transfer volume of scrubber, cm²/cm³
A_p = cross-sectional area of scrubber, cm²
h_G = heat transfer coefficient, gas to liquid, cal/cm²-s-°K
T_L = temperature of liquid bulk, °K

The equations given above are used along with enthalpy and material balances for the total system of gas, liquid, and suspended particles to form a mathematical model for condensation and growth. The model was solved through a finite difference method on an electronic computer for several situations which are discussed below.

PREDICTION OF CONDENSATION

The condensation model was used to predict the particle condensation ratio, f_p, (which is the fraction of the total condensate which goes to the particles) as a function of several parameters. The conditions investigated are as follow:

1. Scrubber type - one sieve plate
2. Inlet gas - saturated from 310°K to 350°K
3. Water - uniform bulk temperature from 310°K to 325°K
4. Particle number concentration - 10^7 to $10^9/cm^3$
5. Particle diameter - 0.1 to 1.0 μm
6. Liquid phase heat transfer coefficient - 0.01 to 0.1 cal/cm^2-s-°K
7. Condensation can occur when the gas is saturated

The computed values are plotted on Figures 3 through 7. As can be seen, the figures show the following:

(Figure) 3. "f_p" does not depend much on "d_p"
4. "f_p" decreases significantly with "T_L"
5. "f_p" decreases with "T_G" to an extent which depends on "T_L"
6. "f_p" increases slightly with "n_p" above $10^7/cm^3$
7. "f_p" increases with "h_L" up to "h_L" ≈ 0.1 cal/s-cm^2-°K

It was found in computations not reported here that "f_p" decreases significantly with "n_p" below about 10^6 particles/cm^3. Industrial emissions generally have particle number concentrations on the order of 10^7, and greater. The liquid phase heat transfer coefficient is an important parameter but unfortunately, predictions of its magnitude vary considerably depending on which correlation is used. The value of 0.1 appears to be the best supported by the literature for mass transfer on perforated plates.

For a combination of parameters such as might be encountered in a practical situation a value of "f_p" ≈ 0.25 appears to be reasonable. Given this one can compute the amount of particle growth that will result from a given condensation ratio (i.e., g water condensed/g dry gas = q" = condensation ratio). If the particle size distribution and the scrubber characteristics are known one can predict the overall penetration that will be achieved in the scrubber.

INERTIAL IMPACTION DURING BUBBLE FORMATION

During the formation of bubbles on a sieve plate the jets of gas emerging from the perforations impact on the liquid. Particles are thus deposited on the liquid surface by inertial impaction. Particle collection can be determined from:

$$Pt_i = \exp\left(- \frac{40\ F^2 d_p^2\ \rho_p\ C'\ u_h}{9\ \mu_G\ d_h}\right) \tag{8}$$

where F = foam density, volume fraction liquid
d_p = particle diameter, cm
ρ_p = particle density, g/cm^3
C' = Cunningham slip correction factor, dimensionless
u_h = gas velocity in the perforation, cm/s
μ_G = gas viscosity, poise
d_h = diameter of perforation, cm
Pt_i = penetration of particles of diameter d_p, fraction

PERFORMANCE PREDICTION METHOD

The sequence of steps to be followed in predicting the performance of an F/C scrubber system involving a sieve plate column is as follow:

1. Determine the initial particle size distribution.
2. Compute particle penetration from the saturator based on the saturator collection efficiency characteristics and the initial particle size distribution. No growth occurs in the saturator.
3. Compute particle penetration due to inertial impaction during bubble formation on the first plate. Use the particle size distribution leaving the saturator and the collection efficiency relationship for sieve plate given in equation (8).
4. Calculate the condensation ratio corresponding to the scrubber operating conditions, from this compute "f_v", the volume fraction of gas condensing, and then calculate the penetration due to diffusiophoresis according to equation (9)

for a conservative estimate or equation (10) for an optimistic estimate

$$1 - Pt_D = 0.85\ (f_v)\ (1-f_p) \tag{9}$$

$$1 - Pt_D = 0.85\ f_v \tag{10}$$

The diffusiophoretic penetration applies equally to all particle sizes so it will not change the size distribution but will decrease the particle concentration.

5. Determine the particle size distribution leaving the condenser from the values of "q'" and "f_p". Figure 8 is a size distribution plot showing lines for the particles before and after condensation. The conditions used for this plot were:

Initial d_{pg} = 0.75 µmA = dry mass median diameter
σ_g = 2.5 = geometric std. deviation
n_p = 10^9/DNcm^3 (Dry Normal cm^3, @ 0°C)
q' = 0.3 g/g
f_p = 0.25

6. Compute the particle penetration function for the remaining stages of the scrubber, based on the penetration for one stage given by equation (8). The penetration for a given particle diameter on one stage is "Pt_i". For "N" stages of equal efficiency the penetration for a given particle diameter is "Pt_i^N".

7. Use the relationship between "Pt_i^N" and "d_p" from step 5 and the grown size distribution from step 5 to compute the overall penetration due to inertial impaction after growth.

8. To summarize, the total overall penetration for the F/C scrubber $\overline{Pt}$ will be the product of the following:

a. "$\overline{Pt}_a$" due to impaction in the saturator
b. "$\overline{Pt}_b$" due to impaction in the condenser
c. "$\overline{Pt}_c$" due to diffusiophoresis in the condenser
d. "$\overline{Pt}_d$" due to impaction in stages after the condenser.

Thus,

$$\overline{Pt} = \overline{Pt}_a \times \overline{Pt}_b \times \overline{Pt}_c \times \overline{Pt}_d \tag{11}$$

COMPARISON WITH DATA

Predictions based on the model described above were made for a number of experimental determinations on a 100 m^3/min sieve plate F/C scrubber. Some examples of comparisons of predictions with experimental results are shown in Figures 9 and 10. The correlation shown in Figure 9 is the best obtained and that in Figure 10 is representative of the average case.

CONCLUSIONS

The revised model is much simpler to use than our previous version and it appears to give very good predictions. It also offers the opportunity for easy modification to suit specific situations. The fraction condensing on the particles is a key quantity and it needs more study for plates and other contacting systems.

REFERENCES

1. Calvert, S., J. Goldshmid, D. Leith, and D. Mehta. Scrubber Handbook. A.P.T., Inc., EPA Contract No. CPA-70-95. NTIS No. PB 213-016. August, 1972.

2. Calvert, S., J. Goldshmid, D. Leith, and N. Jhaveri. Feasibility of Flux Force/Condensation Scrubbing for Fine Particulate Collection. A.P.T., Inc., EPA Contract No. 68-02-0256, NTIS No. PB 227-307. October, 1973.

3. Calvert, S., and N. Jhaveri, and T. Husking. Study of Flux Force/Condensation Scrubbing of Fine Particles. A.P.T., Inc., EPA Contract No. 68-02-1082. August, 1975.

4. Calvert, S., and S. Yung. Study of Horizontal Spray Flux Force/Condensation Scrubber. A.P.T., Inc., EPA Contract No. 68-02-1328, Task No. 10. July, 1976.

5. Whitmore, P.J. Diffusiophoretic Under Turbulent Conditions, Ph.D. Thesis, University of British Columbia, 1976.

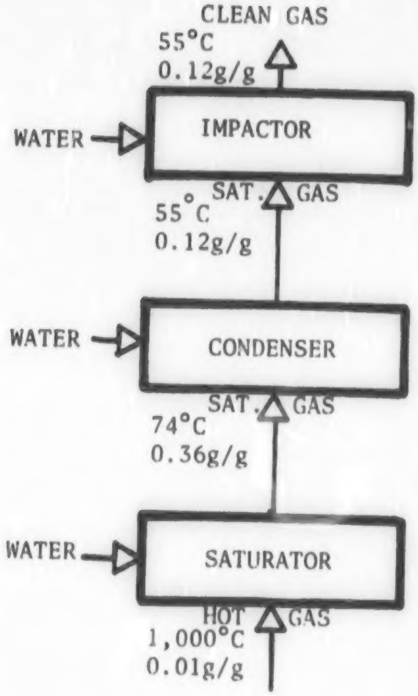
CLEAN GAS
55°C
0.12g/g
WATER
IMPACTOR
SAT. GAS
55°C
0.12g/g
WATER
CONDENSER
SAT. GAS
74°C
0.36g/g
WATER
SATURATOR
HOT GAS
1,000°C
0.01g/g

Figure 1. Generalized F/C Scrubber System.

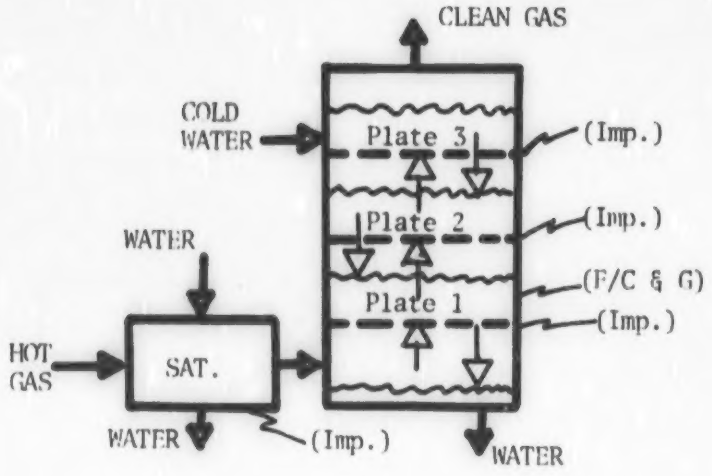
CLEAN GAS
COLD WATER
Plate 3
(Imp.)
Plate 2
(Imp.)
WATER
(F/C & G)
Plate 1
(Imp.)
HOT GAS
SAT.
WATER
(Imp.)
WATER

Figure 2. Multiple plate F/C scrubber system.

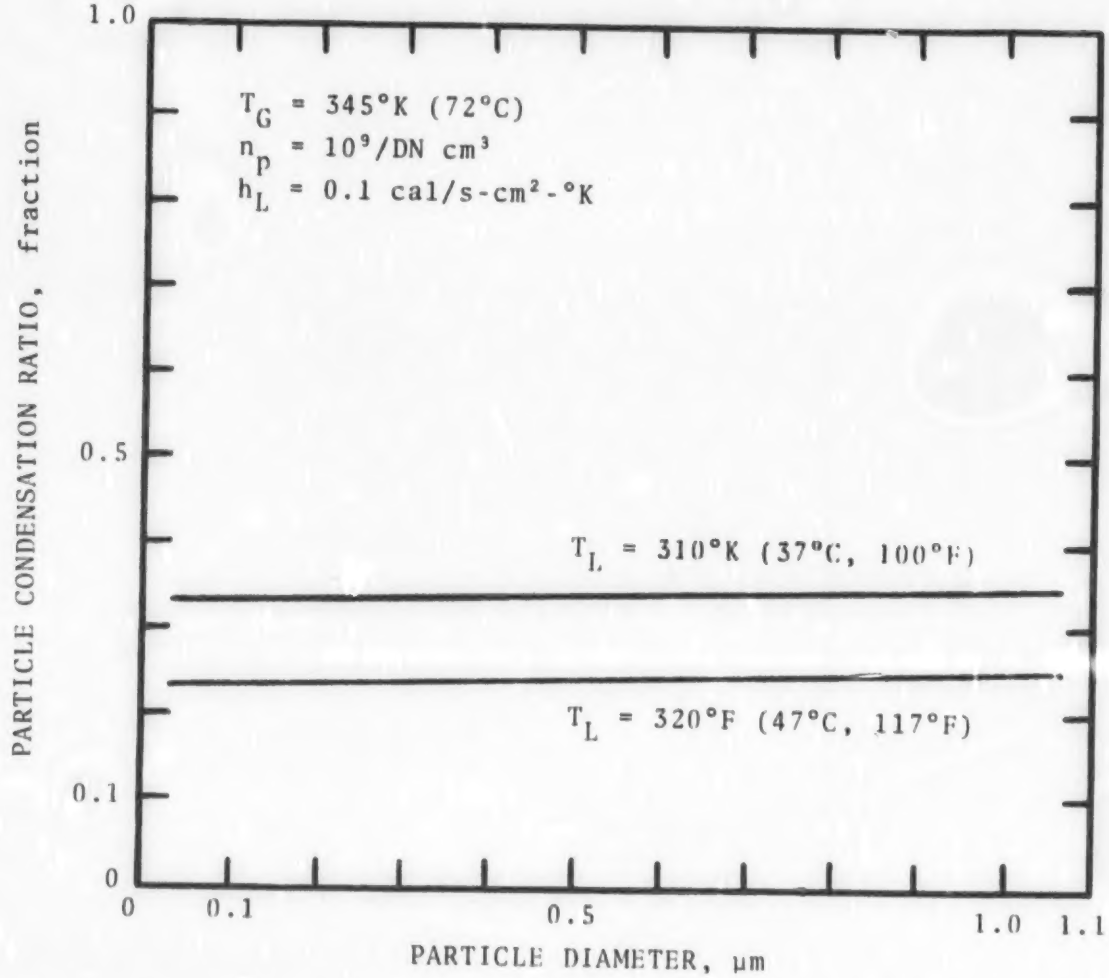

Figure 3. Effect of particle diameter on condensation ratio.

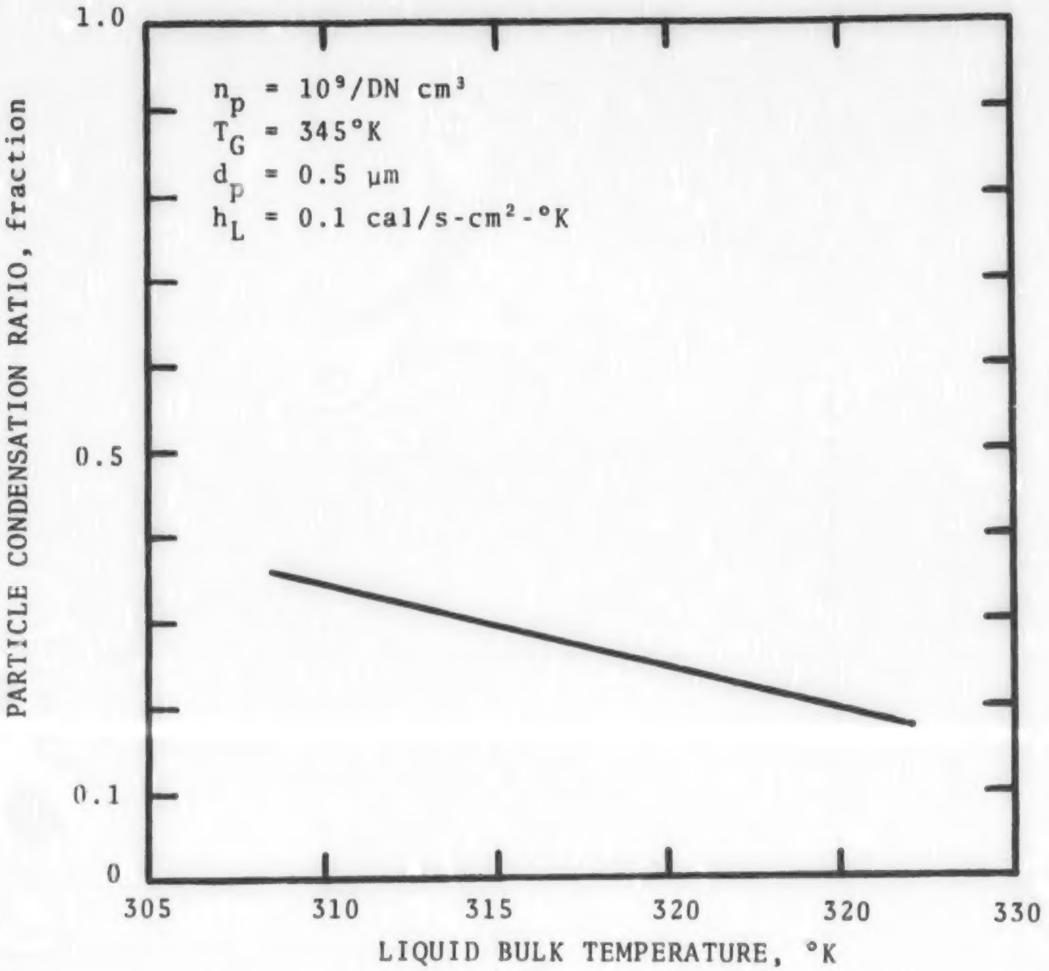

Figure 4. Effect of liquid bulk temperature on condensation ratio.

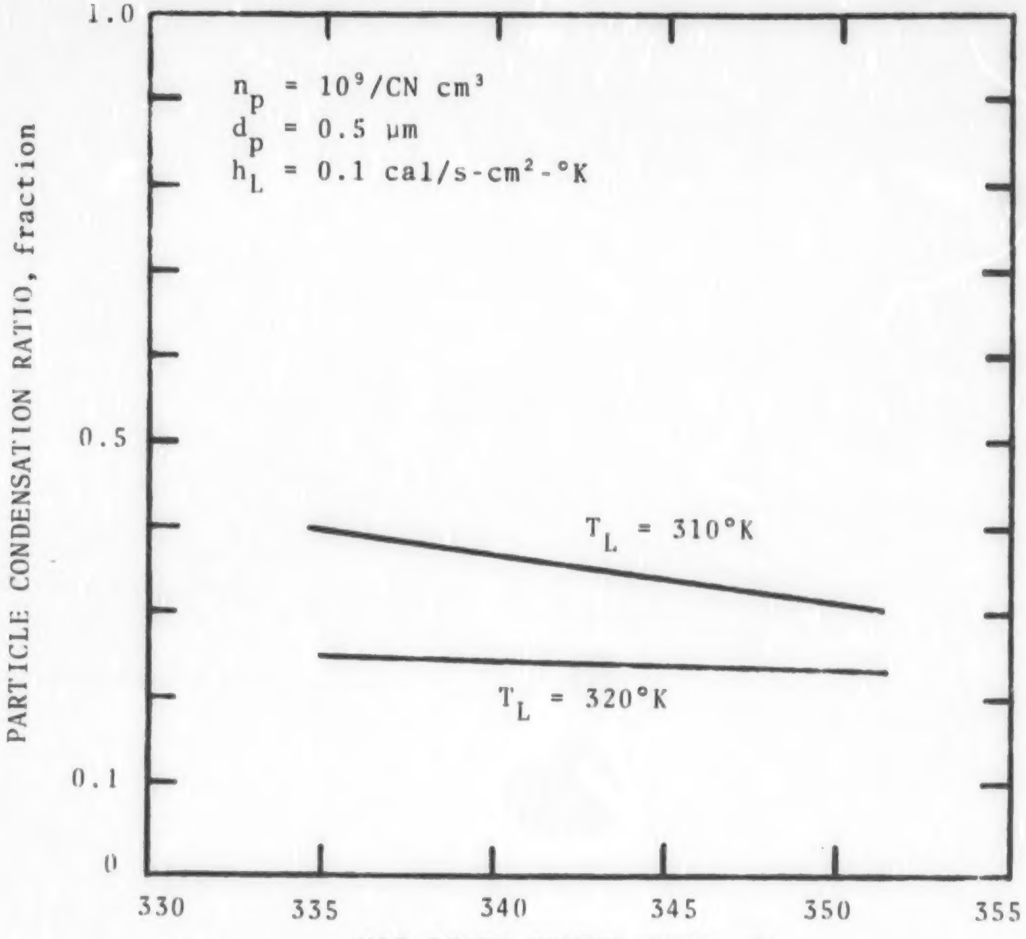

Figure 5. Effect of gas inlet temperature on condensation ratio.

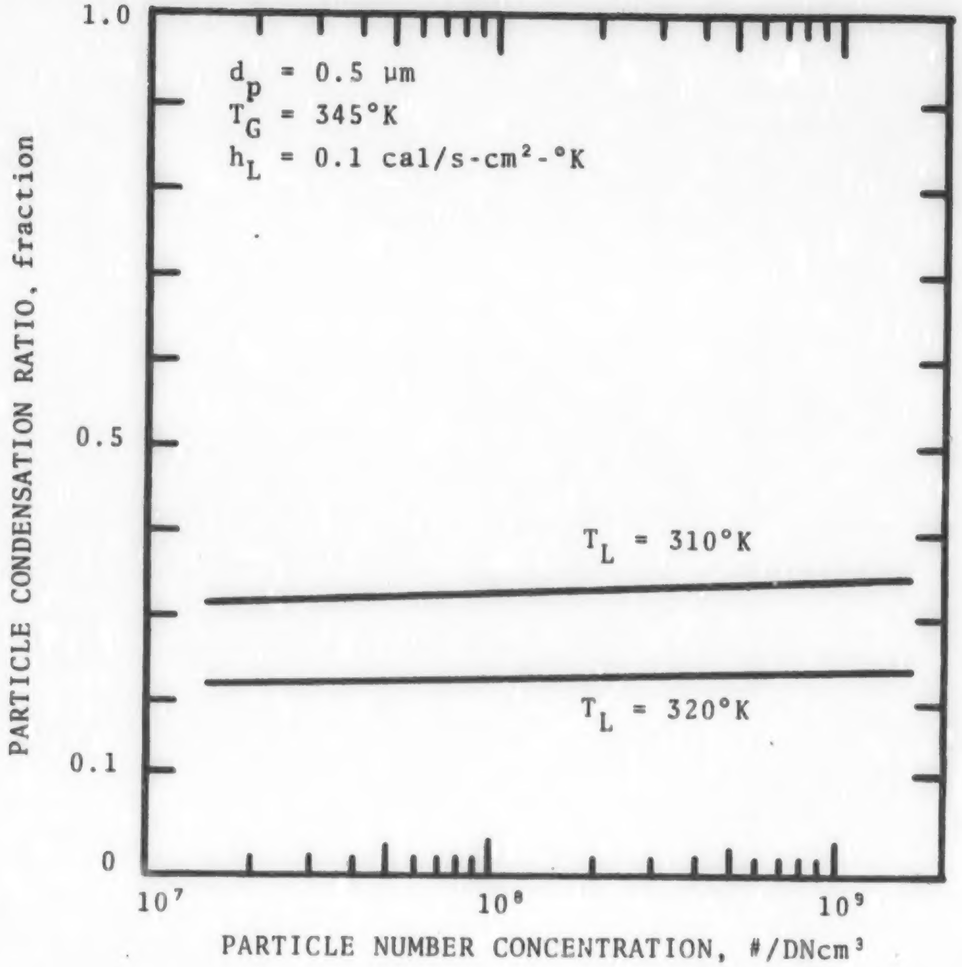

Figure 6. Effect of particle number concentration on condensation ratio.

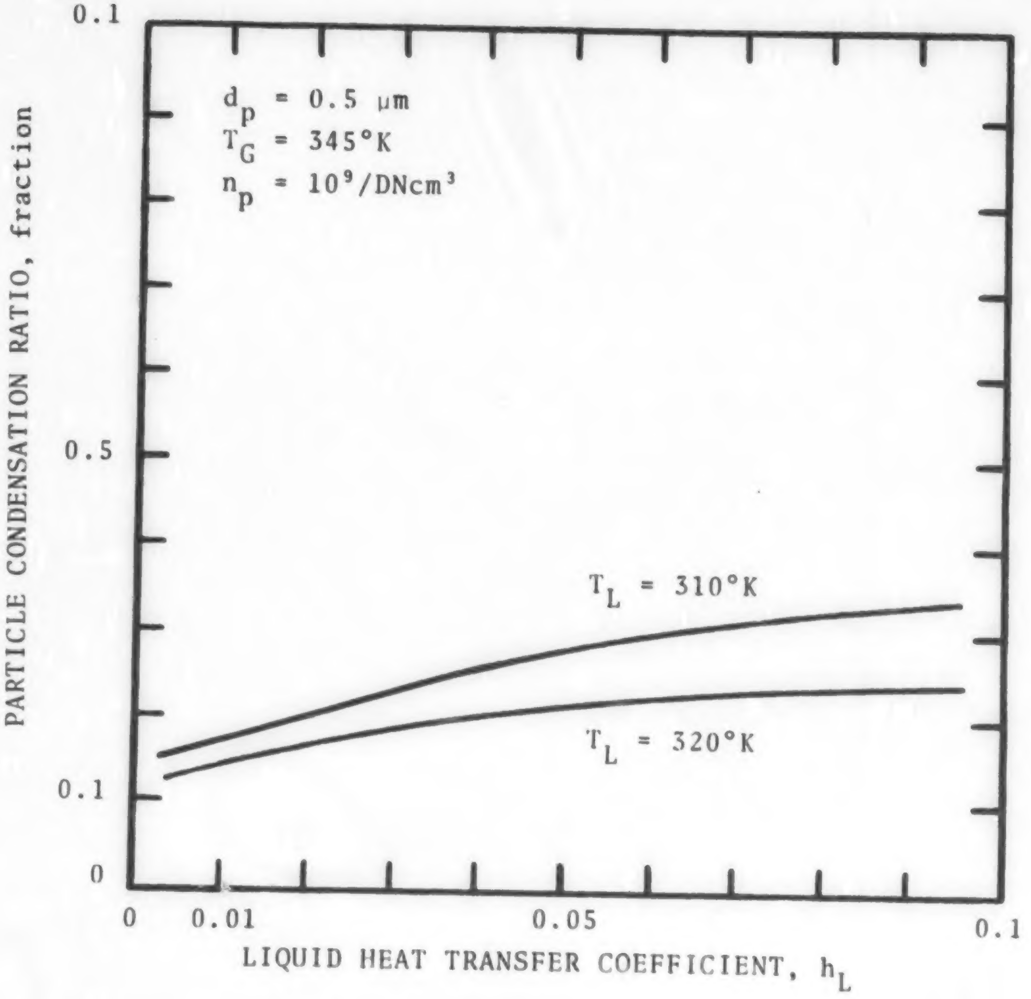

Figure 7. Effect of liquid heat transfer coefficient on condensation ratio.

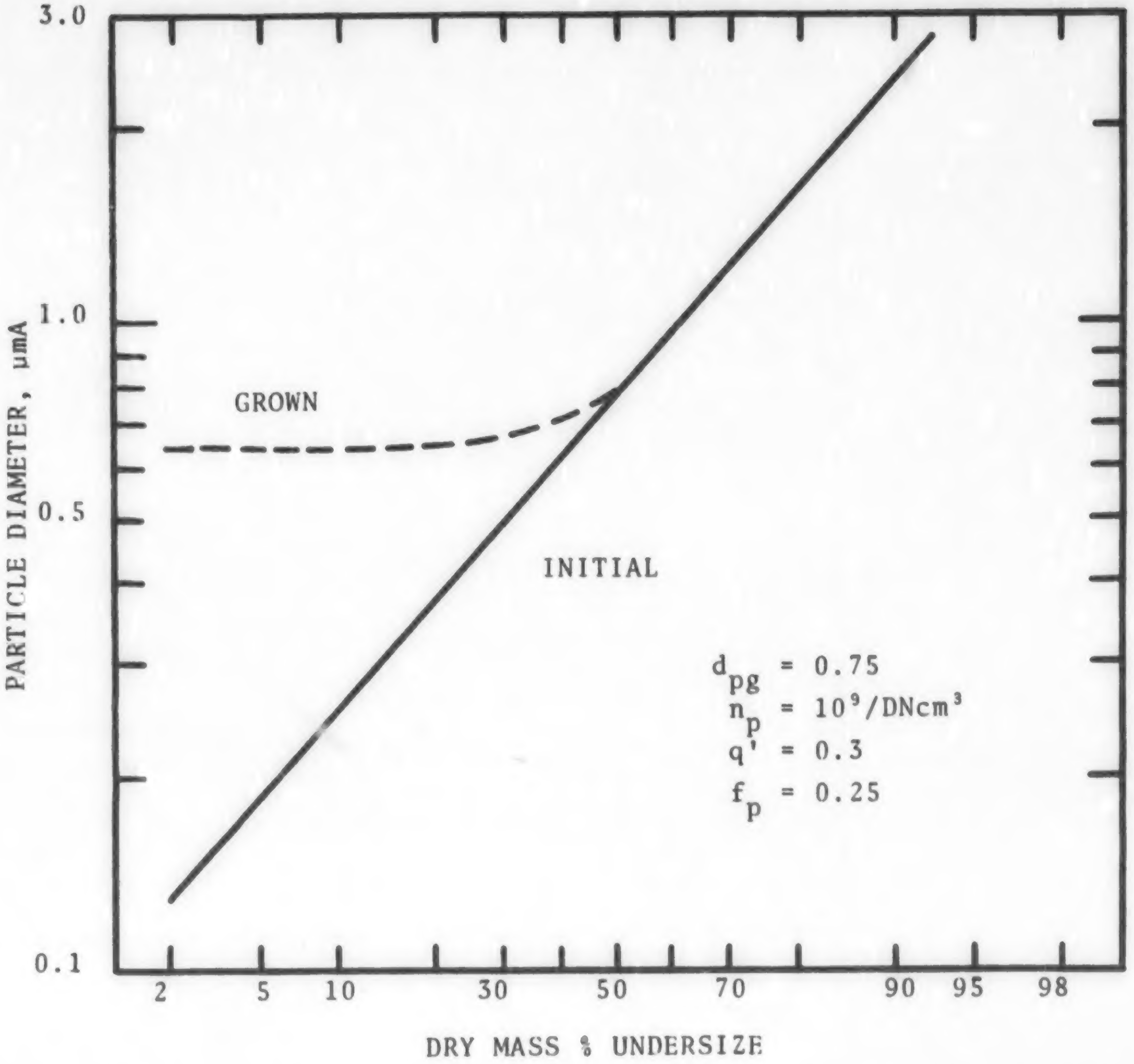

Figure 8. Particle size distribution before and after condensation.

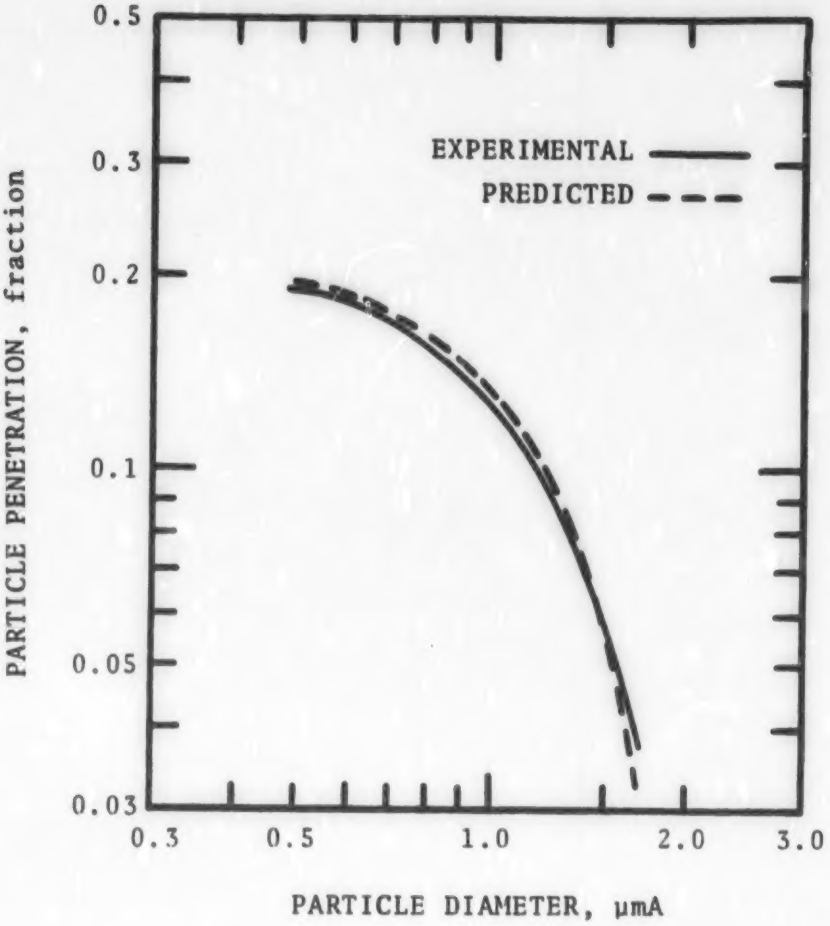

Figure 9. Particle penetration versus aerodynamic diameter for Run 64.

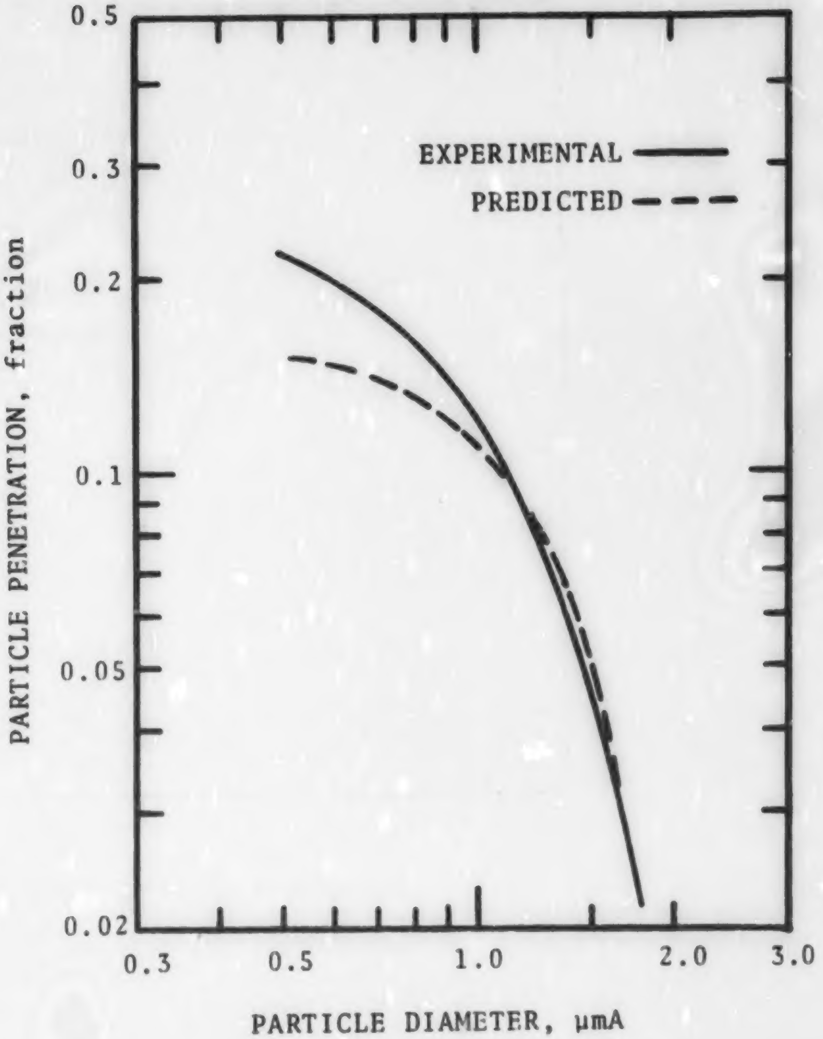

Figure 10. Particle penetration versus aerodynamic diameter for Run 69.

INTERFACIAL SURFACE EFFECTS ON PARTICLE COLLECTION

G. Woffinden
D. Ensor
G. Markowski

Meteorology Research, Inc.
464 W. Woodbury Road
Altadena, California 91001

L. Sparks

Industrial Environmental Research Laboratory
Environmental Protection Agency
Research Triangle Park, North Carolina 27711

J. Berg

Department of Chemical Engineering
University of Washington
Seattle, Washington 98105

ABSTRACT

A theoretical analysis was made to show the effects of interfacial sufrace tension on collection efficiency of solid particulates by liquid water droplets. For wet scrubber applications, it was assumed that particulates had diameters ranging from 0.05 to 3 μm, and collecting droplets had diameters ranging from 20 to 200 μm.

The theory indicates that as a particle and droplet impact, the air or vapor layer between them takes time to flow out. If the film thinning time is less than the impact time (particle stopping time), the particle and droplet will coalesce. If the thinning time is longer, the particle will rebound and will not be collected by the droplet.

Initial theoretical results indicate that, after impact, capture (coalescence) will occur in most cases that are considered to be representative of a typical wet scrubber. The primary effect of reducing droplet surface tension is a deeper penetration by the particle into the droplet before stopping because of the lower resistive force. The deeper penetration increases film thinning time and, therefore, may actually reduce collection efficiency.

Experiments are being conducted to evaluate the results of the analytical study. Two types of experiments are being considered: (1) ultrahigh speed photography of the coalescence process between individual particles and droplets, and (2) evaluation of surface tension variation effects in a laboratory-scale simulated scrubber.

Initial theoretical work has been completed. Experimental work is currently being planned and conducted. A final analytical study will relate results of the theoretical mechanism study and the experimental evaluations to current scrubber modeling techniques.

INTERFACIAL SURFACE EFFECTS ON PARTICLE COLLECTION

The objective of this study was to evaluate the effect of interfacial surface tension on collection efficiency of a wet scrubber.

SCRUBBER MODEL

The effect of surface tension is not obvious in most of the current wet scrubber analytical models[1]. Penetration (one minus the collection efficiency) in the Calvert model, for example, is given by Equation 1:

$$P = \exp\left[- \frac{2Q_L \ V \ \rho_L \ d}{55 \ Q_G \ \mu} \left| F \ (k, f) \right| \right] \qquad (1)$$

where P = average penetration
Q_L = volumetric flow rate of gas phase
Q_G = volumetric flow rate of liquid phase
V = velocity of gas phase
μ = viscosity of gas
ρ_L = density of liquid
d = diameter of liquid drops
$F(k, f)$ = function of inertial parameter, k, and unknown factors, f

Surface tension, as such, is not one of the parameters listed; however, surface tension influences droplet breakup and, therefore, the resultant droplet diameter, d. Surface tension also affects the Stokes number indirectly because it is a function of droplet size. The interfacial surface properties can also have a significant effect on the "F" factor because it is primarily a collection efficiency factor that includes both collision and coalescence probabilities. It is assumed that surface tension does not have a direct effect on collision probability, but that it could have an effect on coalescence after impact.

Limited experimental studies on the effects of surfactants in scrubbers have been performed by Bughdadi[2]. He concluded that addition of surfactant (0.1 percent Triton CF-10) improved the collection efficiency of a venturi scrubber, especially at low liquid-to-gas flow ratios. He reported that the overall collection efficiency improved from 99.66 percent to 99.93 percent at 18ℓ water/28 m^3 of gas (4 gal/1000 ft^3). He attributed the improvement to easier penetration of the collected particulates into the scrubber water droplets, thus providing more effective wetting. He also observed the reduction in spray droplet sizes with surfactant additives.

Wolfe[3] has shown experimentally that spray droplet size is proportional to the square root of the surface tension:

$$d = c\sigma^{1/2} \tag{2}$$

where d = droplet diameter
c = constant
σ = liquid surface tension

The maximum surface tension of scrubber water is approximately 72 dynes/cm (pure water). Additives and normal contaminants in operating scrubbers will typically reduce the surface tension to 50-60 dynes/cm. If a surfactant is added, the surface tension can be further reduced to 20-30 dynes/cm. Therefore, the maximum possible reduction, from 72 to 20 dynes/cm, will reduce the spray droplet diameter by only 50 percent at most. In actual practice, a maximum reduction of 30 percent is more realistic. The effect of droplet size reduction on scrubber efficiency is not easily determined from the scrubber model, Equation 1. The droplet size affects the "F" factor which includes individual droplet collection efficiency and other unknown factors. Decreasing the size of droplets will increase the number of droplets so that droplet/particle collision efficiency will be improved, particularly for small particles. When the droplets get small enough that they are no longer removed from the gas stream by the entrainment separator, the scrubber efficiency will become very low. The droplets in a scrubber are usually very large (on the order of 50 to 200 μm diameter) compared to the particles being scrubbed (the most difficult particles to remove are typically 0.05 to 3.0 μm diameter). When there is a large difference in size between the droplet and particle and the particle is in close proximity to the liquid surface, the droplet surface can be considered as an infinite flat plane. In general, a reduction in droplet size tends to reduce penetration of particles, i.e., it increases the scrubber collection efficiency. The changes, however, are expected to produce second order effects.

THINNING LAYER COALESCENCE MODEL

As already indicated, particle capture by liquid droplets is a two step process: (1) collision, and (2) coalescence after collision. There is virtually no effect of surface tension on collision probability because surface tension, by itself, produces no forces that extend far beyond the surface. The surface tension of the droplet, however, can have significant effects on the particle dynamics at close range, i.e., at the time of collision.

Analytical models relating the physical and chemical mechanisms that control coalescence were reviewed and compared. The film thinning model is the most widely accepted theory of coalescence.

The film thinning model assumes that as a particle collides with a water droplet, a thin layer of air or vapor is trapped between the particle and the deformed surface of the droplet. This air layer prevents immediate coalescence. The layer thins under the forces involved in the collision processes; thinning is opposed by the layer's viscous forces. If the layer thins sufficiently before the colliding particle rebounds, the layer ruptures and coalescence occurs. Figure 1 illustrates the collision and film thinning model. The solid particle has penetrated its maximum distance, x_m, into the surface of the much larger water droplet, and an air layer has been trapped between the particle and the droplet. F_s denotes the force between the particle and droplet and depends on a number of parameters, including the droplet surface tension, internal pressure, particle velocity, and particle radius. The particle/droplet contact time during the collision (before rebound) is calculated either analytically or numerically, depending on the assumptions made. The contact time is then compared with the thinning time. If the thinning time is less than the contact time, coalescence is assumed to occur.

The time for the trapped layer to thin is calculated using Reynold's formula[4]:

$$t = \frac{3}{4\pi} \frac{A^2}{F_s} \eta \left(\frac{1}{\delta^2} - \frac{1}{\delta_o^2} \right) \qquad (3)$$

where
t = thinning time
A = area of contact
η = bulk viscosity of air
δ = film thickness at maximum particle penetration distance
δ_o = initial film thickness
F_s = force between the particle and the droplet

If δ_o is larger than 2δ, its effect on the thinning time, t, is small. It is, therefore, normally neglected.

Results of the current study indicate that, although general trends in coalescence probability may be predicted by the model, modifications will be required for specific quantitative predictions. The following model restrictions could account for the observed differences:

1. Calculations performed to date (Emory,[5] Lang,[6] Jayaratne[7]) have used the average force acting on the particle during collision and the area at maximum penetration in Equation 3 to calculate thinning time, t. However, the thinning time is actually dependent on the time average ratio of the square of the contact area, A^2, and the force, F_s, exerted by the liquid surface. Models examined calculated the force as:

$$F_s = \alpha A^a \tag{4}$$

where
F_s = force exerted by the liquid surface
α = a constant depending on velocity
a = 1 or 1/2
A = contact area

Thus, the thinning time is estimated as

$$t \cong C_o \frac{A^2}{A^a \delta^2} \tag{5}$$

where C_o = constant, including all other constants in Equations 3 and 4. Before the particle forms a trapped air layer, the area, A, is zero and the thinning time also becomes zero since a is 1 or less. Thus, the model appears to predict that the thinning layer collapses before penetration begins. Of course, the layer does not collapse completely, but the above argument implies that the layer thins much more rapidly at the start of penetration than is accounted for by the ratio of average force and maximum contact area.

2. The calculated thinning time is strongly dependent on the assumed shape of the depression created by the impacting particle. Figure 2 shows two models that have been used. The area of contact is proportional to θ^2 and the thinning time is proportional to θ^4. The difference in thinning time between these models is likely to be an order of magnitude. Model 2 also predicts a smaller droplet resistive force and, thus, a considerably longer contact time before rebound.

3. Thinning time is strongly dependent on δ, the separation at which surface forces cause rupture of the film. Uncertainty exists in estimating this unstable film thickness. Jayaratne[7] suggests a thickness of 1000 Å, and Emory[5] indicates that it may be as thin as 50 Å. This factor of 400 difference introduces uncertainty in thinning time.

4. The noncontinuous nature of the air film, when its thickness is less than the mean free path of approximately 1000 Å is expected to decrease its stability, and therefore decrease the thinning time. Any electrostatic charge or induced molecular polarization is is also expected to reduce film stability.

5. Any surface roughness in the colliding particle can shorten the thinning time. Analysis of Equation 3 indicates that the thinning time is sensitive to roughness either through reducing the effective area, A, or the rupture distance, δ.

6. Collision at a small grazing angle causes a particle to deflect rather than rebound in the opposite direction. Many models have not attempted to include this effect. It is clear that the impact angle is important; however, the overall effect in actual scrubber applications is not obvious.

7. Davis[8] predicts a marked decrease in film viscosity when the thickness is less than the mean free path. In this case, the effective viscosity is nearly directly proportional to the film thickness. When this effect is included in the calculation of thinning time from Equation 3, the thinning time is reduced by a factor on the order of 5.

8. The electric double layer at a water surface produces the effect of a small negative surface charge. Therefore, a short-range repulsive force, proportional to the dipole moment, is generated between two droplets in close proximity[9]. Silica particles adsorb a water layer from the atmosphere and, therefore, acquire an electric double layer similar to that of a water droplet. For initial stages of coalescence, they, therefore, can be considered as water droplets. Double-layer forces generally are estimated to be smaller than those produced by the viscous film thinning effects[10]. There is evidence, however, that the double layer may have a coalescence retarding effect under some conditions. This effect was used to explain stability of water droplets floating for long periods on a water surface[11]. Similar experiments have been conducted in our laboratory. Droplets of polar liquids are generally, but not always, more stable floaters than those of nonpolar liquids. Other mechanisms, such as electroviscous effects or gas adsorption on the liquid surface, may have an effect also. It has been shown that addition of surfactants

can increase the stability of floating droplets. This effect could be the result of increased polarization of the surface double layer. The effects from surface polarization must be treated separately from those due to surface tension alone.

If the film thinning model or a modified thinning model is valid, it predicts that the surface tension of scrubber droplets will have only a secondary effect on particle collection efficiency due primarily to reduced size of scavenger droplets. A reduction in surface tension reduces the pressure exerted on the particle during impact. Since the particle will then have less resistance, it penetrates deeper into the droplet. This deeper penetration produces a longer, narrower path for the vapor film, and the thinning time is increased. The increased thinning time results in reduced capture probability because the particle may rebound before the film ruptures.

EXPERIMENTS

Simple laboratory experiments were devised to measure film thinning times and the effects of surface energy on the thinning times. These experiments were planned to evaluate, at least qualitatively, the film thinning theory.

Initial experiments have been performed, and additional experiments are in progress. In these experiments, the impact and coalescence process for a water droplet and a glass sphere (representing a fly ash particle) was observed with a high speed motion picure camera looking through a microscope. The water droplets were approximately 1000 to 3000 μm diameter and were suspended on the end of a microliter syringe needle. The glass spheres, were made by drawing a glass rod into a fine fiber and forming a ball on the tip end. The particles ranged from 40 to 4000 μm diameter. The suspending rods were as small as 10 μm diameter. Rods 10 μm diameter without a sphere on the end were also used to represent 10 μm diameter particles.

The experimental setup is shown in Figures 3 and 4. The supporting syringe and glass rod were mounted on three-dimensional micromanipulators so that they could be moved independently within the field-of-view of the camera. The glass particle was caused to impact the water droplet by rapidly advancing the horizontal traverse mechanism of the particle support, Figure 5. Radioactive polonium strips were mounted near the particles and droplets to eliminate electrostatic charges. Radiation from the polonium ionizes the air so that surface charges bleed off. Experiments without the polonium tended to give shorter and more variable film thinning time measurements. The camera used was a Beckman and Whitley Dynafax, operating at a top speed of 26,000 pictures per second, with individual frame exposure times of 2.5 μsec. The camera is a continuous writing, rotating drum camera with 224 frames.

Illumination was provided by a Xenon flash lamp system. The system is designed to provide a square-wave light pulse with nearly uniform intensity over the picture taking time of 1 drum revolution. In order to eliminate the effects of heat and electromagnetic fields produced by the flash lamp discharge, a fiber optic light pipe was used. The light pipe made it possible to move the lamp away from the event being photographed.

Coalescence delay time was measured as a function of particle size. The effects of impact velocity and surface tension are to be determined in future studies. Figures 6 through 12 are typical photographic sequences showing the coalescence process. Film thinning time was taken as the coalescence delay time; i.e., the time from first contact until a liquid meniscus was first discernable. For example, in Figure 10 the delay time was taken as 12 frames at 39 μsec/frame, for a total delay time of 468 μsec. The 39 μ sec is determined by the framing rate, which was normally held constant at 26,000 frames/sec, except for Figure 6 which was taken at 10,000 frames/sec, giving a time per frame of 100 μsec. The magnification in Figure 6 is also reduced.

The camera speed was measured to within ±5 percent. A measurement uncertainty of ±1/2 frame at each end of the thinning time measurements introduces an additional potential error of ±39 μsec. A thinning time of 1,000 μ sec, therefore, has a random experimental variation of approximately ±10 percent while a thinning time of 100 μ sec has a random variation of approximately ±50 percent.

Figure 13 is a comparison of experimental results with theoretical predictions based on the film thinning model of Emory[5]. The experimental results are consistent and reasonably reproducible; however, they differ from the theoretical predictions by as much as 2 orders of magnitude for larger droplets. For the large particle experiments, the particles were nearly the same size as the water droplets. An error could, therefore, be introduced by the false assumption that the droplet was large compared to the solid particle. Some of the random experimental variation could also be due to uncontrolled parameters including: ambient temperature, relative humidity, water purity, and particle cleanliness. No special control of these factors was made; however, because of the limited ranges of variations they are not expected to have large effects. Ambient temperatures ranged from 19 to 22°C (67-72°F). Relative humidity ranged from 40 to

49 percent. Freshly distilled water was used for the droplets. Glass particles were initially clean when formed on the end of glass support rods in a torch flame. They were allowed to remain in the ambient atmosphere for at least several days with no additional cleaning or treatment prior to use in the experiments. In many cases, the particles were used repeatedly in successive tests. Water was blotted from the bead surface at the end of a test run, and the bead was allowed to dry in the nominal ambient 45 percent relative humidity atmosphere for at least 15 minutes prior to performing a subsequent test with the same particle. An adsorbed monolayer of water probably existed on the particle surface for all tests, since it is almost impossible to preclude such a layer in an ambient atmosphere. Also, a similar water layer probably will exist on fly ash particles in a scrubber.

CONCLUSIONS

1. An impacting solid particle appears to remain in contact with a water droplet for a finite measurable time before wetting or coalescence occurs. This coalescence delay time can be interpreted as equivalent to the film thinning time.

2. The film thinning models of droplet coalescence and experimental results from the MRI studies show the same general trends even though there are large differences under some conditons. At least some of these differences, hopefully, can be resolved by additional development of the model and the experiments.

3. The film thinning model is probably the best model available, even though it appears that modifications are needed to provide more valid predictions.

4. Reduction in surface tension of the scrubber liquid appears to produce only second order effects on collection efficiency; i.e., through reductions of spray droplet sizes, or through reduced penetration resistance during particle impact. The magnitude of these effects is not yet known.

5. Electrostatic fields appear to be effective in increasing coalescence efficiency. Charge effects can produce large reductions in film thinning times. Therefore, addition of electrostatic fields in a wet scrubber could probably increase the particulate collection efficiency.

ACKNOWLEDGMENTS

Gratitude is expressed to Patrick A. O'Donovan, Aerojet General Corporation, for providing high speed photographic equipment.

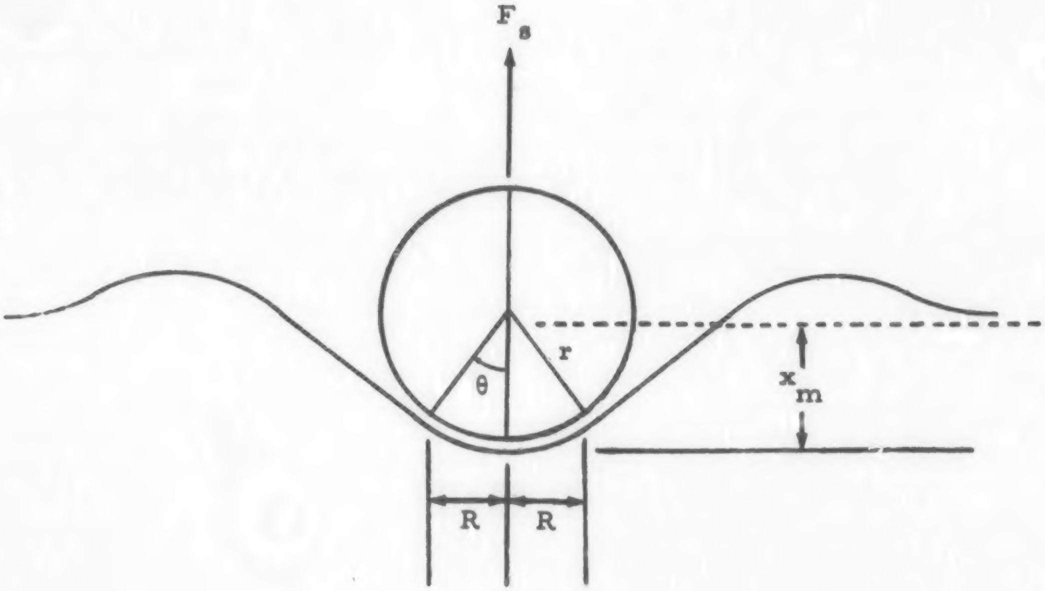

Figure 1. Model for collision of particle and liquid droplet.

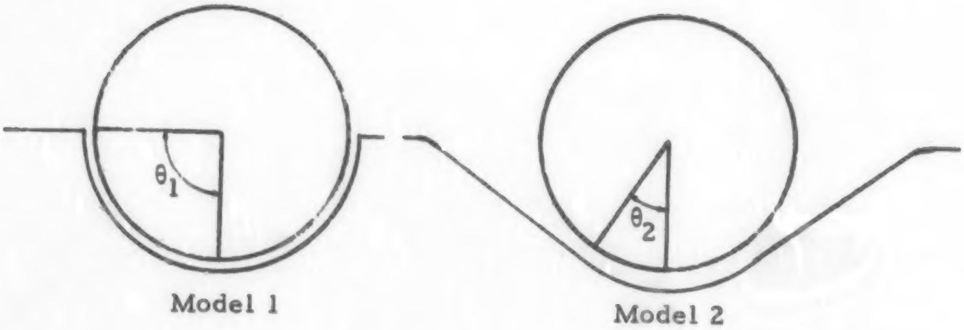
θ$_1$
θ$_2$
Model 1
Model 2

Figure 2. Models for surface deformation.

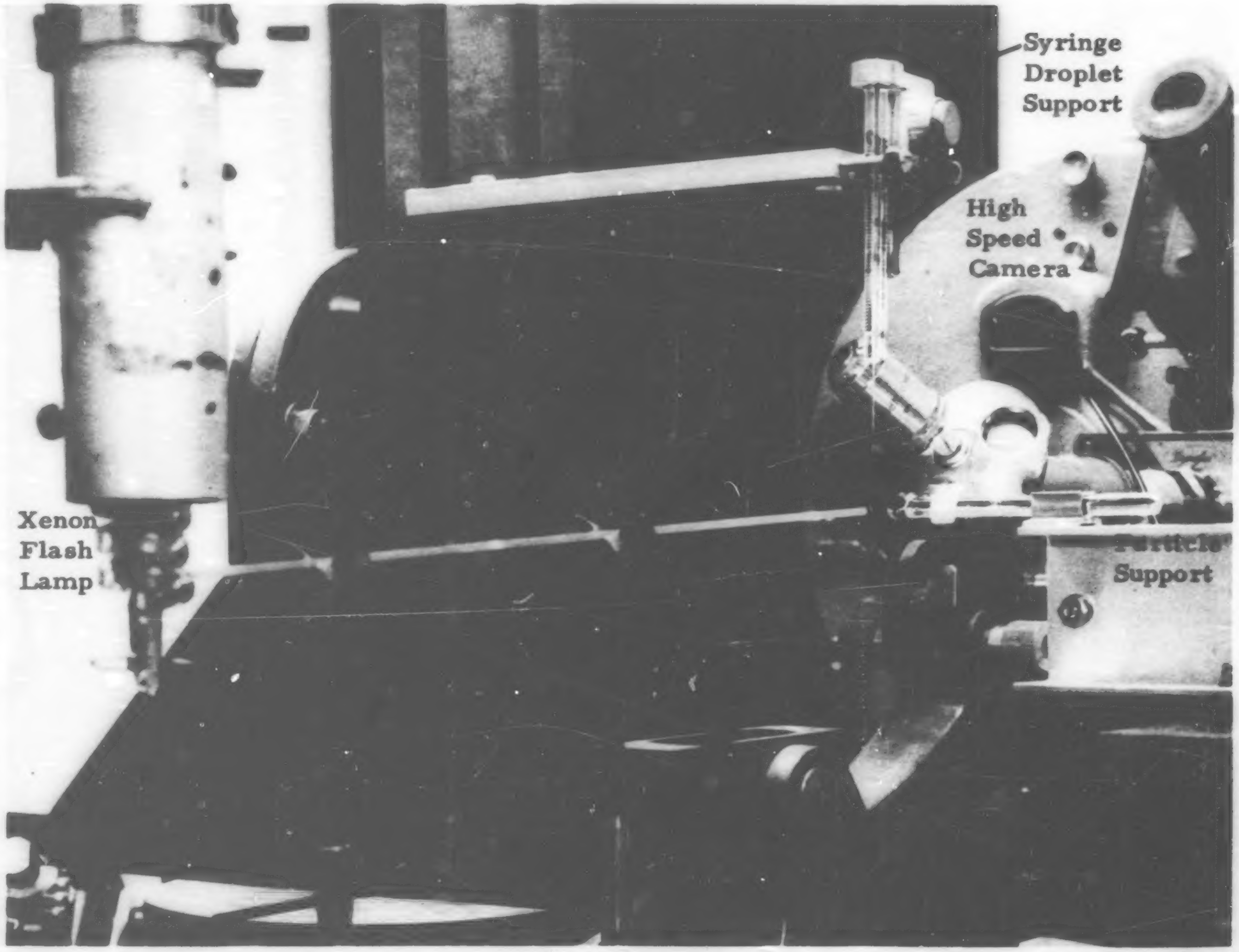
Syringe Droplet Support
High Speed Camera
Xenon Flash Lamp
Particle Support

77-084

Figure 3. High speed cine microscope equipment used for experimental evaluation of coalescence mechanisms.

Reproduced from
best available copy.

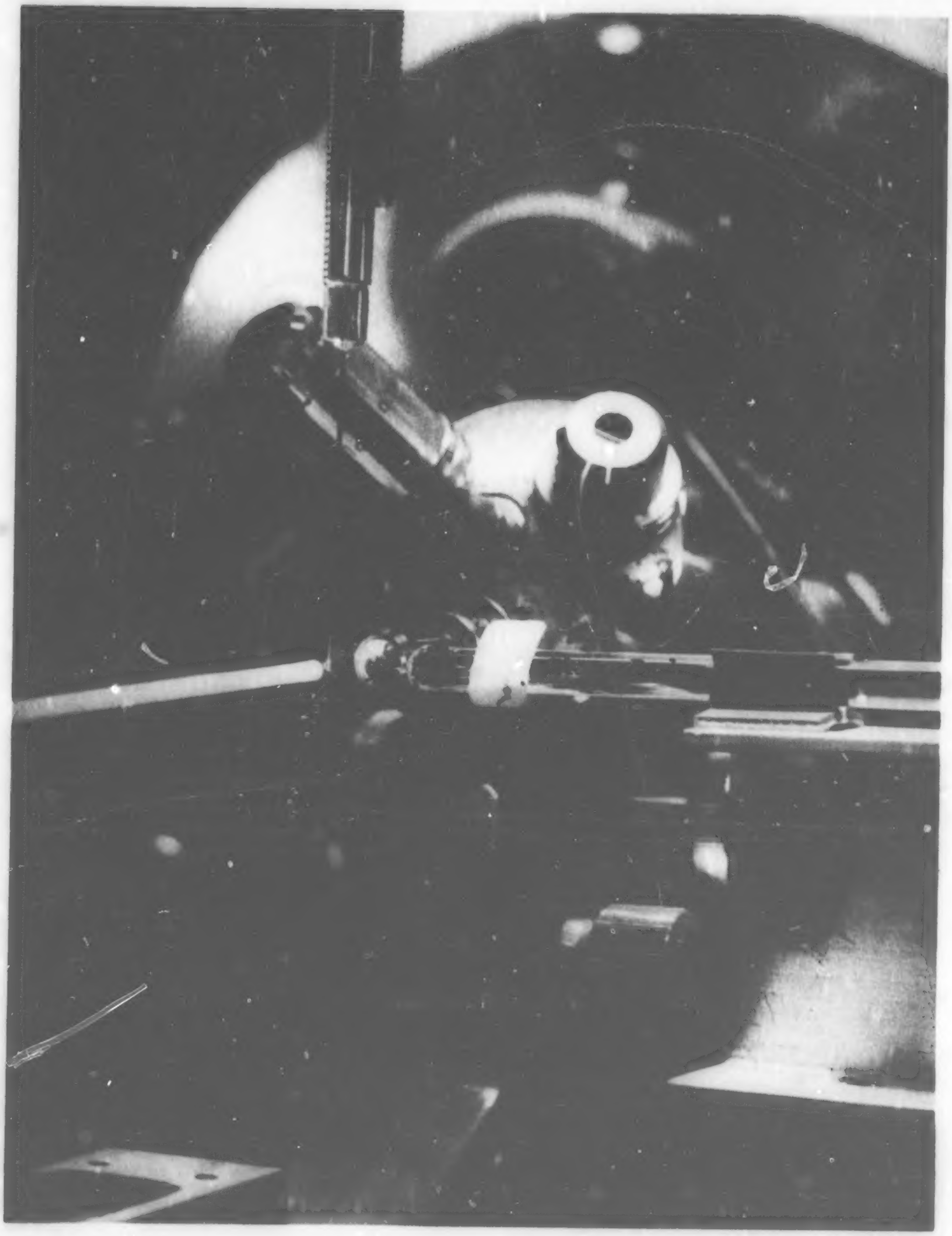

77-083

Figure 4. Glass rod with simulated fly ash particle mounted on traversing mechanism.

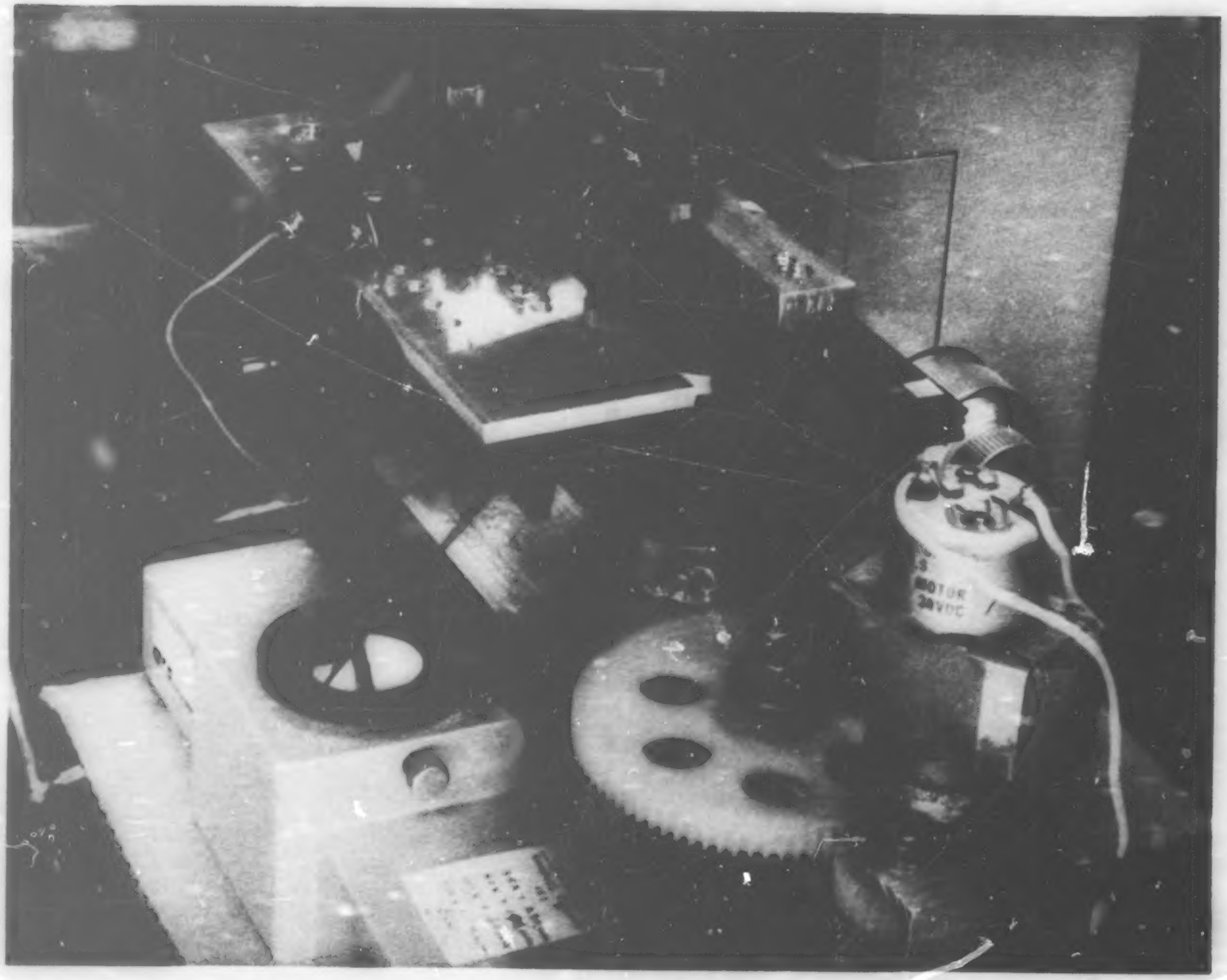

Figure 5. Traversing mechanism for impacting particles into water droplets.

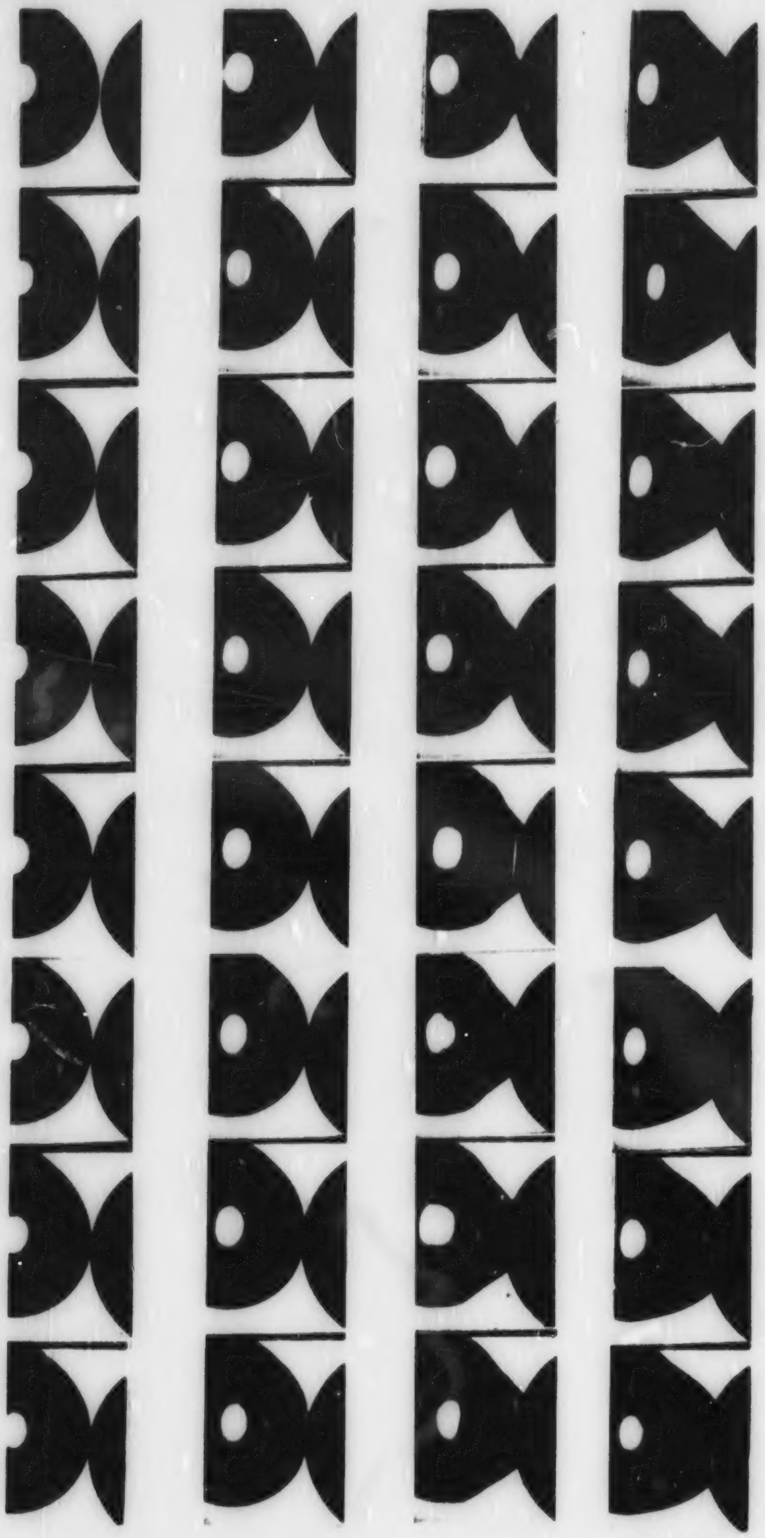

77-115

Figure 6. Coalescence of 2800 μm diameter glass particle with water droplet, 1200 μsec delay (10,000 pps).

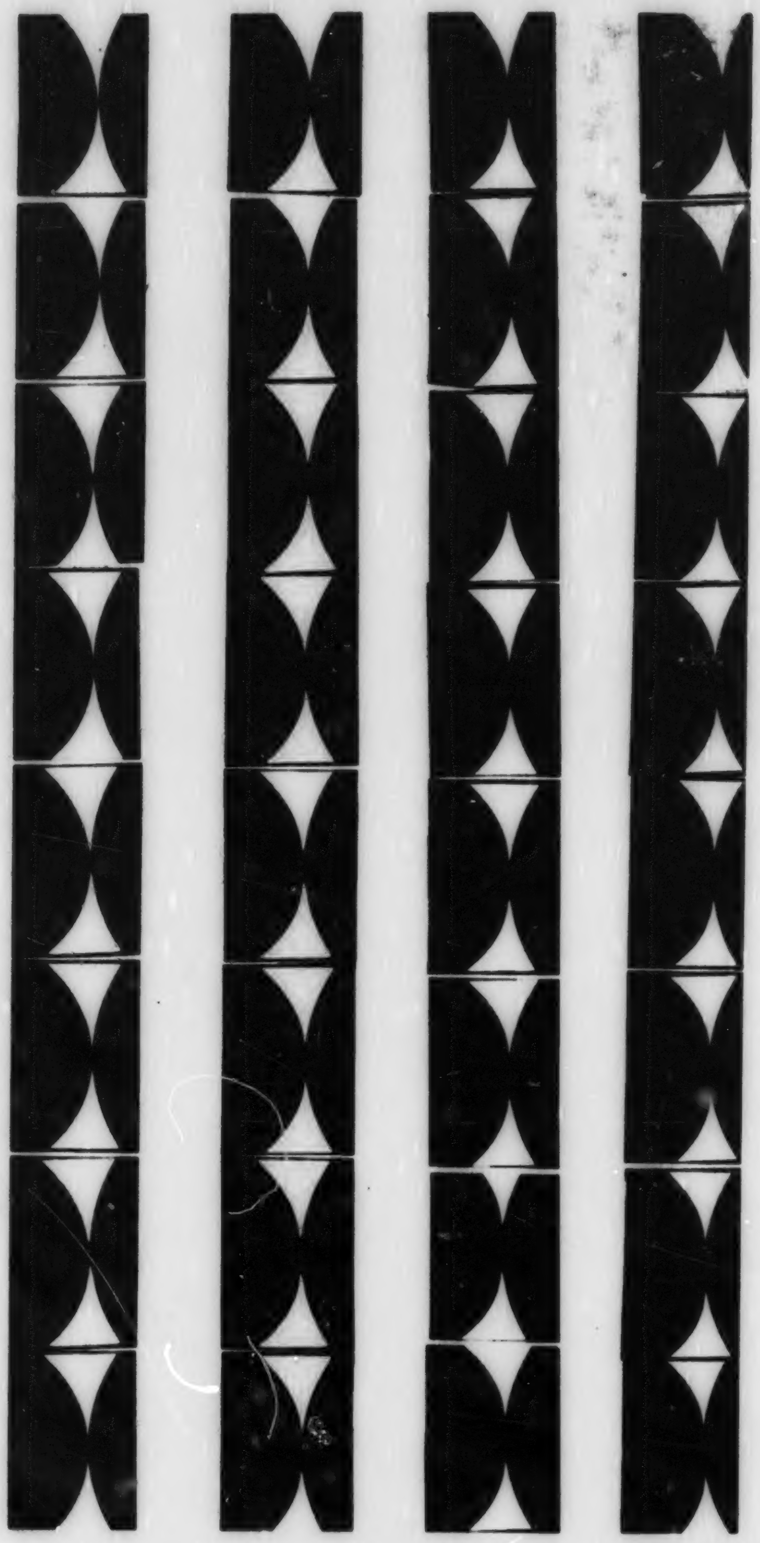

77-116

Figure 7. Coalescence of 2800 μm diameter glass particle with water droplet, 2067 μsec delay.

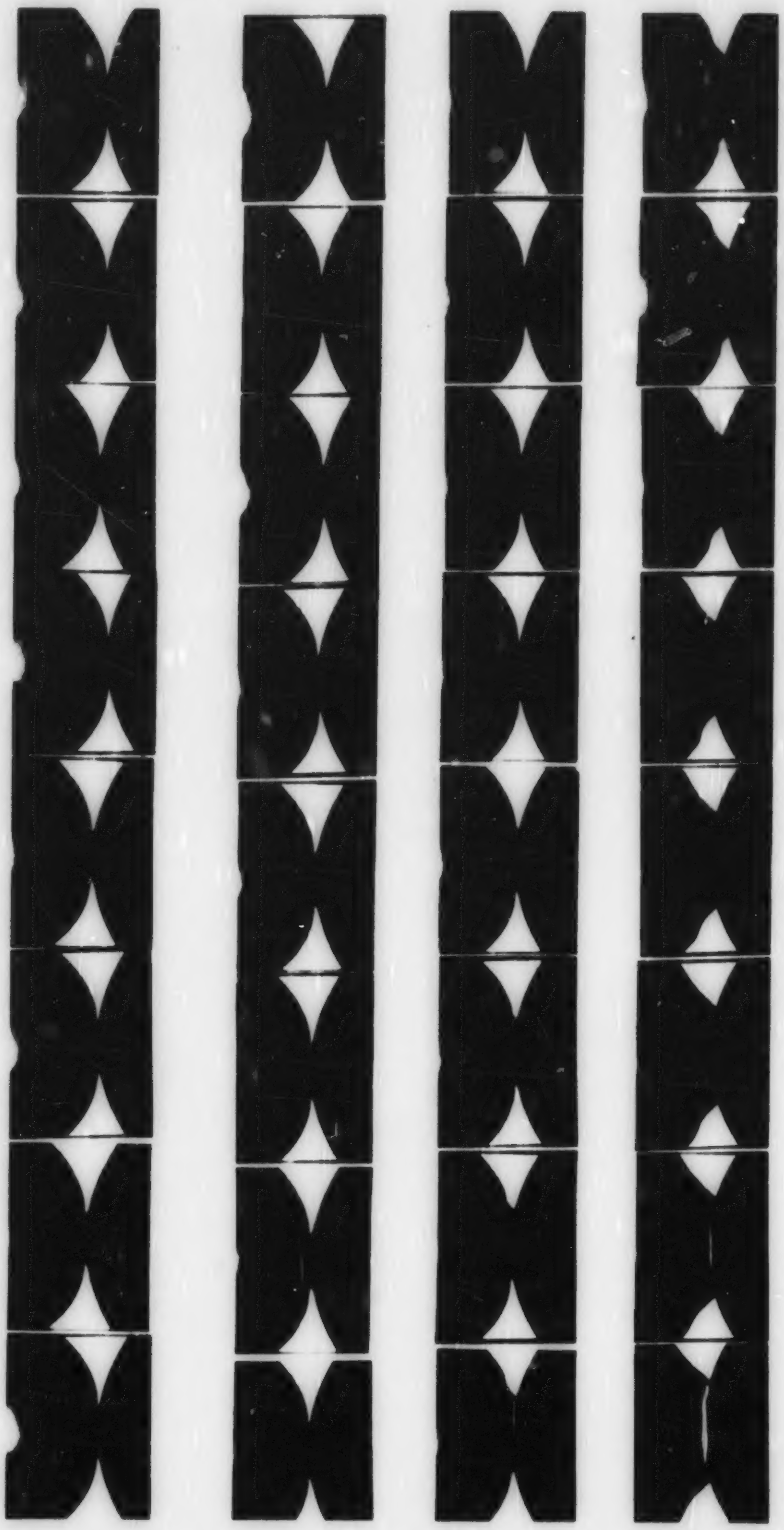

77-117

Figure 7. Continued.

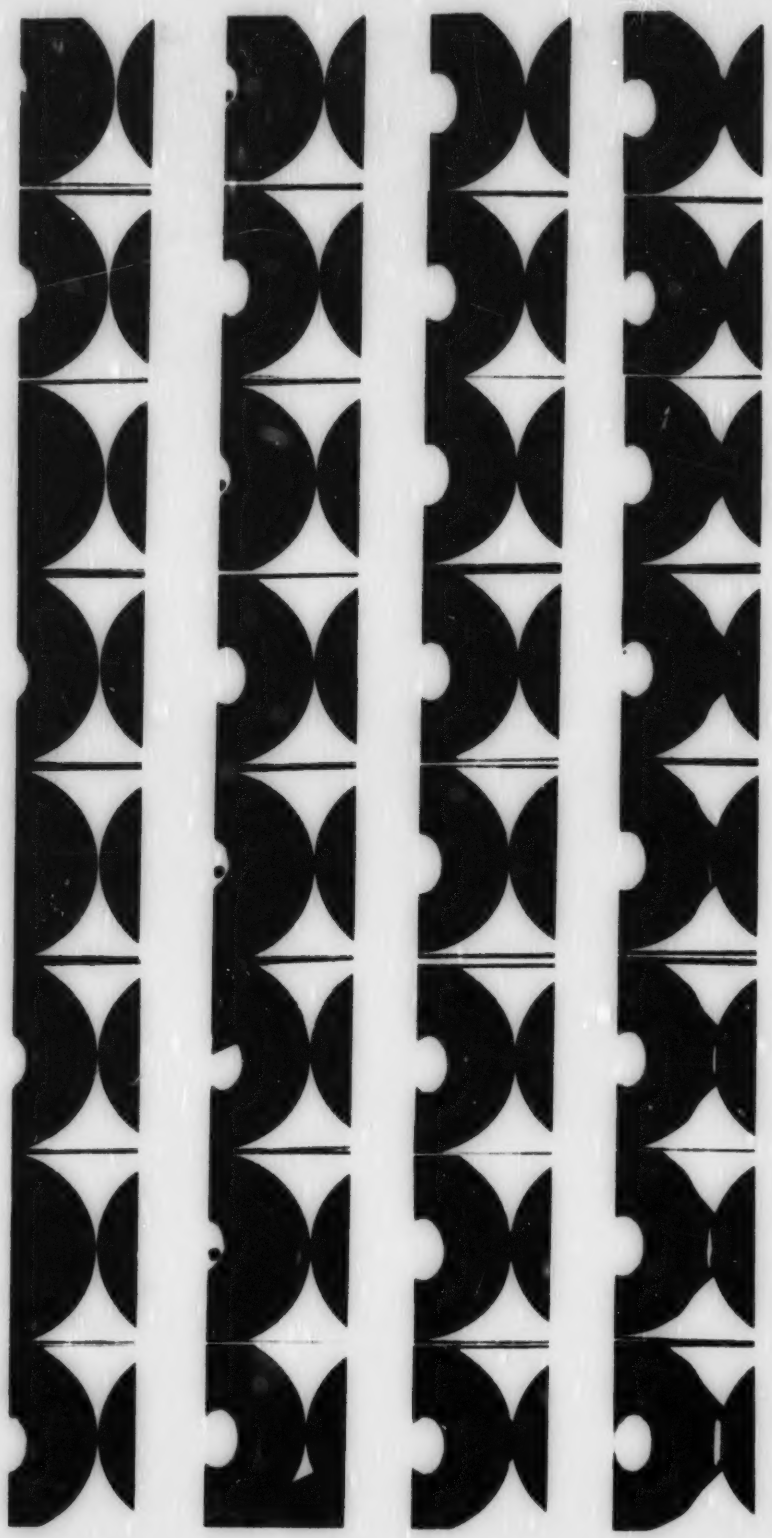

77-118

Figure 8. Coalescence of 1700 μm diameter glass particle with water droplet, 585 μsec delay.

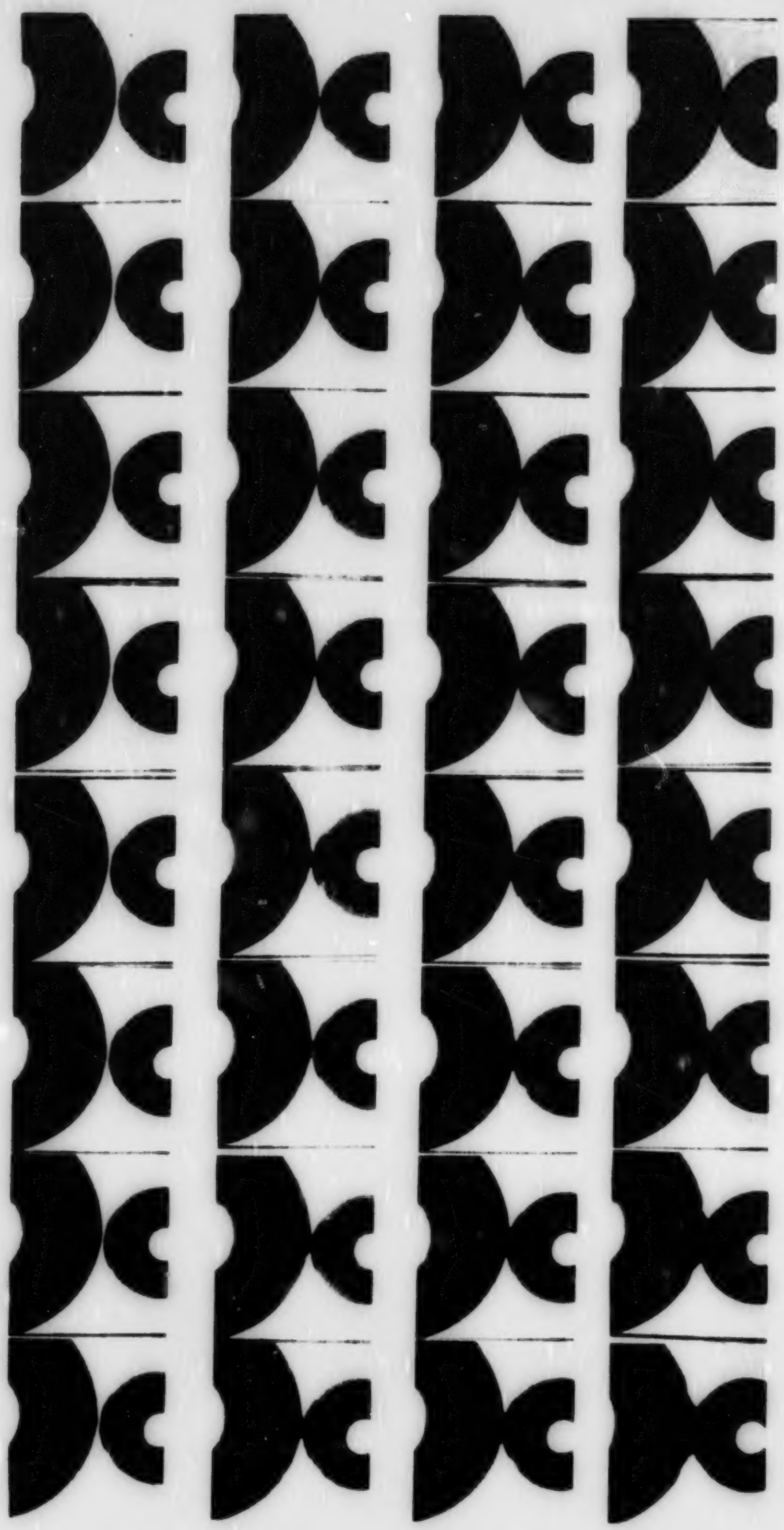

77-119

Figure 9. Coalescence of 1000 μm diameter glass particle with water droplet, 780 μsec delay.

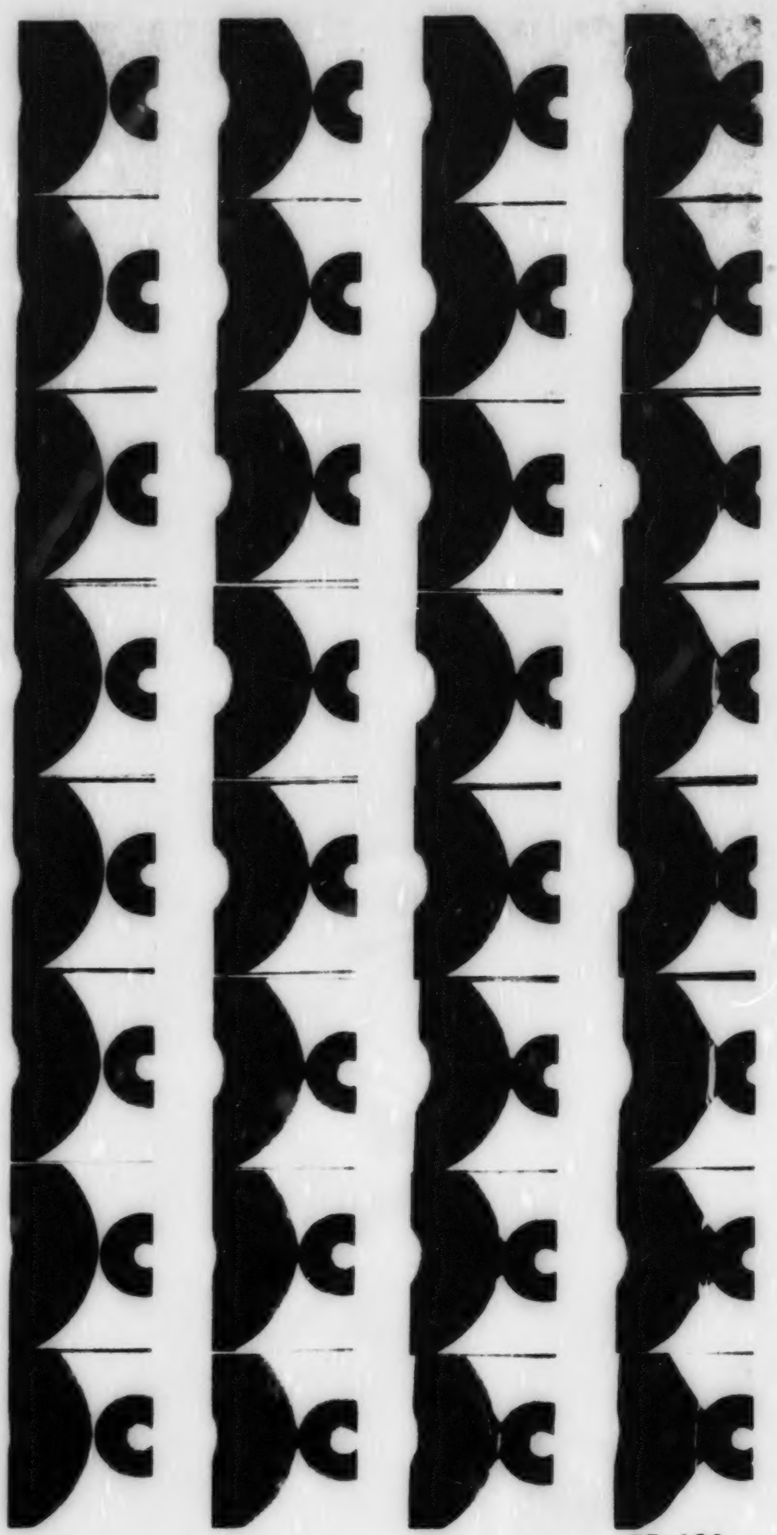

Figure 10. Coalescence of 725 μm diameter glass particle with water droplet, 468 μsec delay.

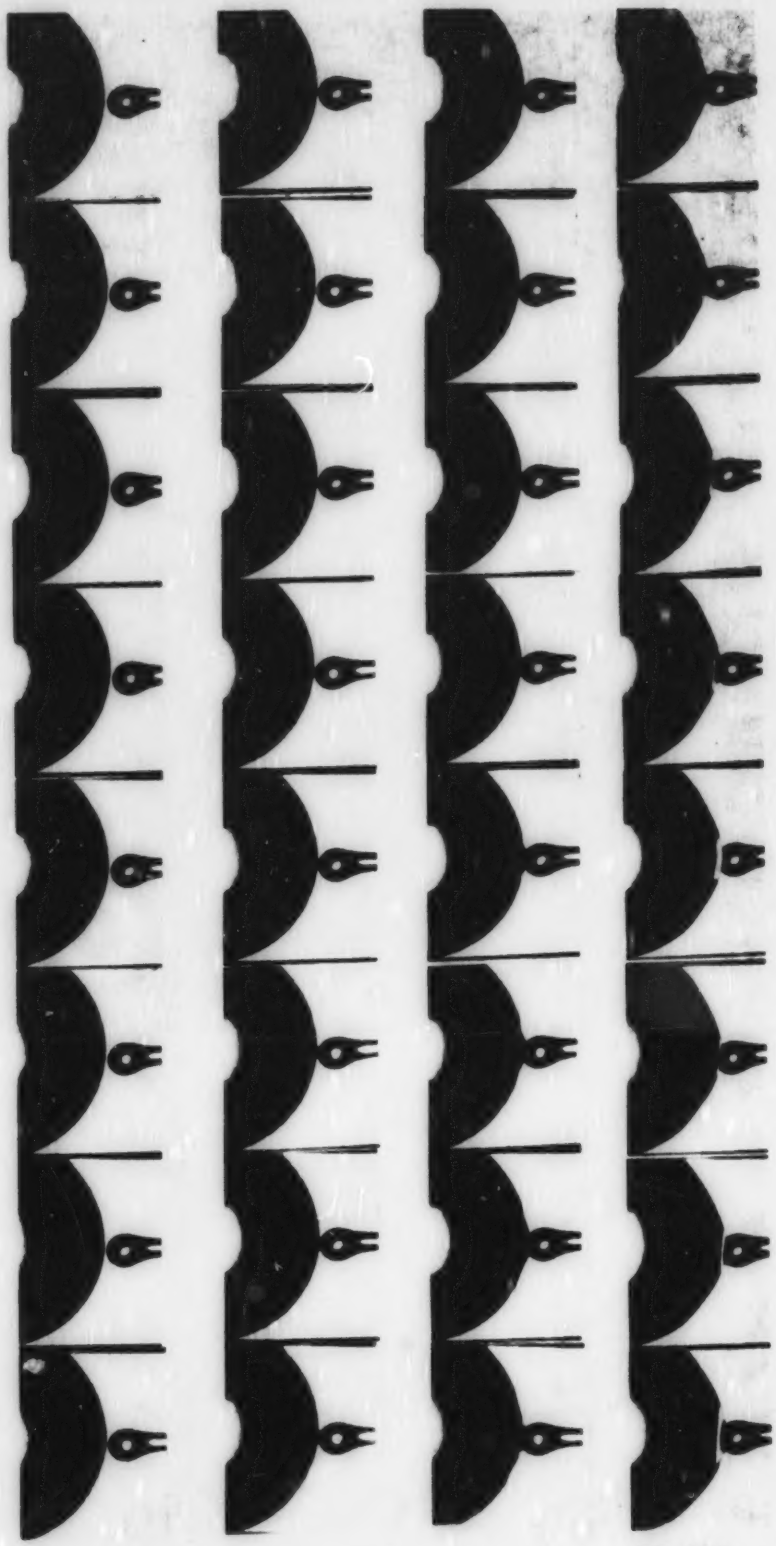

Figure 11. Coalescence of 275 μm diameter glass particle with water droplet, 351 μsec delay.

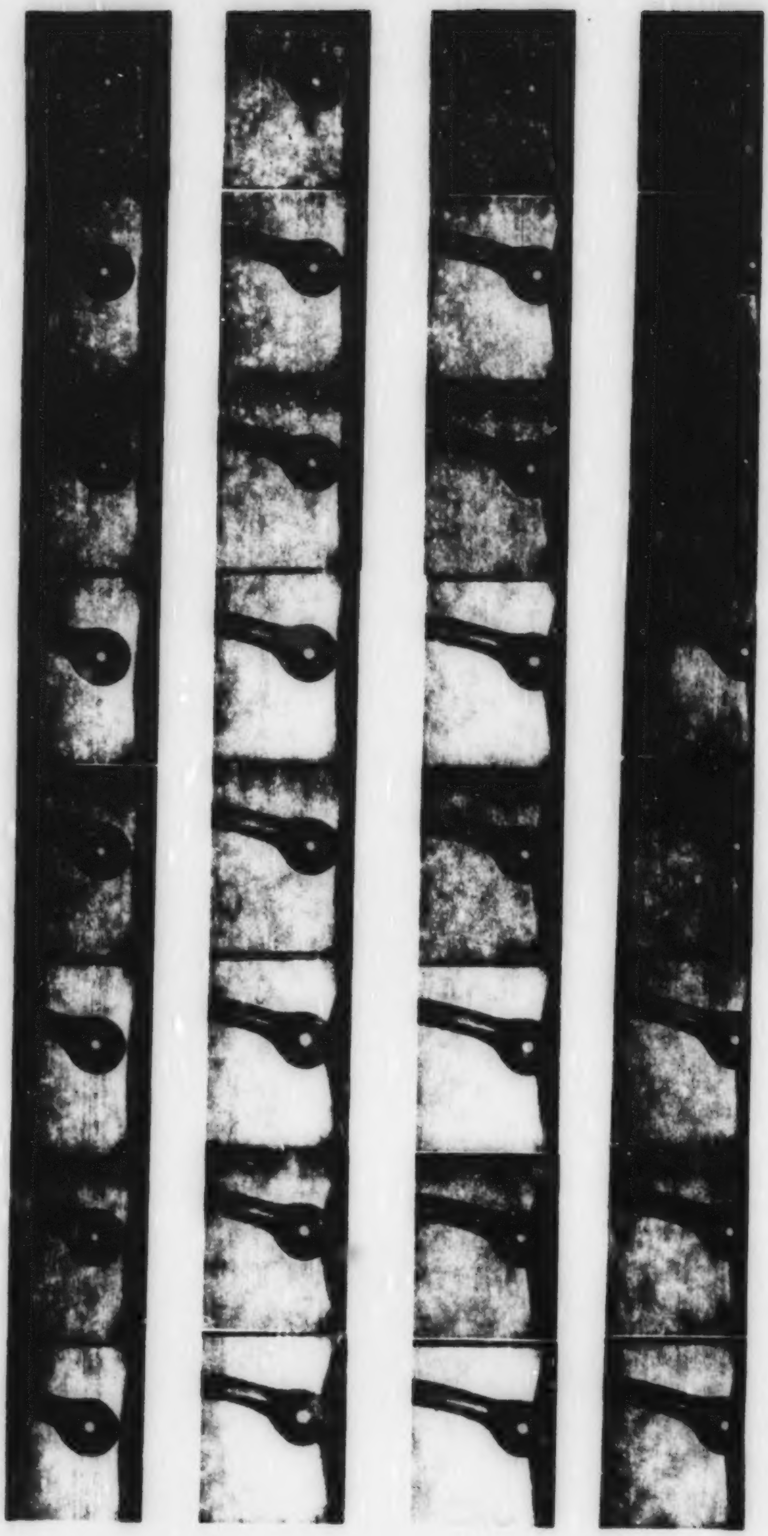

77-122

Figure 12. Coalescence of 100 μm diameter glass particle with water droplet, 156 μsec delay.

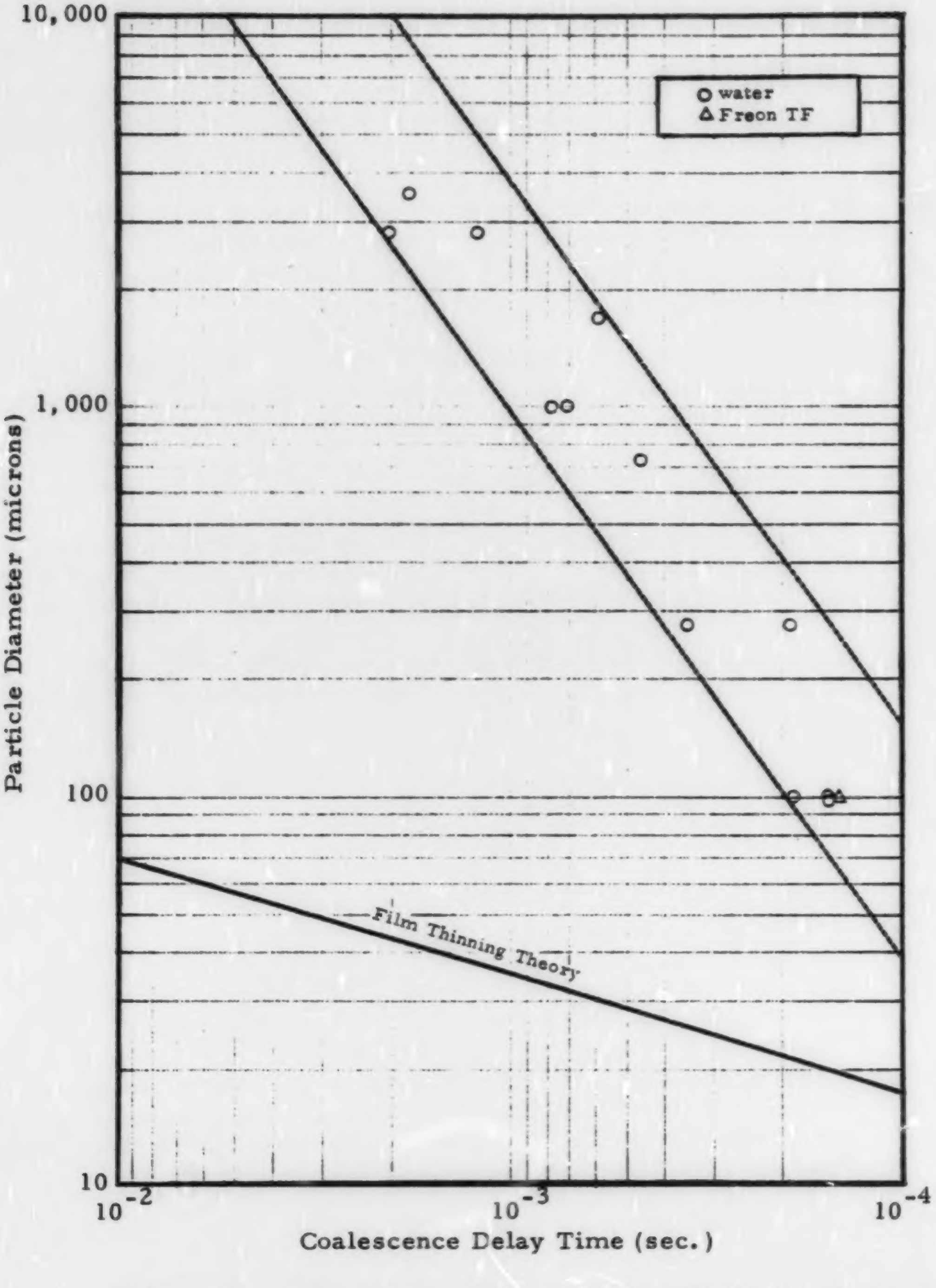

Figure 13. Comparison of theoretical predictions and experimental measurements of coalescence delay time.

REFERENCES

1. S. Calvert, J. Goldshmid, D. Leith and D. Mehta, "Wet Scrubber System Study, Volume I, Scrubber Handbook," APT, Inc. Report No. EPA-R2-72-118a, NTIS No. PB 213016, 1972.

2. S.M. Bughdadi, "Effect of Surfactants on Venturi Scrubber Particle Collection Efficiency," M.S. Thesis, Department of Thermal and Environmental Engineering, Southern Illinois University of Carbondale, 1973.

3. H.E. Wolfe and W.H. Andersen, "Kinetics, Mechanism, and Resultant Droplet Sizes of the Aerodynamic Breakup of Liquid Drops," Aerojet-General Corporation Report No. 0395-04(18)SP, 1964.

4. O. Reynolds, Phil. Trans. Roy. Soc., A(177):157 (1886).

5. S. Emory and J. Berg, "The Effect of Liquid Surface Tension on Solid Particle-Liquid Droplet Coalescence," University of Washington, Task Report EPA Contract No. 68-02-2109. (To be published)

6. S.B. Lang, "A Hydrodynamic Mechanism for the Coalescence of Liquid Drops," Ph.D. Thesis, Lawrence Radiation Laboratory Contract 7405-eng-48, 1962.

7. O.W. Jayaratne and B.J. Mason, "The Coalescence and Bouncing of Water Drops at an Air/Water Interface," Proc. Roy. Soc., A(280): 545 (1964).

8. M.H. Davis, "Collision of Small Cloud Droplets: Gas Kinetics Effects," J. Atmos. Sci., (29):911 (1972).

9. A.W. Adamson, Physical Chemistry of Surfaces, Second Edition, Interscience Publishers, New York, New York, 1960.

10. N. Arbel and Z. Levin, "The Coalescence of Water Drops, I. A Theoretical Model of Approaching Drops," Department of Geophysics and Planetary Sciences, Tel Aviv University, Ramat Aviv, Israel, February, 1977.

11. C.L. Strong, "The Amateur Scientist," Sci. Am., (230):104 (1973).

EPA MOBILE PARTICULATE COLLECTORS

A: PROGRAM INTENTIONS

Dale L. Harmon
Particulate Technology Branch
Industrial Environmental Research Laboratory
Research Triangle Park, N. C. 27711

B: CUPOLA FOUNDRY PARTICLE CONTROL WITH VENTURI AND SIEVE TRAY SCRUBBERS

D. L. Zanders
S. P. Schliesser
Monsanto Research Corporation
Research Triangle Park, N. C. 27711

ABSTRACT

The following two papers describe the EPA mobile particulate control units and the results of tests using the mobile scrubber unit to control the particulate emissions from an iron foundry cupola.

EPA MOBILE PARTICULATE COLLECTORS
PROGRAM INTENTIONS

Dale L. Harmon
Particulate Technology Branch
Industrial Environmental Research Laboratory
Research Triangle Park, N. C. 27711
April 1977

Introduction

The Environmental Protection Agency and predecessor organizations have been involved in development of systems for control of emissions from industrial sources for many years. The EPA R&D program for particulate control is designed to establish engineering design techniques and performance models, and to improve the collection capability and economics of control devices for particulate matter. The objective is the development and demonstration of control technologies capable of effectively removing large fractions of the under 3 micron diameter particles from effluents.

In 1973, EPA funded the design and construction of a mobile fabric filter unit, the first of a series of three mobile research units built for the assessment of the collectibility of particulate emissions from industrial sources. These units house the three types of conventional particulate collectors (fabric filter, wet scrubber and electrostatic precipitator) that are generally used by industry at the present time.

Actual data on particle collection efficiency of conventional particulate collectors is sparse. Actual operating data for the optimization of collection efficiency and cost is not readily available. Design of control equipment is presently based on projections from historical data which has been developed by manufacturers for their own devices and is proprietary. This information is not standardized and cannot be extrapolated to other devices. On-site testing prior to control device selection is seldom attempted and the possibility of alternative devices is poorly defined. The EPA mobile units are highly versatile and will be used to investigate the applicability of these control methods to the control of fine particulate emitted from a wide range of sources. The relative capabilities and limitations of these control devices will be evaluated and documented. This information, supplemented by data from other EPA particulate programs, will permit selection by equipment users of collection systems that are technically and economically optimum for specific applications. Operation of the mobile units will be coordinated with other EPA laboratories and regions to provide, when possible, field data on specific problem sources. Capabilities of the three mobile units are tabulated in Table I.

Fabric Filter Unit

The original mobile fabric filter unit was built by GCA Corporation for EPA and was mounted on an open 1360 Kg truck. The equipment could be operated on the truck or could be removed and operated at locations not accessible to the truck. The mobile filter unit can be adapted to cleaning by mechanical shaking, pulse jet or low-pressure reverse flow.

Filtration can be conducted at cloth velocities as high as 0.1 m/s with a pressure differential up to 50 cm of water, and at gas temperatures up to 290°C. Cleaning parameters can be varied easily over broad ranges. One to seven filter bags of any fabric media, 1.2 to 3m long and up to 30 cm in diameter may be used. Gas flows used are from 0.012 to 0.13 m^3/s, as determined by cloth velocity, bag size and bag number.

The mobile fabric filter unit in the above configuration operated on effluents from a brass and bronze foundry, a hot mix asphalt plant, a coal-fired boiler, a lime kiln and a pulp mill recovery boiler. Operation of the unit from the open truck was not satisfactory due to problems resulting from the weather, so the filter system was installed in a 12m closed trailer in October 1976. Since then the unit has been used to determine the performance of a fabric filter on air emissions from a cyclone collector used on the St. Louis Refuse Processing Plant. The unit is scheduled to be operated on a power plant burning a western subbituminous coal this month (April).

Wet Scrubber Unit

The second mobile unit received by EPA was the wet scrubber. This unit, built by the Naval Surface Weapons Center at Dahlgren, Va., was delivered in December 1974. The scrubber unit is in a 12m trailer and contains a venturi scrubber and a sieve tray scrubber. Maximum gas flow rate through the scrubbers is 0.28 m^3/s. Maximum L/G ratio is 0.01 m^3/m^3. The unit can treat gas at temperatures up to 480°C.

Figure I is a flow schematic of the scrubber unit. The inlet, through the side of the trailer, is equipped with four banks of electrical heaters to prevent heat loss of the effluent stream in the duct. A presaturator in the mobile unit precools the gas down below 175°C before treatment by the scrubbers. The presaturator can be bypassed if precooling is not required. After the presaturator the gas flow goes to either the sieve tray scrubber or the venturi scrubber.

The sieve tray scrubber is a four-tray tower designed for ease of operation and maintenance. Aluminum support plates secure each tray holder on three sides. High-density polyethylene flanges, bolted directly to the tray holders, are sealed on the holder side with O-rings. These flanges are individually machined to fit 46 cm OD Pyrex glass column sections, and hold an O-ring which seals against the outside diameter of the glass section. A clearance of approximately 0.16 cm on either end of each glass section allows the glass to "float" free of compressive or tensile stresses between tray holders. Three sets of trays are provided with varying hole diameters and hole spacing. The open area is the same for all trays. Trays are changed by unscrewing the two wing nuts on each tray cover, removing the cover and the old tray, inserting a new tray, and replacing the cover. One man can change the trays in about 5 minutes.

Three interchangeable venturis with different throat diameters are provided with the venturi/cyclone scrubber. The maximum pressure drop with the smallest venturi is about 250 cm w.c. Each throat is 30 cm long and accepts water dumped radially 5 cm from the throat entrance. After leaving the venturi, the scrubbed gas enters a cyclone which removes large droplets and/or particles and provides a drain for the scrubbing liquid.

A demister is located in the duct following the scrubbers to remove entrained droplets from the scrubbed gas stream before entering the blower and discharging to the atmosphere through a stack mounted on the trailer.

A 1700 liter capacity supply tank provides water for the entire system. After passing through the scrubbers, the scrubbing liquor drains to a sump tank mounted under the trailer. The liquid is pumped from the sump tank to an Industrial Filters Company deep-bed gravity filter mounted above the supply tank.

In both the scrubber and fabric filter mobile unit, a section of the trailer is partitioned off for a control room and analytical laboratory.

The mobile scrubber unit has been operated on a coal-fired power plant, on a lime kiln in a pulp and paper mill and on a gray iron foundry.

Electrostatic Precipitator Unit

The mobile electrostatic precipitator was delivered to EPA in September 1976. This system was also designed and built by the Naval Surface Weapons Center. The mobile ESP facility consists of two separate units mounted in 12m freight vans. Figure II is a floor plan of the two units. The first unit is the process van which houses a five-section ESP and all auxiliary equipment. This equipment consists of a diffuser section, a blower and cooling system, a screw conveyor for removal of collected material and transformer-rectifiers for high voltage connections. Each section of the ESP has a separate power supply which provides up to 50,000 volts and 7 milliamps DC. The precipitator is designed to operate at flow rates up to 1.4 m^3/s at temperatures up to 480°C.

The second unit is a control/laboratory van containing all process controls, monitors and recorders plus provisions for an analytical laboratory and equipment storage.

The mobile ESP facility is scheduled to be taken to the field for the first test in May 1977. It will be used to evaluate the effects of sodium conditioning on a low-sulfur western coal.

Summary

The original objective in building the mobile particulate control units was to operate all three units on the same source to compare the relative capabilities and limitations of the control methods on a given source. In practice the units, more frequently, have been used individually to answer specific control problems. These versatile mobile units should find wide applications in the future to fill both of these needs.

Table I. MOBILE PARTICULATE COLLECTOR CAPABILITIES

Characteristic	Mobile Fabric Filter	Mobile Scrubber	Mobile ESP
Trailer Length, m	12	12	12 (each of two)
Type Particulate Collector	1. Shake Clean 2. Pulse Clean 3. Reverse-Flow Clean	1. Venturi 2. Sieve Tray	1. 5-section ESP
Flow Rate, m^3/s	0.012 to 0.13	0.14 to 0.28[a]	0.47 to 1.4
Maximum ΔP, cm w.c.	50	250	66
Maximum Temperature, °C	290	480	480
Maximum Duct Length, m	30	30	30

---

[a] Sieve Tray limited to 0.24 m^3/s

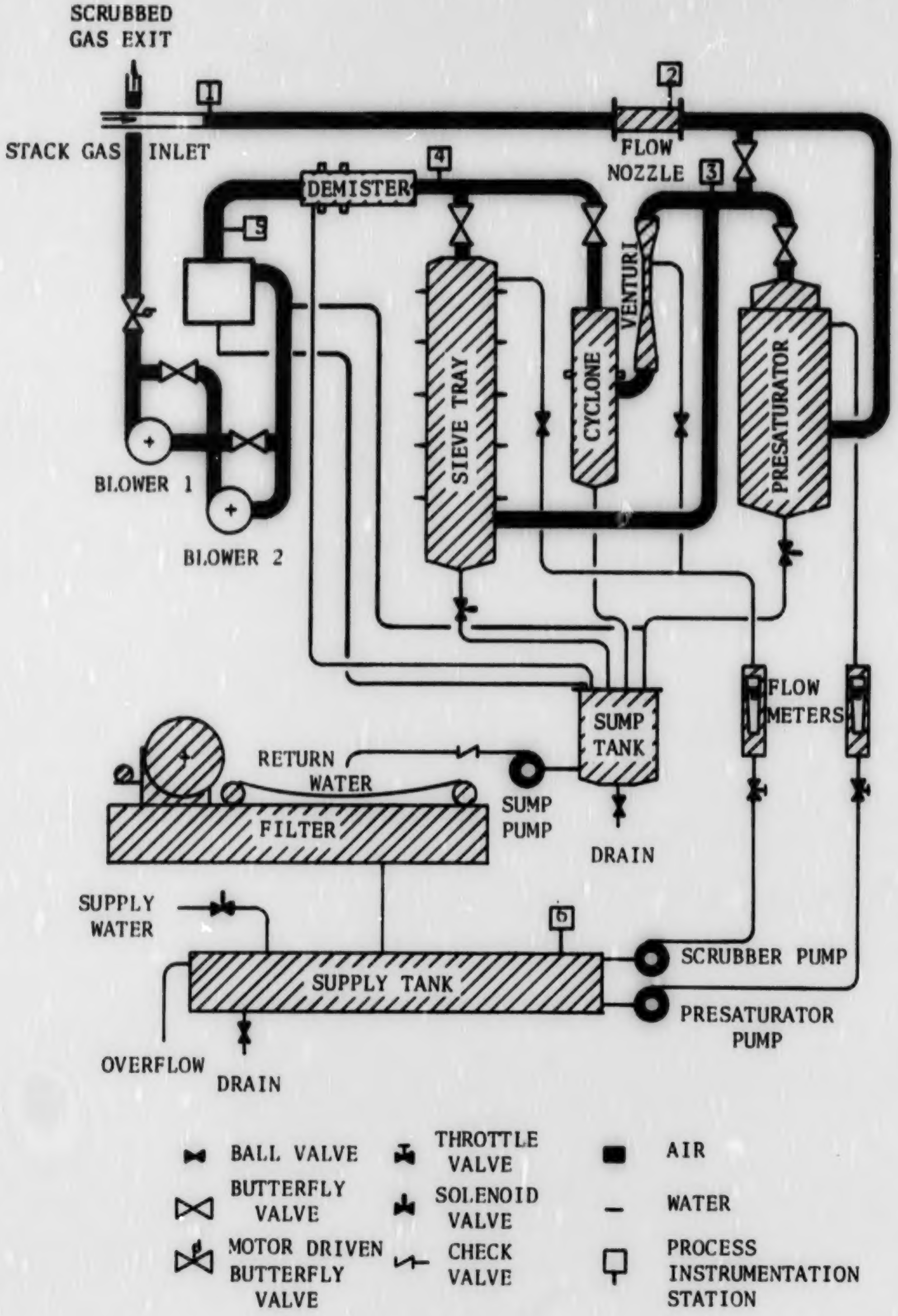
SCRUBBED
GAS EXIT
1
2
STACK GAS INLET
FLOW
NOZZLE
3
4
DEMISTER
5
VENTURI
SIEVE TRAY
CYCLONE
PRESATURATOR
BLOWER 1
BLOWER 2
FLOW
METERS
SUMP
TANK
RETURN
WATER
SUMP
PUMP
FILTER
DRAIN
SUPPLY
WATER
6
SCRUBBER PUMP
SUPPLY TANK
PRESATURATOR
PUMP
OVERFLOW
DRAIN
BALL VALVE
BUTTERFLY
VALVE
MOTOR DRIVEN
BUTTERFLY
VALVE
THROTTLE
VALVE
SOLENOID
VALVE
CHECK
VALVE
AIR
WATER
PROCESS
INSTRUMENTATION
STATION

Figure 1. Scrubber Flow Schematic.

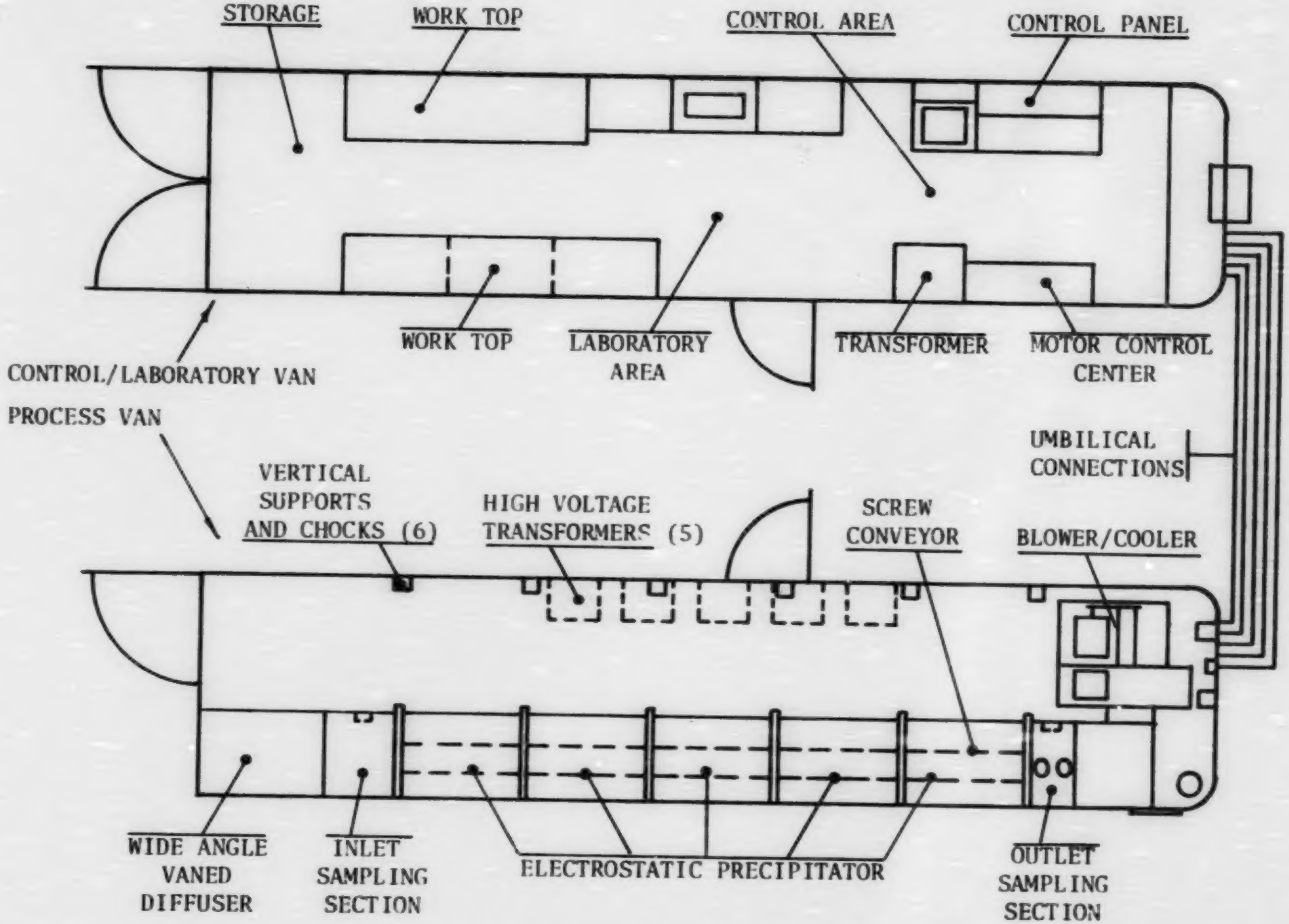
STORAGE
WORK TOP
CONTROL AREA
CONTROL PANEL
WORK TOP
LABORATORY AREA
TRANSFORMER
MOTOR CONTROL CENTER
CONTROL/LABORATORY VAN
PROCESS VAN
UMBILICAL CONNECTIONS
VERTICAL SUPPORTS AND CHOCKS (6)
HIGH VOLTAGE TRANSFORMERS (5)
SCREW CONVEYOR
BLOWER/COOLER
WIDE ANGLE VANED DIFFUSER
INLET SAMPLING SECTION
ELECTROSTATIC PRECIPITATOR
OUTLET SAMPLING SECTION

Figure 2. Plan View of Mobile ESP Facility.

CUPOLA FOUNDRY PARTICLE CONTROL WITH VENTURI AND SIEVE TRAY SCRUBBERS

by

D.L. Zanders and S.P. Schliesser
Monsanto Research Corporation

This paper shows results obtained from field testing the Industrial Environmental Research Laboratory mobile pilot scrubber unit on effluent from an iron foundry cupola.

SCRUBBER SYSTEM

The scrubber unit is mounted in a 40 ft trailer and has a processing capability of about 500 cfm of effluent gas depending upon operating conditions. Inside the trailer, two scrubber units are arranged as shown in Figure 1. The top half of the schematic shows the gas flow path - the bottom half the liquor flow path.

A stack gas slipstream is drawn through the unit beginning at the top left of the schematic, through a flow measuring device, presaturator, and into either one of two particle removal devices. These are followed by a mist eliminator, I.D. fans and a scrubbed gas exit stack.

Scrubbing medium is supplied to either unit from the supply tank. Liquor returns to the system from the bottom of the scrubber units into a sump tank, where it is then pumped to a solids removal filter. Clarified liquor is returned to the supply tank. Provisions are incorporated to treat the liquor in the filter bed and supply tank areas. Make-up liquor is attained through a piping arrangement to the supply tank.

One scrubber is a venturi type, with capability to vary the throat diameter. The other scrubber is a four tray tower with sieve type trays. This unit has the capability of varying tray hole size and spacing. Both units were tested on the cupola foundry.

PROGRAM INTENT AND SITE SELECTION

Intent of the testing program was to determine the fine particle collectability (3 micron and below) of these conventional type control devices as represented by the pilot scrubber system and measured by impactors and mass collection devices.

A commonly occuring foundry operation was selected based upon its previously determined fit within the ranges of over twenty characteristics of iron foundry operations in the following areas:

a. Feed Metal and Furnace Characteristics

b. Charge Characteristics

c. Fuel Characteristics

d. Effluent Characteristics

The selected cupola was a nominal four ton per hour hot blast operation producing gray iron castings.

TESTING PROGRAM

Sampling was conducted over a two month period, encompassing both inlet and outlet particle size distributions and mass loadings under varying operating conditions for each scrubber system.

Venturi Unit - Plans

Test plans for the venturi scrubber were to:

a. Look at collection performance as a function of pressure drop and liquid/gas ratio

b. Look at the dependency of collection efficiency on throat velocity

c. Investigate cooling and humidification effects

d. Look at the relationship between efficiency and pressure drop

A range of operating conditions were covered during the testing period as shown in Table 1.

TABLE 1

Range of Conditions

Variable	Range
Pressure Drop (in. H_2O)	20-60
Gas Rate (acfm)	250-600
L/G (gpm/kcfm)	6-30
Throat Velocity (ft/sec)	225-400

Venturi Unit - Results

Data obtained by varying the L/G ratio at fixed throat velocity are shown in Figure 2. Removal efficiency improved slightly but steadily through the studied range.

Varying throat velocity affected overall mass collection efficiency as shown in Figure 3. The influence here is considerably more noticeable.

Pressure drop influence is depicted in Figure 4, over the range of 20-60 inches of water.

The effect of additional humidification was looked at by operating at the same conditions with and without the use of the presaturator unit. This effect is illustrated in Figure 5.

A considerable body of data was gathered on the fractional removal efficiency of the venturi unit during the course of the testing program. This data includes fractional removal efficiency curves, cumulative size distributions and outlet differential size distributions. An illustration of commonly occuring data patterns is shown in Figure 6. This graph shows removal efficiency as a function of particle size from approximately 0.5 to 4.0 microns, as well as the measured effect on low and submicron particle removal by varying pressure drop in the venturi. The wide range of removal efficiencies measured indicate a high need to optimize operating conditions for a venturi type scrubber to attain the fine particle removal efficiency potential of such a device.

Sieve Tray Unit - Plans

The other unit in the EPA mobile scrubber system, the sieve tray scrubber, is not commonly applied to control foundry emissions. Test conditions covered were similar to the venturi regarding L/G ratios, but the pressure drop range was appreciably lower. Conditions covered for the sieve tray scrubber are shown in Table 2.

TABLE 2

Sieve Tray Testing Conditions

Variable	Range
Pressure Drop (in. H_2O)* **	12-15
L/G Ratio (gpm/kcfm)* **	10-30

* at two sieve hole sizes

** with and without humidification

Overall mass removal efficiency varied from 45-70% by weight (below the performance of the venturi unit) dependent primarily upon the liquid to gas ratio, with smaller effects observed from sieve plate hole size and pressure drop across the column.

Data gathered on the effect of L/G ratio for both small and large hole sieve trays used (.125 and .250 inch holes) indicated a divergent difference in performance characteristics as shown in Figure 7.

Examination of pressure drop influence showed fairly large data scatter cycling between 45-65% removal efficiency.

Humidification with the presaturator produced a slight increase in the overall collection efficiency of the tray scrubber.

Fractional removal efficiency for the tray scrubber was characterized by a very sharp drop in removal efficiency below the two micron level, with poor removal efficiency characteristics on submicron particles. An illustration of this is shown in Figure 8.

CONCLUSIONS

The following information and indications have been drawn from the test data gathered:

Venturi Scrubber

a. Measured overall mass removal efficiency varied from 45-96 weight% depending upon operating conditions

b. Throat velocity significantly affected overall mass removal efficiency

c. Gas presaturation appears to be beneficial to fractional removal efficiency in the low and submicron particle sizes, particularly in the submicron range

d. Measured fractional removal efficiencies as high as 70-80 weight% were achieved in the low and submicron particle sizes through optimization of scrubber system operating conditions

Sieve Tray Scrubber

a. Measured overall mass removal efficiency varied from 30-70 weight% depending on the operating conditions

b. Fractional removal efficiency showed a sharp decline below the 2 micron size, with poor removal in the submicron range

c. Presaturation of the incoming gas stream had a slight beneficial effect on removal efficiency

d. Over the range of variables tested, no optimization of fine particle removal efficiency was attained.

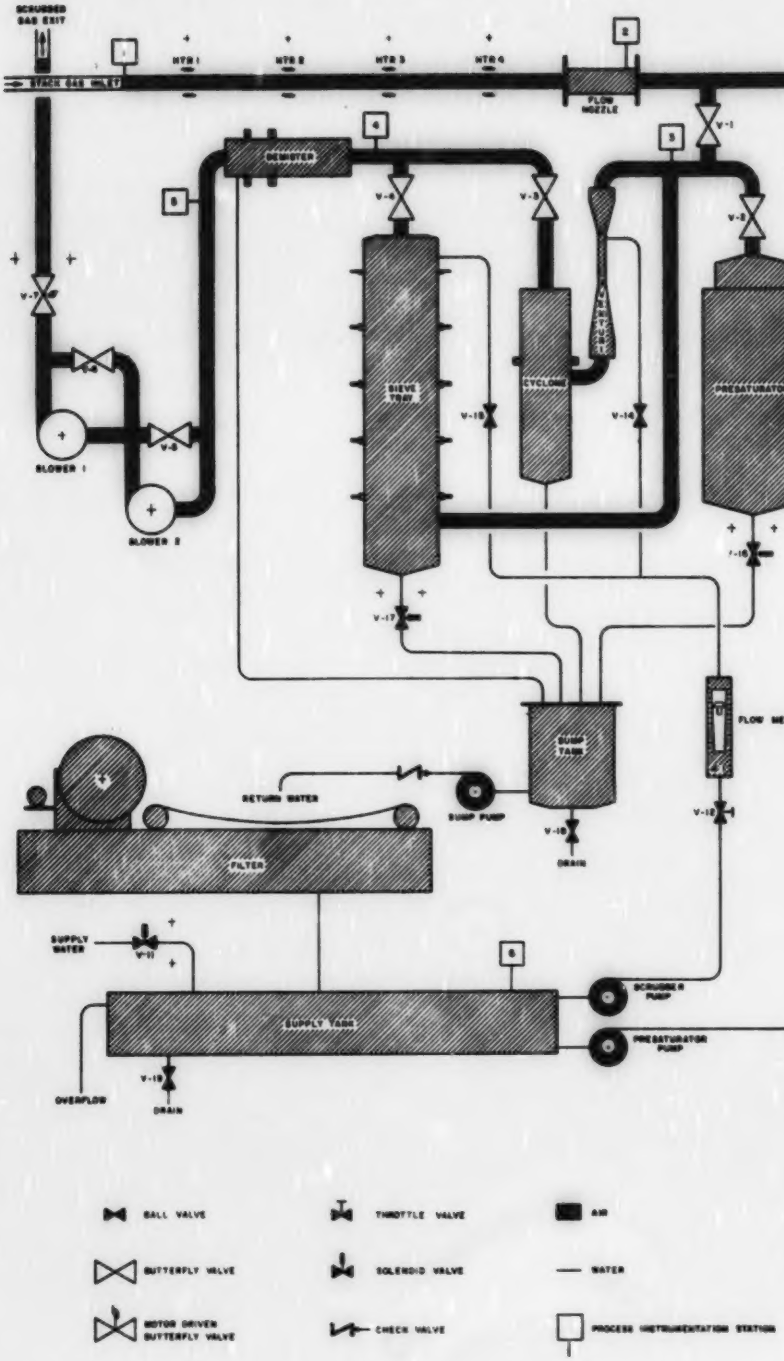
SCRUBBED GAS EXIT
STACK GAS INLET
1
HTR 1
HTR 2
HTR 3
HTR 4
2
FLOW NOZZLE
V-1
3
4
DEMISTER
5
V-4
V-3
V-2
V-7
V-8
V-9
BLOWER 1
BLOWER 2
SIEVE TRAY
CYCLONE
PRESATURATOR
V-15
V-14
V-16
V-17
SUMP TANK
FLOW METERS
RETURN WATER
SUMP PUMP
V-18
DRAIN
V-12
V-13
FILTER
SUPPLY WATER
V-11
6
SUPPLY TANK
SCRUBBER PUMP
PRESATURATOR PUMP
V-19
OVERFLOW
DRAIN
BALL VALVE
THROTTLE VALVE
AIR
BUTTERFLY VALVE
SOLENOID VALVE
WATER
MOTOR DRIVEN BUTTERFLY VALVE
CHECK VALVE
PROCESS INSTRUMENTATION STATION

Figure 1. Scrubber Flow Schematic.

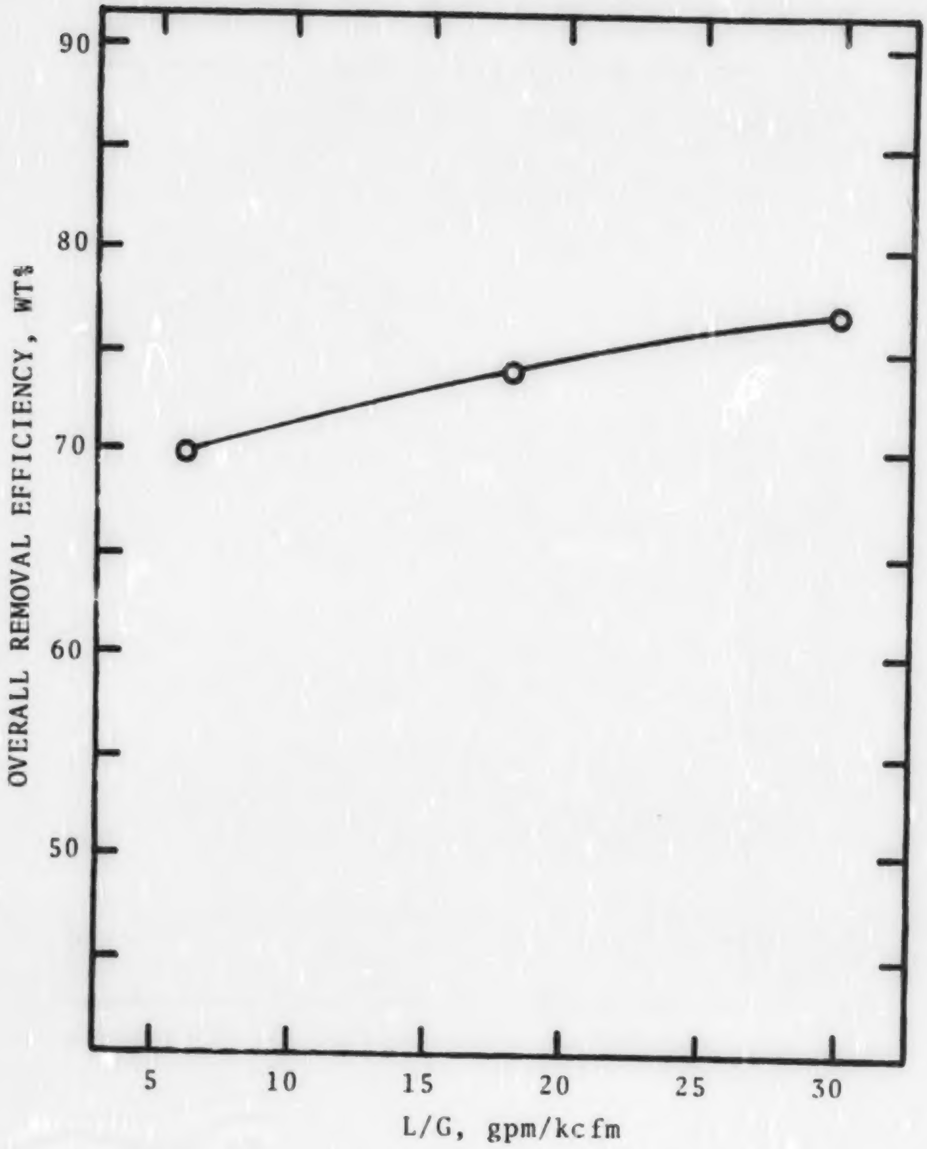

Figure 2. Effect of L/G ratio on Venturi Scrubber.

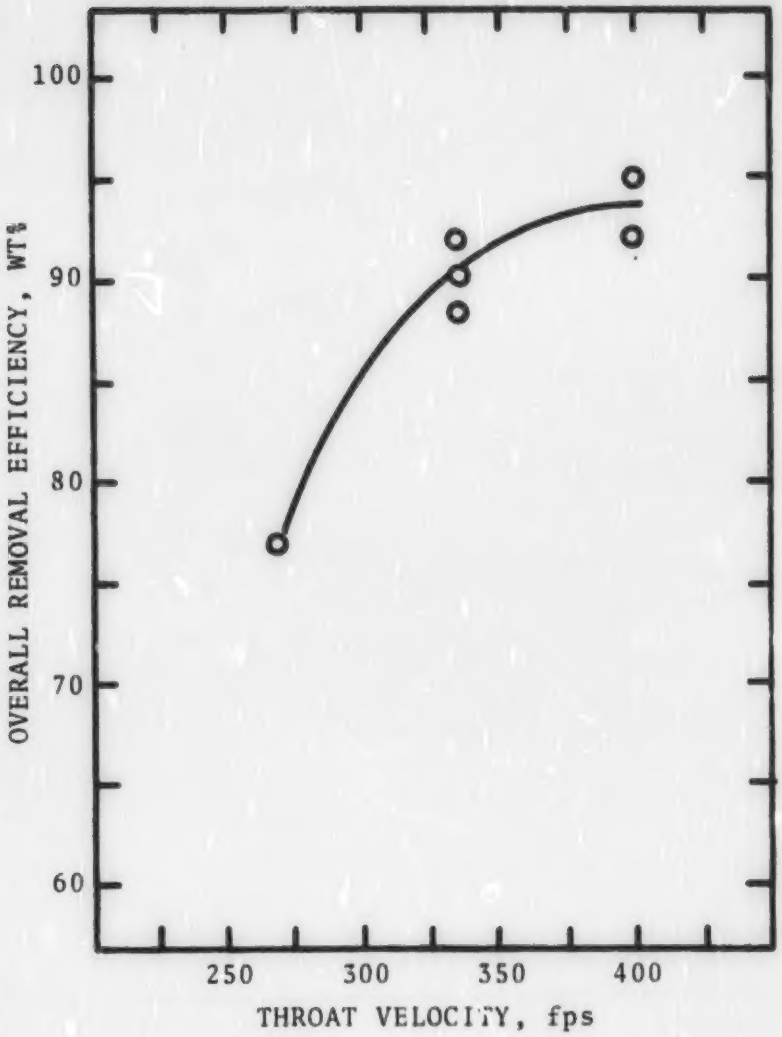

Figure 3. Effect of throat velocity on Venturi Scrubber.

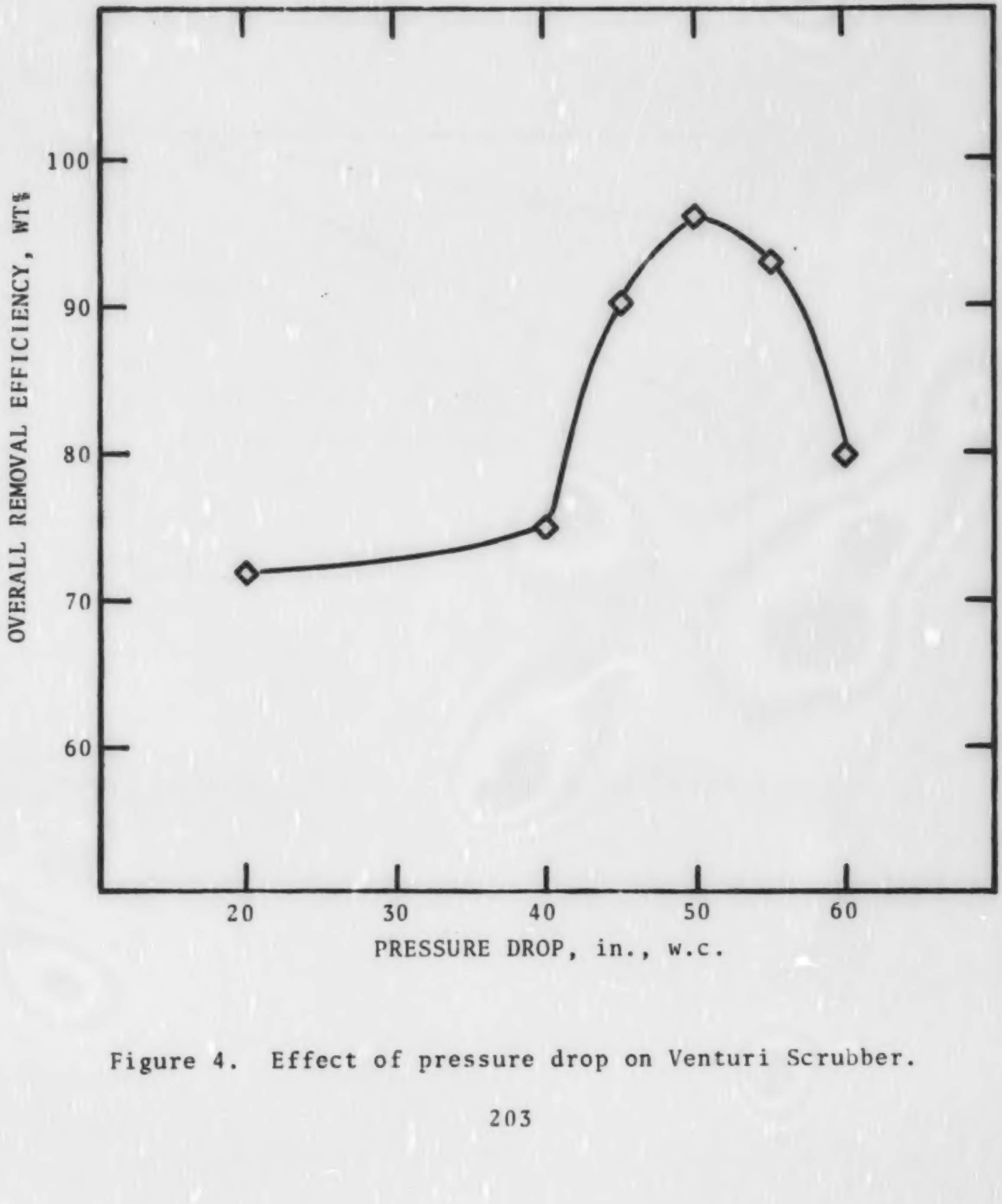

Figure 4. Effect of pressure drop on Venturi Scrubber.

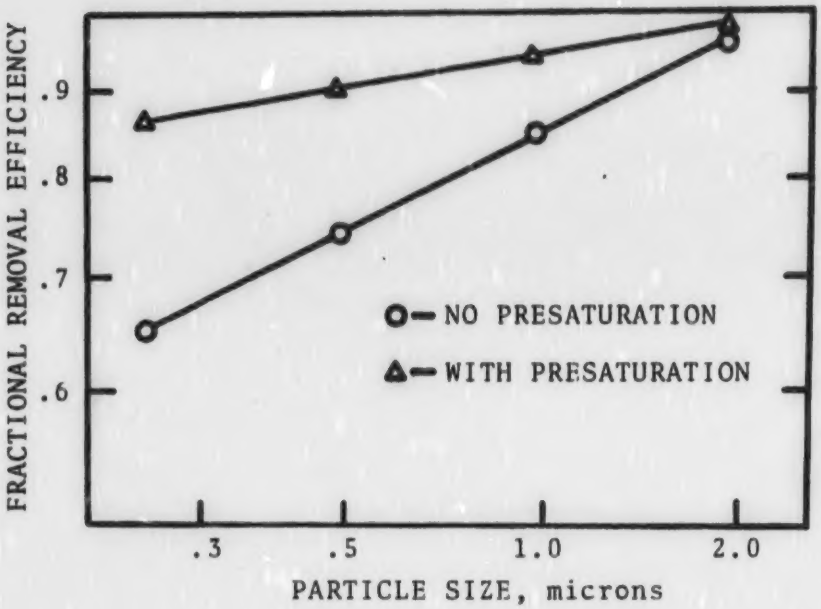

Figure 5. Effect of presaturation on Venturi Scrubber.

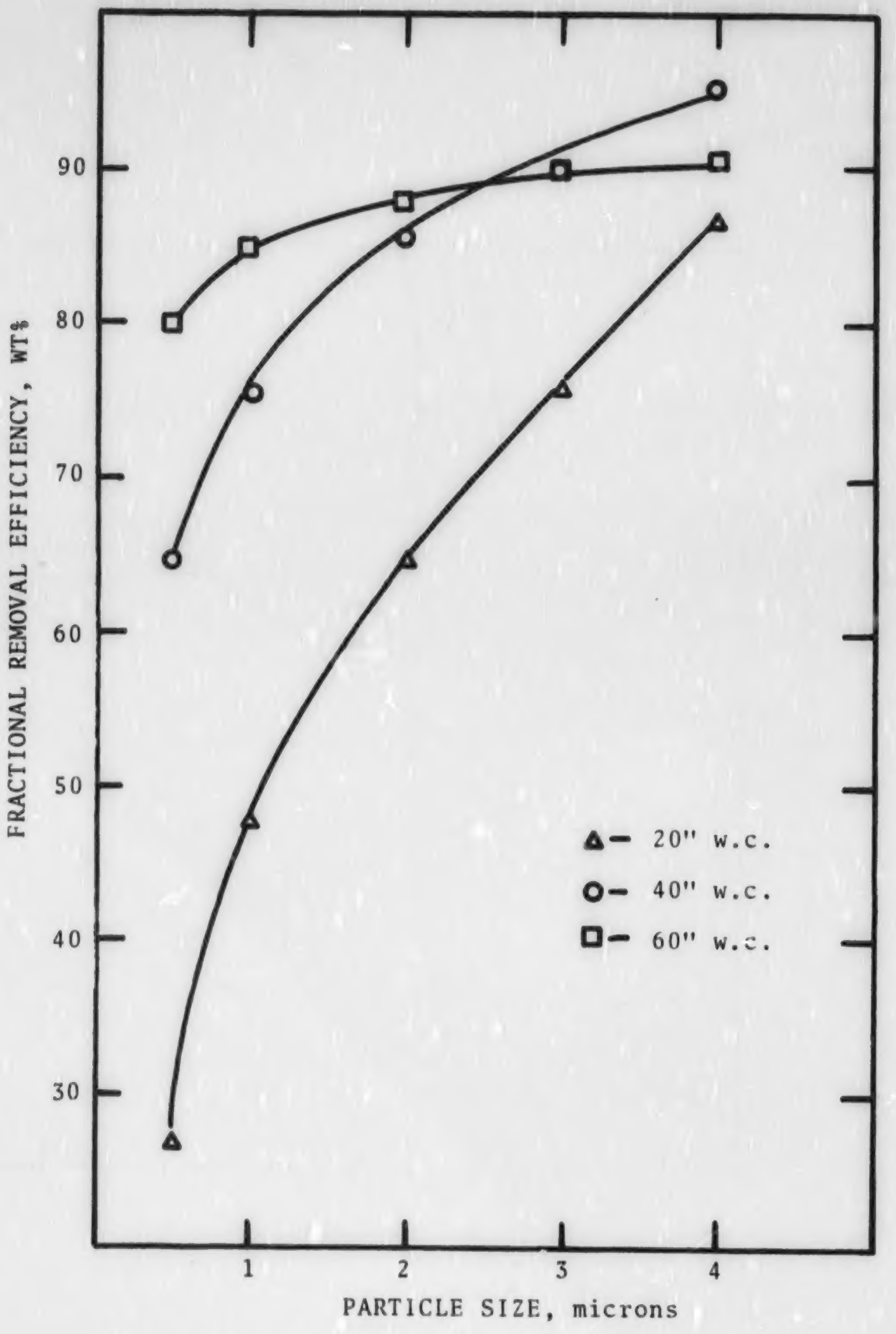

Figure 6. Fractional removal efficiency for Venturi Scrubber.

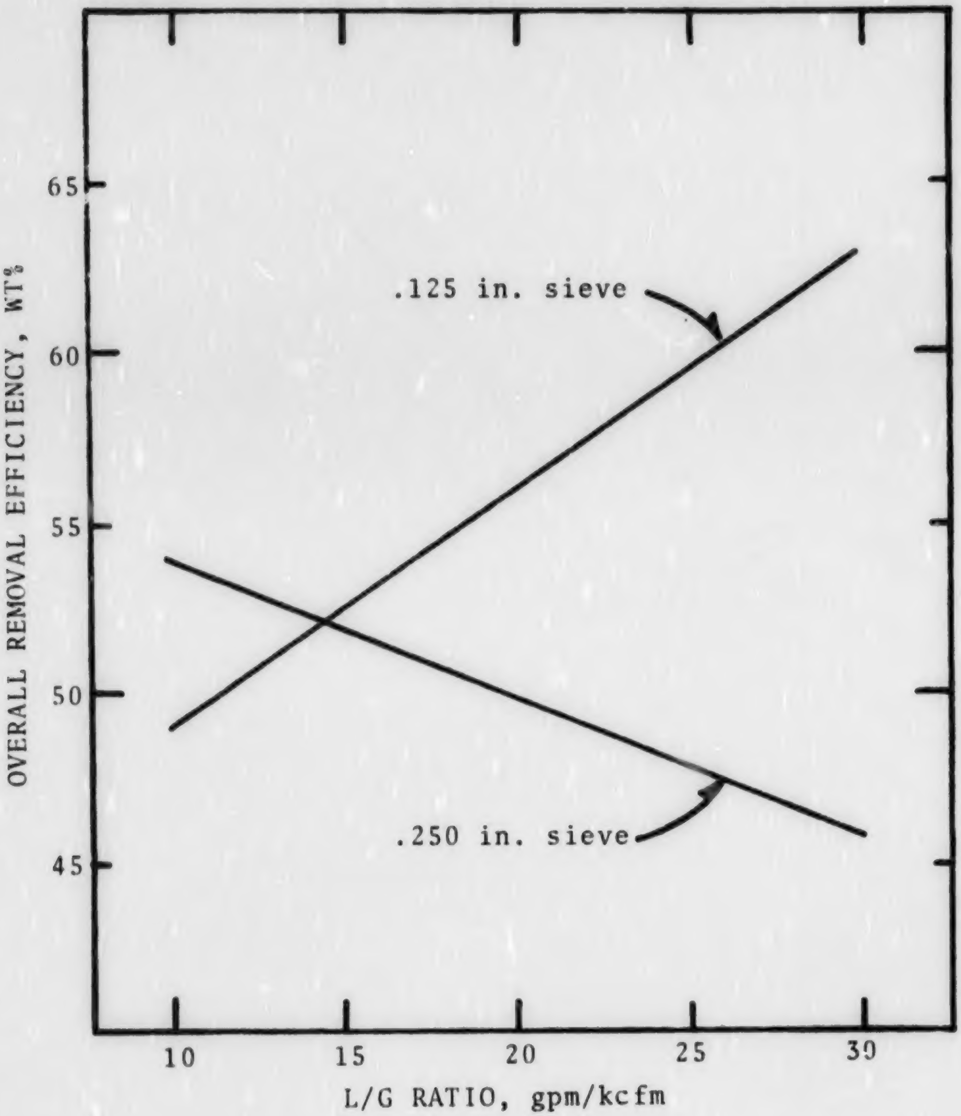

Figure 7. Effect of L/G ratio on Sieve Tray Scrubber.

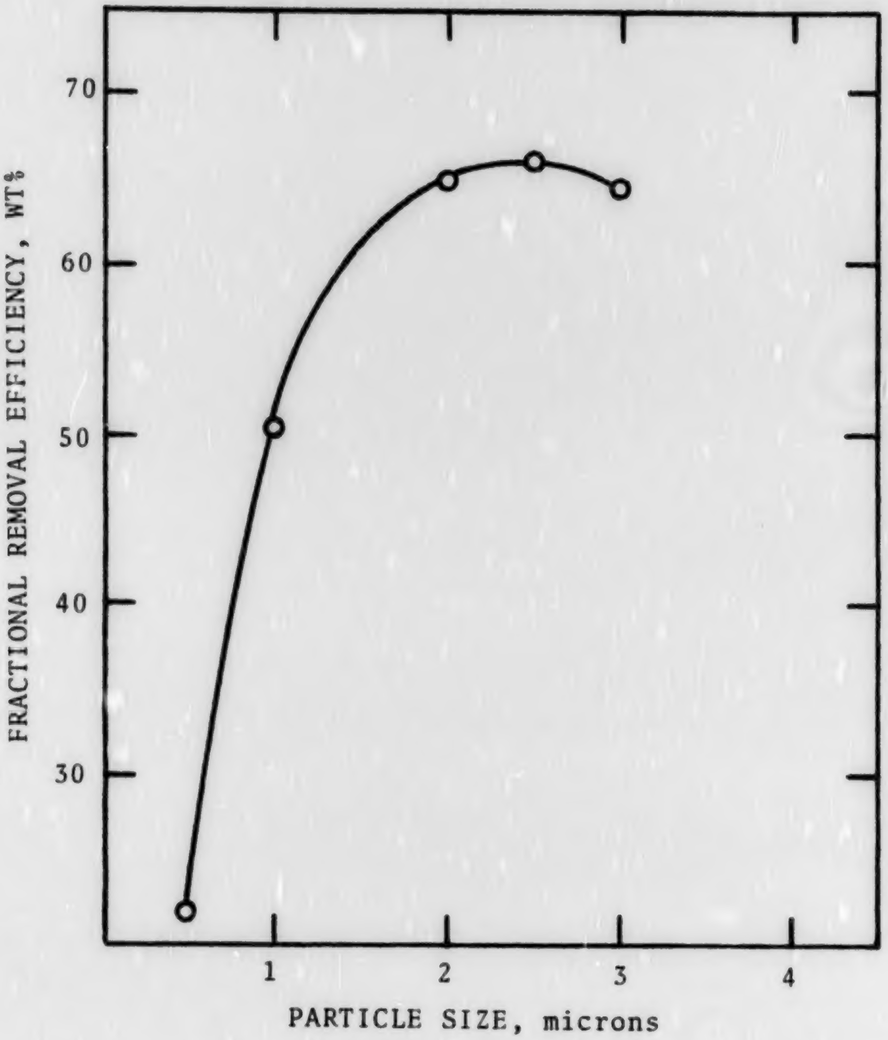

Figure 8. Fractional efficiency of Sieve Tray Scrubber.

FIELD TEST OF A VENTURI SCRUBBER
IN RUSSIA

Dennis C. Drehmel
Particulate Technology Branch
Industrial Environmental Research Laboratory
U.S. Environmental Protection Agency
Research Triangle Park, N.C. 27711

This paper discusses the performance test of a high pressure drop venturi scrubber operating on an electric arc furnace at the Nikopol Ferroalloy Plant in the Ukrainian Soviet Socialist Republic. The overall scrubber collection efficiency averaged about 99.9 percent, with greater than 98.6 percent for submicron particles. These tests were performed as part of a technology exchange program between the U.S. and the U.S.S.R.

Preceding page blank

FIELD TEST OF A VENTURI SCRUBBER IN RUSSIA

Introduction

Because of the adverse effect of pollution on public health and welfare, the United States of America and the Union of Soviet Socialist Republics have independently developed pollution control methods to protect the environment from liquid, solid, and gaseous contaminants. In 1972, with recognition of the mutual benefits that could be gained from technology exchange, the United States and the U.S.S.R. signed a bilateral agreement pledging cooperation on environmental protection. As a part of this agreement, a working group on stationary source air pollution control was formed by the U. S. Environmental Protection Agency and the U.S.S.R. Research Institute of Industrial and Sanitary Gas Cleaning to define joint programs.

The planned cooperative programs encompass several areas of air pollution control technology, including particulate emission control. High mass-collection efficiencies are now achieved on particulate emissions from industrial processes in both countries by utilizing electrostatic precipitators, fabric filters, wet scrubbers, and novel devices. Growing concern for the health and environmental effects of fine particulate emissions (3 microns or smaller) has resulted in a need for further improvement of conventional control techniques and for the development of new techniques for fine particulate control.

In order to exchange technology on fine particulate control, a joint testing program was established. Soviet specialists would visit the U.S. to test with U.S. experts a hot-side electrostatic precipitator and U.S. experts would join Soviets to test a high efficiency scrubber in the U.S.S.R. This paper discusses the second part of that program. The high efficiency scrubber selected was a high pressure drop venturi scrubber on an electric arc furnace at the Nikopol Ferroalloy Plant in the Ukrainian Soviet Socialist Republic.

Description of the Test Site and Scrubber

The Nikopol Ferroalloy Plant produces silicomanganese with electric arc furnaces each of which consists of a rectangular bath and six oval electrodes. The electrodes are supplied power by three 21,000 KVA transformers. The rectangular bath is 20.3 m long by 6.0 m wide by 3.2 m high and has three tapholes. The furnaces operate continuously except for scheduled outages averaging one day per month.

The gases leaving the furnace are primarily carbon monoxide (64-88%) and carbon dioxide (7.5-24.0%). Other constituents are shown in Table 1. The gases contain as much as 20 g/Nm^3 of particulate matter which is primarily silica (12-15%) and manganese oxide (10-16%). The particulate size is initially small; that is, substantially less than 1 μm. However, the particles agglomerate to shift the mass median diameter to as high as 3 μm.

The particulate control system consists of a series of scrubbers shown in Figure 1. The first scrubber, which is item 1 in Figure 1, is an inclined gas line (500 mm in diameter) into which water is sprayed by two centrifugal injectors. The second scrubber (item 2) is a spray chamber (1000 mm in diameter) which contacts the gas countercurrently. The third scrubber (item 3) is a venturi scrubber (100 mm in diameter) with a pressure drop of 22 to 24 kPa. The venturi scrubber is followed by a cyclone mist eliminator (item 4). The scrubbing water flow rate for each injector in the inclined scrubber and for the venturi scrubber is 7 m^3/hr. Also shown in Figure 1 are the exhaust draft fan (item 5), the filter press (item 6), the liquor recycle pump (item 7), the sedimentation tank (item 8), and the cooling tower (item 9).

Experimental

Measurements to determine performance of the venturi scrubber were made before the venturi and after the mist eliminator. Figure 2 shows the location of the sampling ports. Because sampling ports were not available in the gas line before the venturi, ports in the spray chamber scrubber were used for inlet sampling and the water to the spray chamber scrubber was turned off. Outlet sampling was conducted on a long run of gas line after the mist eliminator.

Mass concentrations and mass emission rates were determined using an EPA Method 5 probe. However, only single point sampling was used because of the small duct sizes and because of the problems in maintaining gas tight seals to prevent combustion of the carbon monoxide rich flue gas. Particle size measurements were made using cascade impactors: Brink at the inlet; and Andersen at the outlet. Both impactors used glass fiber collection substrates for the stages and a glass fiber final filter for collecting particles which penetrated the impaction stages.

Results and Discussion

Particulate concentrations into and out of the venturi scrubber are shown in Table 2. The average inlet concentration is 5.19 g/Nm^3; outlet, 5.94 mg/Nm^3 and the average efficiency is 99.89 percent. Results of particulate sizing data give a log normal size distribution with an average mass median diameter (MMD) at the inlet of 1.7 μm with a geometric deviation (σg) of approximately 2. At the outlet the MMD is 0.42 μm and the σg is between 2 and 3. The fractional efficiencies are given in Table 3. The collection efficiency for particles greater than 1 μm in diameter is greater than 99.9 percent. As the particle diameter decreases to 0.3 μm the efficiency decreases to 98.6 percent.

The total penetration of the scrubber may be predicted by equation 8.2-12 of the Scrubber Handbook(1). This equation combines an assumed log normal particle size distribution with the equation for penetration of a monodispersed aerosol through a venturi scrubber. Equation 8.2-12 can be solved by integrating with respect to particle size. This integration was made using the extremes in gas flow rate which gave the extremes in throat velocity and hence the extremes in total penetration. For a flow rate of 2180 Nm^3/hr, the throat velocity is 76.04 m/s and the predicted efficiency if 99.84 percent. For a flow rate of 2500 Nm^3/hr, the throat velocity is 88.42 m/s and the predicted efficiency is 99.94 percent. The predicted overall efficiencies bracket the observed overall efficiency of 99.89 percent.

With respect to fractional efficiencies, the efficiency for a single particle size may be calculated from equation 5.3.6-5 of the Scrubber Handbook. The predicted values from this equation are greater than 99.9 percent for all particle sizes noted in Table 3 except for 0.3 µm. At this smallest particle size, the predicted efficiency ranges from 93.8 to 98.2 percent depending on the velocity in the throat used in the calculations. When all experimental and predicted fractional efficiencies are compared, the predicted values differ from experimental ones by less than 0.7 percentage units and are higher for all particle sizes except for 0.3 µm where the predicted value is lower.

Conclusions

A high pressure drop venturi scrubber at the Nikopol Ferroalloy Plant (USSR) was tested for total and fractional collection efficiency of electric arc fume. At a pressure drop of 22 to 24 kPa, the overall efficiency of the scrubber ranged from 99.86 percent to 99.92 percent. The collection efficiency for particles larger than 1 µm in diameter was greater than 99.9 percent and for those smaller than 1 µm was greater than 98.6 percent. These experimental results are consistent with predicted values from theoretical equations.

Acknowledgements

The author wishes to acknowledge the work of Soviet specialists and technicians who used the U. S. equipment to produce the raw data from these tests. Moreover, Mr. Bruce Harris of the U. S. Environmental Protection Agency and Mr. Joseph McCain of Southern Research Institute supervised the taking and reduction of the measurement data at the Nikopol Ferroalloy Plant. The SR-52 program for integration of the scrubber equations to calculate all penetrations was provided by Dr. Leslie Sparks of the U. S. Environmental Protection Agency.

Table 1. Properties of Nikopol Electric Arc Flue Gas

Composition by volume percent

CO	64-88
O_2	0.4-1
CO_2	7.5-24.0
H_2	3.0-6.0
CH_4 and N_2	<8

Dry gas density - 1.3 kg/Nm^3

Heat value - 9000 KJ/Nm^3

Water vapor content - less than 20%

Particulate concentration - 15 to 20 g/Nm^3

Particulate composition in percent of mass

S_1O_2	12-15
MnO	10-16
CaO	4-5
NiO	3-4
Al_2O_3	1-3
C	7-10

Table 2. Results of Concentrations Measurements at Inlet and Outlet of Nikopol Scrubber

Day (July)	Inlet g/Nm^3	Outlet mg/Nm^3	Efficiency %
28	4.37	3.55	99.92
29	5.69	5.85	99.90
30	4.76	6.49	99.86
30	3.72	4.77	99.87
31	- - -	5.85	- - -
31	7.42	9.13	99.88
Overall	5.19	5.94	99.89

Table 3. Nikopol Scrubber Fractional Efficiency

Aerodynamic Diameter μm	Inlet Incremental Concentration mg/m^3	Outlet Incremental Concentration mg/m^3	Collection Efficiency %
5.0	1500	0.85	99.94
3.0	5700	0.59	99.99
2.0	7400	1.14	99.98
1.3	6100	1.29	99.98
0.8	1050	1.63	99.84
0.5	400	2.60	99.35
0.3	280	3.90	98.61

Figure 1. **NIKOPOL SCRUBBING APPARATUS**

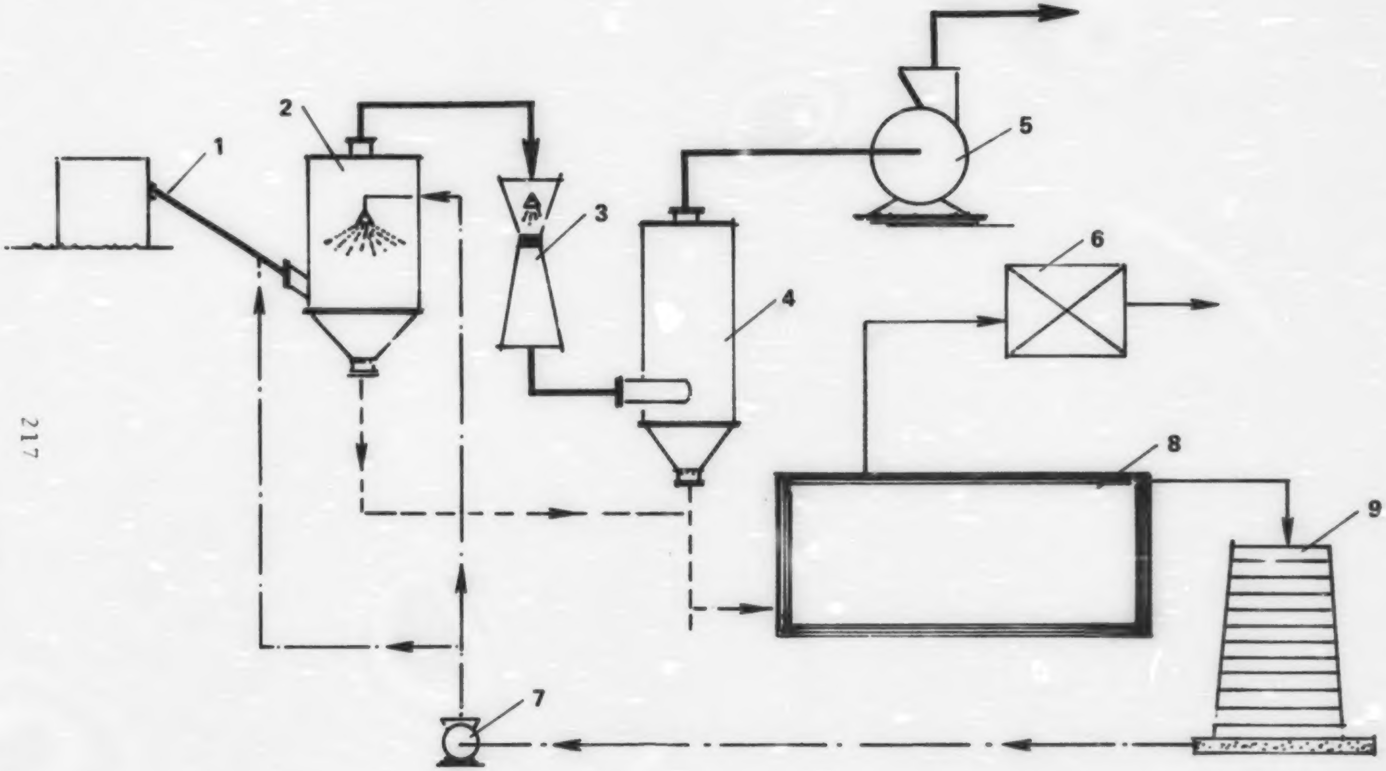

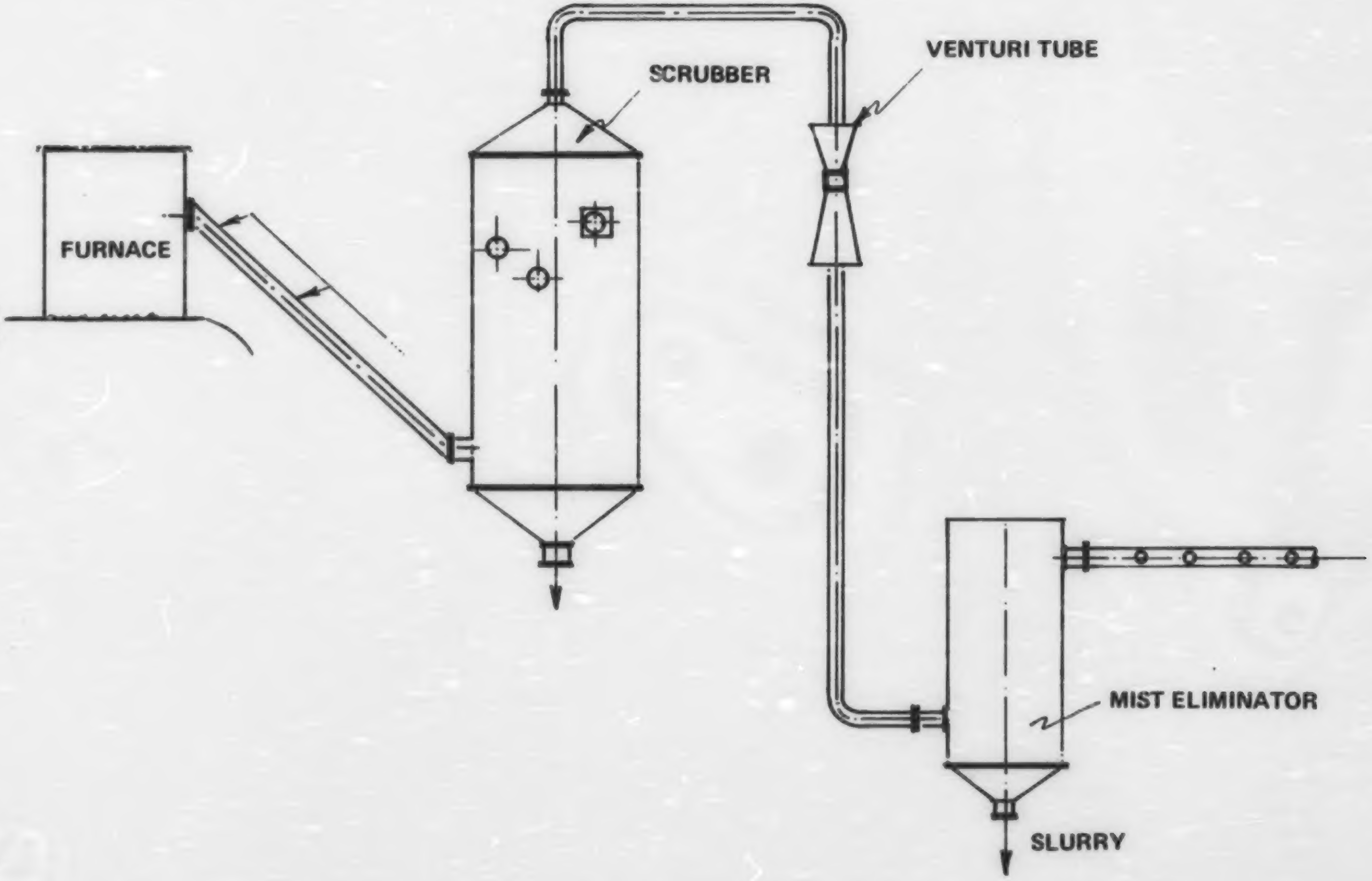
FURNACE
SCRUBBER
VENTURI TUBE
MIST ELIMINATOR
SLURRY

Figure 2. Nikopol Scrubber Sampling Port Locations

Reference

1. S. Calvert, J. Goldshmid, D. Leith, and D. Mehta, Scrubber Handbook, EPA Report No. EPA-R2-72-118a, NTIS No. PB-213-016, August 1972.

A.P.T. FIELD EVALUATION OF FINE PARTICLE SCRUBBERS

Seymour Calvert
Shui-Chow Yung
Harry Barbarika
Gary Monahan

Air Pollution Technology, Inc.
San Diego, California 92117

Leslie E. Sparks
Dale L. Harmon

U.S. Environmental Protection Agency
Industrial Environmental Research Laboratory
Research Triangle Park, North Carolina

ABSTRACT

The performance of thirteen industrial scrubber systems have been determined experimentally. The performances are reported in terms of grade penetration curve and cut/power relation.

The measured performances of these scrubbers are compared with predictions of design equations. In cases where design equations are not available, they are developed from basic theories. Except for the design equation for the mobile bed scrubber, design equations for other types of scrubbers tested give reasonable performance predictions.

The scrubber performance, expressed as the cut diameter versus power relationship developed by Calvert has been verified and extended with the performance data.

Preceding page blank

INTRODUCTION

The need for more reliable data on the fine particle collection efficiency of air pollution control scrubbers has become increasingly apparent as control requirements have grown more demanding. Major efforts, such as the Wet Scrubber System Study (Calvert et al.,1972), which resulted in the issuance of the "Scrubber Handbook", have augmented our ability to design better scrubbers and to predict their performance. Design methods, including mathematical models, have been developed from basic theory plus whatever good data were available, but to a large extent they were untested. Thus, one could not confidently predict performance for present scrubber designs and operating conditions or extrapolate into better combinations of design and operation.

It is very difficult to compare scrubber performances in different situations without knowing efficiency as a function of particle size, commonly called "grade efficiency". Even on an empirical basis, there had been so few carefully and properly conducted performance tests that the capabilities of existting systems were not known. Because of a predominant concern for only the outlet particulate loading or emission rate, collection efficiency in terms of overall particle mass was rarely tested. The few data which had been published were generally unsatisfactory for use because of inadequate methodology, undefined parameters, insufficient quantity, and similar inadequacies.

The program reported here was supported by EPA over the past 5 years and was initiated in response to the need for additional reliable performance data on fine particle scrubbers. The objectives were to obtain data on fine particle collection efficiency as a function of particle size for scrubbers operating on representative industrial emission sources and to reconcile the performance data with existing mathematical models.

FIELD SAMPLING METHOD

The method of approach to the program objectives involved a number of experimental determinations to obtain collection efficiency data, the acquisition of information on system characteristics and behavior, and computations which utilized the performance data and mathematical models. Over the course of the program the methods and apparatus used were generally improved and were modified to suit each specific test situation, but the main features were similar and will be described here.

The most important experimental measurements were those regarding particle size and concentration. In the beginning of the program the size range of primary interest was from a few tenths to a few microns diameter, which is within the measurement range of a cascade impactor. Later the size range was extended downward by an order of magnitude and it was necessary to use a diffusion battery in addition to the cascade impactor. The apparatus and methods used are outlined below:

1. Gas velocity distribution and parameters had to be measured at the inlet and outlet of the scrubber in order to define the following:

   a. conditions for isokinetic sampling,
   b. particle concentration per unit volume of dry gas, and
   c. gas flow rate.

Methods to measure these parameters are:

Parameter	Equipment	Method
Gas velocity and flow rate	Standard pitot tube or calibrated type "S" pitot tube; differential pressure gauge.	EPA method 1; EPA method 2.
Gas temperature	Calibrated thermocouple or mercury filled glass-bulb thermometer.	
Humidity	Thermometers.	Wet and dry bulb temperature measurement on a flowing sample withdrawn from the duct.
Pressure	Inclined water manometer or a pressure gauge.	Measured by means of a static pressure tube inserted in the duct.

2. The most essential part of the scrubber performance tests is the determination of particle size distribution and concentration (loading) in the inlet and outlet of the scrubber. For accurate determination of particle size distribution, a mechanism that collects particles and causes neither formation nor break up of aggregates is necessary. Cascade impactors come close to meeting these requirements.

In a cascade impactor, particles are classified by inertial impaction according to their mass. The larger ones are collected on the plate opposite the first stage and the smallest on the plate opposite the last stage. A.P.T. uses Brink, Andersen University of Washington Mark III, and a cascade impactor of A.P.T.'s own design for particle size fractionation. These impactors (except Brink) classify particles into seven size groups and are capable of sizing particles down to about 0.1 μm diameter.

In order to minimize probe losses all tests were made with the impactors in the duct and with the inlet nozzles appropriately sized to give isokinetic sampling. A modified EPA Method 5 train was used to monitor the sample gas flow rate.

In some tests, a pre-cutter was used to remove either the heavy particle loading from inlet samples or the entrained liquid from outlet samples. A cyclone separator with about a 3 μmA cut diameter was first used but a round jet impactor with about an 8 μmA cut diameter was found to have better characteristics and was adopted for use for both inlet and outlet sampling. The impactors were either given time to reach the duct gas temperature or heated to prevent moisture deposition.

To increase the weighing accuracy, each impactor collection plate was lined with light-weight substrate. Generally, either greased aluminum foil or a glass fiber filter paper substrate was used. Impactor substrates and backup filters were weighed with an analytical balance to the nearest tenth milligram (10^{-4}g).

Particle size distribution and loading measurements were conducted simultaneously at the scrubber inlet and outlet. The method minimizes the effects of particle size distribution changes caused by fluctuations in the operation parameters. Since the program objective was to investigate scrubber performance on fine particles, the sampler was held at one location in the duct for the duration of each sampling run. This is an adequate technique for obtaining good samples of particles smaller than a few microns in diameter because they generally are well distributed across the duct.

RESULTS

A summary of the scrubbers tested is given in Table I. The first ten scrubbers in Table I are classified as conventional scrubbers. The last three are novel devices because they are different in some manner from conventional technology.

The dashed lines in Figures 1 through 10 are experimental grade penetration curves. They were computed from simultaneous inlet and outlet particle size/concentration data. The penetrations were obtained from a plot of the cumulative particle mass concentration versus particle aerodynamic diameter. We use the symbol "µmA" for aerodynamic diameter, which is equal to particle diameter (d_p) in µm (microns) times the square root of the particle density (ρ_p) in g/cm³ times the square root of the Cunningham slip correction factor (C'). The computation of penetration (penetration is equal to 1 minus efficiency) as a function of particle diameter is based on the following equations.

Overall penetration can be defined as:

$$\overline{Pt} = \frac{1}{C_{pt}} \int_o^{C_p} (Pt)_{d_p} \, dCp \qquad (1)$$

Penetration for particles with diameter d_p is given by:

$$(Pt)_{d_p} = \frac{f(d_p)_{outlet}}{f(d_p)_{inlet}} = \frac{\left[\frac{dC_p}{d(d_p)}\right]_{outlet}}{\left[\frac{dC_p}{d(d_p)}\right]_{inlet}} \qquad (2)$$

"$\left| dC_p/d(d_p) \right|$" is the slope of the cumulative mass versus aerodynamic diameter plot. It may be obtained either by a stepwise graphical procedure or by fitting a mathematical function to the data point and then evaluating the slope analytically.

DISCUSSION

Comparison of the experimental results with mathematical models was done wherever models were available. Table II is a list of the design equations taken from the "Scrubber Handbook". All these equations are based on particle collection by inertial impaction.

The predicted grade penetration curves are represented by the solid lines in Figures 1 through 10. By comparing the predicted and the measured grade penetration curves, we can either verify or reject the design equations. The results of this comparison are summarized as follows:

1. Valve tray on urea prilling tower - No specific performance model was available for a valve tray so it was necessary to develop one. We used the model for sieve plates because the gas jets emerging from the slots between the valve cap and the tray impinge on a liquid froth similar to the round gas jets on a sieve plate. The model compared well with the data after accounting for particle growth due to water vapor condensation.
2. Vaned centrifugal on KCl dryer - The collection efficiency of this scrubber could not be accounted for simply by centrifugal deposition caused by the internal vanes. A gas atomized spray model gave predictions which agreed with the data.
3. Mobile bed on coal-fired boiler - No satisfactory model is available. The mobile bed design equation is a semi-empirical correlation proposed by Bechtel based on the data reported by UOP. It was developed on the assumption that collection efficiency is due to inertial impaction on the balls.
4. Venturi on coal-fired boiler - The model for a venturi in terms of particle cut diameter correlated with pressure drop agrees well with the experimental results.

5. Wetted fiber on NaCl dryer - Heated impactors were used in the field sampling. Thus, the measured particle size is that of a dry particle. In the scrubber, dry particle size is not the actual size the scrubber will see. The scrubber sees a wet particle which is larger. We did not measure the wet particle size in the field. Common salt particles are highly hygroscopic. According to Junge (1963) the physical diameter of the particle will increase to about 5 times that of the dry salt particle at high humidity and about double at 75% relative humidity.

   Wet particle diameter was calculated from dry particle diameter with the assumption that its physical diameter is doubled. Calculation results are shown in Figure 5. The filters in the filter pad were ellipsoidal in shape with the longer axis normal to the direction of gas flow. Therefore, its collection efficiency should lie somewhere between the collection efficiencies of a ribbon and a cylinder.

   It can be seen that the model agrees with the calculations for wet particles.
6. Impingement plate on NaCl dryer - A model based on impingement from round jets gives good agreement with the data after allowing for particle growth due to condensation.
7. Venturi rod on cupola - The venturi model gives a good prediction for particles larger than about 1.0 μmA but does not account for low penetration for the sub-micron particles.
8. Venturi on asphalt dryer - The venturi model prediction agrees with the performance data.
9. Venturi on borax fusing furnace - The model agrees with data for particles with diameter larger than 1 μmA. For particles smaller than 1 μmA diameter, the model predicted penetration a few percent higher than measured.
10. Variable rod on cupola - The model predicted penetration higher than that measured.

CUT/POWER RELATIONSHIP

When scrubbers are operated at different pressure drops it is very difficult to evaluate and to compare their performances based only on grade penetration curves. We have developed a useful correlation called the cut/power relationship for this purpose and others. The cut/power relationship is a plot of the cut diameter given by the scrubber against pressure drop or power input, as illustrated in Figure 11. Cut diameter is the particle diameter whose collection efficiency is 50%. The solid lines in this graph were calculated theoretically from the design equations presented in the "Scrubber Handbook."

The performance cut diameters determined experimentally in this program were plotted against measured pressure drop in Figure 11. (In cases where penetration curves do not reach 50%, the reported cut diameters were equivalent cut diameters calculated by the method presented by Calvert, 1974). As can be seen, curves for impingement and sieve agree with the data. The line for venturi scrubber from the previous correlation slightly overestimates the pressure drop. The dashed line fits the experimental data determined in this study and is based on a revised method we have developed for predicting venturi scrubber pressure drop (ref: Yung et al., 1976).

NOVEL DEVICES

Under the novel device test program, we have tested a CHEAF, an electrostatic scrubber, and a charged droplet scrubber.

Electrostatically Augmented Scrubber

The electrostatic scrubber is designed by Air Pollution Systems. It is essentially a venturi scrubber with a charging electrode placed ahead of the throat. The unit we tested is a pilot scale unit with a capacity of about 28 m^3/min (1,000 CFM). The experimental data are shown in Figure 12 for the scrubber system with the charger off and with the charger on.

The scrubber manufacturer did not have a design model so we had to develop one. With minor modifications, the design equations for the venturi scrubber apply. In a venturi scrubber the most important unit mechanism responsible for particle collection is the collection by drops and the predominant collection phenomenon is inertial impaction. When particles are charged, then, in addition to the inertial force, electrostatic forces are present that force the particle towards the drop; i.e., increase the collection efficiency of the drop.

Calvert et al. (1973) calculated the theoretical total collection efficiency due to particle deposition caused by flux forces plus inertial force. A plot of single drop collection efficiency against inertial impaction parameter with flux deposition number, N_{FD}, as the parameter is presented in Figure 13. Flux deposition number is defined as:

$$N_{FD} = \frac{u_F}{u_o} = \frac{\text{Particle deposition velocity}}{\text{Gas velocity past drop}} \tag{3}$$

Assuming Stokes' law holds, the particle deposition velocity is given by:

$$u_F = \frac{C' \, Q_p \, E}{3 \pi \mu_G \, d_p} \tag{4}$$

Single drop collection efficiency, η, is related to scrubber penetration by an equation given by Calvert for a venturi:

$$(Pt)_{d_p} = \frac{2 \, Q_L \, \rho_L \, d_d \, u_{Gt}}{55 \, Q_G \, \mu_G} \int_{f_a}^{0} \eta \, df \tag{5}$$

This model was applied to predict the collection efficiency of the A.P.S. scrubber both with the charger on and with the charger off. Figure 12 shows the predicted A.P.S. scrubber performance along with experimental curves. As can be seen, the predictions and data cross each other for both conditions. The design equations predict a higher penetration than actually measured in the sub-micron region.

Wetted Fibrous Bed

The CHEAF system is primarily a wetted fibrous bed scrubber system. It consists of water sprays to wet and clean the filter medium, a rotary drum containing a fibrous "sponge" filter medium, and a water bath reservoir for cleaning the rotary filter. Particle collection is due to filtration by the rotary filter.

The CHEAF unit we tested was on a diatomaceous earth dryer exhaust. The experimental results are shown in Figure 14. The grade penetration curve for wet particles in the figure was calculated from the penetration curve for dry particles and particle growth data.

The prediction of particle penetration for the CHEAF required the development of mathematical models because none were available from the literature. We can mathematically represent the filter as a fiber bed consisting of an array of equally spaced cylinders. The "Scrubber Handbook" gave the following equation for the prediction of particle penetration of a clean fibrous bed:

$$(Pt)_{d_p} = \exp\left[-S\eta\right] = \exp\left[-\frac{4\ \ell(1-\varepsilon)}{\pi\ d_f}\ \eta\right] \qquad (6)$$

where "η" is the effective collection efficiency of a single fiber in the bed by all collection mechanisms.

By assuming negligible interaction among fibers, the collection efficiency of a fiber in a fiber bed can be approximated by the collection efficiency of an isolated fiber. This assumption might slightly underestimate the fiber efficiency but, since the fibers are not all oriented normally to the gas flow direction, collection efficiency will be lowered slightly.

The pressure drop across the fiber bed is the sum of the drag losses of all fibers. We used the drag coefficient for an isolated cylinder, to be consistent with the assumption of negligible interaction among fibers.

$$\Delta P = 6.5 \times 10^{-4}\ \frac{\ell(1-\varepsilon)\ \rho_G\ C_D\ u_G^2}{d_f} \qquad (7)$$

Equations (6) and (7) were used to predict the performance of the CHEAF. The result is shown in Figure 15, a plot of cut diameter versus pressure drop for various fiber diameters. The cut diameter versus pressure drop relation is highly dependent on the diameter of the fiber, but not much on the solidity factor. The circle in the figure represents the data we determined experimentally. The fiber diameter and the porosity of the filter medium of the scrubber were not disclosed to us because they were proprietary data. Therefore, we could not determine how well the model predicts the performance.

It is possible to compare our model with the data of Rei and Cooper (1976) for tests on a pilot scale unit of the CHEAF. They reported the volume fraction void of the filter medium to be 97% and the fiber diameters to be 64 μm, 44 μm, and 36 μm for foams with 18, 26, and 33 pores per cm. They also reported the measured cut diameter was somewhere below 0.5 μmA for pressure drops ranging from 40 to 90 cm W.C. The dashed line in Figure 15 shows their data, which are consistent with our predictions.

Charged Droplet Scrubber

The charged droplet scrubber was developed by TRW Systems. Instead of charging the particles, as in the case of APS electrostatic scrubbers, the TRW charged droplet scrubber charges the water drops. The water flows out of small diameter tubes which also act as electrodes. The water is atomized as it jets from the tubes. Particle collection of this scrubber is due to inertial impaction and the electrostatic force that exists between the particle and the water drop. The 680 m^3/min (24,000 CFM) unit we tested was used to control emissions from a coke oven.

Figure 16 shows the experimental data. A mathematical model for the charged droplet scrubber was developed by TRW. We did not compare the model prediction with data in this study.

CONCLUSIONS

In conclusion, the field sampling program reported here has attained its major objectives. We obtained meaningful performance data and have verified or developed several mathematical models. Except for the design equation for the mobile bed scrubber, design equations for the scrubber types tested in this program give reasonable performance predictions. In cases where "Pt" was lower than predicted it could be accounted for by particle growth due to water condensation.

The cut/power relationship has many useful applications. It can be used to compare and evaluate scrubbers, to make preliminary scrubber selections, and to estimate the minimum pressure drop of a scrubber for it to attain the required performance. We have verified and extended this relationship in this study.

ACKNOWLEDGEMENT

The work upon which this paper is based was performed pursuant to Contracts 68-02-0285, 68-02-1328, 68-02-1496, and 68-02-1869 with the Environmental Protection Agency.

NOMENCLATURE

C_D = drag coefficient, dimensionless

C_p = particle concentration, g/cm³

C_{pt} = total particle concentration, g/cm³

C' = Cunningham slip factor, dimensionless

d_c = collector diameter, cm

d_d = drop diameter, cm

d_f = fiber diameter, cm

d_h = diameter of perforation, cm

d_p = particle diameter, μm

d_{pa} = aerodynamic particle diameter, μmA

d_{pg} = mass median particle diameter, μmA

E = field strength, kV/cm

F = foam density, dimensionless

f = empirical constant, dimensionless

f_a = empirical constant = 0.5

$f(d_p)$ = frequency distribution of particles

K_p = inertial impaction parameter, dimensionless

K_{Pt} = inertial parameter in the venturi throat, dimensionless

ℓ = thickness of filter pad, cm

N_{FD} = flux force deposition number, dimensionless

n = number of stages, dimensionless

$\overline{Pt}$ = overall penetration, fraction or percent

$(Pt)_{d_p}$ = penetration for particles with diameter d_p, fraction

NOMENCLATURE (continued)

Q_G = gas volumetric flow rate, m^3/s

Q_L = liquid volumetric flow rate, m^3/s or ℓ/s

Q_p = electrical charge carried by the particle, coulomb

S = solidity factor, dimensionless

T_G = gas temperature, °C

u_F = particle drift velocity, cm/s

u_G = gas velocity, cm/s

u_{Gi} = interstitial gas velocity, cm/s

u_{Gt} = gas velocity in the venturi throat, cm/s

u_h = velocity of gas through perforation, cm/s

u_o = gas velocity, past drop, cm/s

z = static bed height, cm

Greek

ε = porosity, fraction

ℓ = filter pad thickness, cm

η = single drop or single fiber collection efficiency, fraction

μ_G = gas viscosity, poise

ρ_G = gas density, g/cm^3

ρ_L = liquid density, g/cm^3

ρ_p = particle density, g/cm^3

σ_g = geometric standard deviation

Δp = pressure drop, cm W.C.

Table 1. SUMMARY OF SCRUBBERS TESTED

No.[a]	Control Device	Source	Q_G Am^3/min	Q_L/Q_G ℓ/m^3	T_G, °C		Pressure Drop cm W.C.	Inlet Size Distribution		$\overline{Pt}$ %	Performance Cut Diameter (μmA)
					In	Out		d_{pg}, μmA	σ_g		
1	Valve tray (Koch Flexitray)	Urea prilling tower	86	0.7	27	17	30	1.1	1.5	54	1.0
2	Vaned centrifugal (Ducon)	KCl dryer	465	0.26	196	78	8	>100	-	3	1.3
3	Mobile bed (UOP/TCA)	Coal fired utility boiler	18,000	6.6	143	85	30	5	2.5	6	0.48
4	Venturi (Chemico)	Coal fired utility boiler	13,400	1.8	163	54	25	3.8	5	2.7	0.67
5	Wetted fiber filter (Encort Corp)	Salt dryer	1,590	0.24	38	32	19	10	4.8	2.7	0.64
6	Impingement plate (Sly Impinjet)	Salt dryer	238	0.15	85	38	30	>100	-	10	1.3
7	Venturi rod (Engineering Hydrofilter)	Foundry cupola	1,274	2.4	88	65	273	1	2	0.4	0.25
8	Venturi (AAF)	Asphalt batch plant	800	1.3	149	57	66	10	3	0.3	0.37
9	Venturi (AAF)	Borax calciner & fusing furnace	1,200	1.7	80	55	110	1	3	2.5	0.2
10	Variable-rod venturi (National Dust Collector)	Foundry cupola	1,010	2.1	35	20	180	.75	1.8	1.5	0.18
11	CHEAF (Johns-Manville)	Diatomaceous earth calciner & dryer	710	0.75	63	60	48-53	.85	4	5	0.8
12	Electrostatic scrubber (Air Pollution Systems)	TiO_2 test dust	23	1.8	16	16	40	1	2.1	8.5	0.35
13	Charged droplet (TRW)	Coke oven	680	0.05	120	60	10	1.4	2.1	88-94	0.35

[a] Numbers cited in Figure 11.

Table 2. DESIGN EQUATIONS FOR VARIOUS SCRUBBER TYPES

SCRUBBER TYPE	DESIGN EQUATIONS
Sieve and valve tray	$(Pt)_{d_p} = \exp\left[-40F^2 \; K_p\right], \quad K_p = \frac{d_{pa}{}^2 \; u_h}{9 \; \mu_G \; d_h}$ $0.38 < F < 0.65$
Mobile bed	$(Pt)_{d_p} = \exp\left[-9.5 \times 10^6 \left(\frac{Q_L}{Q_G}\right)^{3.3} \left(u_G \; \rho_G\right)^{3.66} \; K_p \frac{z}{d_c}\right]$ $K_p = \frac{d_{pa}{}^2 \; u_{Gi}}{9 \; \mu_G \; d_c}$
Venturi and gas atomized spray	$(Pt)_{d_p} = \exp\left[\frac{2 \; Q_L \; u_{Gt} \; \rho_L \; d_d}{55 \; Q_G \; \mu_G} \; F(K_{Pt}, f)\right]$ $F(K_{Pt}, f) = \frac{1}{K_{Pt}}\left[1.4 \ln\left(\frac{K_{Pt} \; f + 0.7}{0.7}\right) + \frac{0.49}{0.7 + K_{Pt} \; f} - (K_{Pt} \; f + 0.7)\right]$
Wetted fiber filter	$(Pt)_{d_p} = \exp\left(-\eta \; S\right)$ $S = \frac{4 \; \ell \; (1-\varepsilon)}{\pi \; d_f}$
Impingement	$d_{pa_{50}} = \left(\frac{1.37 \; \mu_G \; n \; d_h{}^3}{Q_G}\right)^{0.5}$

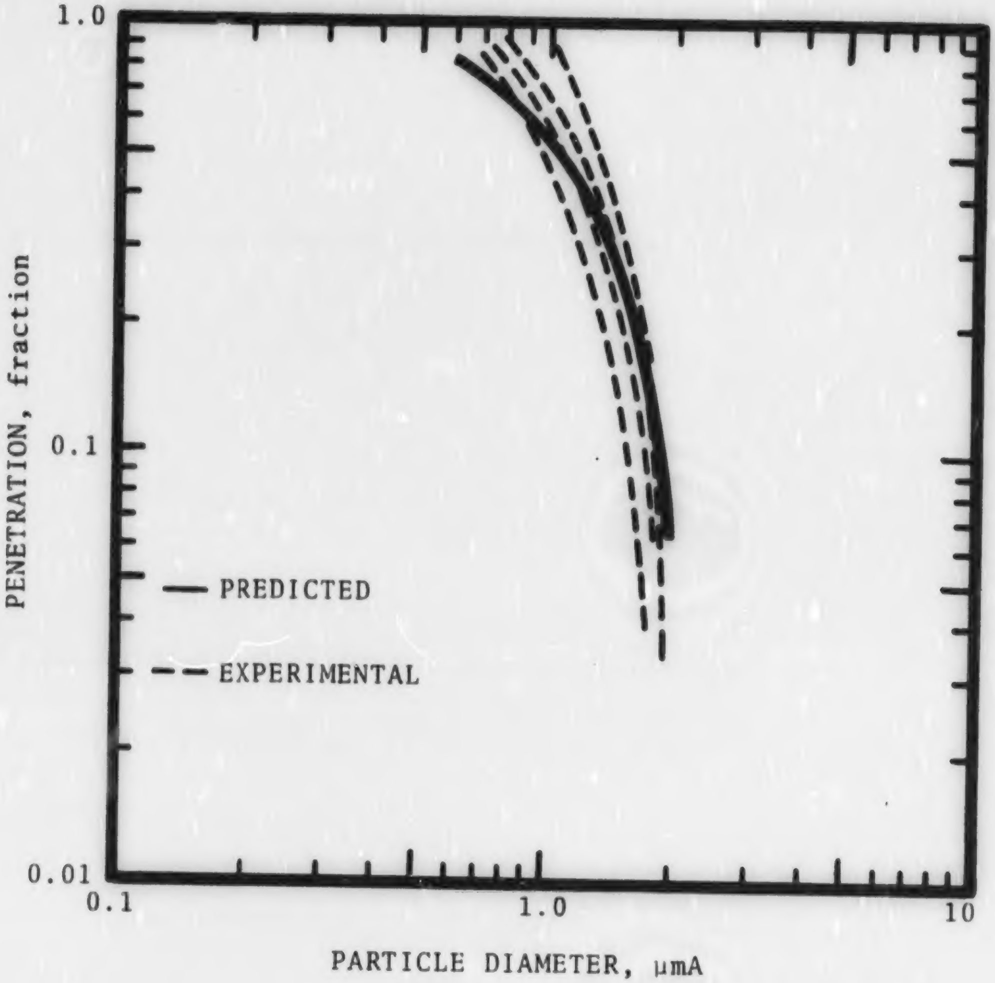

Figure 1. Predicted and experimental penetrations for Koch Flexitray.

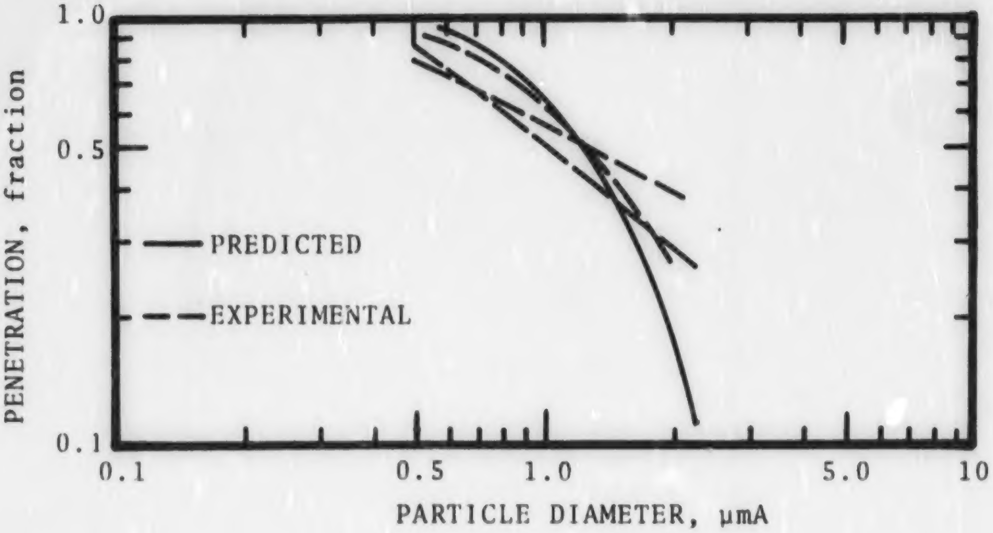

Figure 2. Predicted and experimental penetrations for Ducon Multivane scrubber.

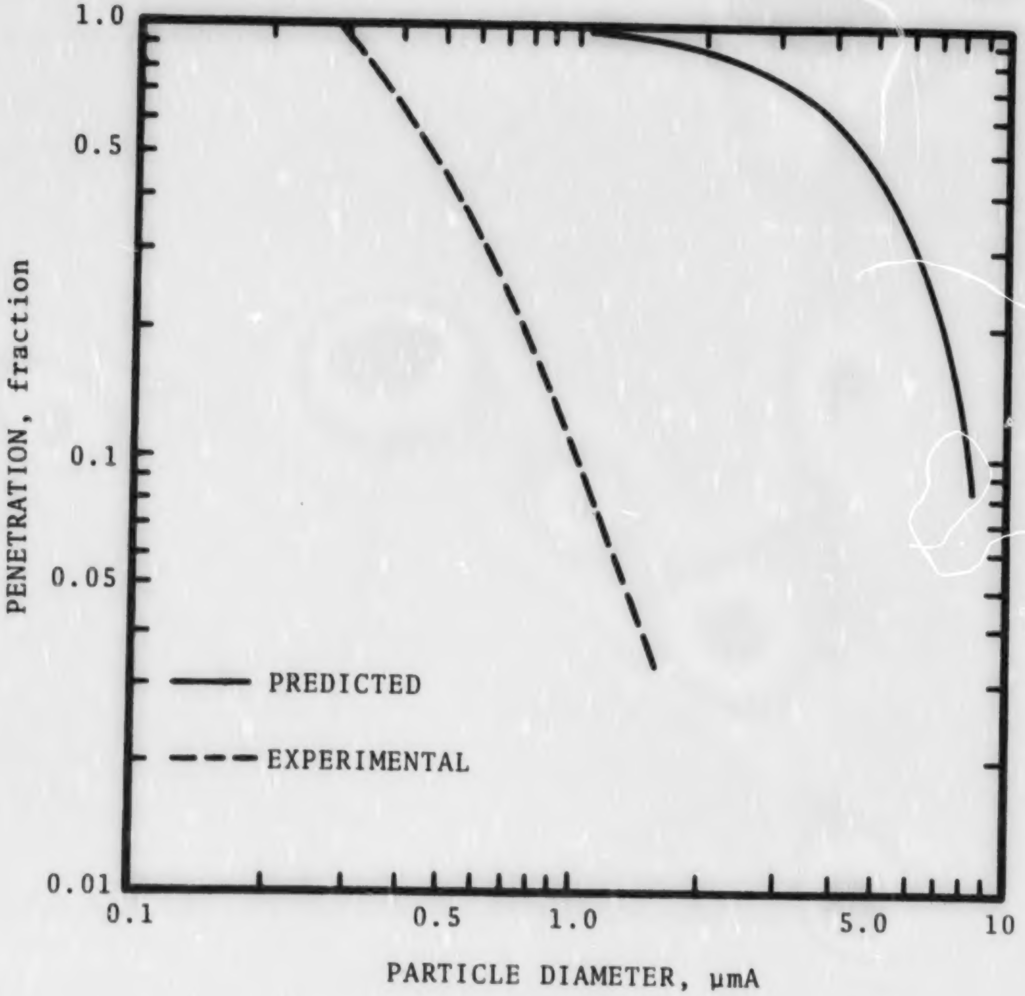

Figure 3. Predicted and experimental penetration for mobile bed scrubber.

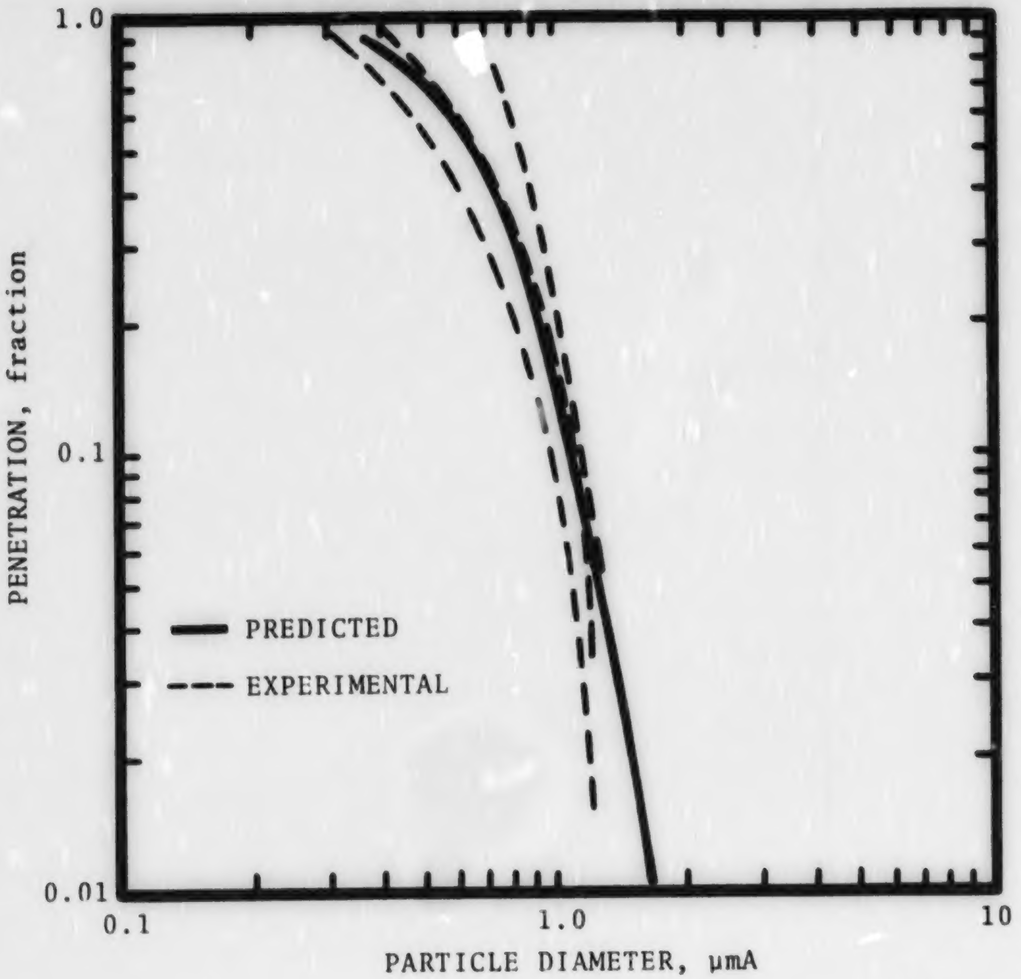

Figure 4. Predicted and experimental penetrations for Chemico venturi.

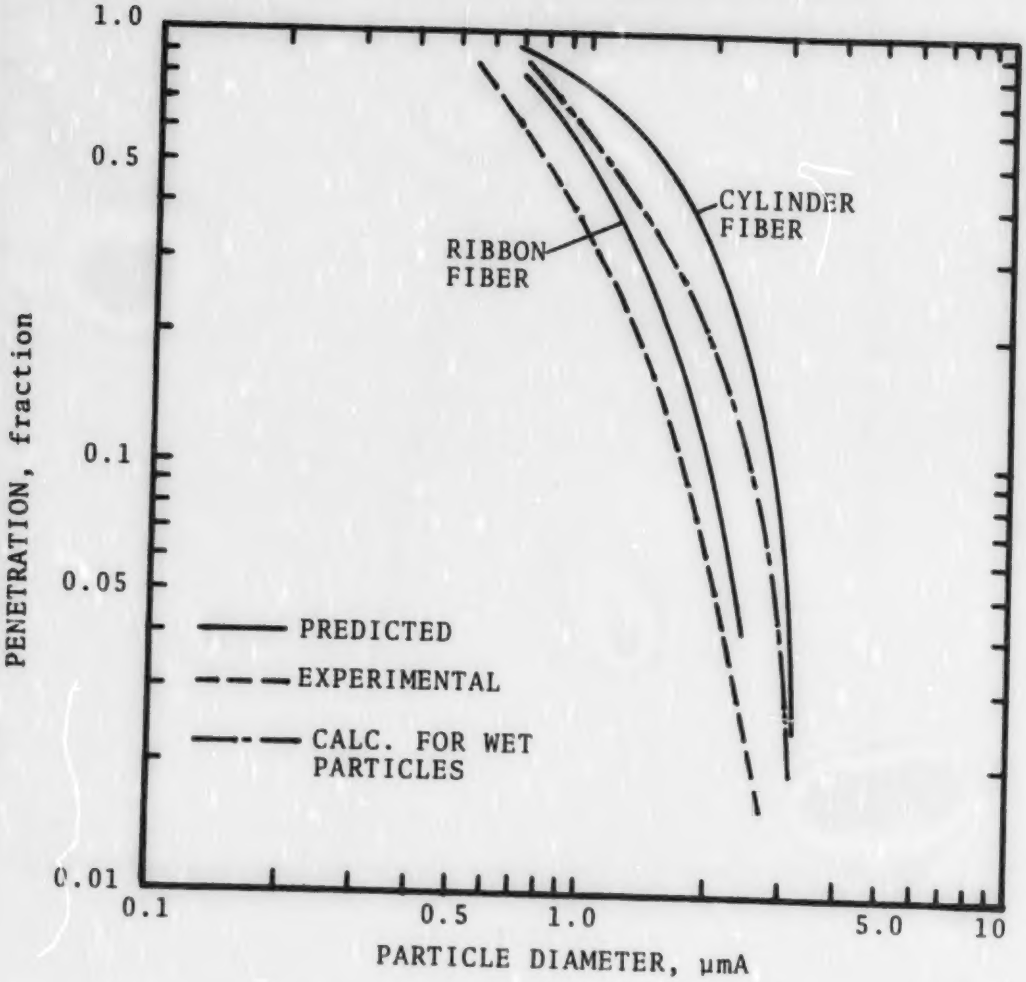

Figure 5. Predicted and experimental penetrations for Encort wetted fiber scrubber.

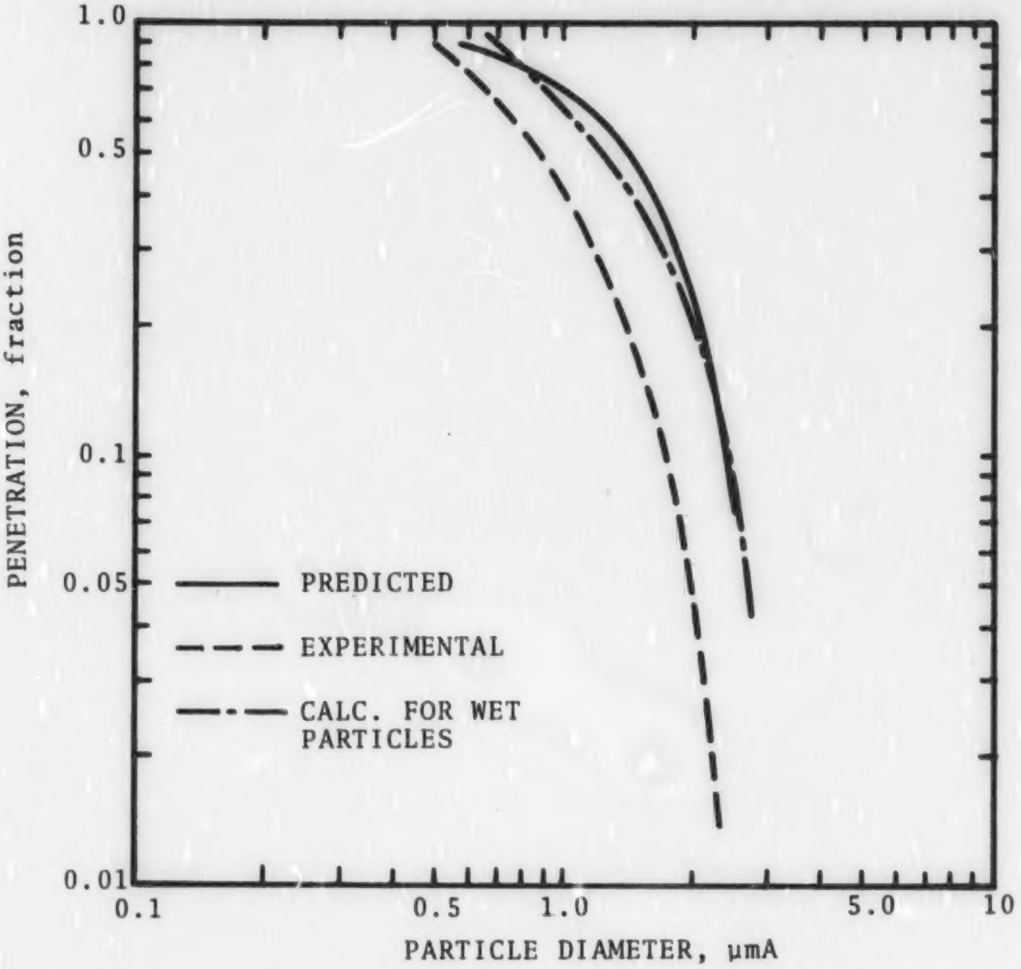

Figure 6. Predicted and experimental penetration for Sly Impinjet.

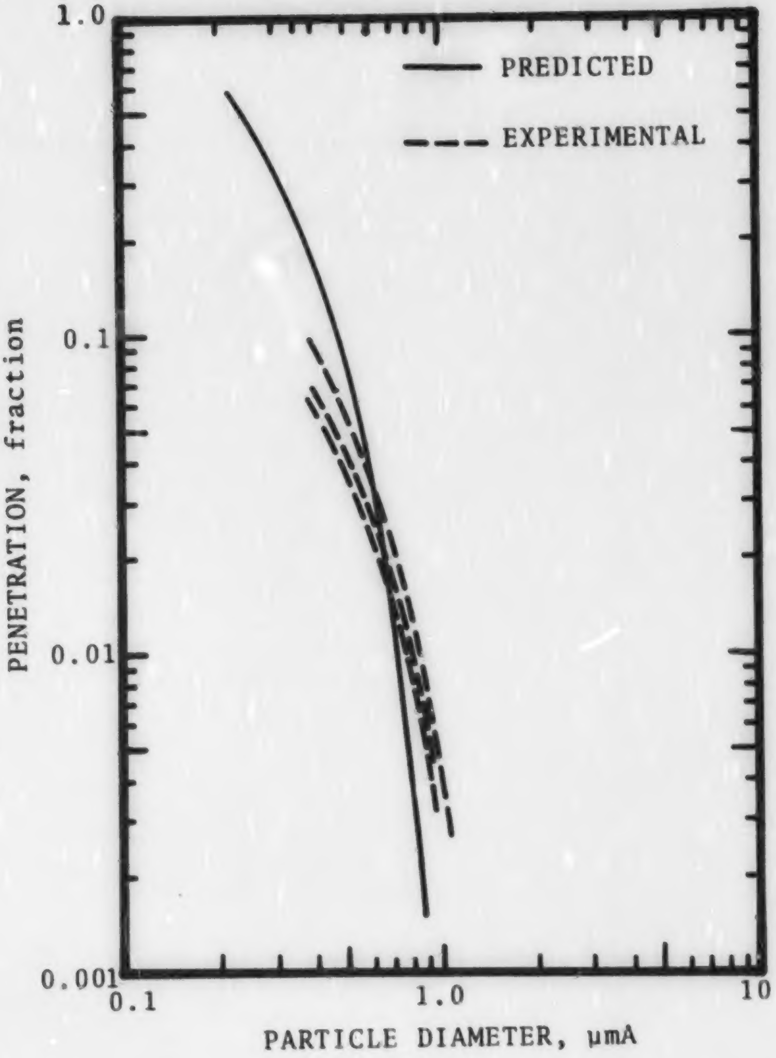

Figure 7. Predicted and experimental grade penetration curves for venturi rod scrubber.

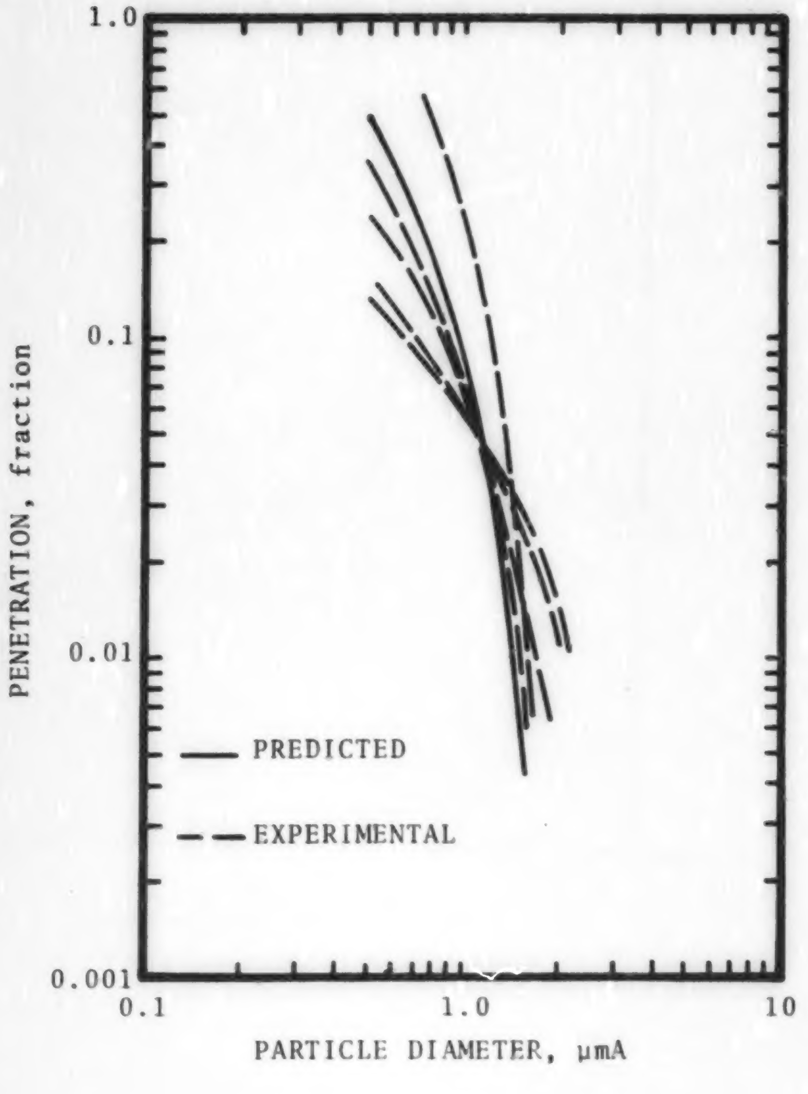

Figure 8. Predicted and experimental penetrations for AAF Kinepactor 32.

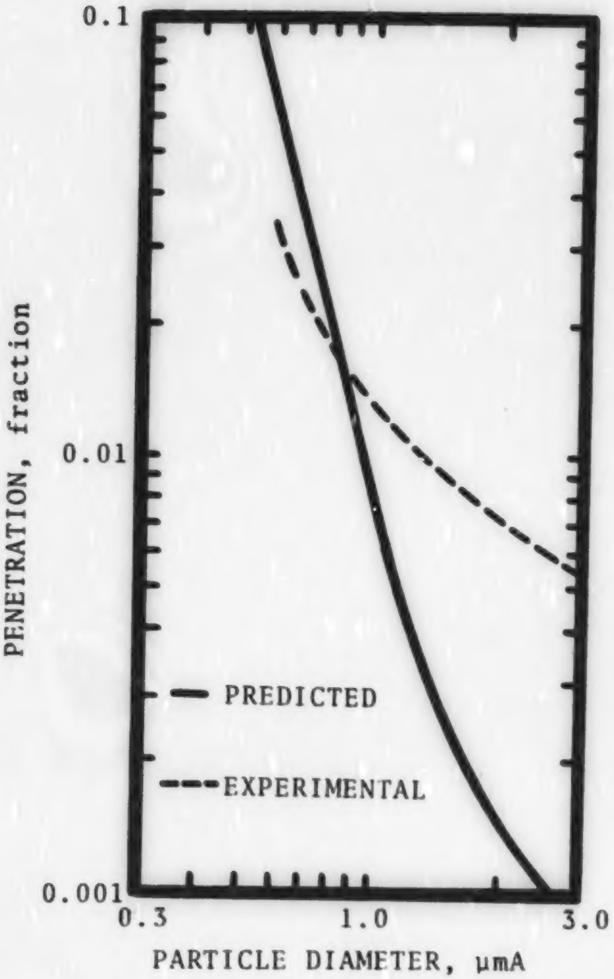

Figure 9. Predicted and experimental grade penetration curves for AAF Kinepactor 56.

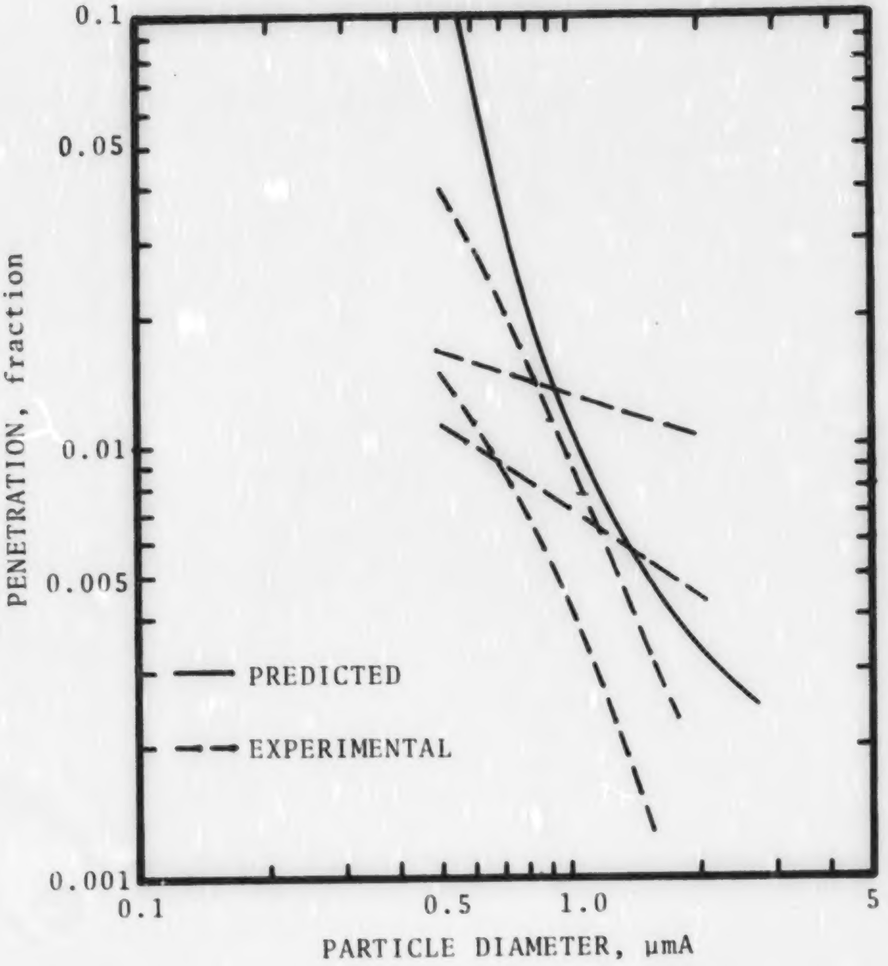

Figure 10. Predicted and experimental penetrations for variable rod scrubber.

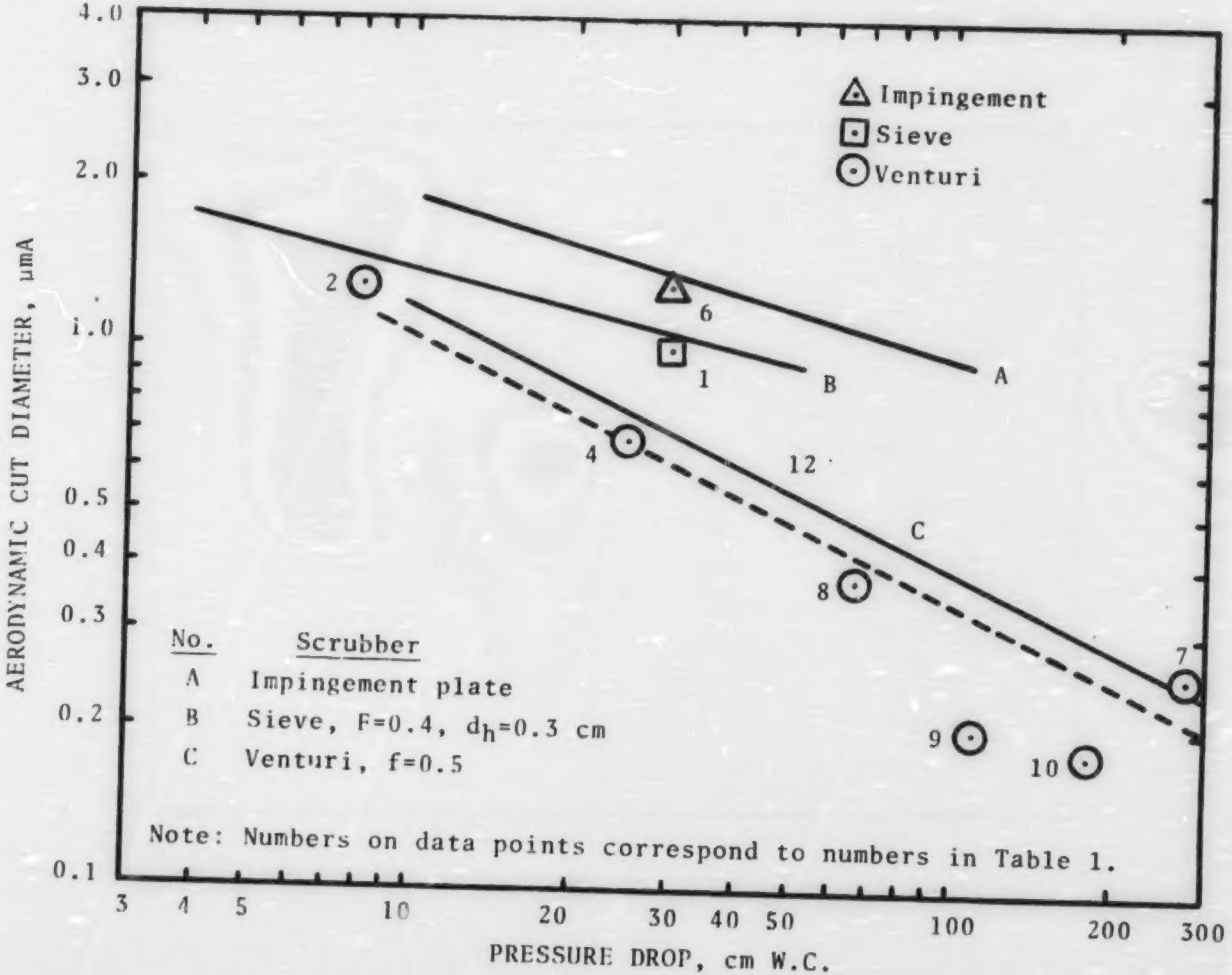

Figure 11. Theoretical and experimental cut diameters as a function of pressure drop for several scrubber types.

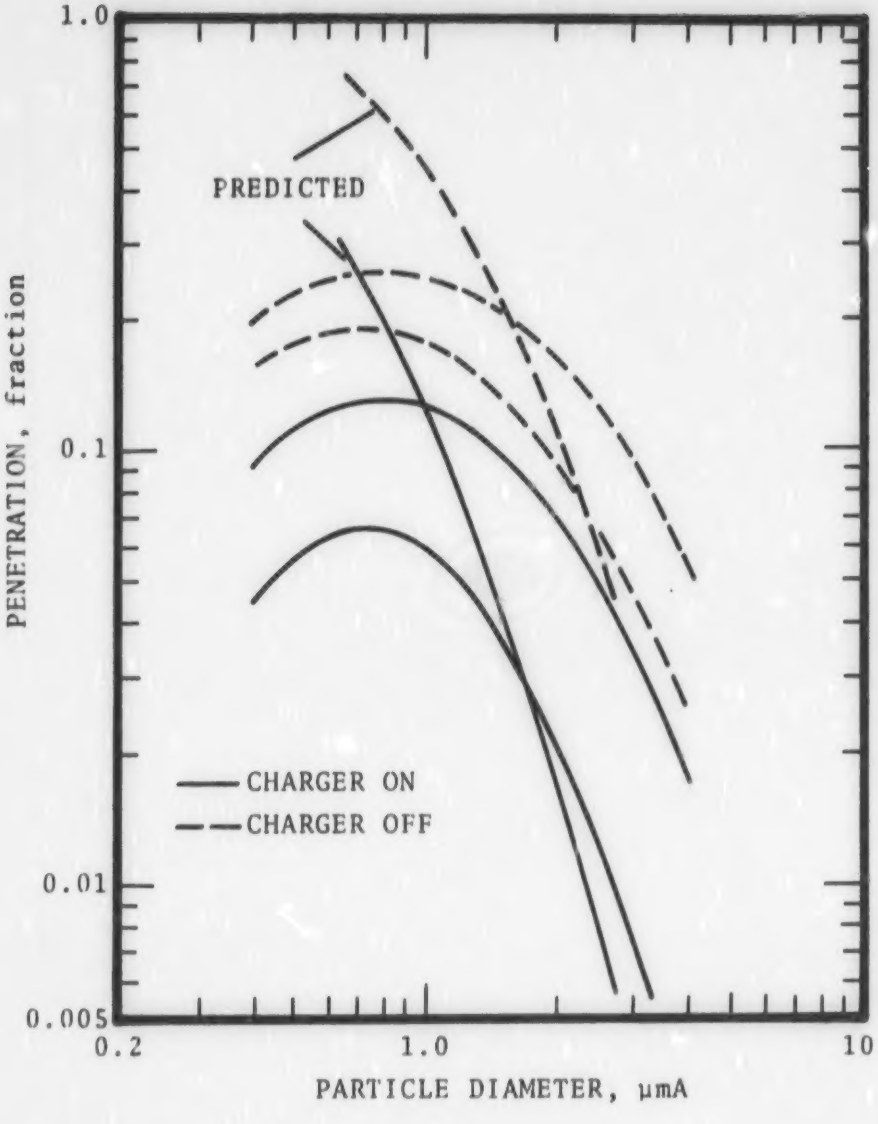

Figure 12. Predicted and experimental penetrations for APS electrostatic scrubber.

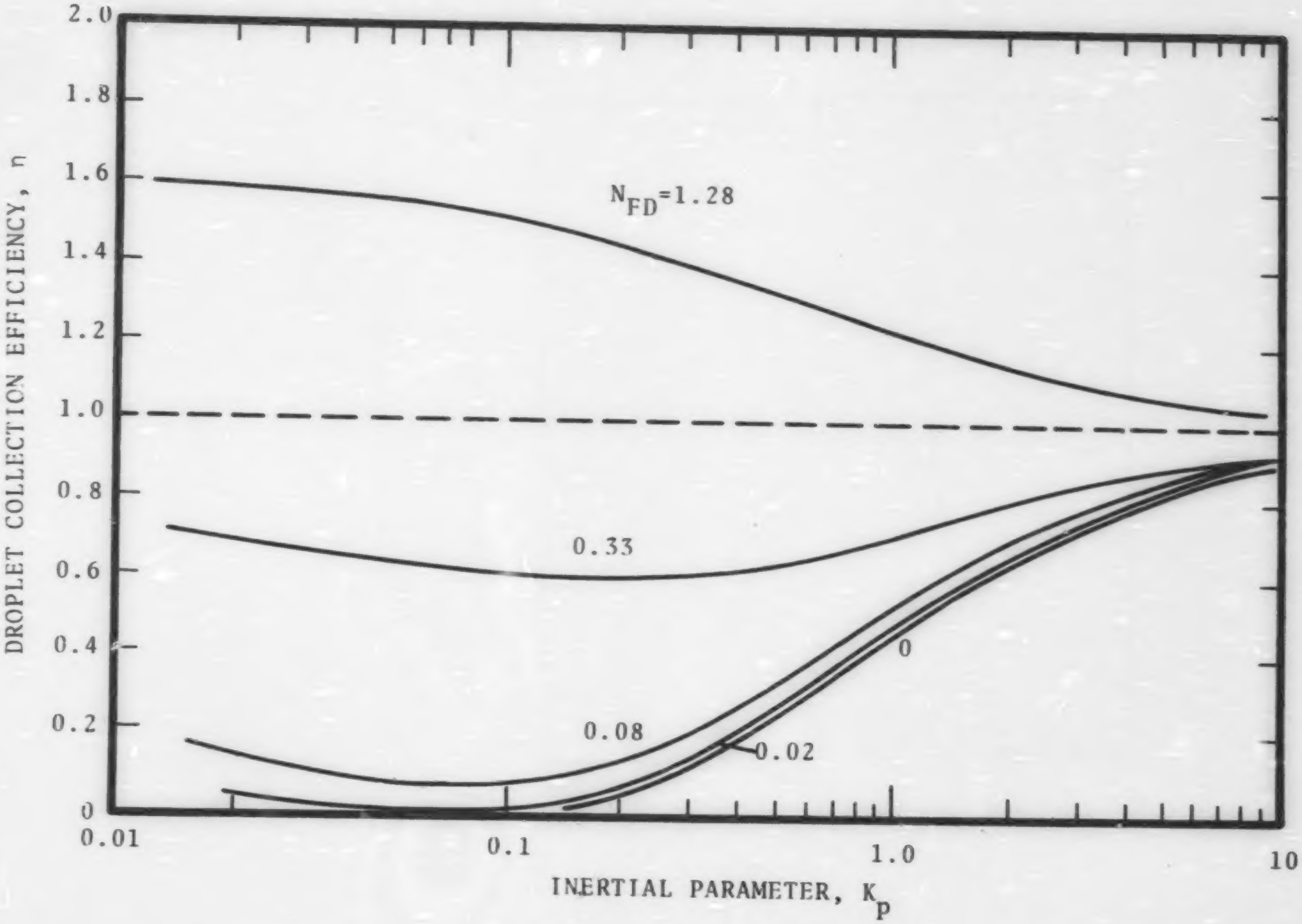

Figure 13. Collection efficiency of single drop versus inertia parameter at N_{Re_d}=9.6 with N_{FD} as parameter.

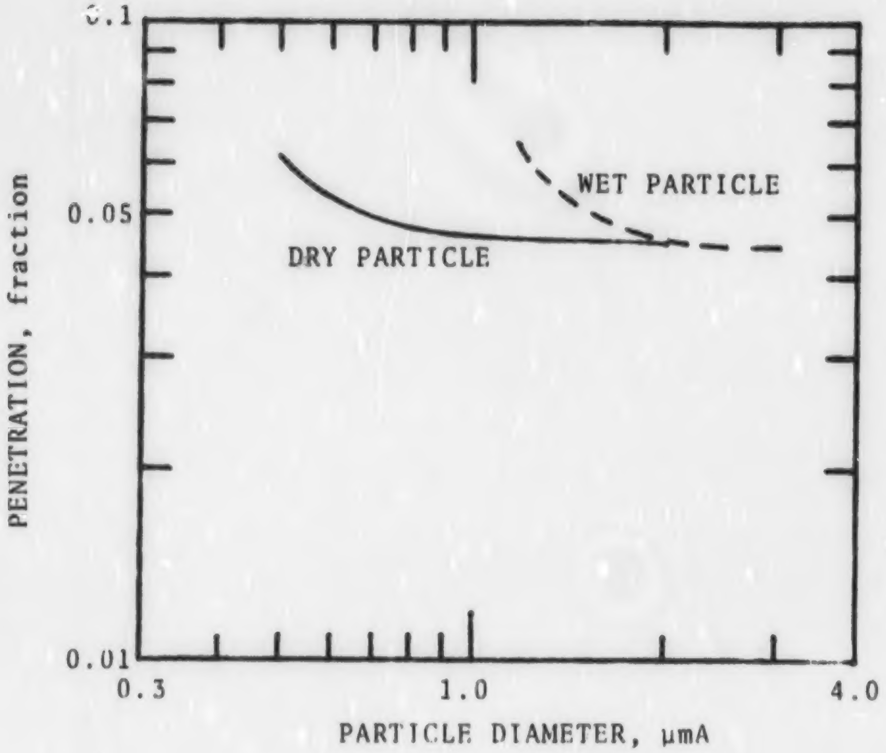

Figure 14. Experimental grade penetration curve for CHEAF.

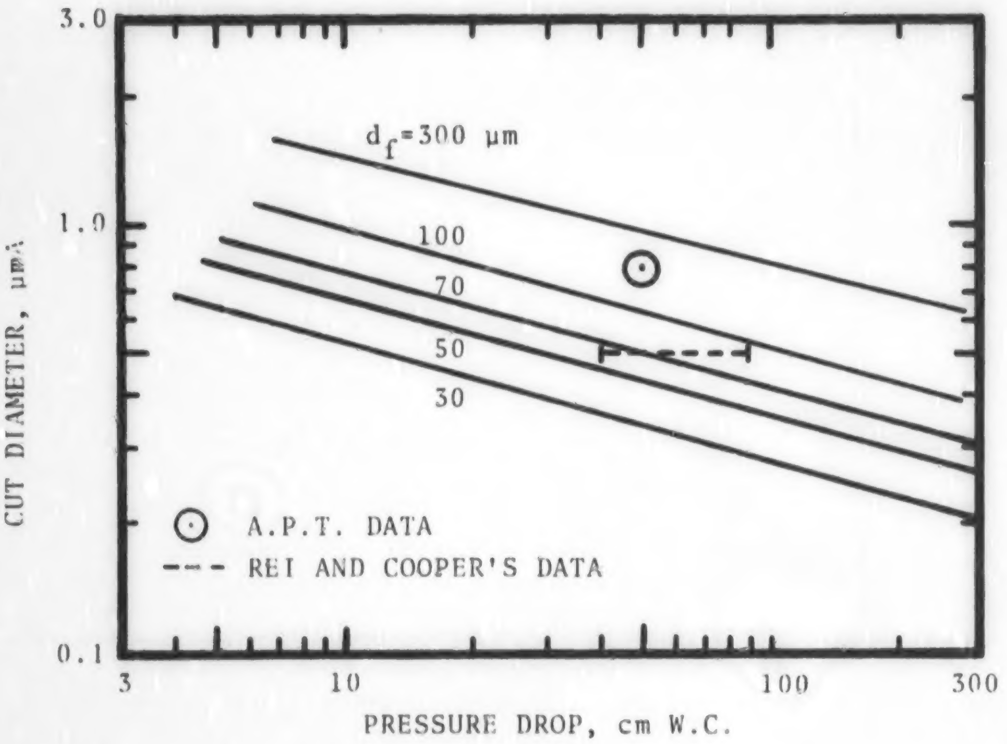

Figure 15. Cut diameter versus pressure drop for fibrous bed.

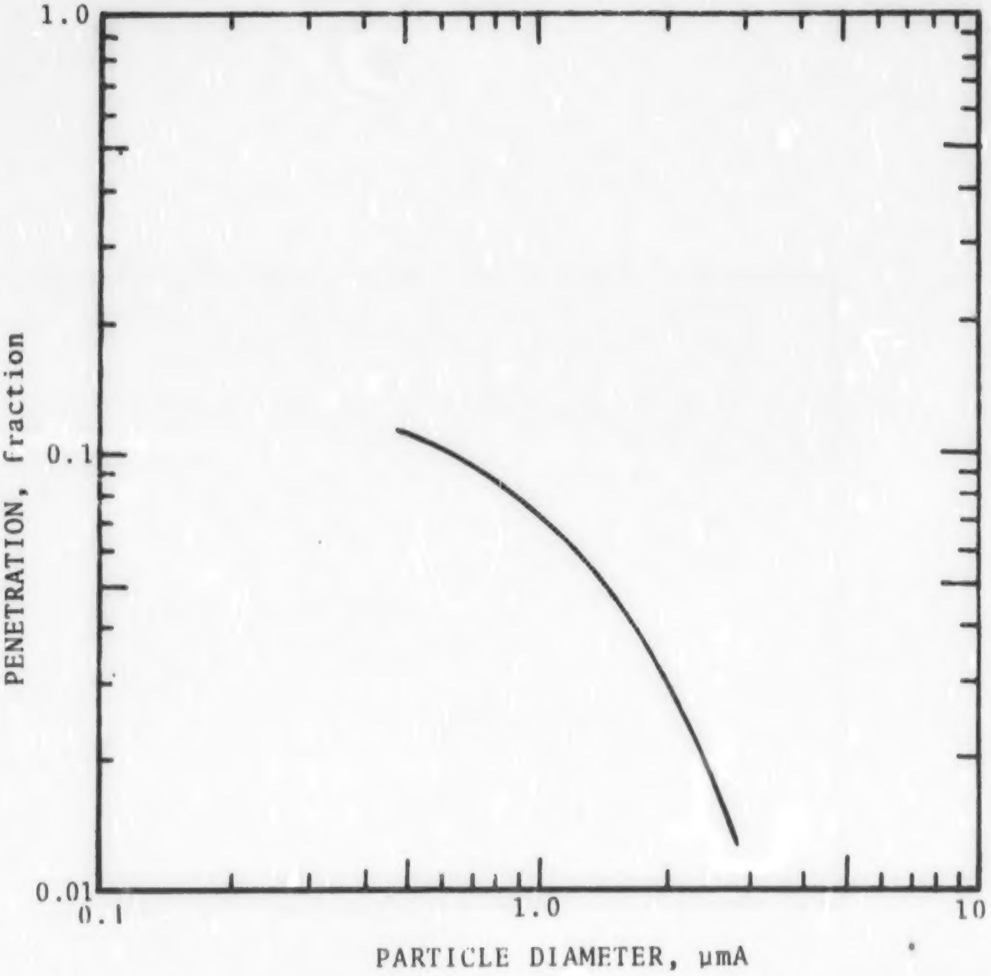

Figure 16. Experimental penetration curve for charged droplet scrubber

REFERENCES

1. Calvert, S., J. Goldshmid, D. Leith, and D. Mehta. "Wet Scrubber System Study, Volume I, Scrubber Handbook." EPA-R2-72-118a (NTIS PB 213-016), August 1972.

2. Calvert, S., J. Goldshmid, D. Leith, and N.C. Jhaveri, "Feasibility of Flux Force/Condensation Scrubbing for Fine Particulate Collection," EPA 650/2-73-036 (NTIS PB 227-307), October 1973.

3. Calvert, S., "Engineering Design of Fine Particle Scrubbers," J. of A.P.C.A., 24, No. 10, p. 929, October 1974.

4. Yung, S., S. Calvert, and H. Barbarika, "Venturi Scrubber Performance Model," Final report to EPA, Contract 68-02-1328, Task 13 (1976) (in printing).

5. Junge, C.E., "Air Chemistry and Radioactivity," Academic Press, 1963.

6. Rei, M.T., and D.W. Cooper, "Laboratory Evaluation of the Cleanable High Efficiency Air Filter (CHEAF)", EPA-600/2-76-202 (NTIS PB 256-698/AS), July 1976.

RESULTS OF FLUE GAS CHARACTERIZATION TESTING AT THE EPA ALKALI WET-SCRUBBING TEST FACILITY

Richard G. Rhudy and Harlan N. Head
Bechtel Corporation

ABSTRACT

A series of tests were conducted at the EPA Alkali Wet Scrubbing Test Facility located at the Shawnee Steam Plant, Paducah, Kentucky, to measure mass loading and the size distribution of the particulates emitted from the lime and limestone wet scrubbers. The tests were designed to determine the effects of operating variables on emission levels. Two different scrubbing trains were tested, a TCA and a venturi followed by a spray tower. Flue gas feed for the unit was supplied from Unit 10 of the Shawnee Steam Plant either directly from the boiler or after the electrostatic precipitator.

Mass emissions from the venturi/spray tower system were in compliance with the EPA New Source Performance Standards while the mass emissions from the TCA system approached or exceeded the EPA standard for the conditions tested. Mass penetration by particle size, measured from 0.3 to 10 microns, was generally higher for the TCA system than for the venturi/spray tower system over the range of variables tested.

Slurry entrainment was small. It appeared primarily as particulate emissions greater than 2 microns actual diameter.

Preceding page blank

RESULTS OF FLUE GAS CHARACTERIZATION TESTING AT THE EPA ALKALI WET-SCRUBBING TEST FACILITY

Introduction

The EPA Alkali Wet Scrubbing Test Facility, located at the Shawnee Steam Plant, Paducah, Kentucky, is a lime/limestone throwaway process demonstration facility operated under EPA direction. The purpose of the test facility is to demonstrate the commercial feasibility of lime and limestone wet scrubbing of coal fired power plant exhaust gases.[1,2,3] At the test facility, a venturi followed by a spray tower and a TCA (turbulent contact absorber) are operated to remove both particulates and SO_2 from flue gas generated by the coal fired boiler. As a part of this project, a Flue Gas Characterization Program is being conducted to answer a number of questions concerning the flue gas emissions from the lime and limestone wet scrubbers.

First, mass loading data was needed to determine the conditions under which EPA New Source Performance Standards for mass emission could be met. Second, a measurement of the extent to which scrubbers generate particulates through scrubber reaction-product entrainment was desired, especially in the fine ($< 2\ \mu$) particulate range. And third, because of concern over the health hazards of sulfates,[4] it was desired to determine the effect of scrubbers on sulfuric acid vapor (SO_3) emissions and, using this data, to estimate total sulfur emissions (i.e., SO_2, SO_3, and reaction-product sulfates).

An intensive testing period to explore the effect of major operating variables on each system has been completed. This paper reports the results only of the mass loading and size distribution tests. SO_3 emission results will be reported elsewhere. Routine testing is being continued to monitor long term trends as opposed to the periodic spot checks made in the past.

Experimental

Test Program

The test series on both the venturi/spray tower and TCA systems were designed to determine the effect of major operating variables on mass removal and particulate size distribution.

Variables investigated on the venturi/spray tower system were flue gas rate, slurry rate, MgO addition, venturi pressure drop, mist eliminator configuration, and percent solids recirculated. Variables investigated on the TCA system were flue gas rate, liquor rate, MgO addition, and mist elimination wash scheme. MgO is used as an additive in lime/limestone systems to increase sulfur dioxide removal. The mist eliminators were washed intermittently on top with fresh water (8-hour sequential cycle with one of the six nozzles activated for 4 minutes every 80 minutes) while three modes of bottom wash were evaluated as follows:

- High frequency intermittent fresh water (HI), 4 min/hr at 1.5 gpm/ft^2, shut off during testing
- Low frequency intermittent fresh water (LI), 6 min/4 hr at 1.5 gpm/ft^2, shut off during testing
- Continuous diluted clarified liquor (C), at 0.4 gpm/ft^2, left on during testing

For one run on each system, flue gas feed to the scrubber was obtained from downstream of the electrostatic precipitator (ESP) to check scrubber performance on flue gas with low grain loading. Flue gas feed for all the other runs came from a takeoff just downstream of the boiler air preheaters. Listed in Table 1 are the run conditions for the venturi/spray tower system tests, and in Table 2, the conditions for the TCA system tests.

Sampling Locations

Both the inlet and outlet of each scrubber were sampled. The duct work at these locations was forty inches in diameter. Two eight-point traverses, 90° apart, were performed for each mass loading and size distribution test. The inlet sample ports were located ahead of the saturation sprays at the scrubber inlet where the gas temperature was approximately 300-330° F. The outlet sample port was located after the reheater at the scrubber outlet where the gas temperature was approximately 250° F. The sample ports were about two duct diameters upstream and six duct diameters downstream of the nearest obstruction.

Test Methods

The procedure used for measuring particulate mass loading was a modification of EPA Method Five.[5] A Hi-Volume sampling train manufactured by the Aerotherm Division of Acurex Corporation was used. The major differences in test conditions between sampling at Shawnee and a typical Method Five application were (1) increased sampling flow rate (2 cfm versus 0.75 cfm typical for EPA Method Five), (2) filter temperatures in the 350°F to 400° F range to prevent acid (SO_3) condensation, and (3) the first two impingers filled with $NaCO_3$ solution to remove SO_2 and to provide corrosion protection for the pump and dry gas meter.

Particulate size distributions were measured with out-of-stack heated inertial impactors.[6] A Brink Model BMS-11 impactor was used for inlet sampling and a Meteorology Research Inc. (MRI) model 1502 impactor was used for outlet sampling.

To obtain representative size distribution measurements, sampling traverses were made. The flow rate through the impactor was held constant to ensure constant impactor stage cut sizes. The sampling nozzle was chosen to provide average duct velocity at the nozzle inlet. Because of the uniformity of the duct velocity profile, ± 10 percent of the isokinetic sampling rate could be maintained by sampling at the average duct velocity.

Because all size distribution measurements were taken out of stack to facilitate temperature control, a fraction of the particulate was deposited in the probe. For the outlet size distributions, the estimated probe fallout included a significant fraction of the particulate in the size range of the first three stages. Thus, it was necessary to combine the probe wash and the first three stages when computing grain loadings as a function of particle size. For the inlet measurements no correction was required.

Results

Venturi/Spray Tower System

Included in Table 1 are the results of the mass loading tests performed on the venturi/spray tower system.

As expected, the venturi operating conditions had the greatest effect on particulate removal. Average outlet mass loading ranged from 0.019 gr/dscf at a venturi pressure drop of 9 in. H_2O and 600 gpm slurry rate (Run VFG-1C) to 0.036 gr/dscf at ~ 3 in. H_2O and 140 gpm slurry rate (Run VFG-1P). Even at a venturi pressure drop of 3 in. H_2O, the venturi/spray tower system was capable of meeting EPA New Source Performance Standards (NSPS) for mass emissions from coal fired power plants (0.052 gr/dscf assuming 30 percent excess air in the flue gas). However, the EPA NSPS opacity requirement will probably limit the maximum particulate concentration allowable for a commercial size stack.

Future testing will concentrate on defining the relationships between opacity and mass loading. Preliminary results of the first of these tests on the TCA system are discussed under the TCA results.

Average outlet mass loading for the run with low inlet fly ash concentration (Run VFG-1B, flue gas from after the electrostatic precipitator) was 0.005 gr/dscf. Calculations based on size distribution measurements suggest there should be no problem with opacity at this level and it is apparent that entrainment from the circulating scrubber slurry must be less than this value.

To further quantify the amount of entrained scrubber reaction products, the particulate from one outlet-mass-loading filter was analyzed for each of Runs VFG-1A, VFG-1B, and VFG-1C. Table 3 presents the results of wet chemical and semi-quantitative spectrographic analyses of these solids. By assuming all the calcium and magnesium in the samples were present as hydrated reaction products (as noted in Table 3), the mass loading of entrained scrubber reaction products was estimated. For the VFG-1B analysis, the resultant value was 0.002 gr/dscf while for the VFG-1A and VFG-1C analyses, the value was approximately 0.006 gr/dscf. However, the runs were made at the same operating conditions (see Table 1), and the entrainment values should be the same. The values for Runs VFG-1A and VFG-1C may be high because a portion of the calcium collected from these runs existed in the fly ash emitted from the scrubber and should not have been included in the reaction-product emission estimation. Scanning electron microscope (SEM) photographs of the outlet-mass-loading filter indicated that the emitted solids were predominately fly ash particles.

Inlet and outlet grain loadings as a function of aerodynamic particle size were calculated[7] using mean values of all the measurements for each run. These values are plotted for runs with high fly ash loading in Figure 1 and for the run with low fly ash loading in Figure 2. The outlet particulate size distributions, like the mass loading results, appeared to be fairly independent of operating variable level for the runs with high fly ash loadings. The outlet size distribution for the run with low fly ash (Run VFG-1B) exhibited a similar shape but had lower values reflecting the reduced grain loading.

Mass penetration as a function of aerodynamic particle size, determined graphically from Figures 1 and 2, are plotted in Figure 3 for all runs with high fly ash loading and in Figure 4 for the run with low fly ash loading. Penetration appeared to be fairly independent of run variable level. Mass penetration for the high fly ash loading tests appeared to vary from about 20 to 50 percent for 0.1 micron particles to less than 1 percent for particles larger than 5 microns. For the tests with low fly ash loading, mass penetration was the same for 0.1 micron particles but penetration increased to approximately five percent for particles larger than 5 microns.

For the Shawnee particulate emissions, a 2 micron actual diameter corresponds to a 3.1 micron aerodynamic diameter.[8] Using this relationship, the impactor data was split into mass emission greater than and less than 2 microns actual diameter. Mass emission of particles less than 2 microns actual diameter from the venturi/spray tower system was insensitive to run variable level, averaging ~ 0.016 gr/dscf for all of the high grain loading runs. Emission of particles greater than 2 microns averaged ~0.006 gr/dscf for all runs except Run VFG-1A (MgO addition) and Run VFG-1P (minimum venturi). The data for these runs was not of sufficient quality to estimate a mass emission for the greater than two micron diameter particulate. For the low fly ash run, emissions less than 2 microns actual diameter averaged 0.002 gr/dscf while emissions greater than 2 microns actual diameter averaged 0.003 gr/dscf.

SEM photographs (see Figures 5 and 6) of the scrubber outlet impactor particulate from Run VFG-1A captured on the third stage (7.8 to 9.3 microns actual cut size) and sixth stage (1.1 to 1.2 micron actual cut size) revealed that very little emitted reaction products were visible on the sixth stage (deposits appeared to be all spherical fly ash) while crystals of $CaSO_3 \cdot 1/2H_2O$ (the rosettes) were visible on stage three. These SEM photographs confirmed the presence of scrubber slurry reaction products and indicated they were concentrated in the larger size range.

TCA System

Presented in Table 2 are the results of the mass loading tests conducted on the TCA system. The average outlet mass loading ranged from 0.042 to 0.065 gr/dscf for the high inlet fly ash loading tests and was 0.026 gr/dscf for the test with low fly ash loading.

The average mass emission values with high inlet fly ash loading were in the range of and sometimes exceeded the EPA New Source Performance Standards for particulate emissions. Preliminary results of mass loading versus opacity measurements indicate that removals in the 0.020 to 0.025 gr/dscf range would be required to meet the EPA opacity standard for a 500 MW plant with a single stack (assuming a 70 ft/sec exit velocity). This value is well below the mass emission requirements. Further tests are planned to confirm the mass loading/ opacity relationship.

Non-dispersive infrared and thermo-gravimetric analysis of the particulate on a single outlet filter from the run with low fly ash loading indicated that emissions from entrained scrubber reaction products were in the 0.005 gr/dscf range. Based on this single analysis, the outlet loadings appeared to be predominately fly ash. Preliminary results from air/slurry entrainment tests on the TCA system indicated a slurry (~ 40 percent fly ash and ~ 60 percent slurry reaction products) entrainment value between 0.003 and 0.005 gr/dscf. This value is in agreement with the low reaction product emission value and supports the conclusion that over 90 percent of the TCA emission is fly ash. Similar tests are scheduled for venturi/spray tower system.

The highest emission values experienced under base case conditions occurred with a continuous diluted clarified liquor mist eliminator underwash (Run TFG-1C). Changing to an all fresh water mist eliminator wash scheme (Run TFG-2B) reduced emissions.

Reducing the circulating slurry rate had no effect on the emissions (Run TFG-2E), but reducing the gas rate (Run TFG-2D) tended to reduce the emissions. MgO addition (Run TFG-2A) tended to increase emissions although this run did not have the highest emission rate since it used a fresh water mist eliminator wash scheme.

Inlet and outlet grain loadings as a function of aerodynamic particle size were calculated[7] using mean values of the measurements for each run and are plotted for runs with high fly ash loading in Figure 7 and for runs with low fly ash loading in Figure 8. The inlet distributions were similar to the venturi/spray tower measurements, confirming that the scrubber inlet size distributions were the same even though they were taken from the boiler outlet duct at different points.

Mass penetration as a function of aerodynamic particle size is plotted for the runs with high inlet fly ash loading and low inlet fly ash loading, in Figures 9 and 10, respectively. The mass penetration for the high fly ash loading runs varied from about 40 to 90 percent for 0.1 micron particles to less than 2 percent for particles larger than 5 microns. For the low fly ash loading runs, penetration was between 25 and 70 percent for 0.1 micron particles and about 10 percent for particles larger than 5 microns.

For the high fly ash loading runs, emission of particles less than 2 microns actual diameter averaged ~ 0.025 gr/dscf except for the low gas rate run (TFG-2D) and the low slurry rate run (TFG-2E) where the average was higher at ~ 0.037 gr/dscf. In a TCA, this decreased removal efficiency would be expected with slurry or gas turndown because of decreased sphere activity in the beds. Emission of particulates with diameters greater than 2 microns averaged ~ 0.028 gr/dscf except for the base case with a continuous mist eliminator wash (TFG-2C) and the MgO addition run (TFG-2A) where the emissions averaged ~ 0.055 and ~ 0.038 gr/dscf, respectively. The low fly ash loading run averaged 0.003 gr/dscf less than 2 microns actual diameter and 0.025 gr/dscf greater than 2 microns actual diameter.

From this data it would appear that slurry entrainment after evaporation in the reheater contributes mostly to the large size fraction of the emissions. For example, the continous diluted clarified liquor underwash (TFG-2C versus TFG-2B) consisting of water and dissolved solids significantly increased emissions only in the greater than 2 micron fraction. Also, when the gas rate (TFG-2C versus TFG-2D) or the liquor rate (TFG-2C versus TFG-2E) was reduced, the fine particulate increased but the larger particulate decreased. This probably resulted from a decrease in slurry entrainment . MgO addition which increased the total dissolved solids also resulted in an increase in emission for the larger sizes.

System Comparison

Run VFG-11 and TFG-2B from Tables 1 and 2 were chosen to compare the relative flue gas cleaning capabilities of the two systems under typical operating conditions for attaining 80 percent SO_2 removal. These runs were made under conditions of similar percent solids recirculated (15 percent) and mist eliminator wash scheme (fresh water wash with the bottom wash off during testing). The mist eliminator type (threepass, open-vane chevron) was the same for both systems.

The venturi/spray tower gas rate was 35,000 acfm compared with 30,000 acfm for the TCA system. However, particulate removal in the venturi/ spray tower system appeared to change little with gas rate (Run VFG-1C versus Run VFG-1D) and a correction to 30,000 acfm was assumed to be neglible.

Comparison of the two systems showed that the estimated average outlet mass loading value was ~0.026 gr/dscf for the venturi/spray tower system versus ~0.048 gr/dscf for the TCA system. The average mass emission of particulate less than 2 microns actual diameter was ~0.016 gr/dscf for the venturi/spray tower versus ~0.026 gr/dscf for the TCA system. Mass emission greater than 2 micron actual particle diameter was ~0.008 gr/dscf on the venturi/spray tower system versus ~0.027 gr/dscf for the TCA system. The less than and greater than 2 micron data come from the impactor runs which add up to slightly different values than the mass loading averages.

It should be emphasized that this comparison is only valid for the scrubbers at Shawnee under the conditions specified and is not meant as a blanket generalization about the relative capabilities of the two types of scrubbers. Possible design modifications and economic factors must also be considered on any final system evaluation.

Conclusions

Analysis of the flue gas emissions at the Shawnee Test Facility has shown that mass emission is higher for the TCA system than for the venturi/spray tower system under typical conditions. Indeed, the TCA mass emission approached or exceeded the EPA New Source Performance Standards for mass emission while the venturi/spray tower emission was consistently below the standard.

Scrubber reaction product emission represented only a small percentage of the total mass emission. Size distribution run results and scanning electron microscope photographs indicated that most of the scrubber reaction product emission was confined to the larger particle sizes.

Additional measurements of the magnitude and size distribution of the scrubber reaction product emission are to be made.

Measurement of mass penetration through the scrubbers as a function of particle size indicated that there was no massive generation of particulate, (i. e., outlets greater than inlets) and that penetration became significant in the range of one micron and smaller where it varied from 25 to 90 percent. Under comparable conditions, the relative mass penetration for the TCA system was greater than for the venturi/spray tower system.

Controlled Variables	VFG-1A	VFG-1B		VFG-1C	VFG-1D	VFG-1E	VFG-1F	VFG-1G	VFG-1I	VFG-1P
Gas Rate, acfm @ 130°F	35,000	35,000	35,000	35,000	20,000	35,000	35,000	35,000	35,000	35,000
ST Gas Velocity, ft/sec	9.4	9.4	9.4	9.4	5.4	9.4	9.4	9.4	9.4	9.4
ST Slurry Rate, gpm	1,400	1,400	1,400	1,400	1,400	1,400	0	1,400	1,400	1,400
Venturi Slurry Rate, gpm	600	600	600	600	600	375	600	600	600	140
Venturi ΔP, in. H_2O	9	9	9	9	9	4.5 - 6.0	9	9	9	2.8 - 3.2
Percent Solids Recirculated	8	8	8	8	8	8	8	8	15	8
Fly Ash Loading	High	Low	Low	High	High	High	High	High	High	High
Alkali	Lime	Lime	Lime	Lime	Lime	Lime	Lime	Lime	Lime	Lime
Mist Elim. Configuration	chevron	chevron	chevron	chevron	chevron	chevron	chevron	chevron + York	chevron	chevron
Mist Elim. Wash Scheme[1]	LI	LI	LI	LI	LI	LI	LI	LI	LI	LI
MgO Addition	Yes	No	No	No	No	No	No	No	No	No
Uncontrolled Variables										
Gas Vel. at Mist Elim., ft/sec	9.4	9.4	9.4	9.4	5.4	9.4	9.4	9.4	9.4	9.4
System ΔP Range, in. H_2O	13.3 - 13.8	13.1 - 13.8	13.6 - 14.0	13.7 - 14.3	10.2 - 10.8	9.5 - 10.5	12.5 - 13.2	14.1 - 15.5	13.7 - 14.3	6.9 - 7.3
Total Dissolved Solids, ppm	13,200 - 18,000	2,500 - 5,200	7,000 - 9,500	7,700 - 9,600	6,000 - 8,800	5,400 - 8,000	7,200 - 10,000	8,300 - 9,400	6,600 - 9,000	6,900 - 8,100
Flue Gas Measurements										
Mass Loading Inlet										
Average, gr/dscf	4.41	0.070	0.367	6.17	4.53	5.11	5.14	6.05	5.18	5.63
Range, gr/dscf	3.66 - 5.50	0.039 - 0.096	0.118 - 0.609	4.82 - 8.39	3.68 - 5.78	3.77 - 7.90	3.72 - 6.41	3.90 - 8.76	3.70 - 6.06	5.13 - 6.66
Mass Loading Outlet										
Average, gr/dscf	0.032	0.005	0.005	0.019	0.026	0.028	0.027	0.021	0.026	0.036
Range, gr/dscf	0.023 - 0.046	0.003 - 0.007	0.003 - 0.009	0.013 - 0.023	0.018 - 0.039	0.020 - 0.037	0.022 - 0.037	0.018 - 0.024	0.017 - 0.037	0.031 - 0.040
Mass Loading Removal										
Average, %	99.3	92.0	98.3	99.7	99.4	99.4	99.5	99.6	99.5	99.4
Range, %	99.0 - 99.4	82.1 - 96.3	96.5 - 99.3	99.5 - 99.8	99.1 - 99.6	99.1 - 99.7	99.4 - 99.6	99.4 - 99.8	99.4 - 99.7	99.3 - 99.5
Test Philosophy	MgO add'n.	Low inlet fly ash loading.		Basic operating conditions.	Low gas rate.	Minimum venturi.	Venturi only.	Basic operating conditions. York demister added.	High percent solids recirculated.	Repeat of Run VFG-1E at correct conditions.
Comments		TDS low due to non-equilibration of clarifier.	TDS raised by $CaCl_2$ add'n. Boiler upset conditions caused higher inlet grain loading.			Flowmeter probe caused high flow to venturi. Desired 140 gpm.		Demister plugged after 55 hrs. of operation.		

[1] LI is an abbreviation representing a low frequencey, fresh water, top and bottom mist eliminator wash scheme. The bottom wash was shut off during testing

Table I. Flue Gas Characterization Program results for the Venturi/Spray Tower system.

Controlled Variables	TFG-2A	TFG-2B	TFG-2C	TFG-2D	TFG-2E	TFG-2F	706-2A
Gas Rate, acfm @ 300°F	30,000	30,000	30,000	20,000	30,000	30,000	30,000
Scrubber Gas Velocity, ft/sec	12.5	12.5	12.5	8.4	12.5	12.5	12.5
Slurry Rate, gpm	1200	1200	1200	1200	600	1200	1200
Percent Solids Recirculated	15	15	15	15	15	15	15
Fly Ash Loading	High	High	High	High	High	High	Low
Alkali	Limestone	Limestone	Limestone	Limestone	Limestone	Limestone	Limestone
Mist Eliminator Configuration	chevron	chevron	chevron	chevron	chevron	chevron	chevron
Mist Eliminator Wash Scheme [1]	HI	HI	C	C	C	no wash	HI
MgO Addition	Yes	No	No	No	No	No	No
Uncontrolled Variables							
Gas Velocity at Mist. Elim., ft/sec	8.2	8.2	8.2	5.5	8.2	8.2	8.2
TCA Beds ΔP Range, in. H_2O	5.6 - 7.4	7.0 - 9.0	7.0 - 8.5	4.4 - 5.1	4.4 - 5.0	5.6 - 7.2	8.0 - 10.0
Mist Eliminator ΔP Range, in. H_2O	0.47 - 0.50	0.45 - 0.60	0.48 - 0.60	0.18 - 0.20	0.45 - 0.55	0.44 - 0.50	0.40 - 0.60
Total Dissolved Solids, ppm	50,000 - 55,000	7,300 - 9,500	5,000 - 10,000	5,700 - 7,400	4,600 - 6,300	6,400 - 8,700	7,000 - 9,000
Flue Gas Measurements							
Mass Loading, Inlet							
Average, gr/dscf	4.67	6.07	5.82	6.13	5.69	4.53	0.124
Range, gr/dscf	3.55 - 5.61	5.14 - 7.59	4.77 - 7.51	4.23 - 6.86	4.39 - 6.61	3.67 - 5.43	0.065 - 0.225
Mass Loading, Outlet							
Average, gr/dscf	0.055	0.048	0.064	0.056	0.065	0.042	0.026
Range, gr/dscf	0.034 - 0.092	0.037 - 0.058	0.058 - 0.080	0.051 - 0.065	0.054 - 0.088	0.035 - 0.046	0.018 - 0.032
Mass Loading Removal							
Average, %	98.8	99.2	98.9	99.1	98.8	99.1	74.0
Range, %	98.3 - 99.4	98.9 - 99.4	98.4 - 99.2	98.7 - 99.2	98.4 - 99.1	99.0 - 99.2	53.8 - 85.8
Test Philosophy	MgO addition.	Basic operating conditions. HI wash scheme.	Basic operating conditions. C wash scheme.	Low gas rate.	Low liquor rate.	Basic operating conditions. No wash.	Low inlet fly ash loading.
Comments	Noticeable scale particles were found on the outlet mass loading filter.						

(1) Wash Schemes: HI, high frequency fresh water bottom wash with the bottom wash off during testing; C, continuous diluted clarified liquor bottom wash left on during testing. With both schemes a low frequency fresh water top wash was used.

Table II. Flue Gas Characterization Program results for the TCA system.

Specie	VFG-1A			VFG-1B			VFG-1C		
	TVA Lab	Bechtel Lab[(1)]		TVA Lab	Bechtel Lab[(1)]		TVA Lab	Bechtel Lab[(1)]	
		1	2		1	2		1	2
Ca, wt. %	7.4	3.7	5.4	6.6	10.0	10.4	3.7	4.0	7.4
Mg, wt. %	0.4	1.3	0.4	0.3	3.6	1.0	0.2	1.4	0.6
Fe, wt. %	6.2	5.2	9.1	7.1	3.1	5.8	4.6	3.1	6.0
Al, wt. %	1.9	2.0	5.9	1.1	1.1	3.1	2.9	3.4	9.1
Total Sulfur, wt. %	13.5	9.8	--	15.3	11.7	--	12.0	10.3	--
Reaction Products									
Calculated wt. % (2)	32.5	22.5	24.4	28.6	61.3	48.2	16.2	24.4	33.6
Calculated Grain Loading, gr/dscf	0.008	0.005	0.006	0.001	0.003	0.002	0.003	0.005	0.007

Notes: (1) Two methods were used: 1 = wet chemical methods and 2 = semi-quantitative spectrographic.

(2) Assumes: $Ca \equiv CaSO_3 \cdot 1/2H_2O + CaSO_4 \cdot 2H_2O$ such that oxidation is 20 percent and all MgO was converted to $MgSO_4 \cdot 7H_2O$

Table III. Selected Venturi/Spray Tower outlet mass loading solids analysis and resulting calculated reaction products emission.

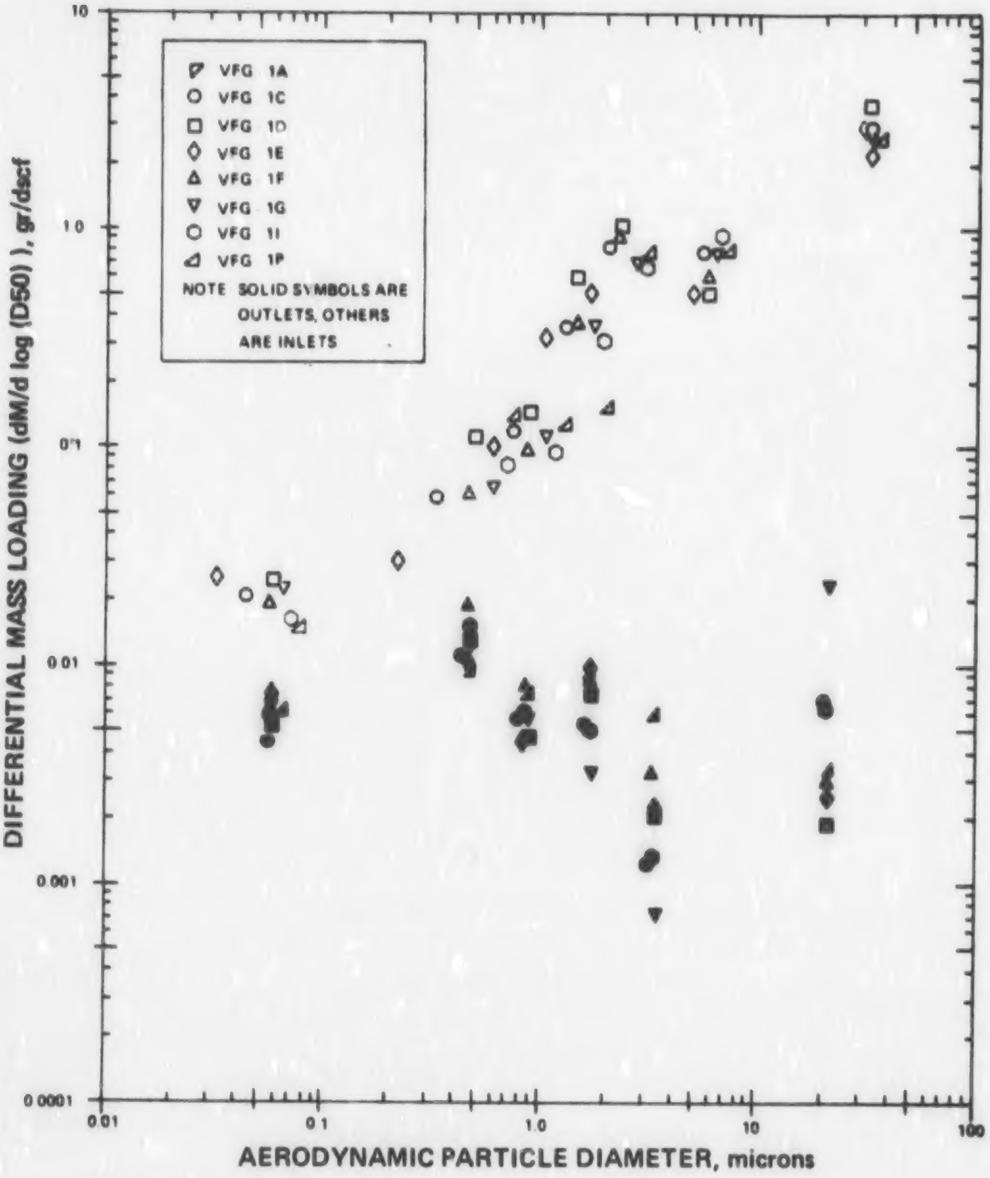

Figure 1. Mean differential mass loading versus aerodynamic particle size for all Venturi/Spray Tower system high fly ash loading runs.

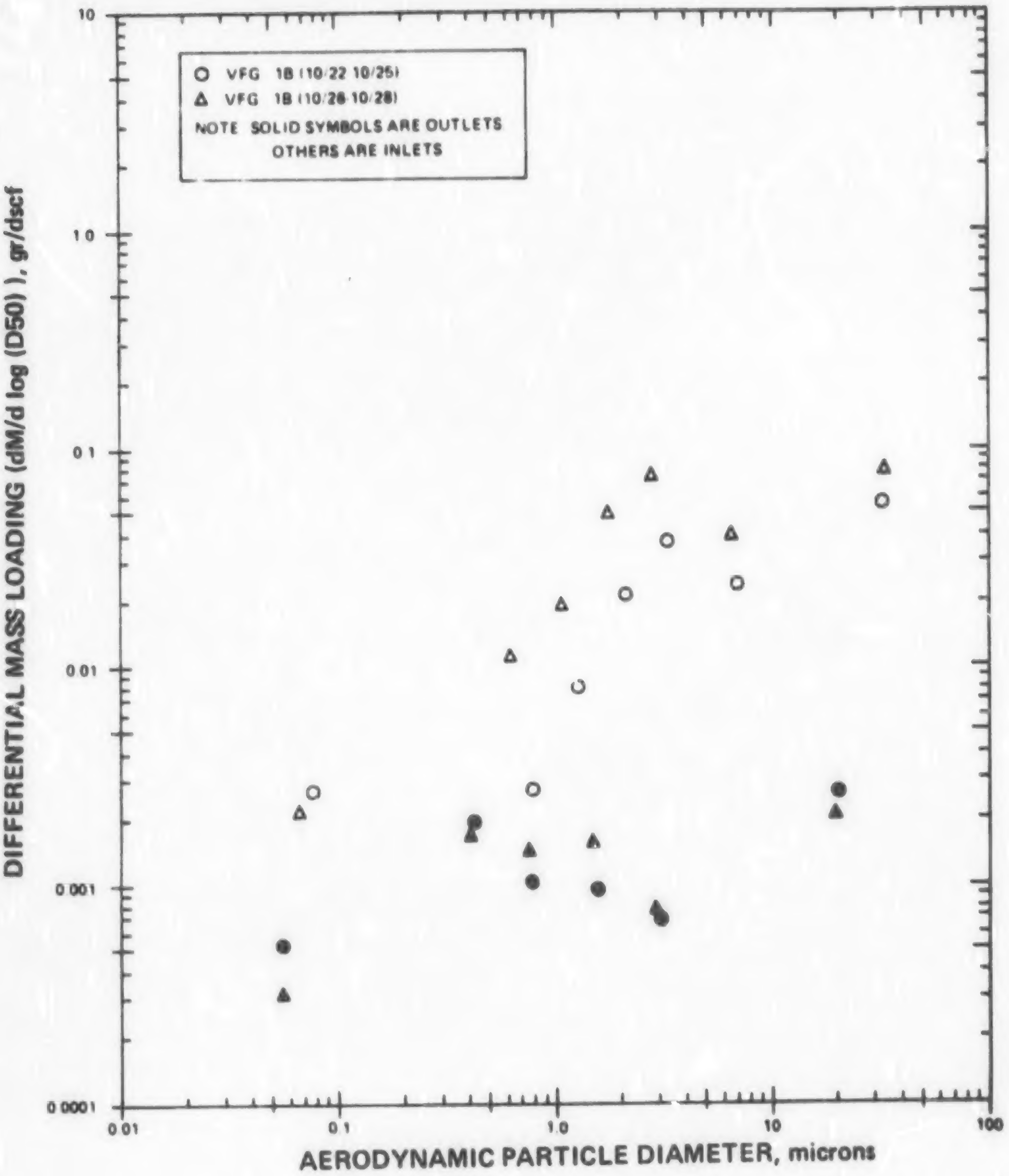

Figure 2. Mean differential mass loading versus aerodynamic particle size for the Venturi/Spray Tower system low fly ash loading run.

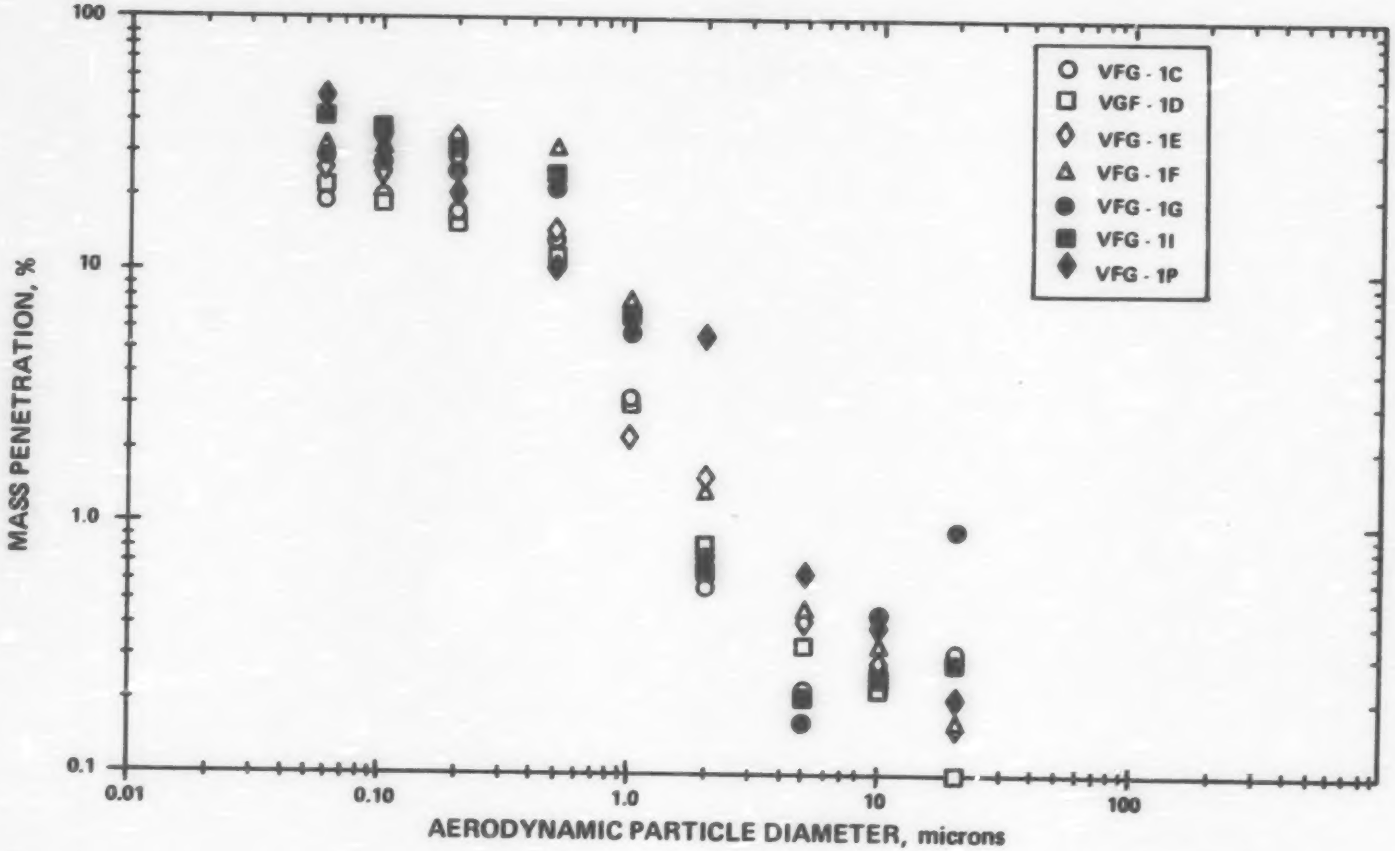

Figure 3. Mass percent penetration versus aerodynamic particle diameter for all Venturi/Spray Tower high fly ash loading runs.

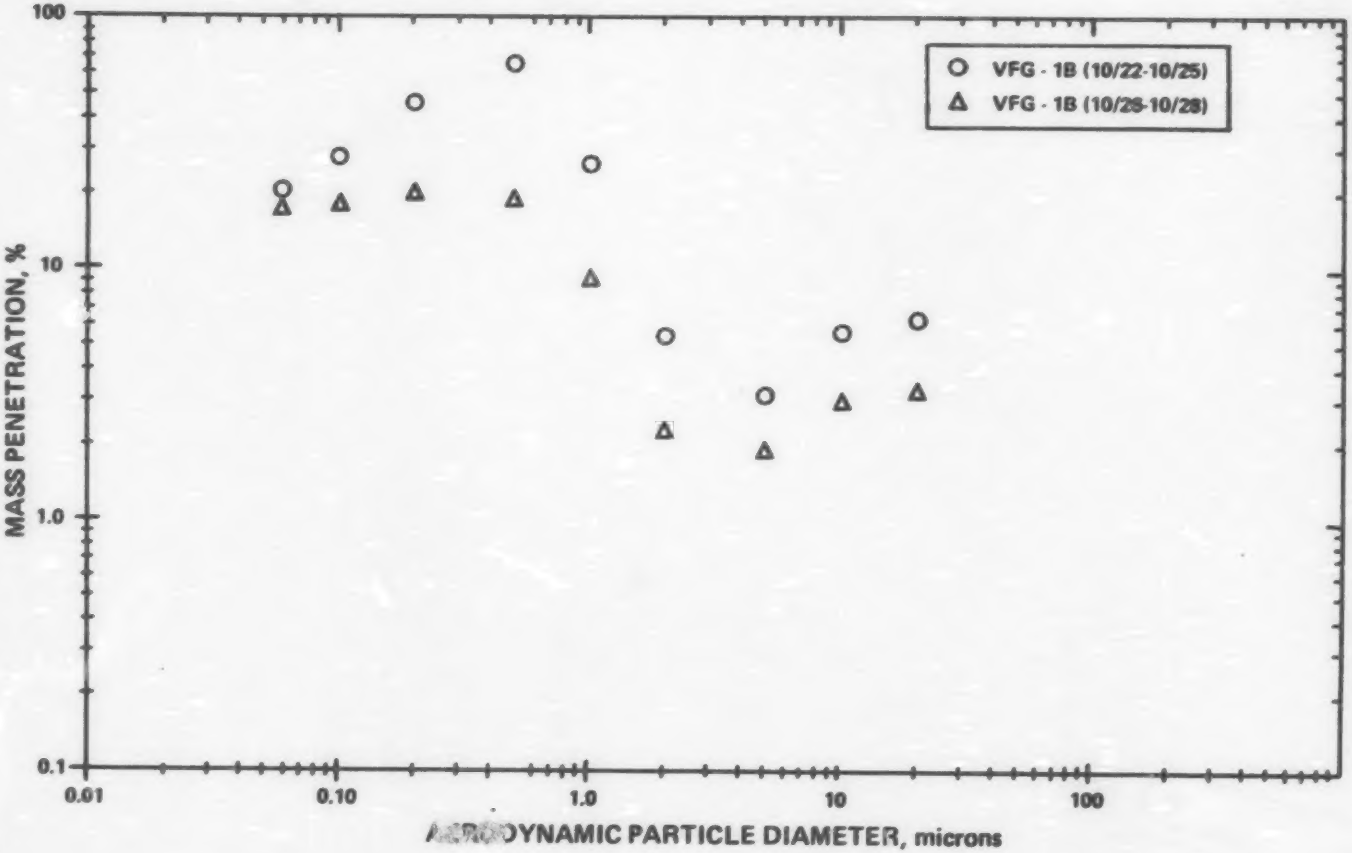

Figure 4. Mass percent penetration versus aerodynamic particle diameter for Venturi/Spray Tower low fly ash loading Run VFG-1B.

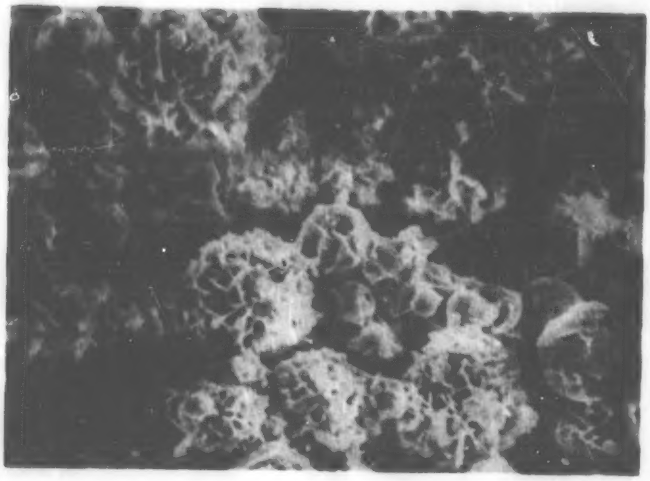

Figure 5. Particulate on third stage of outlet impactor during Venturi/Spray Tower run VFG-1A. Magnification 2000X.

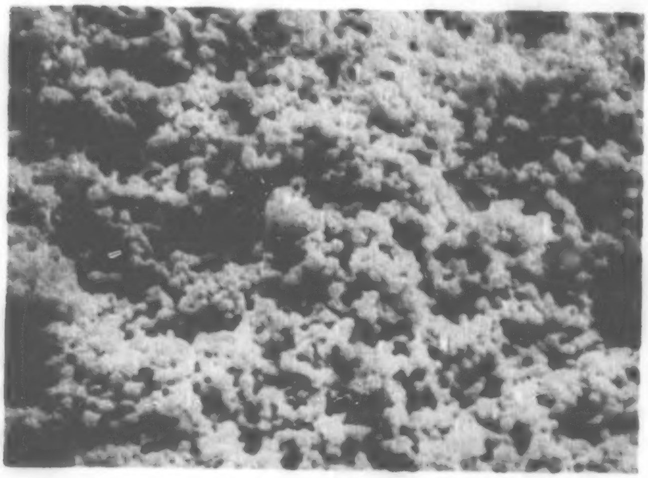

Figure 6. Particulate on sixth stage of outlet impactor during Venturi/Spray Tower run VFG-1A. Magnification 5000X.

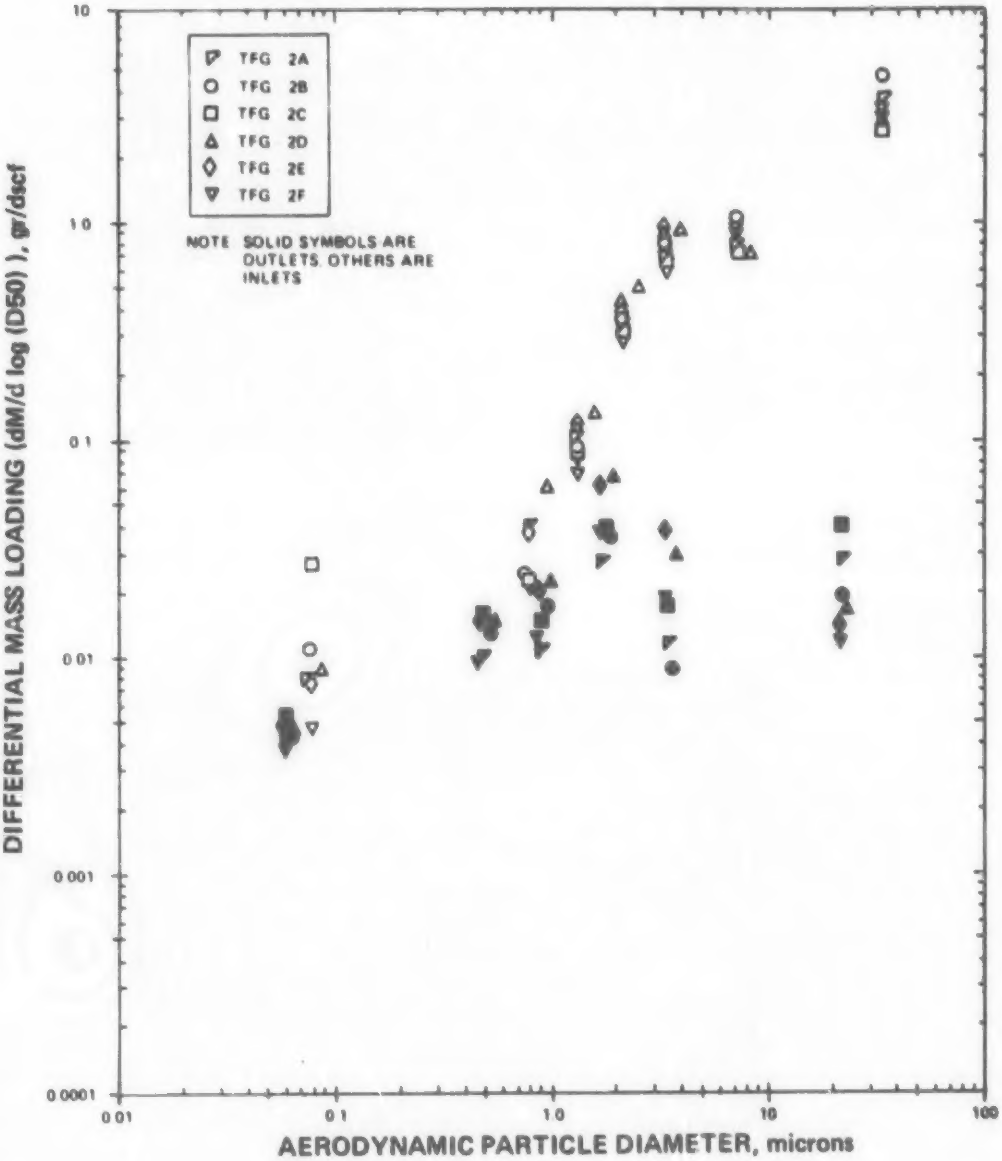

Figure 7. Mean differential mass loading versus aerodynamic particle size for all TCA system high fly ash loading runs.

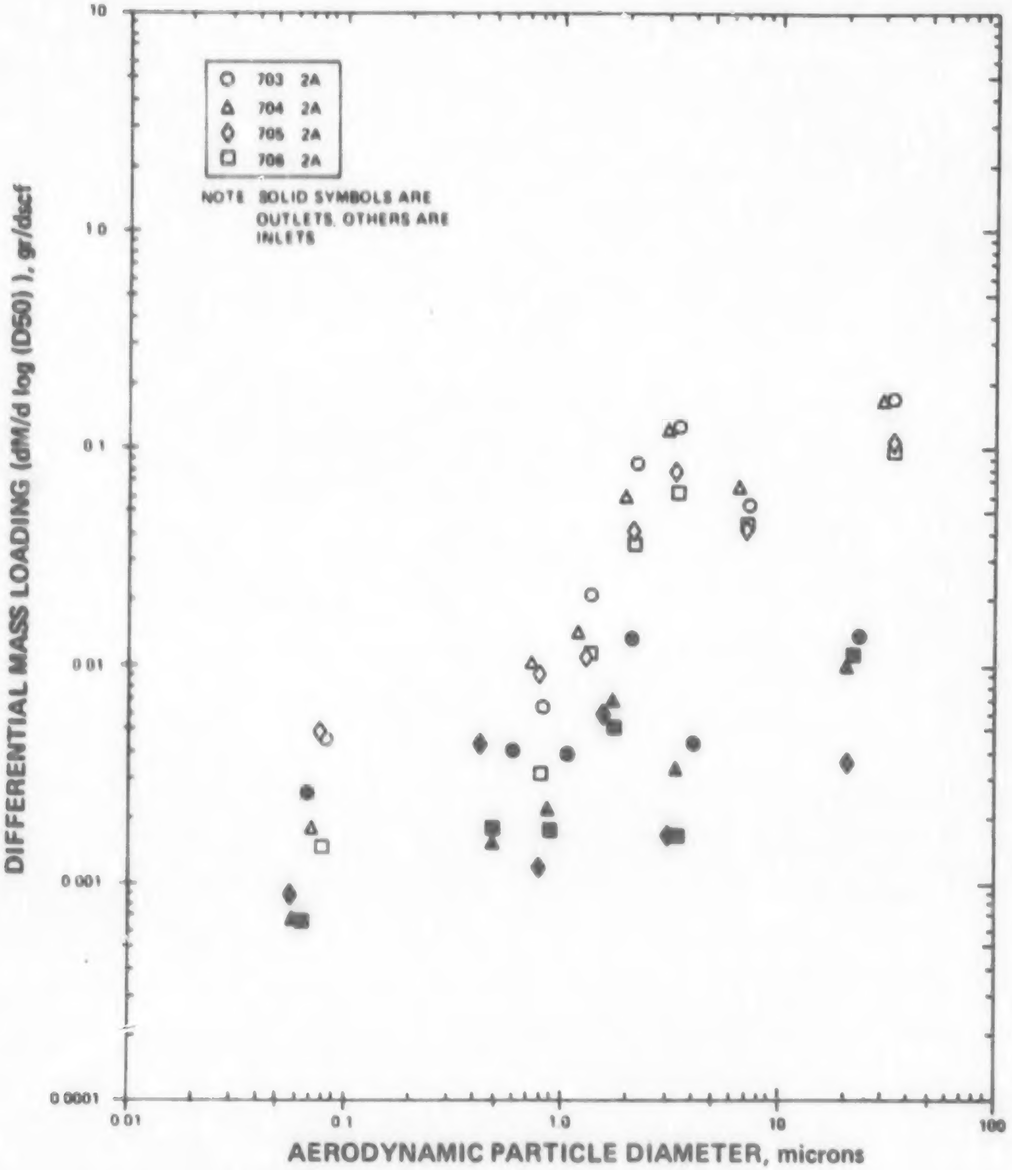

Figure 8. Mean differential mass loading versus aerodynamic particle size for all TCA system low fly ash loading runs.

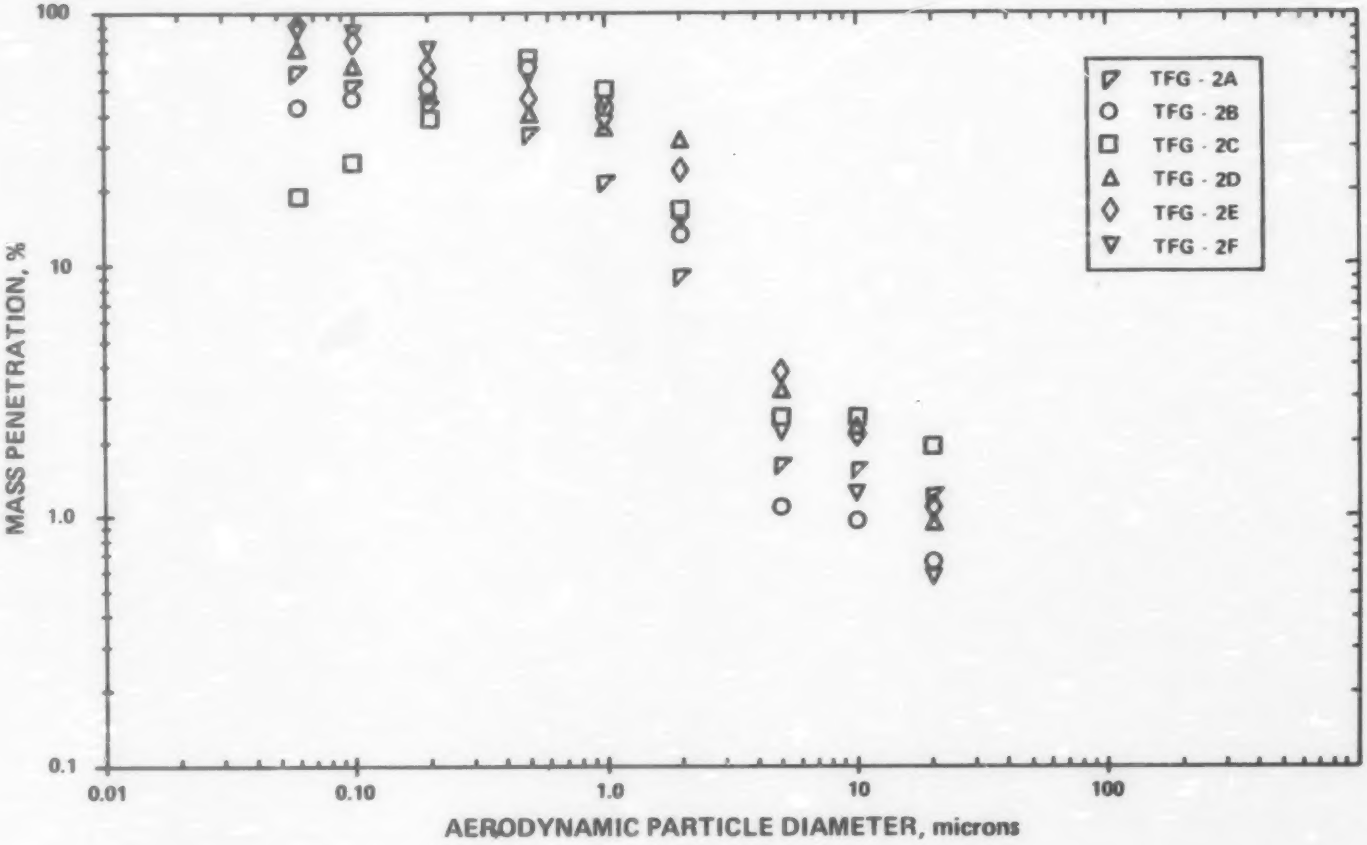

Figure 9. Mass percent penetration versus aerodynamic particle size for all TCA high fly ash loading runs.

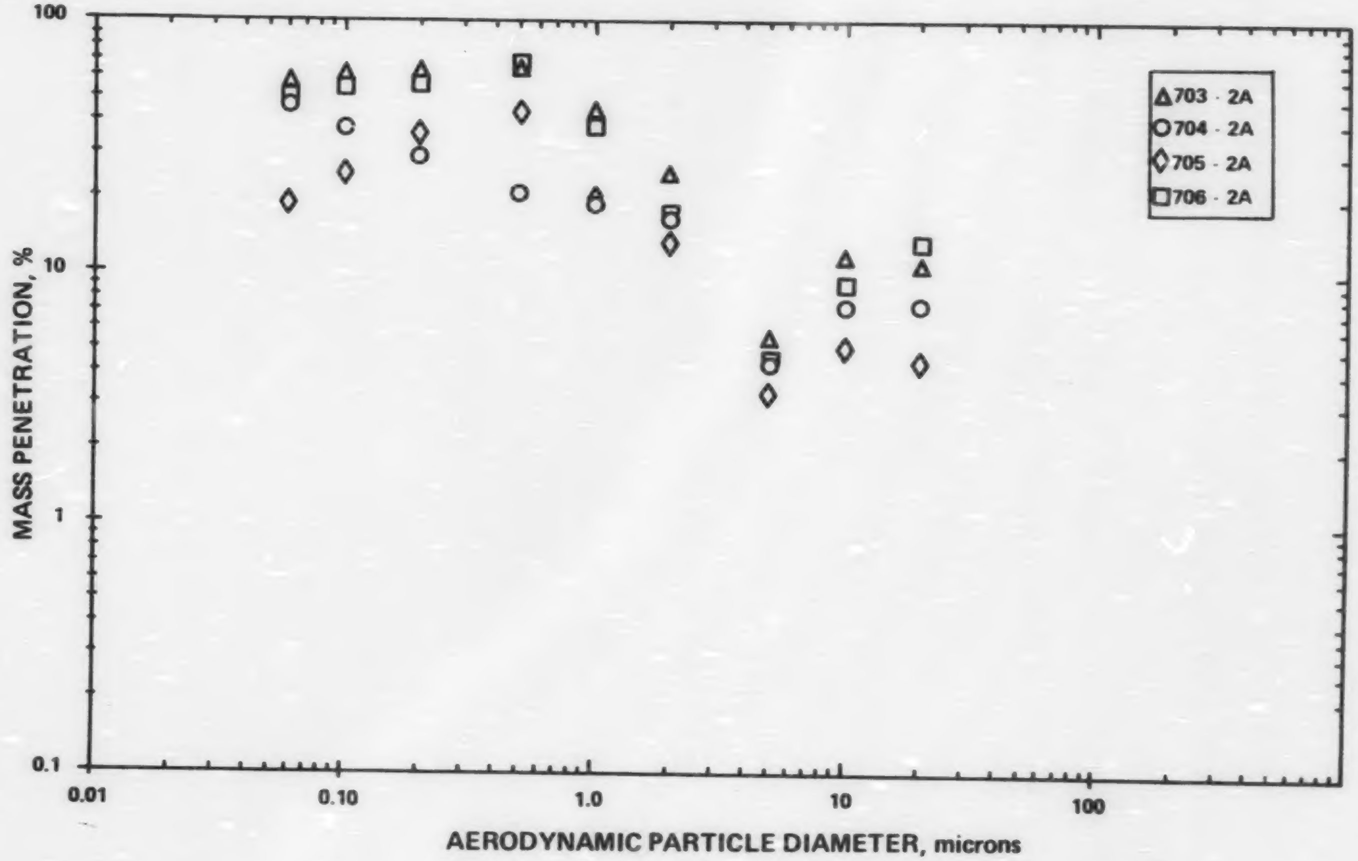

Figure 10. Mass percent penetration versus aerodynamic particle size for all TCA low fly ash loading runs.

References

1. Bechtel Corporation, EPA Alkali Scrubbing Test Facility: Summary of Testing through October 1974, EPA Report 650/2-75-047, June 1975.
2. Bechtel Corporation, EPA Alkali Scrubbing Test Facility: Advanced Program First Progress Report, EPA Report 600/2-75-050, September 1975.
3. Bechtel Corporation, EPA Alkali Scrubbing Test Facility: Advanced Program Second Progress Report, EPA 600/7-76-008, September 1976.
4. M. P. Schrag and A. K. Rao, Fine Particle Emissions Information System: Summary Report (Summer1976), EPA Report 600/2-76-174, June 1976.
5. Federal Register, Vol. 36, No. 247, 12/23/71, p. 24888.
6. TRW Corporation, Procedures for Aerosol Sizing and SO_3 Vapor Measurement at TVA Shawnee Test Facility, Document No. 24916-60390-RU-01, 1977.
7. D. B. Harris, "Tentative procedures for particulate sizing in process streams - cascade impactors", IERL, EPA , Research Triangle Park, N. C., ppm. 30-32, February, 1976.
8. R. H. Perry, Chemical Engineers' Handbook, fifth edition, McGraw-Hill Book Co., New York, 1973, p. 5-61.

THE WATERLOO SCRUBBER

Donald R. Spink
Francis A.L. Dullien
Peter L. Douglas

Department of Chemical Engineering
University of Waterloo
Ontario, Canada N2L 3G1

ABSTRACT

The body of information presented in this paper is directed to all those poor souls who are faced with tough particulate removal problems and frustrated because only expensive and high energy-consuming solutions are available to contend with the problem. A simple and yet highly effective scrubber is described with examples detailed for application to treatment of particulate-laden hot gases and implied for treatment of cooler gases, e.g., those less than 100°C.

THE WATERLOO SCRUBBER

Introduction

The purpose of this paper is to

a) describe the Waterloo Scrubber and point out its many features

b) present laboratory and plant data to illustrate the abilities of the Waterloo Scrubber to effectively remove fine particulate

c) present a theoretical, mathematical model which appears to account for the removal efficiencies observed

Figure 1 is a photograph of our laboratory scrubber installation which clearly illustrates the simplicity of this scrubber. The main components are the duct work, the slightly modified fan and a means to introduce a fine mist or fog into the duct upstream from the fan. The cross-section of the Waterloo Scrubber, shown in Figure 2, illustrates its simplicity. The major modification to the fan is to include a drain at the lowest point in the fan casing as shown in Figure 2, along with the water seal used to receive the agglomerated spray and contained particulates. A source for introducing a fine spray of water or other liquid is also shown. While we have studied a number of fine-spray-producing devices, the so called "sonic" nozzles appear to be most suited for two reasons: their energy consumption is modest, and wear, tear and maintenance is minimal. One disadvantage of sonic nozzles is that, when properly tuned, they can be somewhat noisy and therefore distracting. Insulation of the duct may be required depending on the location of the scrubber.

There are three criteria which are necessary for the proper operation of the Waterloo Scrubber:

1) The mist or fog of droplets introduced must be fairly fine, i.e., normally on the order of from 5 to 50 μm in a reasonably uniform distribution.

2) The fan must turn at a relatively slow speed so as to provide not only the necessary degree of turbulence but of even greater importance, the requisite residence time for the contact, agglomeration and elimination of the liquid mist and particulates originally contained in the dirty gas stream.

3) The number of liquid mist droplets introduced to the system must be in proportion to the number of particulates to be removed from the system; however, as dust loadings increase the ratio of liquid droplets to dust particles can be reduced and visa versa.

If the mist or fog of liquid is introduced into the system by condensation of water vapour, such as would occur if a hot, saturated gas stream were suddenly cooled by the introduction of a small stream of cold air, in that the vapour is caused to condense in situ, such condensation will normally take place on the surfaces of the dust particles within the duct, thereby causing these to grow. This is especially true when the dust particles are hydrophilic and even more so when they are hygroscopic. Under such conditions, less energy is consumed and it is found that the amount of water so produced on condensation need not be as great an amount as would have to be furnished by an atomizing nozzle. We'll come back to this point shortly.

If a finely dispersed liquid mist is introduced into most scrubbers, a significant number of the fine mist "particles" will not be captured. Thus, the removal of acid mists, for example, is often a serious problem to many chemical and metallurgical industries. Conventional "demisters" are also ineffective in the removal of fine mists or fogs. Thus, one of the important features of the Waterloo Scrubber is its ability to remove fine mists or fogs from a gas stream.

Experimental Methods

Standard testing procedures were employed for all experimental studies reported here. These procedures include isokinetic sampling and the use of Joy WP-50 particulate train. Calculations were based on those outlined by the Joy Manufacturing Company in their bulletin WP-50.

All data was statistically examined to ascertain its reproducibility and level of confidence.

Only a limited number of particle size distribution experiments have been conducted, primarily due to the tedious nature of such work and the high degree of uncertainty associated with the results(4). Prior to late 1976, this type of data was determined the "hard way". A dispersed sample was first collected on a polished stub (a source of much controversy), gold plated (vapour deposition), subjected to a scanning electron microscope photograph which was then analyzed on a Quantimet. Some confidence was initially established with this approach when results matched the manufacturer's particle size distribution data very closely for several different pigments tested.

Late in 1976 an Anderson 8 stage, cascade impact sampler was obtained. Initial use of this equipment has been primarily in studies to improve the methods employed to introduce and disperse the test dust into the system. A few scrubber outlet samples have also been collected on the Anderson sampler to determine individual particle size removal efficiencies.

Results

The method of introducing test dust into a scrubber system is one of the most critical steps in the study and development of particulate removal systems in the laboratory. We have employed numerous methods in attempts to develop a superior system and by continuous improvements have now achieved the requisite excellent dispersion of fine powders by the equipment shown in Figure 3. Particle distribution data using an Anderson Cascade impact sampler have confirmed the excellent dispersion achieved with the simple equipment shown in Figure 3. The vibrating feeder delivers a uniform flow of the dust to the throat of an air venturi where a high velocity air jet draws the dust into the system while at the same time effectively dispersing it in the duct of the system.

The test dust employed to the greatest extent in our studies is a pigment-grade aluminum silicate; Figure 4 shows the characteristics of this dust. Also shown on Figure 4 is a typical particle size distribution (count not normalized) for an outlet sample from the Waterloo Scrubber. For this particular experiment and sample, all particles greater than 1.2 µm have been completely removed; this phenomena has been observed for many years with the Waterloo Scrubber.

The ability of the Waterloo Scrubber to completely eliminate a fine mist or fog is believed to be responsible also for the removal of fine particulates in the gas stream. (At the meeting, a short film will be shown at this point which illustrates the ability of the Waterloo Scrubber to completely eliminate a fine mist or fog from a gas stream).

The observed instantaneous elimination of a fine mist or fog by the action of a slowly-turning fan has been analyzed in terms of several "classical" mechanisms of coagulation and precipitation of aerosols, but none of these classical mechanisms account for more than a fraction of the effect observed. The elimination of the fine mist can be fully explained, however, if it is assumed that turbulent diffusion on a scale comparable to the effective stopping distance of the larger drops present in the mist is responsible for the fast agglomeration of the mist to produce larger droplets which are easily removed by the centrifugal action in the fan.

Physical justification for this assumption may lie with the postulated mechanism whereby, for very short periods of time, large directional velocity differences exist between droplets of different size such that the simultaneously existing turbulent diffusion of the particles is made far more effective than has been assumed by existing theories, resulting in a much higher rate of coagulation (or agglomeration) than would be observed either due to a similar velocity difference between the different sized droplets in the absence of turbulence or as a result of turbulent diffusion in the absence of a large velocity difference between the droplets.

The resulting mathematical model, written as a symmetrical expression for the rate of disappearance of small and large droplets (particles) is as follows(5):

$$\frac{d\,n_L}{dt} = \frac{d\,n_S}{dt} = -\pi\,\frac{D_L + D_S}{2}\left(\frac{\varepsilon}{15\nu}\right)^{1/2}\frac{(x_L - x_S)^2_{eff}}{t^2_{eff}}\,n_L\,n_S\,n\,t^2 \quad (1)$$

where n = number of drops in a unit volume
t = time
D = diameter of drops
ε = energy dissipated per unit mass of medium
ν = kinematic viscosity
x = distance travelled by particles (stopping distance)
η = capture coefficient

subscripts

L = large
S = small
eff = effective

This model is based on the assumption that only two sizes of droplets are initially present and in equal number. The introduction of a true size distribution $f(D)dD$ of the drops initially present so as to obtain the droplet size concentration at any time t is presently being developed.

Numerical integration of equation (1) over very short time periods to obtain an approximate solution gives new drop sizes D_L' and D_S' and corresponding new concentrations n_L' and n_S'; this process can then be repeated for successive short time periods to develop the ultimate particle size distribution at any time. Such calculations employing time increments of 0.0005 seconds indicate that virtually all of the particles are large enough after relatively short residence short residence times to be removed by centrifugal action in the fan. While such an approach provides only an approximate solution, the results relate very closely to that observed. Further development and testing of the model are now in process.

We have heretofore emphasized the necessity of a slowly turning fan. Application of equation (1) is in agreement with this concept where t_{eff}, the effective residence time of particles in the fan, must be sufficient to allow the interactions theorized to take place. Such results are expressed in a different fashion as shown in Figure 5. The relationship shown should not be considered as exact but "illustrates" in pictorial fashion what we have observed and what has been reported in the literature(5). At the higher speeds, turbulence increases at the expense of residence time. It should be pointed out that even when the fan is turning relatively slowly, a highly turbulent condition still exists within the casing of the fan. As an example, a fan turning at 600 rpm and delivering 800 cfm of air will have a fan Reynolds Number around 10^5; a larger fan turning at around 230 rpm and delivering 50,000 cfm of air will have a fan Reynolds Number in excess of 10^6. The effective residence time for both situations will be approximately the same.

Another relationship which is important is the very small amount of water normally employed in the Waterloo Scrubber. Injection of less than 0.03 dm^3 of water per m^3 of gas (approximately 3 lbs. per 1000 ft^3) in the form of a mist consisting of droplets ranging in size from about 5 µm to about 65 µm and with a number average droplet diameter of about 20 to 25 µm is normally effective for the removal of fine particulate. Thus, in the process of eliminating particulates from a gas stream, a very small and thus relatively easily handled aqueous discharge stream results.

All of our earlier work employed Spraying Systems pneumatic atomizing nozzles. Figure 6 illustrates the relationship between average mist droplet size and air pressure used for the Spraying Systems nozzle. Figure 6 is related to Figure 7 which shows the number of mist droplets produced per minute, also as a function of air pressure employed when spraying about two pounds of water per minute. Note that at normal operating conditions, some 100 billion water droplets are produced per minute. The drop size distribution obtained with the pneumatic nozzle (Spraying System) at an air pressure of 485 kPa and at a water flow rate of 1.1×10^{-2} dm^3 s^{-1} is shown in Figure 8. The droplet diameters were measured by using the magnesium oxide method developed by May(7), whereby the airborne droplets are allowed to strike a layer of magnesium oxide on a glass slide. The resulting permanent impressions were then measured under a microscope. Work is currently being conducted in obtaining similar information for various sizes of sonic nozzles when operated under different conditions. It appears that equivalent or better performance can be expected when using one or more of the smaller sonic nozzles with less than 101 kPa air pressure. The larger sonic nozzles don't appear to be as effective at producing very fine mists as the smaller sonic nozzles and normally require higher air pressure. Thus, in some cases, several of the smaller sonic nozzles might be more effective than one larger nozzle.

The effect of dust loadings in the dirty gas stream and the effect of air pressure with a Spraying Systems nozzle on particulate removal efficiency is shown in Figure 9 (using aluminum silicate pigment). To achieve higher removal efficiencies when dust loadings are very small, relatively speaking, many more fine water droplets would be required. When dust loadings are very high, removal is made much easier due to particle-particle interactions which tend to form agglomerates without requiring water to assist to any great extent.

Several additional test dusts as supplied by clients have been evaluated in our laboratory facilities. Unfortunately, we did not characterize these test dusts. Tests on carbon black and aluminum oxide, for example, each resulted in complete removal.

A number of tests have also been conducted on the gases eminating from the "recovery" boiler at a kraft pulp mill. In these tests, which were conducted at the Consolidated Bathurst mill at Portage du Fort, Quebec, the gases were first treated by an electrostatic precipitator rated at 95% efficiency. Removal efficiencies of 96% of particulates remaining after the electrostatic precipitator were achieved with the Waterloo Scrubber on these preliminary tests. Unfortunately, we have not yet been able to characterize the particulate emission from the recovery boiler of a kraft mill after passing through an electrostatic precipitator; however, the indicated mean particle diameter is about

0.4 μm. During tests conducted at Consolidated Bathurst, the gases from the electrostatic precipitator were received at 138°C (280°F). We found that when a fine water spray is introduced into a turbulent gas stream at 138°C or thereabouts, evaporation of the smaller droplets takes place in a small fraction of a second(8). Therefore, before we can effectively introduce a fine spray into a hot gas stream, we must cool and humidify the gases to near their dew point. This can be accomplished in a number of ways. In the initial kraft mill tests, we accomplished this task by inserting a total of four Spraying Systems atomizing nozzles in the duct carrying the hot gases; we found that the hot gas was at its dew point after three nozzles so the fourth was placed several meters from the fan scrubber. Unfortunately, this method of gas cooling is fairly high in its consumption of energy since each Spraying Systems nozzle requires about 520 kPa air to be effective; the calculated energy to compress the air used in each of the nozzles is about 370 W (1/2 HP) depending on the actual amount of air used and method of compression (we did not measure air consumption for these tests but used manufacturer's information). It could perhaps be argued that the cooling and humidification of the gases is unrelated to the actual particulate removal step, but nevertheless, it is a required step. Total power consumed for the initial test at Consolidated Bathurst probably falls between 3.95-5.53 kwh/m^3 (2.5 and 3.5 HP/1000 ft^3/min) of gas scrubbed vs. about 1.5 kwh per m^3/min (approximately 1 HP/1000 cfm) when cooler air is being scrubbed in the Waterloo Scrubber.

Once the effectiveness of the Waterloo Scrubber to remove substantial amounts of salt cake fly ash from the recovery boiler off-gas was established, our thoughts were then directed to methods to improve removal efficiencies and reduce energy consumption. It was felt that humidification of the hot gases could be accomplished in a simple packed tower; energy related to such a device would be that required to lift water from the sump to a distributor above the packing, a distance of less than 10 feet, plus energy related to the increase in pressure drop across the system. Rough calculations indicate that a total of less than 1.5 kwh/m^3 would be associated with the operation of the humidification tower.

Once the gases have been cooled and humidified close to their dew point, further cooling of the gas will produce a condensation effect thereby resulting in the formation of a cloud of water droplets within the duct. Such condensation will preferably take place on the surface of dust particles in the gas stream which could conceivably lead to improved removal efficiencies. This approach was first studied with the laboratory scrubber. The problem of producing up to 1/2 m^3/s of gas at its dew point and at approximately 160°F proved to be an interesting problem in itself. A salamander (gas heater) rated at 210,000 kJ/hr was the initial source of hot gas; this was cooled and humidified to some extent by the fine spray from a "sonic" nozzle, and followed by live steam provided at 165°C and about 500 kPa from a 1/2" open line. With minor adjustments, the requisite conditions were achieved. Test dust was introduced as described (vide supra).

In the laboratory tests, the cooling air was allowed to be sucked into the duct through variable-sized slots. The slot openings were varied by sliding a curved cover over a rectangular opening in the round duct. The formation of a mist or fog at the point of injection of the cooler air was readily apparent. Whereas in previous experiments with the aluminum silicate pigment as the test dust, efficiencies of about 96% were about the best achieved without excessive use of atomizing sprays (see Figure 9), all of the experiments employing the condensation approach to introduction of the mist within the duct showed at least 98% particulate removal and approximately half of such tests resulted in complete removal of the test dust.

Accordingly, the installation at Consolidated Bathurst has now been revised to eliminate all of the atomizing sprays. Instead, the energy of the hot gases will be used to provide the saturated situation, using a small packed tower for the humidification. Preliminary tests indicate that the hot gases can be cooled to their dew point with less than 12 ℓm^{-3} circulating flow when the flow of hot gases was in excess of 1/2 $m^3 s^{-1}$ (> 1000 ft^3/min).

A schematic flow diagram of the revised installation at Consolidated Bathurst is shown in Figure 10. In addition to the benefits of this approach as suggested above, water mist, produced by cooling the saturated hot gas stream, will be removed along with particulates by the scrubber and the combined stream returned by gravity to the sump tank below the humidification tower. Preliminary calculations indicate that slightly more water is evaporated in the humidification tower than is removed by the cooling-scrubbing process so that a small amount of water must be added to the system. This means that the strength of the Na_2SO_4 solution contained in the sump tank will slowly build up at a rate proportional to the amount of Na_2SO_4 removed from the hot gas stream. Na_2SO_4 exhibits a solubility of 44 kg/100 kg H_2O at 100°C, so we can assume that the concentration of Na_2SO_4 that can be recirculated to the humidification tower without problems would probably approach 40 kg per 100 kg water. At steady state conditions, a constant and fairly concentrated quantity of Na_2SO_4 solution will be removed from the sump tank and this volume must also be replaced by an equivalent amount of water to maintain a proper water balance. The $NaSO_4$ solution will be recycled back to the mill where further concentration may be conducted before addition to the strong black liquor which is fed to the recovery furnace.

To measure the energy efficiency of the Waterloo Scrubber relative to other scrubbers, the particulate removal efficiency must first be converted to a dimensionless number referred to as a 'transfer unit'. The transfer unit, N_t, is expressed as

$$N_t = \ln\left(\frac{1}{1 - \eta}\right)$$

where η is the collection efficiency and $1 - \eta$ is the penetration.

An efficiency of 96% corresponds then to 3.22 transfer units, 98% to 3.91 transfer units and 99% to 4.61 transfer units.

For a number of different scrubbers operating under different industrial conditions, Semrau has observed that

$$N_t = a\,P_t^{\,b}$$

for which 'P_t' represents the theoretical power input to the scrubbing process, and 'a' and 'b' are constants related to properties of the particulates being scrubbed(9). Figure 11 shows a plot of this relationship between efficiency and horsepower/1000 ft^3/min for wet scrubbers when used to scrub the particulates from a pulp mill recovery boiler emission. The initial tests at Consolidated Bathurst (96% removal efficiency) consumed between 2.5 and 3.5 HP/1000 cfm and this information is shown on Figure 11. Also included is the projected point for the revised system at Consolidated Bathurst. Whether Figure 11 would apply to the capture of particulates after passing through an electrostatic precipitator is not known; certainly, particle size and concentration are greatly different.

To date, all testing of the Waterloo Scrubber has taken place over a rather limited range of 0.25-1.0 $m^3 s^{-1}$ (500 to 2000 cfm) so no real evaluation of scale-up factors has been attempted to date. Based on the mathematical model and numerous other studies, constant residence time is felt to be the most critical element in scaling-up. Interestingly enough, as larger gas volumes are required to be handled, larger fans must be used at lower speeds; however the turbulence in the fan, as expressed by the fan Reynolds Number, increases (vidi supra). Figure 12 illustrates the relationship between fan speed and fan capacity for Waterloo Scrubbers having constant residence time. The relationships described above might indicate a potential for improved particulate removal efficiencies with scale-up to handle larger volumes of gas.

Conclusions

The following items summarize the advantages inferred or confirmed, for the Waterloo Scrubber over competing devices for fine particulate removal:

1) low energy consumption
2) low capital cost
3) low operating cost
4) low maintenance
5) low water usage
6) highly effective for the removal of sub-micron particulates

While many are complaining about the high cost of meeting environmental requirements, the Waterloo Scrubber appears to be a very simple yet highly effective solution to many air pollution problems.

Acknowledgments

The authors are grateful to the Committee on Pollution Abatement Research of Environment Canada for their support of the research and pulp mill testing programs described and to the fine people in the Consolidated Bathurst kraft mill at Portage du Fort, Quebec, who have co-operated with us in such an admirable manner during the test program. The authors also acknowledge the invaluable assistance of the many co-op students at the University of Waterloo who worked on this project and in particular, to Gordon Berthin for his dedicated efforts.

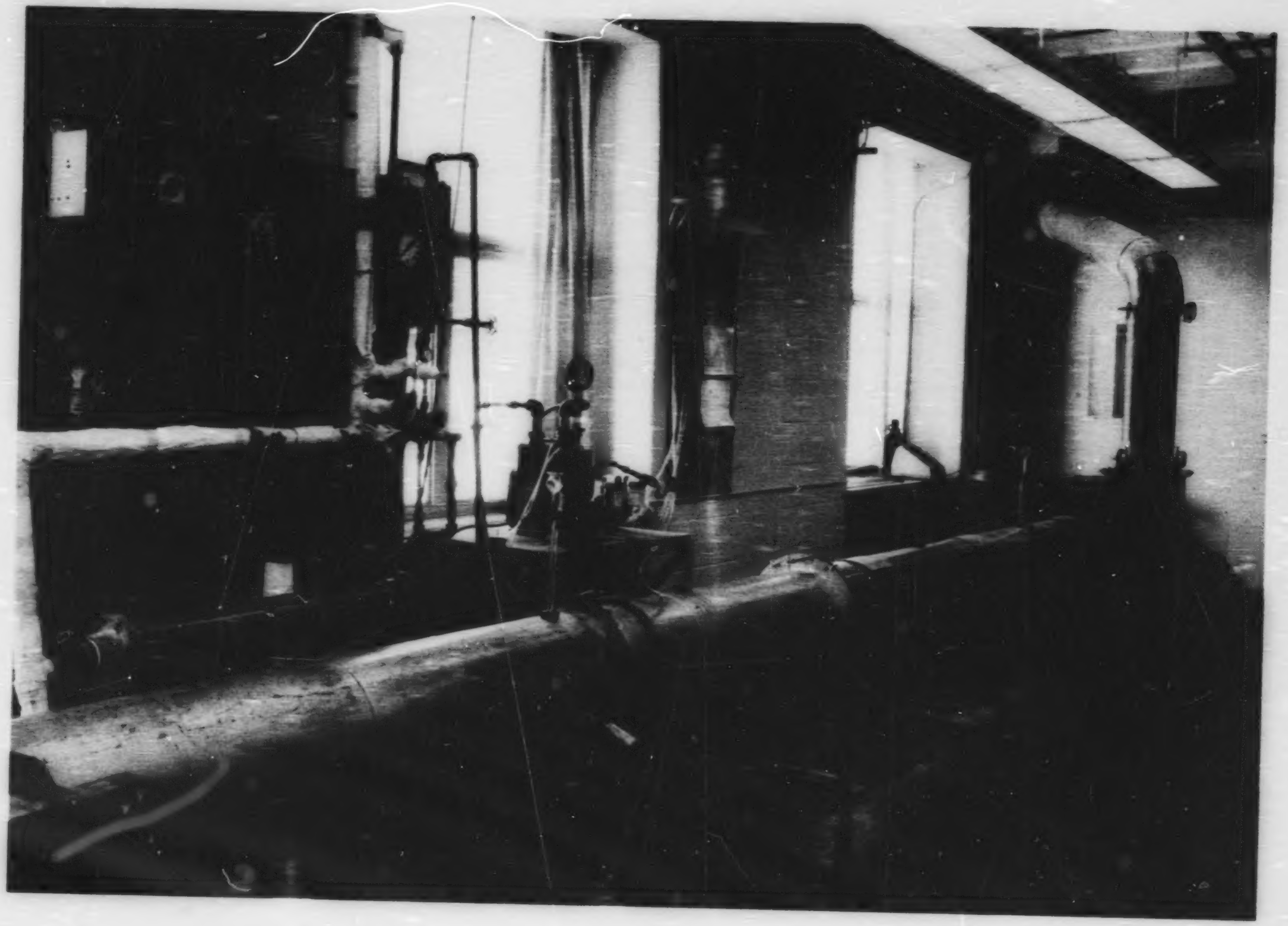

Figure 1. Waterloo Scrubber - laboratory installation.

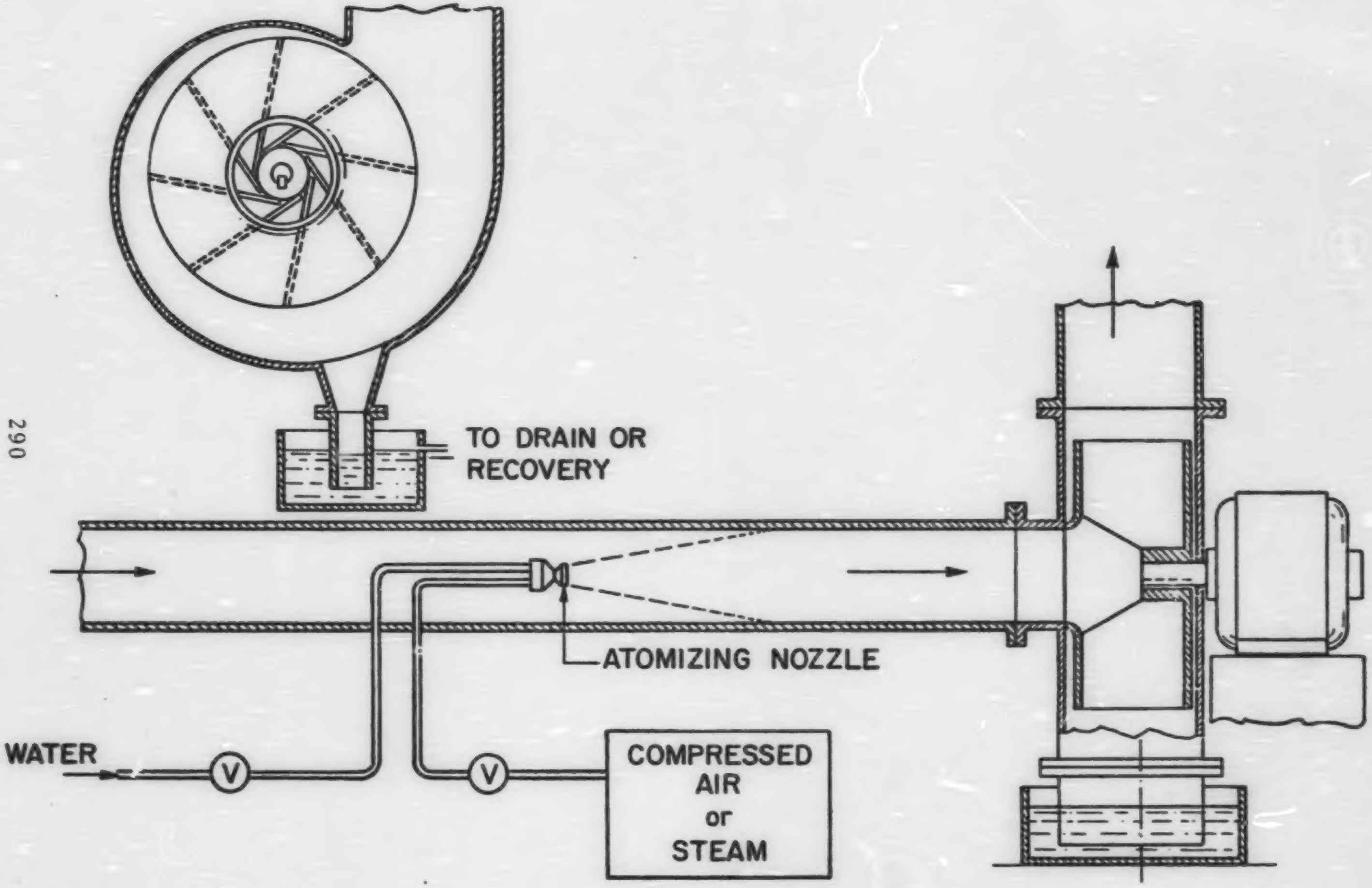
TO DRAIN OR RECOVERY
ATOMIZING NOZZLE
WATER
V
V
COMPRESSED AIR or STEAM

Figure 2. Cross-section details of Waterloo Scrubber.

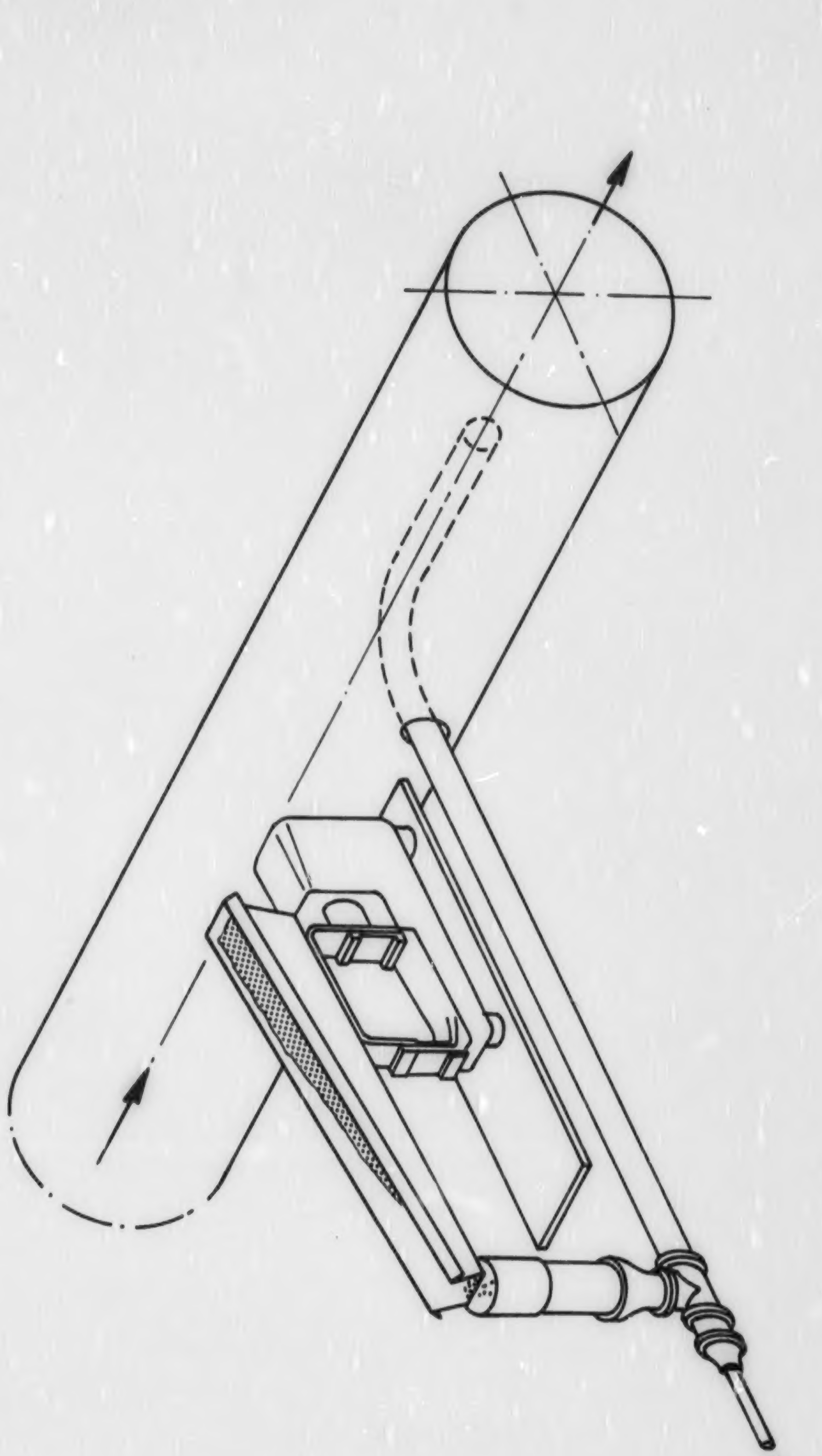

Figure 3. Dust feeding equipment.

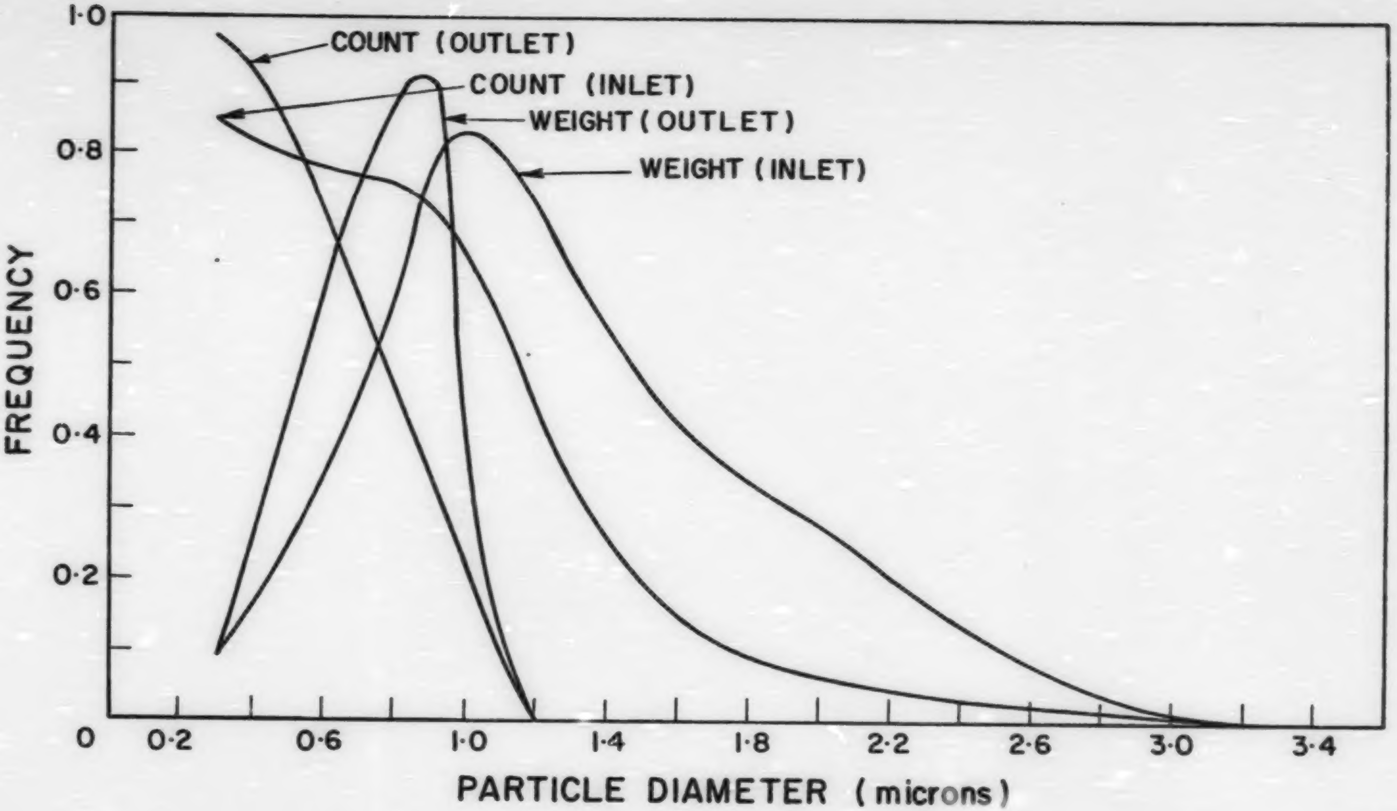

Figure 4. Typical particle size distributions (not normalized) in inlet and outlet duct samples on the Waterloo Scrubber.

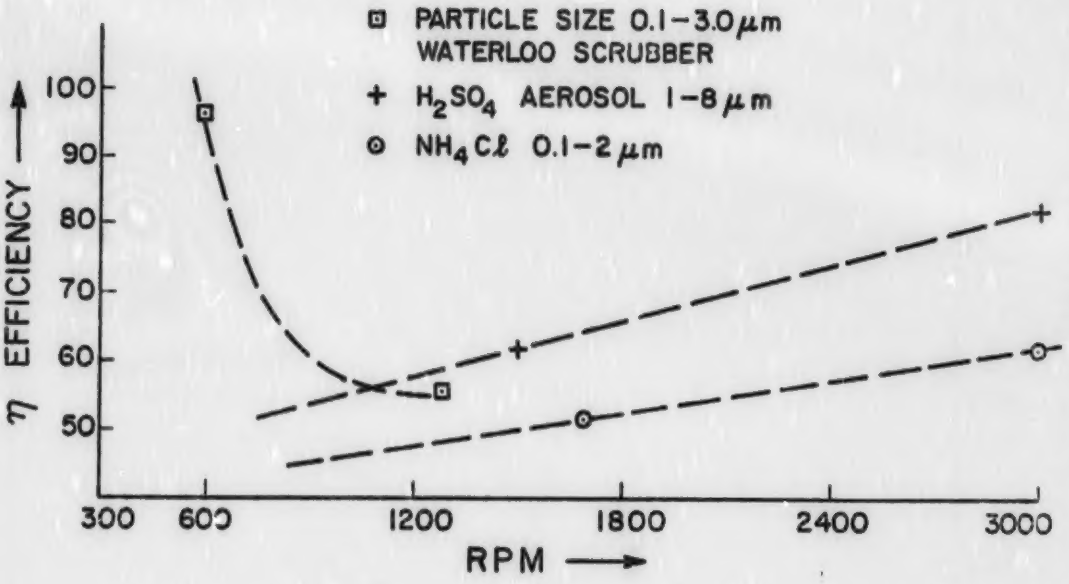

Figure 5. Fine particulate removal efficiency as related to fan speed.

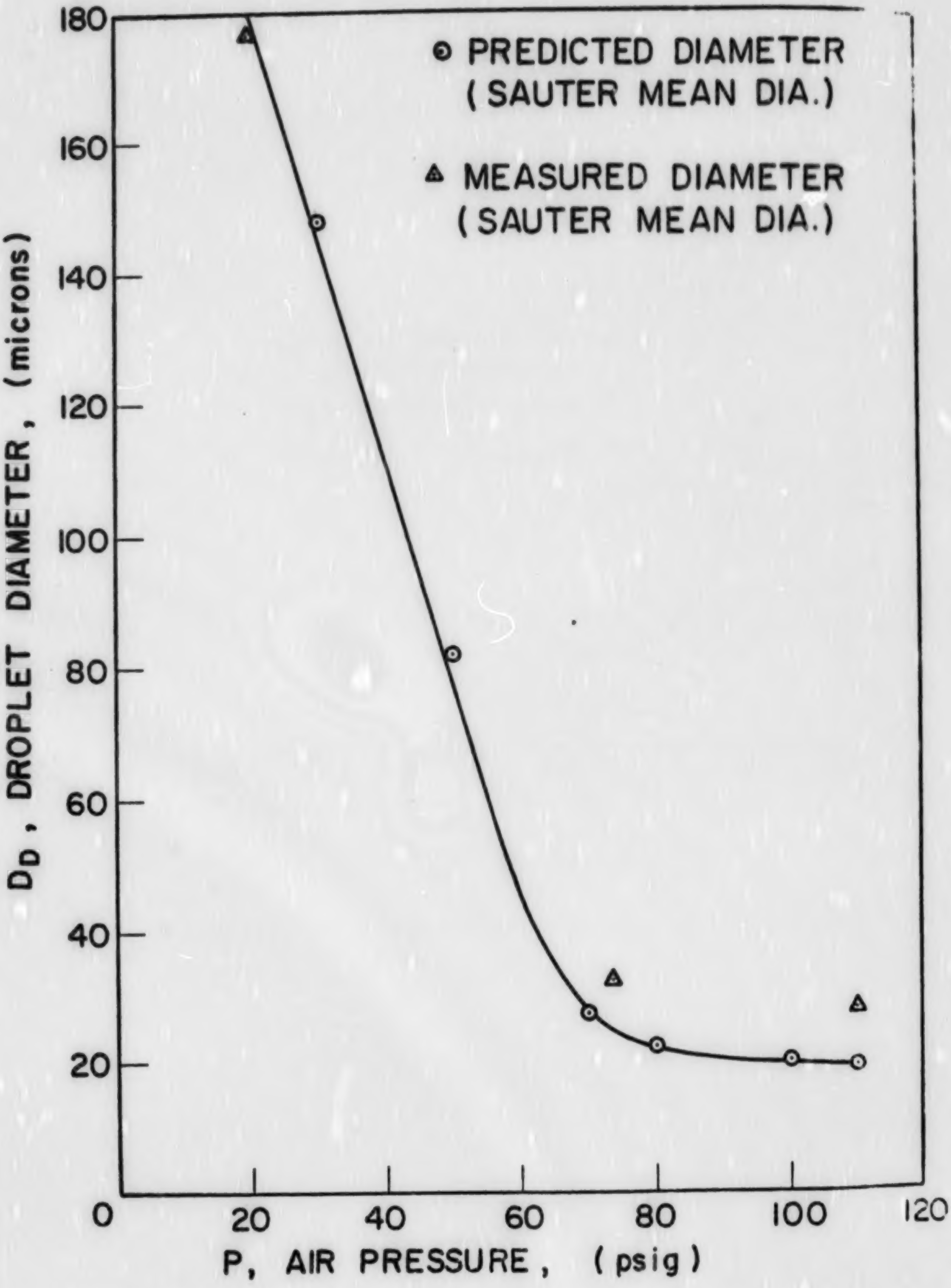

Figure 6. Water droplet size vs. air pressure for Spraying Systems air atomizing nozzle.

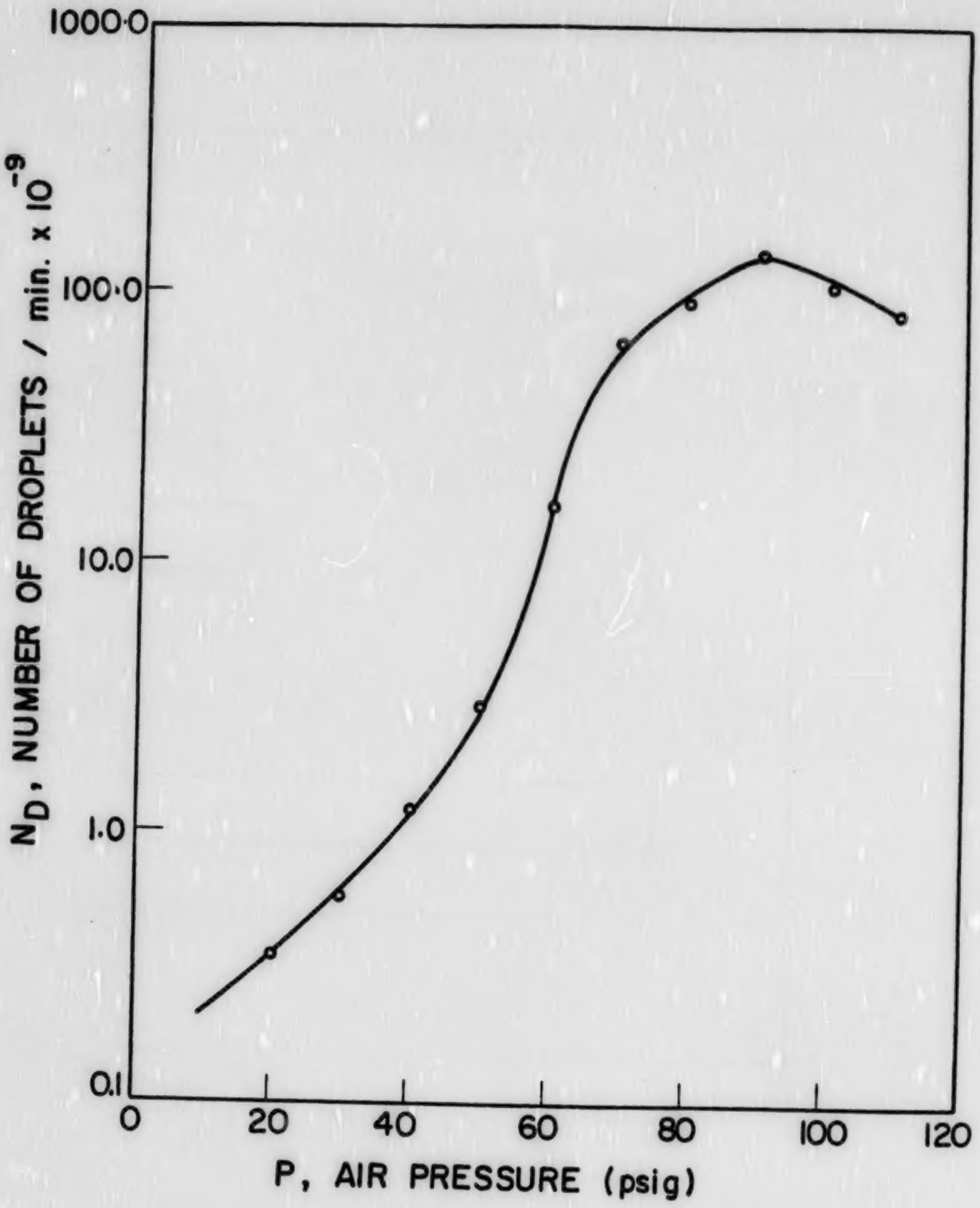

Figure 7. Number of water droplets produced per minute with the Spraying Systems air atomizing nozzle.

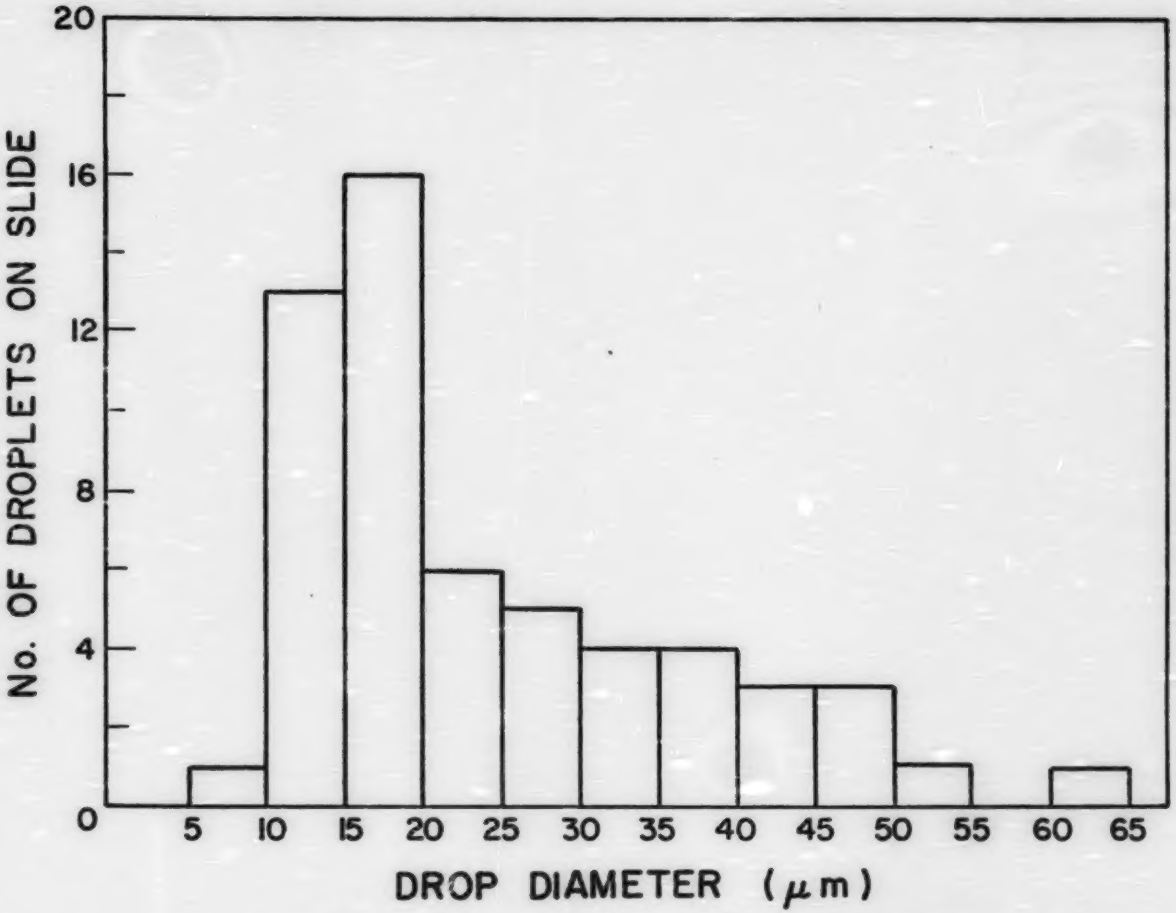

Figure 8. Histogram showing droplet size distribution from a Spraying Systems air atomizing nozzle.

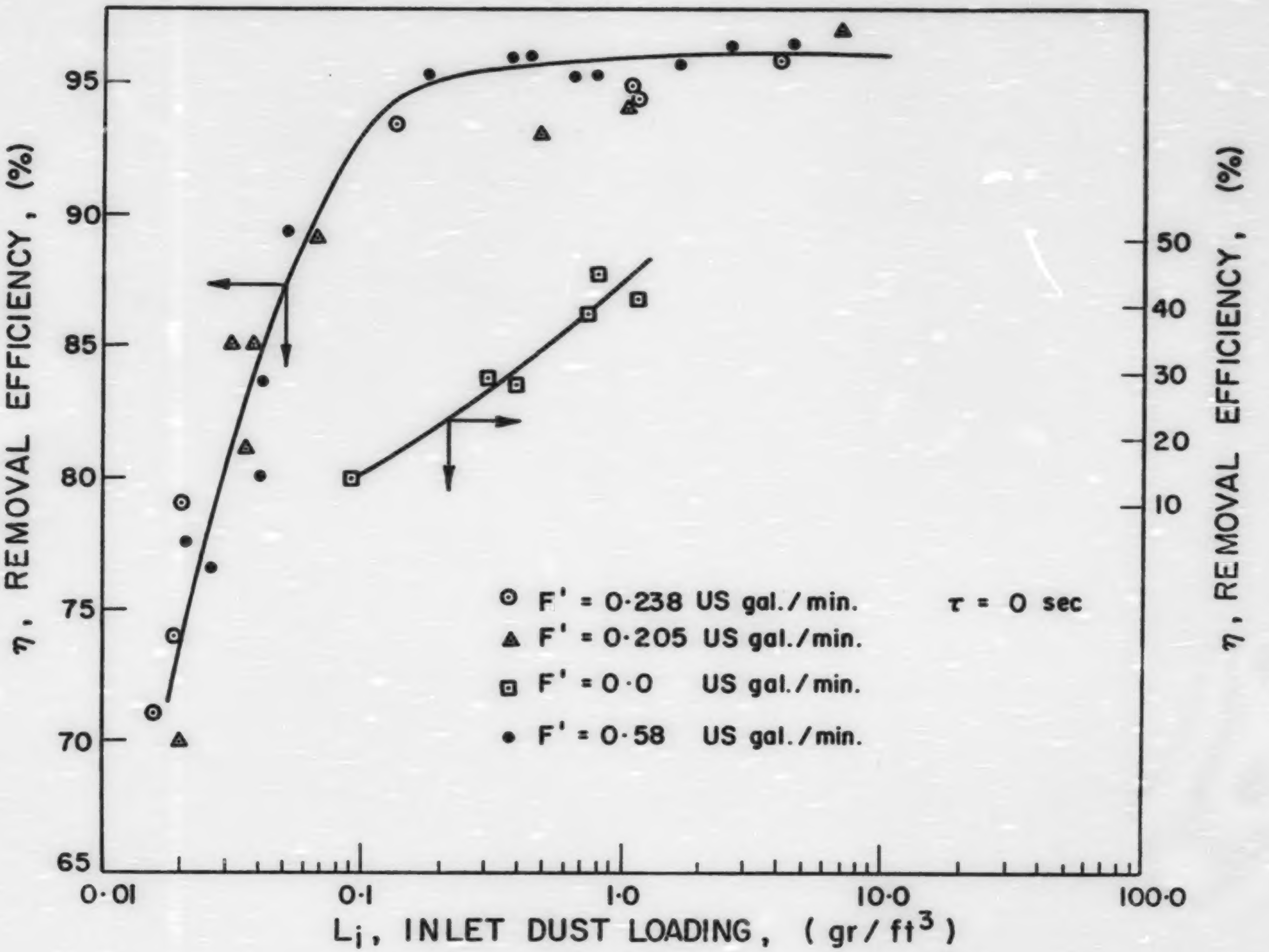

Figure 9. Fine particulate removal efficiency as a function of dust loading and amount of fine water spray used.

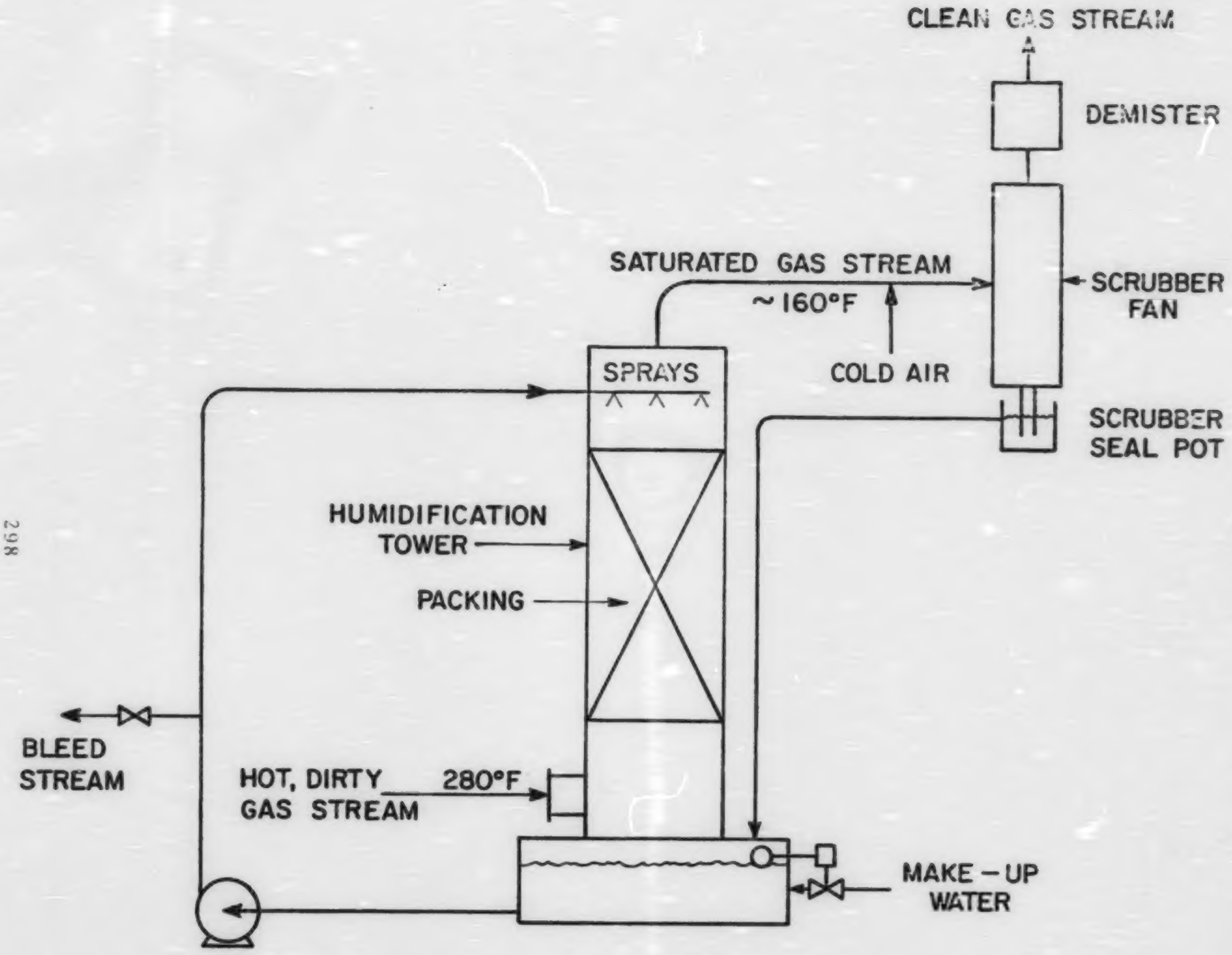

CLEAN GAS STREAM
DEMISTER
SATURATED GAS STREAM
~160°F
SCRUBBER FAN
SPRAYS
COLD AIR
SCRUBBER SEAL POT
HUMIDIFICATION TOWER
PACKING
BLEED STREAM
HOT, DIRTY GAS STREAM
280°F
MAKE-UP WATER

Figure 10. Schematic drawing of the revised Consolidated Bathurst installation.

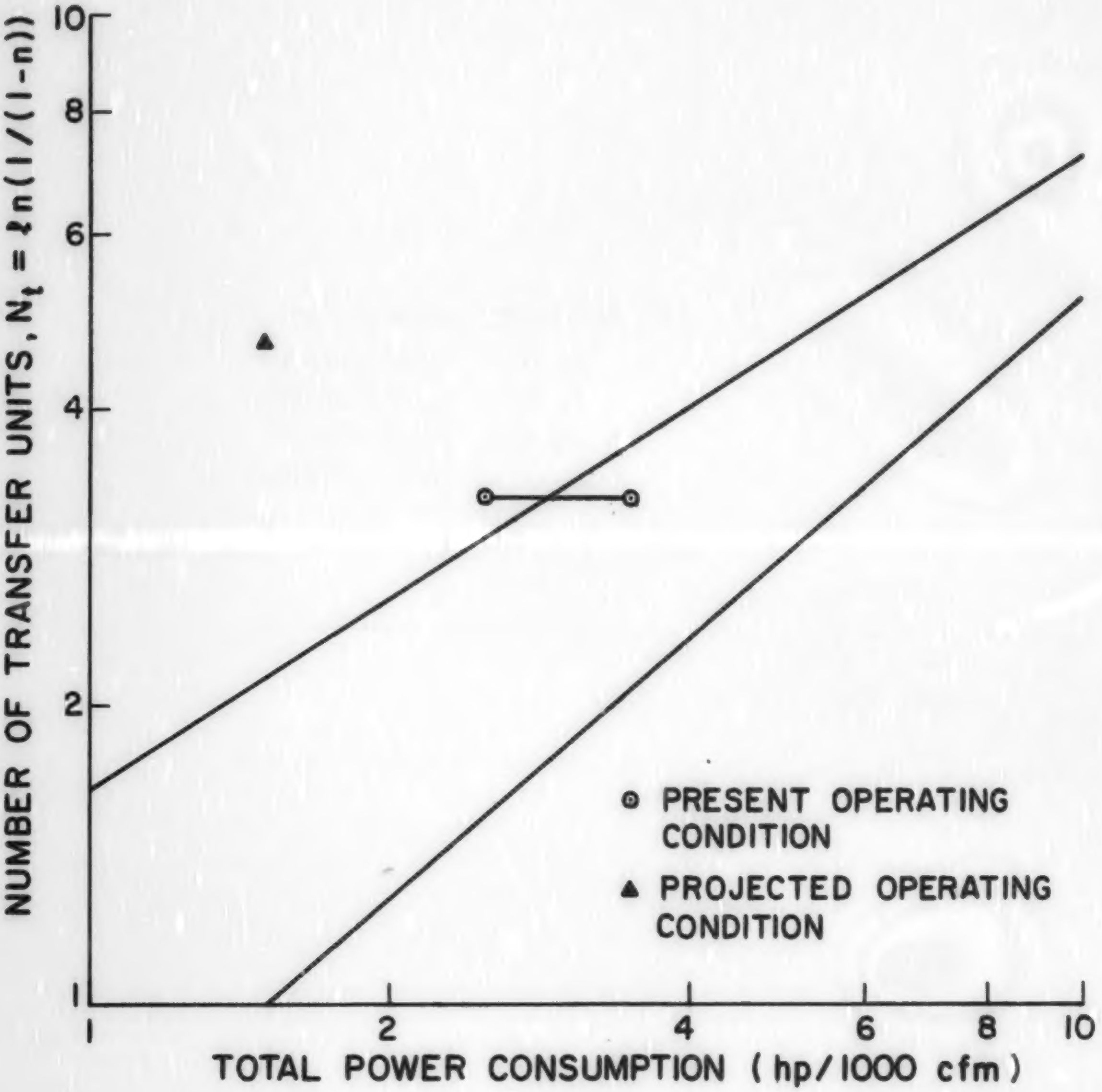

Figure 11. Semrau plot for the recovery boiler on a kraft pulp mill.

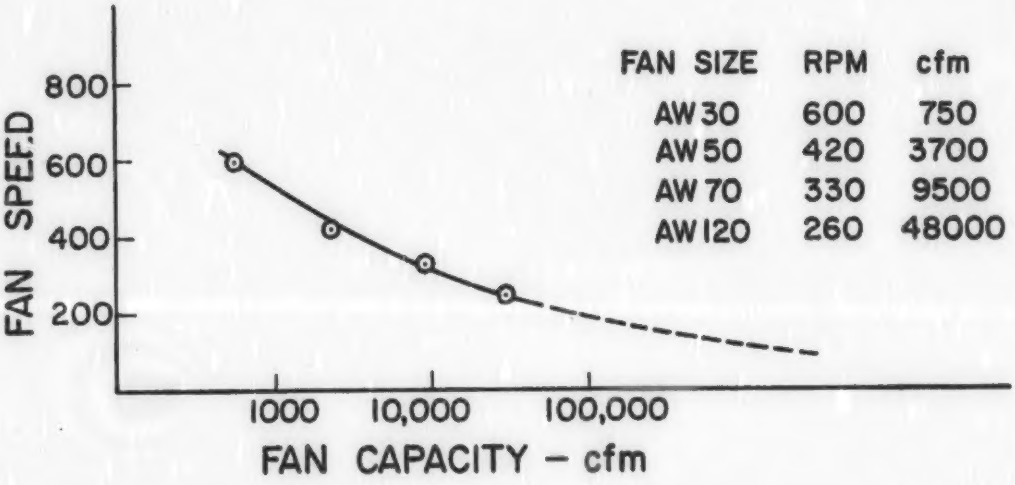

Figure 12. Relationship between fan speed and capacity at constant residence time.

References

1. F.A.L. Dullien and D.R. Spink, U.S. Patent Application, Serial No. 354,638, Gas Scrubber.

2. F.A.L. Dullien and D.R. Spink, U.S. Patent Application, Serial No. 732,383, Gas Scrubber.

3. P.L. Douglas, F.A.L. Dullien and D.R. Spink, "An investigation of the operating parameters of a low energy wet scrubber for fine particulates", Can. J. Chem. Eng., 54, 173 (1976).

4. T.S. Munro, "Construction and preliminary investigations of a wet scrubber of low energy requirement", Masters Thesis, Department of Chemical Engineering, University of Waterloo (1972).

5. F.A.L. Dullien, "The rate played by eddy diffusion in aerodynamic capture of particles", Particle Technology, Nuremberg, European Congress: "Transfer Processes in Particle Systems" Heat, Mass and Momentum Transfer, March 28-30, 1977.

6. G.H. Petersen, U.S. Patent 3,653,187 (April 4, 1972) "Apparatus for agglomerating suspended matter out of gases and vapours and/or for absorbing gas components".

7. R.K. May, "The measurement of airborne droplets by the megnesium oxide method", J. Sci. Instr., 27, 128 (1950).

8. C.W. Lear, W.F. Krieve and E. Cohen, "Charged droplet scrubbing for fine particulate control", Symposium on Electrostatic Precipitators for the Control of Fine Particulate, EPA-650/2-75-016 (1975).

9. K.T. Semrau, "Correlation of dust scrubber efficiency", J. of Air Poll. Contr. Assoc., 10, #3, 200 (1960).

FINE PARTICLE CONTROL WITH UW ELECTROSTATIC SCRUBBER

M. J. Pilat
G. A. Raemhild

University of Washington
Seattle, Washington

D. L. Harmon

U.S. Environmental Protection Agency
Research Triangle Park, North Carolina

ABSTRACT

The UW Electrostatic Scrubber system has been installed in two field portable pilot plants, each in a 40 foot trailer. The UW Electrostatic Scrubber involves the use of electrostatically charged water droplets to collect air pollutant particles charged to a polarity opposite from the droplets. The Mark 1P UW Electrostatic Scrubber pilot plant has been tested at a coal-fired boiler, a magnesium sulfite recovery boiler (pulp mill), and a hog fuel (wood waste) boiler. The Mark 2P UW Electrostatic Scrubber pilot plant has been tested on dioctyl phthalate aerosol, on the emissions from a pulverized coal-fired boiler, and on the emissions from an electric arc steel furnace. Measured overall particle collection efficiencies range from about 25 to 99.8% depending upon the electrostatic scrubber operating conditions and the inlet particle size distribution. The test results illustrate that the addition of electrostatic charging of the aerosol particles and/or the spray liquor droplets can substantially enhance the collection efficiency for fine particles by wet scrubbers.

Preceding page blank

FINE PARTICLE CONTROL WITH UW ELECTROSTATIC SCRUBBER

I. Introduction

A. Objectives of Research Project

The objectives of this on-going research project are to demonstrate the effectiveness of the UW Electrostatic Scrubber for controlling the emissions of fine particulates, to use the portable 1,000 acfm pilot plant in a 40 ft. trailer to obtain the data needed to design larger electrostatic scrubber systems, and to perform preliminary design and economic analyses of full-scale electrostatic scrubber systems.

B. Review of Previous Work

Penney (1944) patented an electrified liquid spray test precipitator involving particle charging by corona discharge and droplet charging by either ion impaction or induction. Penney's system consisted of a spray scrubber with electrostatically charged water droplets collecting aerosol particles charged to the opposite polarity. Kraemer and Johnstone (1955) reported theoretically calculated single droplet (50 micron diameter droplet charged negatively to 5,000 volts) collection efficiencies of 332,000% for 0.05 micron diameter particles (4 electron unit positive charges per particle). Pilat, Jaasund, and Sparks (1974) reported on theoretical calculation results and laboratory tests with an electrostatic spray scrubber apparatus. Pilat (1975) reported on field testing during 1973-1974 with a 1,000 acfm UW Electrostatic Scrubber (Mark 1P model) funded by the Northwest Pulp and Paper Association. Pilat and Meyer (1976) reported on the design and testing of a newer 1,000 acfm UW Electrostatic Scrubber (Mark 2P model) portable pilot plant. The UW Electrostatic Scrubber (Patent Pending) has been licensed to the Pollution Control Systems Corporation (of Renton and Seattle, Washington) for production and sales.

C. UW Electrostatic Scrubber

The UW (Pilat) Electrostatic Scrubber involves the use of electrostatically charged water droplets to collect air pollutant particles electrostatically charged to a polarity opposite from the droplets. A schematic illustration of the UW Electrostatic Scrubber system is presented in Figure 1. The particles are electrostatically charged (negative polarity) in the corona section. From the corona section the gases and charged particles flow into a scrubber chamber into which electrostatically charged water droplets (positive polarity) are sprayed. The gases and some entrained water droplets flow out of the spray chamber into a mist eliminator consisting of a positively charged corona section in which the positively charged water droplets are removed from the gaseous stream.

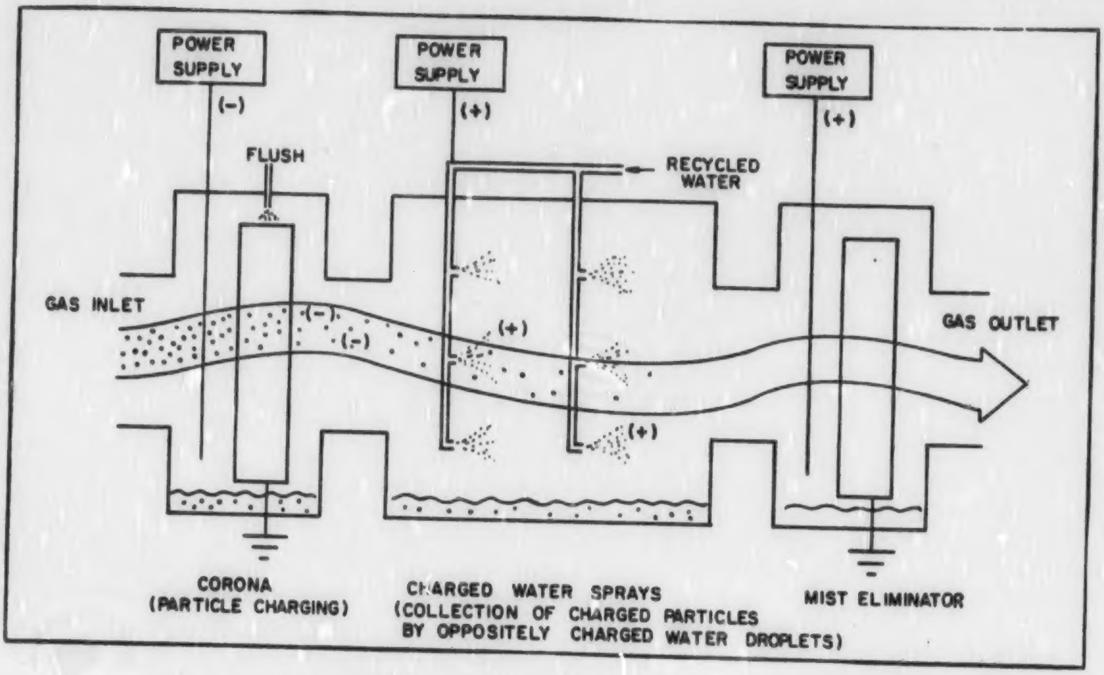
POWER SUPPLY
(-)
POWER SUPPLY
(+)
POWER SUPPLY
(+)
FLUSH
RECYCLED WATER
GAS INLET
(-)
(-)
(+)
(+)
GAS OUTLET
CORONA
(PARTICLE CHARGING)
CHARGED WATER SPRAYS
(COLLECTION OF CHARGED PARTICLES BY OPPOSITELY CHARGED WATER DROPLETS)
MIST ELIMINATOR

Figure 1. UW Electrostatic Scrubber

II. Experimental Method

A. UW Electrostatic Scrubber Pilot Plant

The general layout of the UW Electrostatic Scrubber pilot plant (Mark 2P model) is shown in Figure 2. The system (in the direction of gas flow) includes a gas cooling tower, an inlet test duct with sampling port, a particle charging corona section (corona no. 1), a charged water spray tower (tower no. 1), a particle charging corona section (corona no. 2), a charged water spray tower (tower no. 2), a positively charged corona section to collect the positively charged water droplets, an outlet test duct with sampling port, and a fan. The pilot plant is housed in a 40 ft. long trailer and can be easily transported to emission sources. A photo of the pilot plant (Mark 2P model) located at a steel plant is shown in Figure 3.

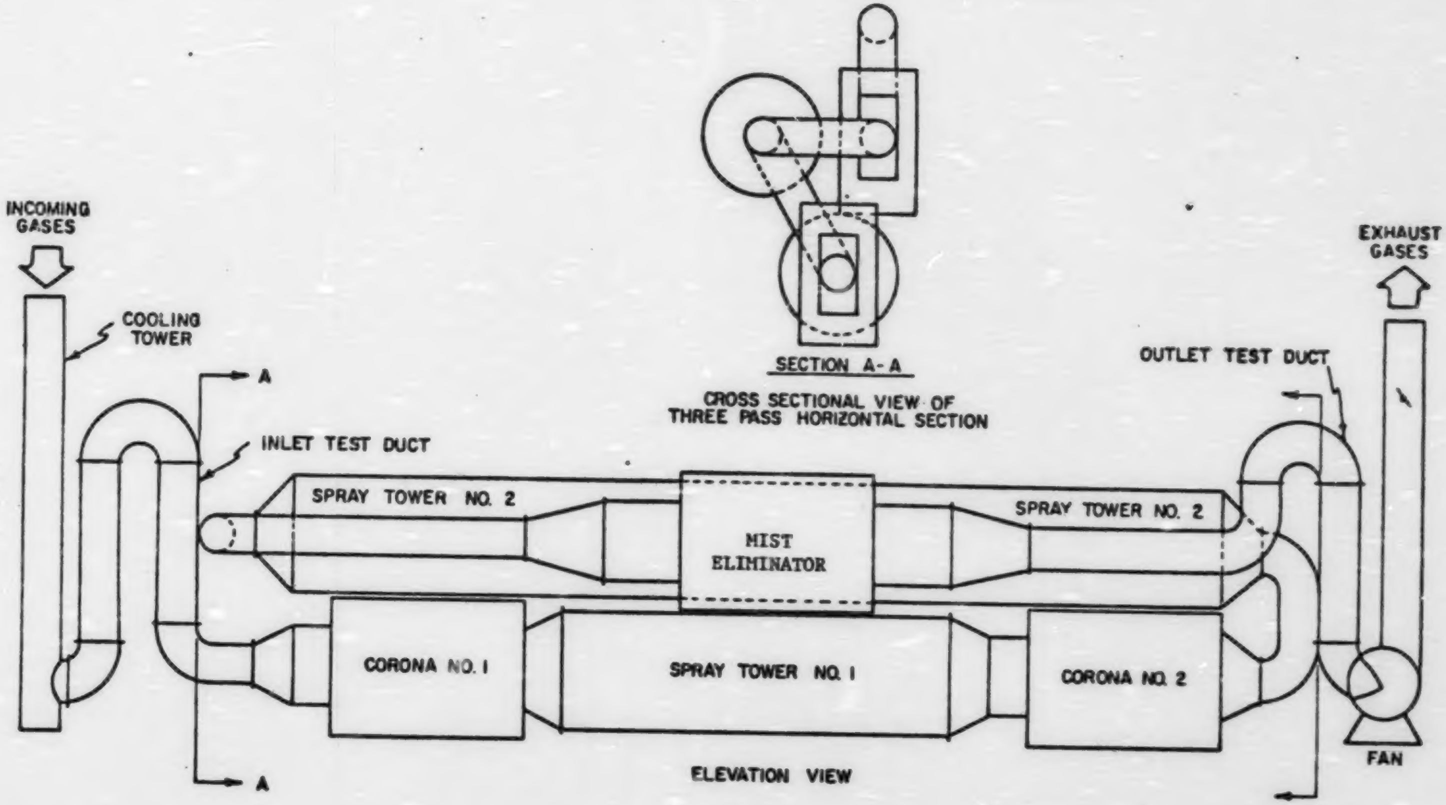
INCOMING GASES
COOLING TOWER
A
INLET TEST DUCT
A
SECTION A-A
CROSS SECTIONAL VIEW OF THREE PASS HORIZONTAL SECTION
EXHAUST GASES
OUTLET TEST DUCT
SPRAY TOWER NO. 2
MIST ELIMINATOR
SPRAY TOWER NO. 2
CORONA NO. 1
SPRAY TOWER NO. 1
CORONA NO. 2
FAN
ELEVATION VIEW

Fig. 2 General Layout of Electrostatic Scrubber Pilot Plant (Mark 2P Model)

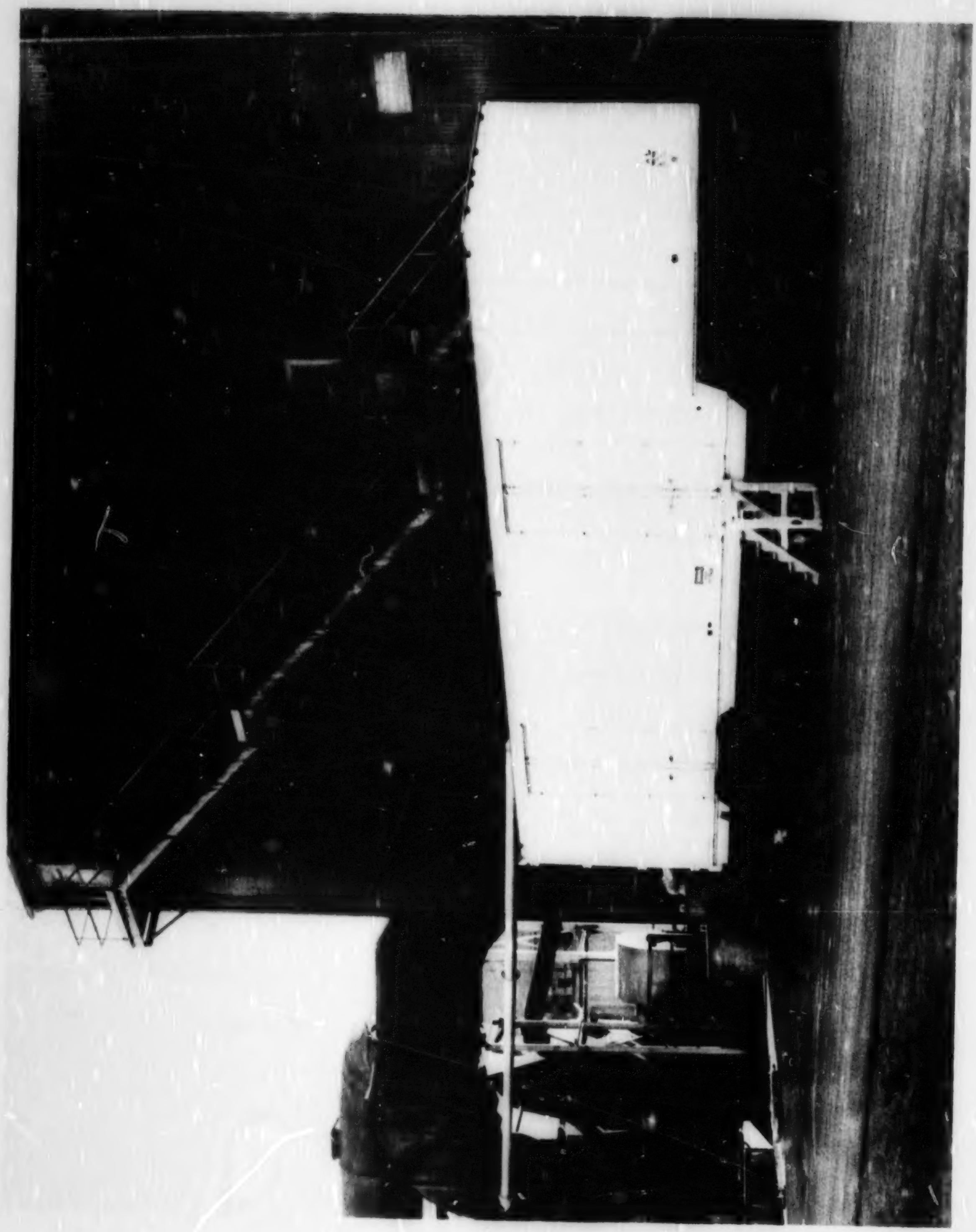

Fig. 3 UW Electrostatic Scrubber Pilot Plant at Steel Plant

B. Test Methods

The particle size distribution and mass concentration were simultaneously measured at the inlet and outlet test duct using UW Mark 3 and UW Mark 5 Source Test Cascade Impactors. During some tests the water charge/mass and aerosol charge/mass were measured. The test parameter and measurement techniques are presented in Table 1.

TABLE 1. Source Test Parameters and Measurement Techniques

Parameter	Equipment
1. Air	
a. velocity and volume	S-type pitot tube with draft gauge
b. temperature	thermometer
c. moisture	wet and dry bulb thermometer and checked by volume of condensate
d. atmospheric pressure	barometer
e. static pressure	Magnehelic gauge
2. Water Spray Towers	
a. water flow	rotometers
b. water charge to mass ratio	digital multimeter
3. Aerosol	
a. mass concentration	UW Mark 3 or 5 Cascade Impactor
b. size distribution	UW Mark 3 or 5 Cascade Impactor
c. aerosol charge to mass ratio	digital multimeter

III. Results

A. Dioctyl Phthalate

In order to check out the newly constructed pilot plant, eight tests were conducted using dioctyl phthalate (DOP) aerosol. The test results are presented in Table 2.

TABLE 2. DOP Test Results

Test No.	Gas Flow at Outlet Duct (acfm)	Water to Outlet Gas Flow Ratio (gal./1,000 acf)	Voltage (KV) Corona #1	Voltage (KV) Corona #2	Voltage (KV) Spray #1	Voltage (KV) Spray #2	Collection Efficiency (%)	Outlet Conc. (gr/scf)
1	744	5.8	0	70	0	25	92.1	0.0007
2	533	8.4	0	70	0	25	94.7	0.0019
3	335	13.4	0	70	0	25	99.7	0.0001
4	515	8.9	70	70	25	25	98.1	0.0024
5	480	12.7	70	70	15	15	95.5	0.0044
6	959	6.4	70	70	25	25	89.0	0.0040
7	969	6.2	0	0	0	0	25.0	0.0227
8	970	6.2	0	0	15	15	49.8	0.0201

B. Coal-Fired Boiler

Three tests were conducted on the emissions from the University of Washington pulverized coal-fired boiler. The boiler was operating at about 67% of its rated capacity during the three tests. Soot-blowing occurred during the second test. The spray liquor used in the scrubber towers was fresh water (no recycling of the liquor). The test results are presented in Table 3.

TABLE 3. Results of Tests at Coal-Fired Boiler

Test No.	Gas Flow at Outlet Duct (acfm)	Water to Outlet Gas Flow Ratio (gal./1,000 acf)	Voltage (KV) Corona #1	Voltage (KV) Corona #2	Voltage (KV) Spray #1	Voltage (KV) Spray #2	Collection Efficiency (%)	Outlet Conc. (gr/scf)
1	997	5.8	65	65	20	20	99.5	0.002
2	974	5.7	60	60	15	15	98.1	0.007
3	1,060	2.4	60	60	20	20	96.1	0.013

C. Electric Arc Steel Furnace

The pilot plant trailer was modified by: (1) increasing the liquor flow rate capabilities, (2) installing a liquor recycle system, (3) improving the purge air supply, (4) installing a spark-rate controller to provide a higher operating voltage to the corona sections, and (5) revising the water spray banks. Then the pilot plant was connected to a duct exhausting from two electric arc steel furnaces. A photo of the pilot plant trailer (the building in the background is a baghouse) at the electric arc steel furnace location is presented in Figure 3. The test results for this emission source are presented in Table 4.

TABLE 4. Results of Tests at Electric Arc Steel Furnace

Test No.	Gas Flow at Outlet Duct (acfm)	Water to Outlet Gas Flow Ratio (gal./1000 acf)	Voltage (KV)				Collection Efficiency (%)	Outlet Conc. (gr/scf)
			Corona		Spray			
			#1	#2	#1	#2		
1	1,783	10.4	70	70	15	15	94.2	0.0057
2	1,484	12.1	35	35	15	15	94.0	0.0025
3	1,553	11.9	70	70	20	20	98.1	0.0024
4	1,032	17.0	70	70	0	0	95.3	0.0016
5	1,474	12.6	70	70	15	15	92.6	0.0395
6	1,428	17.5	70	70	10	10	97.4	0.0025
7	1,391	18.0	70	70	20	20	87.9	0.0075
8	1,281	19.5	50	50	0	0	89.0	0.0978
9	1,470	17.0	50	50	20	20	80.2	0.0750
10	1,214	20.6	50	50	10	10	81.0	0.0811
11	1,331	18.8	70	70	20	20	91.0	0.0430
12	1,281	19.5	70	70	0	0	85.6	0.0178
13	1,210	19.8	0	0	20	20	83.7	0.1042
14	1,225	19.6	0	0	0	0	80.4	0.16797
15	1,259	19.1	0	0	10	10	58.8	0.33031
16	1,255	0	70	70	0	0	87.9	0.07380
17	1,189	21.0	70	70	20	20	93	0.0441
18	1,174	21.3	68	68	10	10	97	0.0285
19	1,163	21.5	68	68	0	0	98	0.0269
20	1,175	21.3	70	70	10	10	98	0.0313
21	1,148	21.8	0	0	10	10	89	0.1151
22	1,221	17.2	70	70	0	10	98.6	0.0194
23	1,247	16.8	70	70	0	10	96.4	0.0258
24	1,293	16.2	65	65	0	0	93.6	0.0315
25	1,184	17.7	70	70	0	0	98.1	0.0074
26	905	23.2	70	70	0	10	99.0	0.00344
27	953	22.0	70	70	0	10	98.9	0.00524
28	1,309	16.0	70	70	0	10	86.5	0.15362
29	1,338	15.7	70	70	0	10	83.7	0.10095
30	1,296	12.3	70	70	10	10	96.6	0.00678
31	1,302	11.5	70	70	2	2	98.6	0.0100
32	1,298	11.6	70	70	2	2	98.8	0.00992
33	1,122	13.4	70	70	2	2	99.6	0.00458

IV. Discussion of Results

A. Dioctyl Phthalate Tests

The particle collection efficiency is related to the gas residence time in the electrostatic scrubber. This is illustrated in Fig. 4, where the particle collection efficiency graph for test no. 4 and test no. 2 are compared (test no. 4 had a 37% longer gas residence time than test no. 2). Test no. 4 had a collection efficiency for 0.5 micron diameter particles of 98.5% compared to 91.5% for test no. 2.

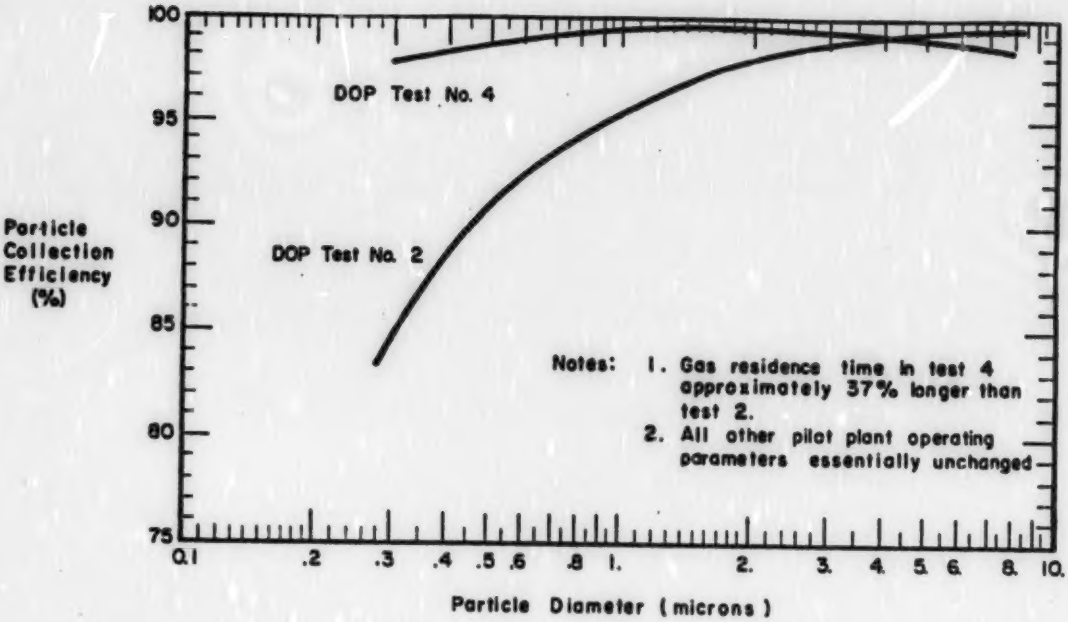

Fig. 4 Influence of Gas Residence Time on Particle Collection Efficiency

The particle collection efficiency at any given particle diameter increases when either the particles or the spray liquor droplets change from uncharged to electrostatically charged conditions. The particle collection efficiency versus particle diameter curves in Fig. 5 show that the collection efficiency for 0.5 micron diameter particles increases from 10% in test 7 (both particles and droplets uncharged) to 23.5% in test 8 (particles uncharged and droplets charged) to 91.5% in test 6 (particles and droplets charged to opposite polarity).

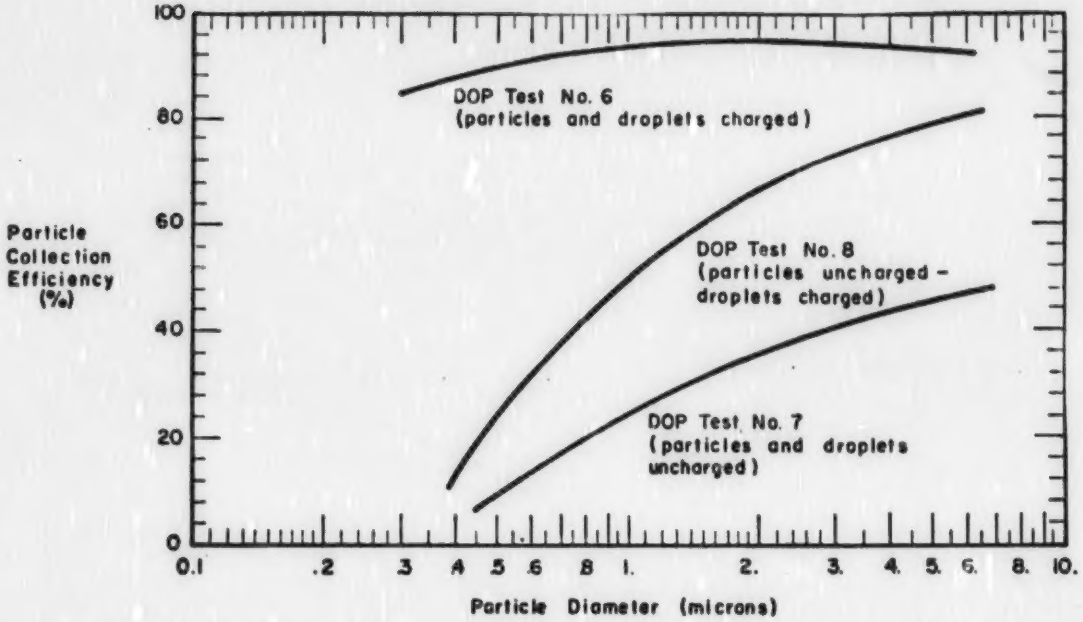

Fig. 5 Influence of Aerosol and Droplet Charging on Particle Collection Efficiency

B. Coal-Fired Boiler

The spray liquor charging voltage affects the particle collection efficiency as is shown in Fig. 6. Increasing the liquor charging voltage increases the particle collection efficiency at any given particle diameter. For example, test 2 (15 kV droplet charging voltage) had a 96.5% collection efficiency for 0.5 micron diameter particles, whereas, test 1 (20 kV droplet charging voltage) had a corresponding 99.1% collection efficiency.

The influence of the water to gas flow rate ratio is illustrated in Fig. 7 where test 3 (2.36 gal./1,000 acf) had a 76.0% collection efficiency for 0.6 micron diameter particles while the corresponding efficiency for test 1 (5.82 gal./1,000 acf) was 97.8%. Thus an increase in the water to gas flow rate ratio provides an increase in the particle collection efficiency at any given particle size.

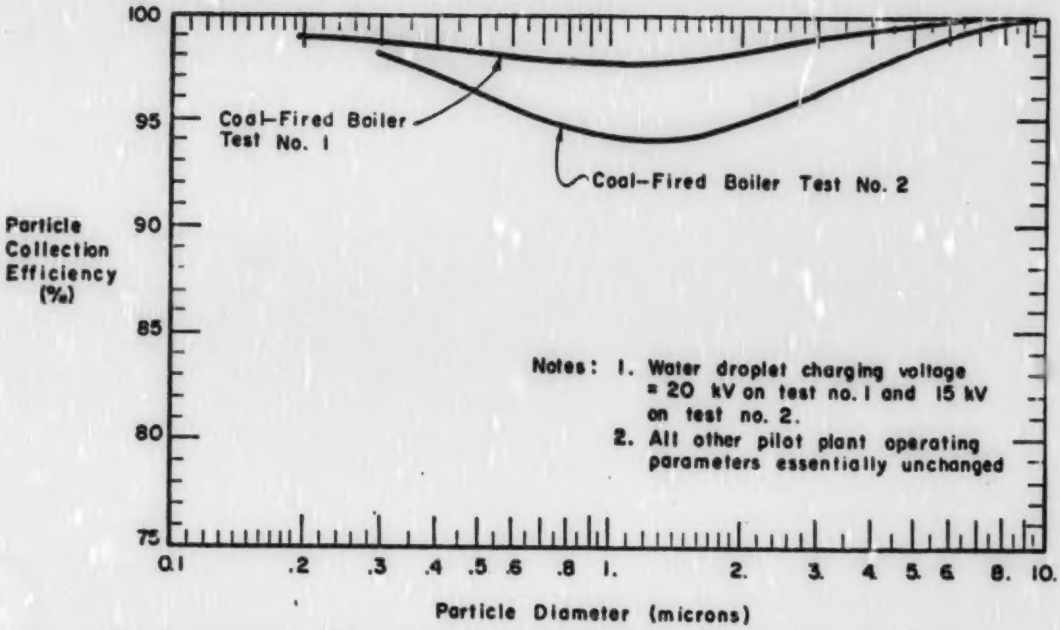

Fig. 6 Influence of Water Droplet Charging Voltage on Particle Collection Efficiency

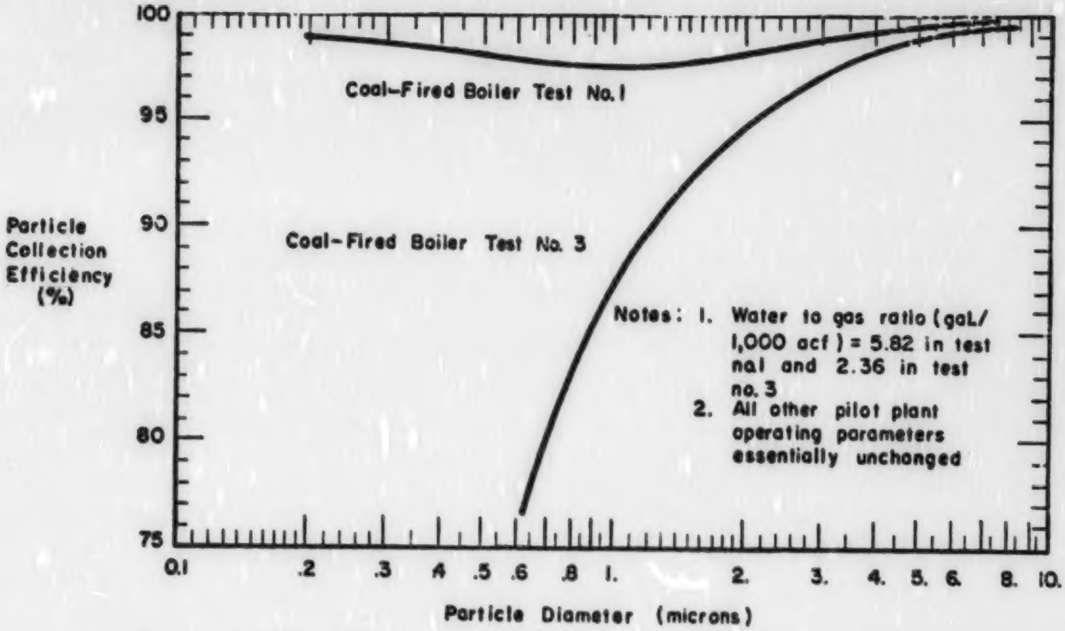

Fig. 7 Influence of Water to Gas Flow Rate Ratio on Particle Collection Efficiency

The overall particle collection efficiencies listed in Table 3 do not include the particles collected in the water spray cooling tower located upstream of the inlet sampling port. The inlet particle concentrations ranged from 0.3 to 0.4 grains/scf as sampled downstream of the spray cooling tower. Therefore, it is expected that considerably higher overall particle collection efficiencies would be calculated if the inlet sampling was conducted at a location upstream of the cooling tower where the particle concentrations are in the 0.5 to 5 grains/scf range. However, the particles removed in the cooling tower are in the larger size range and thus particle collection efficiency versus particle size curves presented in Fig. 6 and 7 should not be significantly affected.

C. The test results for the electric arc steel furnace (Table 4) were obtained during tests conducted from January to May 1977. These are the first tests with the new liquor recycle system. Some problems occurred during the earlier tests. During tests 1 through 16, particle re-entrainment was occurring from the duct downstream of the mist eliminator. This caused the overall particle collection efficiency to be less than expected for these tests. The particle re-entrainment problem was detected by a test performed with clean (atmospheric) air which showed a higher outlet particulate concentration than at the system inlet (clean water was used as the scrubbing liquor). Washing down the duct downstream of the mist eliminator corrected this situation.

During tests 22 to 29, the liquor spray to tower 1 was shut off because it appeared that the spray was flooding the no. 2 corona section. After test 29, the pilot plant was shut down and the spray towers and corona sections were washed down thoroughly. Of the six nozzles in tower 1, the dowstream nozzle fittings were plugged, and the other three nozzles were replaced with nozzles providing a fine mist (manufacturer data specifies 200 to 300 micron diameter droplets). A screen-type mist eliminator was installed at the outlet of tower 1 (inlet to corona 2). Also all the spray nozzles in tower 2 were replaced with the finer droplet nozzles. Tests 30 through 33 were run with both corona sections and both spray towers in operation at a total liquor flow of about 16 gal/minute and a liquor pressure of about 56 psig.

As shown in Fig. 8, the particle collection efficiency versus particle size curves obtained at similar operating conditions are in fairly good agreement. Tests 26 and 27 were conducted with a lower gas volumetric flowrate and correspondingly the corona section SCA and liquor to gas collection efficiencies for these two tests (nos. 26 and 27) were in excess of 99%.

Fig. 9 presents the collection efficiency versus particle size for tests 31 through 33 and shows that the submicron particle collection efficiency for these tests exceeds about 94%. Also these tests illustrate the ability to achieve good particle collection at lower liquor spray voltages and at lower liquor to gas flowrate ratios.

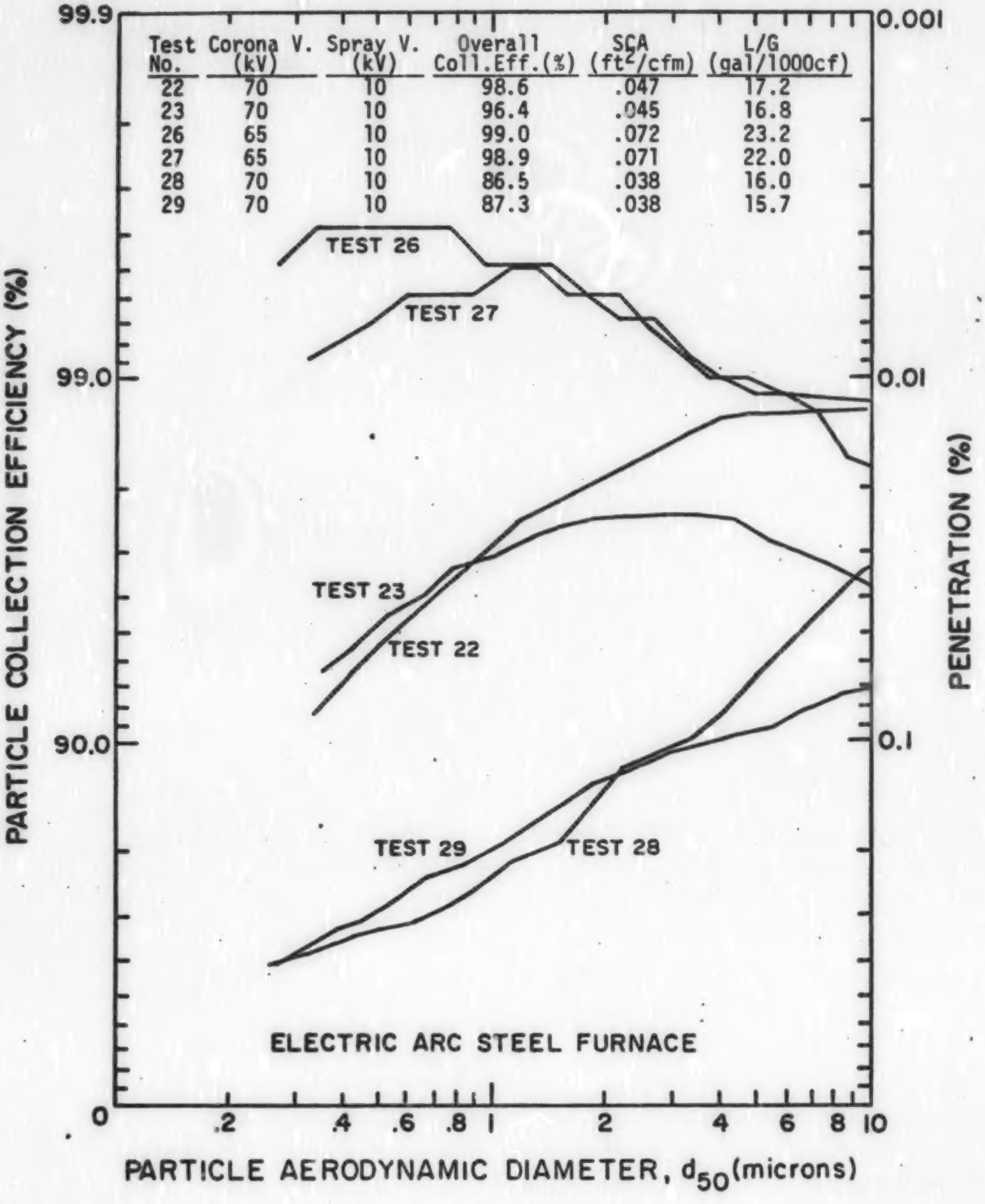

Test No.	Corona V. (kV)	Spray V. (kV)	Overall Coll.Eff.(%)	SCA (ft^2/cfm)	L/G (gal/1000cf)
22	70	10	98.6	.047	17.2
23	70	10	96.4	.045	16.8
26	65	10	99.0	.072	23.2
27	65	10	98.9	.071	22.0
28	70	10	86.5	.038	16.0
29	70	10	87.3	.038	15.7

Fig. 8 Influence of SCA and L/G on Particle Collection Efficiencies

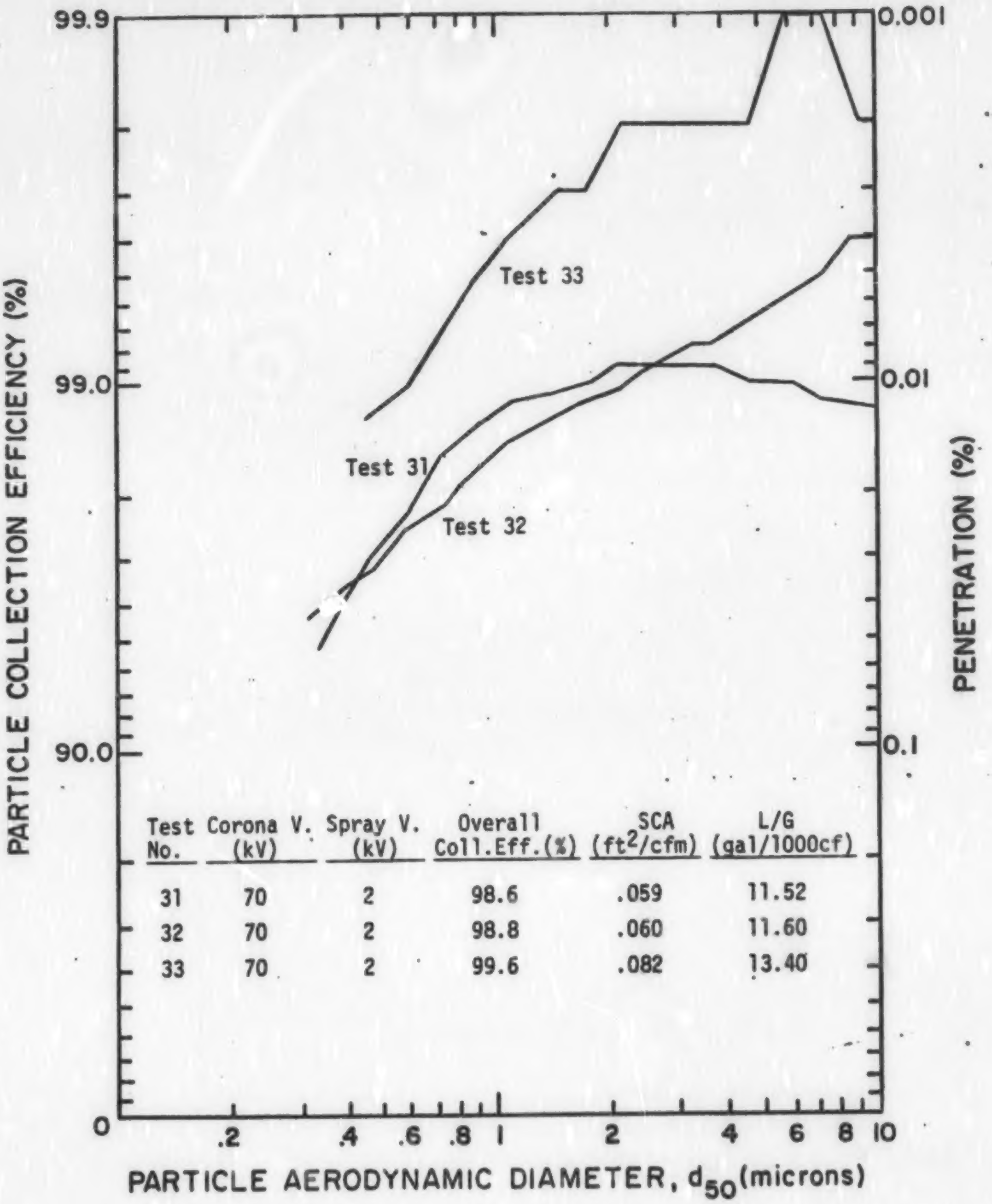

Test No.	Corona V. (kV)	Spray V. (kV)	Overall Coll.Eff.(%)	SCA (ft^2/cfm)	L/G (gal/1000cf)
31	70	2	98.6	.059	11.52
32	70	2	98.8	.060	11.60
33	70	2	99.6	.082	13.40

Fig. 9 Collection Efficiencies at an Electric Arc Steel Furnace

V. Conclusions

The results of tests of the UW Electrostatic Scrubber field portable pilot plants illustrate the capability of high efficiency fine particle collection efficiency at low gas pressure drop (about 0.5 inches of water) and over a range of liquid to gas flowrate ratios (2.4 to 21.8 gal/1000 acf). Measured overall particle collection efficiencies range from about 25 to 99.8% depending upon the electrostatic scrubber operating conditions and the inlet particle size distribution.

Acknowledgements

This research was supported in part by EPA (IERL) Research Grants No. R 803278 and R 8043930 and research grants from Reynolds Metals Company, Alaska Lumber and Pulp Company, Ketchikan Pulp Company, Georgia Pacific Corp., Scott Paper Company, ITT Rayonier Inc., and Publishers Paper Company. The assistance of the Bethlehem Steel Corp., Seattle, is gratefully acknowledged.

References

1. Kraemer, H.F. and H.F. Johnstone (1955) "Collection of aerosol particles in the presence of electric fields" Ind. Engr. Chem. 47 2426.

2. Penney, G.W. (1944) "Electrified liquid spray dust precipitator" U.S. Patent No. 2,357,354.

3. Pilat, M.J., S.A. Jaasund, and L.E. Sparks (1974) "Collection of aerosol particles by electrostatic droplet spray scrubbers" Envir. Sci. & Tech. 8 340-348.

4. Pilat, M.J. (1975) "Collection of aerosol particles by electrostatic droplet spray scrubber" APCA Journal 25 176-178.

5. Pilat, M.J. and D.F. Meyer (1976) "University of Washington electrostatic spray scrubber evaluation" Final Report on Grant No. R-803278, EPA Report No. EPA-600/2-76-100 (NTIS No. PB 252653/AS).

Metric Conversion Factors

Readers more familiar with the metric system are asked to use the conversion factors tabulated below:

Non-Metric	Multiplied by:	Yields metric
ft	30.48	cm
ft^3	28.32	liter
grains/scf	2.288	1 gram/m^3
gal.	3.79	liter
gal./1000 acf	0.1337	liter/m^3
ft^3/min	1.699	m^3/hr
ft/sec	0.3048	m/sec

FINE PARTICLE SCRUBBING WITH LONG STAR STEEL HYDRO-SONIC CLEANERS "THE COALESCER"

Thomas K. Ewan
Jay S. Master

Lone Star Steel Company
Lone Star, Texas 75668

ABSTRACT

Lone Star Steel has developed a family of Hydro-Sonic air cleaners for fine particulate control. These cleaners can also control SO_2 and H_2S with chemical addition and particulate in a single system.

Cleaners are available in a number of different models, sizes and materials to meet varied needs of differing processes.

These cleaners are powered by either: (1) an I.D. or F.D. fan drive, (2) a compressible fluid ejector drive, or (3) combinations of both. The energy range is from <1 BTU per pound of off-gas to 100 BTU per pound of off-gas depending on the pumping and cleaning requirements of the process. The precise amount of energy can be inputted to within 1 BTU per pound of off-gas for a specific cleaning level. Selective particulate size removal can be carried out. The cleaning level is adjustable by varying the energy input. The capital equipment does not have to be changed to effect this.

Aerodynamic technology is employed for high performance cleaning combined with minimum energy utilization:

1. "Free Jet" and shock wave mixing.
2. "Free Jet" formation of droplets shaped into "paddle" and flat-like surfaces.
3. Shaped directional cleaning energy release for fine particulate control also controls opacity. The ejector driven models release the total energy of the system through a narrow cone concentrating cleaning forces.
4. The separation function is performed either by cyclones or by energy recovery modified diffusers.

These cleaners have been under development since 1969 by a R&D team composed of engineers and physicists. We have five years of continuous data taking and development. While the amount of energy inputted is important, we have learned how to achieve high level cleaning by the management and application of that energy in order to achieve high performance and economy at the same time.

FINE PARTICLE SCRUBBING WITH LONE STAR STEEL HYDRO-SONIC CLEANERS

"THE COALESCER"

Introduction

Lone Star Steel Company has developed a patented family of Hydro-Sonic air cleaners for control of particulate, SO_2, H_2S, and precursor gases. These include the compressible fluid driven models (steam or air) or the fan driven models or combinations thereof employing either cyclone or diffusing coalescers for the separation function. These cleaners cover a broad range of cleaning capabilities from meeting regulatory standards to virtual elimination of pollutants. The selection of the cleaner to be employed is made based on the application, the cleaning requirements, and the source of energy available.

While the cleaning performance for the Hydro and Coalescer are the same for particulate, the Coalescer cleaner (a device embodying aerodynamic techniques for cleaning and energy recovery) is discussed in this paper. The Coalescer combines high performance with energy recovery in a single device for the removal of particulate and water soluble gases.

High performance with low energy requirement is achieved by the use of a "Free Jet" mixing stream and water drops of the proper shape, size, number and velocity combined with the use of a specially designed pressure recovery separator (diffuser). The special diffuser is used to provide separation of the cleaned gases from the particulate-containing water and to recover pressure by transforming a portion of the velocity head of the gas stream into a pressure head. The Coalescer Separator, in common with cyclones, demisters or other separation devices performs a separation function, but unlike other separators, the Coalescer recovers a portion of the pressure thereby minimizing the net energy requirement.

The Coalescer system may be powered by a fan or a compressible fluid ejector or combinations thereof. (Figure 3 - Fan Coalescer. Figure 4 - Ejector Coalescer.) The energy requirement for the Coalescer system is low when compared to conventional wet scrubbing for comparable cleaning performance.

Discussion

The Coalescer - How It Works. The operation of the Fan Coalescer and the Ejector Driven Coalescer will be discussed separately.

The Fan Coalescer is a subsonic device in which all of the process offgas is pushed by a fan through a subsonic nozzle, Figure 3. The operating nozzle pressure is from 2" to 50" of water depending on the process to be cleaned.

The Ejector Coalescer is a supersonic compressible fluid drive with no moving parts in the gas stream. The compressible fluid is preferably air or steam. It operates with 15 PSIG to 1000 PSIG or higher driving pressure depending on the available steam or compressed air source.

In the Coalescer cleaners particulate is wetted and the water drops containing particulate are grown to an easy-to-remove size. The mechanisms employed are simple: first, the wetting of the particulate; second, the complete mixing of the particulate and the scrubbing medium; third, the process of growth; and fourth, the process of separation. The processes of wetting and mixing in a "Free Jet", combined with shaped droplets, droplet growth, and separation with energy recovery, distinguish these cleaners from conventional systems.

The wetting of the particulate is achieved initially by the generation of very large numbers of high speed water droplets of the proper shape, number, size and speed to contact the particulate and/or noxious gases.

Figure 5 shows the generation of water droplets of the proper shape, size, speed and number with the subsonic drive while Figure 6 shows the supersonic drive. First, a water droplet is mechanically produced which droplet is in turn injected onto the exhaust of the off-gas stream or onto the compressible fluid ejector stream. When the presized water droplet strikes the high speed stream, operating in a "Free Jet", it is shattered into many smaller droplets and accelerated to high speed. It is desirable to create high speed droplets of a size 10 to 30 times the size of the particulate to be captured since the dust particle may be able to go around or dodge an over-large water drop. The key to the capture of fine particulate and gases is, therefore, the creation of water droplets of the proper shape, number, velocity and size for the particular gas stream. In the "Free Jet" arrangement, it is believed that the water droplets are formed into paddle-like or flat surfaces before contacting the particulate. This increases the surface contact area and assists in direct contact between the particulate and the water. Subsequently, it is believed that the surface tension exerted on the misshapen water droplet causes the droplet to close around and encapsulate the dust particle.

The mixing process immediately follows and overlaps the wetting process. It insures complete wetting of any particles not already wetted by collision. Mixing is accelerated and enhanced in a "Free Jet" as compared to mixing in a confined area or region.

The growth process follows and partly overlaps the mixing process so that a single water drop may contain hundreds of micronic and submicronic dust particles. As a result of the growth of droplets containing particulate into increasingly larger size, the initial size and shape of the particulate in the gas stream has only a small effect on its removal.

Figure 7 illustrates *droplet growth*. A Bertin instrument (France) is used to capture a sample of the mixture in the gas stream. On the left is shown what appears to be a large particle "captured" in a water droplet;

however, this same droplet observed under a microscope after evaporation exhibits the condition shown on the right side of the picture, where dozens of tiny particles appear. This is confirmation of the coalescence of many small particulate-containing droplets into large droplets. The ability to grow particulate-containing droplets into 1000 micron or larger size is important in high performance low energy particulate abatement since separation and removal of such large water drops is easy.

Separation of Cleaned Gas and Particulate-Containing Water Droplets. The separation of the cleaned gas from the water droplets containing the particulate is achieved in a modified diffuser by the use of detached flow, directional forces, velocity control, coalescence and gravity forces at the same time the diffuser recovers pressure. Figures 3 and 4 illustrate schematically the operation of the modified diffuser. There are three controlling interactions—pressure, velocity and direction. Normally in fluid flows and aerodynamics, a diffuser is used for pressure recovery, i.e., to reduce the energy required in a system. The modified diffuser of the Coalescer cleaner provides partial pressure recovery, but its primary function is to separate the particulate-containing water drops from the gas. The modified diffuser thus replaces cyclones, stilling chambers, impactors and/or mist eliminators for the separation function while at the same time providing the added benefit of pressure recovery.

At the entrance to the modified diffuser, the droplet normally moves at a speed in excess of 100 feet per second. At this point, the flow of the gas and water mixture is partially separated (detached) from the diffuser wall so as to direct the particulate laden water drops toward the bottom and away from the cleaned gas. The top of the modified diffuser (as shown in Figures 3 and 4) includes a region of lower pressure which causes recirculation and reentrainment of small droplets and mist. The small droplets are thus returned to the coalescing zone of the diffuser where rapid droplet growth occurs. This process augments the earlier mixing and growth process. Water and particulate separated from the mixture are removed through the drain by gravity forces while the cleaned gas exits in the upward (opposite) direction.

In addition to pressure control and droplet directional control discussed above, a third phenomenon occurring in the modified diffuser is droplet growth as regulated by velocity control. At the entrance to the modified diffuser, the speed of the droplet is usually greater than 100 feet per second. At the exit end of the modified diffuser, the velocity has been reduced by a factor of 5 to 10 because of the increased cross sectional area of the diffuser. Massive coalescing (droplet growth) results from this rapid velocity change. At this point, the particles are encapsulated in water drops grown to a size easy-to-remove by gravity.

The Coalescer cleaners do not seek to remove submicronic and micronic particulate as such, but instead wet the particulate and then grow the droplets containing the particulate to easy-to-remove size.

The Coalescer may be driven either by a fan or a compressible fluid ejector nozzle.

The Subsonic Fan Drive is used to drive the entire off-gas from the process through a subsonic nozzle. It is used in applications where a fan will: provide trouble free service in the off-gas stream; and where the driving energy required is less than 50" H_2O W.C. at the subsonic nozzle. This drive pumps the gas stream and provides the cleaning energy. It meets the needs of most applications where cleaning requirements are in the .0X range. Energy to pump and clean one pound of off-gas, depending on the process and the required draft, is in the <1 to 15 BTU range.

The Supersonic Ejector Drive is used in applications where: it is desirable and/or necessary to have no moving parts in the gas stream; the energy requirement would be greater than 50" W.C. with a fan drive using a subsonic nozzle; there is a hostile environment or very difficult to remove gases or particulate; the standards are highly restrictive; there exists significant quantities of particulate in the submicronic range; and where cleaning is desired in the .00X to .000X grains per SCF outlet. The energy to pump and clean one pound of off-gas, depending on the process and the required draft, is in the 15 to 150 BTU range.

Performance of the Ejector Coalescer

In the compressible fluid Ejector Coalescer, the pumping of the gas stream and the energy to clean the stream are both furnished by a supersonic ejector nozzle. The supersonic nozzle is normally driven by air or steam at a pressure of 15 PSIG or greater. 15 PSIG is necessary to achieve supersonic flow. Some steam driven units are operating in the 500 PSIG range; however, this is not an upper limit. When supersonic flow exists, a series of shock waves is established which aids in the mixing process and insures complete wetting of any particles not already wetted. The shock waves form violent scrubbing zones where intimate contact is forced to occur between the scrubbing medium and the particulate and/or noxious gas and provide the added contact and mixing that make the cleaner superior for fine particulate and SO_2 removal. When using the air drive, the Ejector Coalescer can also provide the oxidizing conditions desired for certain processes, such as SO_2 control. Ejector models are in full scale operation on ore kilns and open hearth furnaces and successful pilot demonstrations have been conducted on a number of other processes.

Performance of the Fan Coalescer

Unlike the ejector models, the Fan Coalescer does have moving parts in the gas stream. This is acceptable in many applications. The performance of the Fan Coalescer has been demonstrated on various processes including coke ovens, sinter plants, ore kilns, galvanizing mills and cupolas in the steel industry. In the paper industry, the Fan Coalescer performance has been demonstrated on recovery boilers, a bark boiler and lime kilns. As shown on the following pages, low energy requirements are combined with excellent performance. This is possible because of the "Free Jet" mixing, droplet shape and other features described earlier.

Performance on specific processes is discussed below. Inasmuch as an open hearth furnace (especially during high heat and oxygen lance) produces extremely large quantities of very fine, difficult to capture particles, it is used as typical of the collection efficiency of the LSS ejector driven Hydro-Sonic cleaners. Other processes discussed in this paper are less difficult to clean and are presented with inlet grain size information vs cleaning performance in grains SCF outlet.

Open Hearth

The ejector drive Hydro-Sonic cleaner on an open hearth furnace including oxygen lance provides controllable cleaning from .0X to .000X grains (partial) per SCF outlet range. Table I shows the scrubber inlet grain loading and the size distribution. Table II shows the scrubber outlet grain loading and size distribution.

Figure 8 shows collection efficiency vs particle size (EPA Report 650/2-74-028).[1]

Electric Furnace

The particle size for an electric furnace (as reported in NTIS PB-203521)[2] is shown in Table III. LSS Hydro-Sonic cleaners consistently provide cleaning well below the .0052 grains SCF outlet EPA regulation on the LSS electric furnace. This is achieved with less than 50 BTU per pound of off-gas pumped and cleaned. (See Figure 9.)

Galvanizing

Table III exhibits the inlet particle size distribution for the processes discussed below.

Zinc dust is readily controlled by use of the low energy Fan Coalescer as shown in Figure 10. The effectiveness of this cleaning on this particulate is such as to provide a clear stack and outlet grain loading many times within standards. The capture of this particulate makes possible the recovery of valuable materials from an off-gas stream. It is being used at Lone Star Steel for the large scale recovery of valuable metals from its open hearth furnaces, in addition to the galvanizing process. The quantity of valuable metals recovered from the galvanizing line is such that a net profit is realized over the cost of cleaning the air. In general, it has been found that as the particulate becomes smaller the concentration and recovery value of the metallic component increases.

Sodium Sulfate Recovery Boiler

A sodium sulfate recovery boiler is readily cleaned using the Fan Coalescer, Figure 11. It provides cleaning well within required standards plus the added feature of capturing and returning to the process valuable material contained in the off-gas. As in the case of the galvanizing mill, a Coalescer on a recovery boiler can, by the capture of fine particulate, reduce the cost of cleaning the off-gas; and, in some applications, provide a net profit over the cost of cleaning. Figure 11 shows the cleaning performance of the Fan and Ejector Coalescer compared with the performance of a Steam Hydro cleaner on the same pulp mill recovery boiler.

Sinter Plants

Sinter Plants are one of the more difficult processes to clean, but the Fan Coalescer is capable of cleaning sinter off-gas to the degree shown in Figure 10. If large quantities of hydrocarbons are present or if more stringent cleaning requirement is required, use of the air or steam Ejector Coalescer rather than the Fan Coalescer is recommended. However, the economics of the Fan Coalescer make it the choice for sinter plants using coke-breeze to meet existing and proposed regulations.

Cupola

Cupolas are used to melt down many forms of "waste" and scrap. Engine blocks, mill scrap, transmissions, and other scrap materials, many of which contain significant amounts of oils and hydrocarbons, are often used. The Fan Coalescer has demonstrated satisfactory cleaning performance on cupolas charged with these materials, Figure 10. In addition to meeting the grain loading requirements with significantly less energy than the so-called "conventional wet scrubbers", the Fan Coalescer will clean a cupola so as to produce a "clear stack".

Coke Oven

Figure 10 shows the performance of a Fan Coalescer in cleaning the off-gases of a coke oven.

All Particulate Processes

Figure 12 shows that the LSS Hydro-Sonic cleaners have the capability to clean any particulate of any size and any inlet grain loading to meet or exceed published air cleaning requirements with reasonable economics. The precise amount of energy required can be inputted. This is adjustable and can be provided on a need required basis to meet changing conditions.

Conclusions

The Coalescer represents new technology in the air cleaning field. It provides high performance, low capital cost and low operating energy requirements. A choice of driving mediums is available: either a fan or a compressible fluid ejector may be used. Normally, steam or air is employed as the compressible fluid with the ejector model. In the ejector models there are no moving parts in the gas stream, and the ejector both pumps and cleans. On both the fan and ejector models, particulate, SO_2, and H_2S may all be controlled in a single unit. The desired cleaning level may be modified by a change in energy supplied to the ejector or fan. In the fan models, an increase in nozzle pressure will provide an increase in cleaning performance. In the ejector models, an increase in the amount of steam or air in relation to the off-gas being pumped and cleaned will provide increased performance.

Lone Star Steel tests with the ejector drive have demonstrated highly effective removal of hydrophobic fumed silica having a near uniform particle diameter of .007 microns. This material rejects water. Analysis of the captured material shows the particulate not wetted, but encapsulated in a film of water. Encapsulating of the dust particle in water is one of the important mechanisms for the capture of fine particulate in the Coalescer cleaner.

These cleaners operate at relatively high gas thru speeds so that residence time in the contact and mixing zone is measured in milliseconds. This allows the building of units of a small size and also provides for savings in the chemicals used to clean off-gas streams containing H_2S, CO_2 and the like. The short residence time allows, for example the removal of H_2S by caustic, but does not permit sufficient time for the CO_2 which may be present to react with the caustic. The Coalescer provides a large number of small high speed water droplets having very high total surface area which enables the cleaners to make instant contact between the droplets, the chemical additive, and the gas to be scrubbed. On all of the processes tested to date, the Coalescer provided excellent performance with relatively low energy. In the Coalescer, a pressure recovery diffuser separator replaces cyclones, demisters, impactors, and stilling chambers. The Coalescer combines air cleaning with pressure recovery—a new and economically advantageous approach in air cleaning.

Table I. Scrubber inlet loading by size interval[a]

Date	Time	Time After Op. Start	Total Load	Dia. (ρ=5.2	Loading in Size Interval, grains/sdcf >6.0	>3.4	3.4-6.0	2.0-3.4	1.3-2.0	.70-1.3	.43-.70	.23-.43	<.43	<.23)
12/11	10:23[b]	3	0.157		.024		.021	.029	.012	.021	.036		.014	
12/09	13:07	10	0.346		.064		.005	.016	.029	.096	.128		.007	
12/07	14:44	15	0.385			.048		.013	.018	.084	.088	.100		.033
12/08	15:03	35	0.182		.029		.008	.003	.014	.020	.043		.065	
12/05	15:00	40	0.129			.048		.017	.008	.005	.013	.029		.008
12/08	09:48	60	0.656		.088		.010	.027	.057	.207	.158		.110	
12/11	11:33	75	1.29			.250		.062	.045	.210	.312	.319		.091
12/08	16:01	90	1.81			.299		.042	.123	.290	.459	.471		.123
12/05	15:57	100	0.784		.176		.010	.027	.080	.225	.171		.094	
12/10	16:12	160	0.656		.075		.000	.002	.016	.152	.252		.159	
12/07	10:46	180	2.55			.109		.028	.139	.430	1.066	.735		.049
12/09	09:54[c]	15	0.507		.063		.006	.009	.035	.118	.205		.070	
12/08	11:45	45	0.768			.203		.038	.070	.161	.142	.125		.029
12/09	16:10[d]	0	0.616			.077		.019	.014	.112	.197	.149		.048
12/11	13:34	19	1.30		.238		.048	.057	.152	.403	.274		.125	
12/06	17:52	22	2.46			.230		.060	.218	.797	.589	.356		.214
12/06	12:18	30	2.20			.346		.066	.180	.678	.469	.273		.188
12/07	11:57	30	1.18		.337		.035	.079	.266	.206	.141		.156	
12/05	11:46	40	2.63			.444		.068	.230	.866	.569	.205		.251
12/05	11:55	50	2.11		.472		.050	.127	.196	.679	.425		.156	
12/09	11:13	55	1.87			.433		.052	.138	.379	.527	.304		.042
12/10	18:15	55	2.02			.134		.075	.170	.622	.572	.248		.200
12/10	11:38	63	1.82		.148		.009	.022	.031	.390	.612		.605	
12/06	18:49	80	2.18		.154		.029	.032	.050	.202	.967		.747	
12/11	14:37	82	1.61			.274		.059	.143	.367	.428	.256		.082
12/06	13:16	86	1.32		.209		.031	.047	.209	.205	.324		.294	
12/10	12:32[e]	7	0.267			.113		.022	.006	.012	.041	.056		.016
				Dia. (ρ=1.	>14	>7.9	7.9-14	4.7-7.9	3.2-4.7	1.8-3.2	1.1-1.8	.69-1.1		<.69)

[a] Samples are ordered to synthesize one complete furnace cycle.

[b] Charge

[c] End of charge to hot metal

[d] Hot metal lance

[e] Tap

Table II. Scrubber outlet loading by size interval

Date(s) & Time(s)	Dec. 6 12:03/ 13:33	Dec. 6 17:45/ 19:15 Dec. 7 11:45/ 13:32	Dec. 7[a] 10:03/ 11:33 13:35/ 14:00	Dec. 8 10:30/ 16:30	Dec. 9 09:30/ 10:25 10:55/ 16:00	Dec. 10 10:15/ 19:15	Dec. 11 09:45/ 16:10
Acc. Position	3	3	3	3	2	3	3
Steam Pressure	250	250	250	300	250	300	300
Scrubber Flow Rate	11,000	11,000	11,000	13,000	15,000	13,000	13,000
#4 Furnace Operations During Measurement	Lance	Lance	Non-Lance	60% NL 40% L	60% NL 40% L	60% L 40% NL	60% L 40% NL
Overall Loading (gr/dscf)	0.0012	0.0012	0.0014	0.00086	0.0016	0.0009	0.0017
Size Interval/Loading Microns/(gr/dscf)							
>6.04	0.00009	0.00013			0.00007	0.00004	0.00015
3.75-6.04	0.00002	0.00005			0.00006	0.00004	0.00010
2.53-3.75	0.00000	0.00006			0.00004	0.00004	0.00009
1.71-2.53	0.00008	0.00004			0.00003	0.00002	0.00012
1.09-1.71	0.00001	0.00001		0.00003[b]	0.00002	0.00002	0.00009
0.52-1.09	0.00008	0.00007		0.00007	0.00006	0.00005	0.00012
0.30-0.52	0.00018	0.00015	0.00040[b]	0.00014	0.00016	0.00014	0.00023
0.18-0.30	0.00017	0.00017	0.00018	0.00012	0.00020	0.00011	0.00017
<0.18	0.00053	0.00052	0.00081	0.00049	0.00091	0.00042	0.00060

[a] Heater failed resulting in large amount of water condensing in impactor.

[b] Value represents the total loading for all particle sizes larger than the minimum size shown for this impactor stage. All impactor stages were not used for these runs.

Table III. Inlet particulate size distribution

Electric Arc Furnace		LSS Galvanizing Blow Box		Sodium Sulfate Recovery Boiler		LSS Cupola (Grey Iron)		LSS Coke Oven Stack	
Size (μ)	%	Size (μ)	%	Size (μ)	%	Size (μ)	%	Size (μ)	%
1-3	20	9-44	61	1-3	35	<3.0	27.4	<12	7.2
0.5-1.0	12	4-9	16.6	.5-1	37	1.5-3	22.8	5-12	2.3
0.1-0.5	21	2.7-4	7.0	.1-5	23	.75-1.5	26.9	3.5-5	3.3
0.05-0.1	5	1.7-2.7	4.9			<.75	22.9	2.2-3.5	7.6
0.01-0.50	5.6	.88-1.7	5.5					1.1-2.2	22.0
		.51-.88	3.2					.7-1.1	21.6
		.35-.51	1.5					.5-.7	12.7
		<.35	.3					<.5	23.3

Where the sum of the percentages is less than 100, the remainder is greater than the largest size shown.

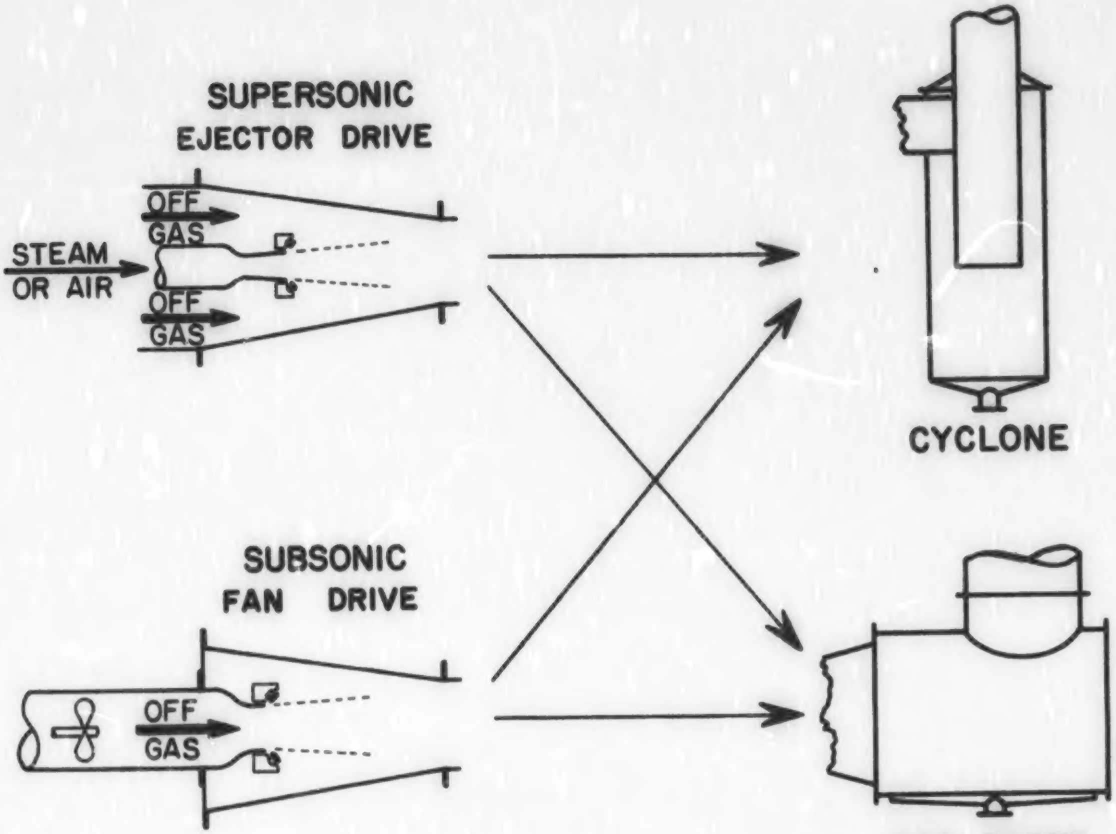
SUPERSONIC
EJECTOR DRIVE
OFF GAS
STEAM OR AIR
OFF GAS
CYCLONE
SUBSONIC
FAN DRIVE
OFF GAS
COALESCER

Figure 1. Hydrosonic cleaners.

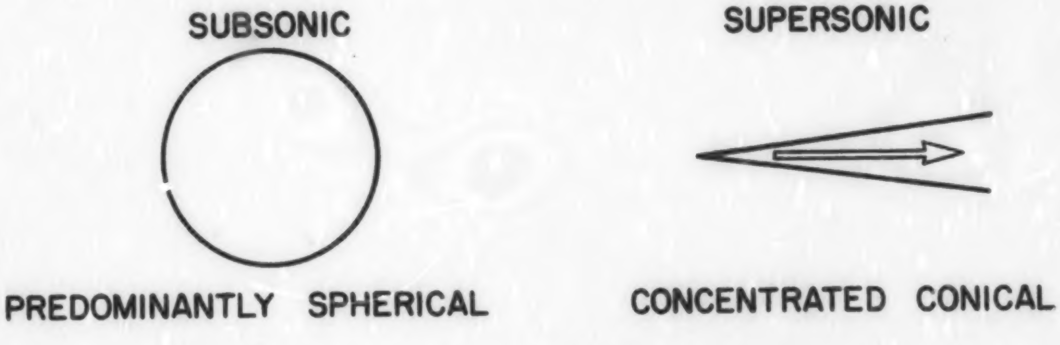
SUBSONIC
SUPERSONIC
PREDOMINANTLY SPHERICAL
CONCENTRATED CONICAL

Figure 2. Energy utilization region.

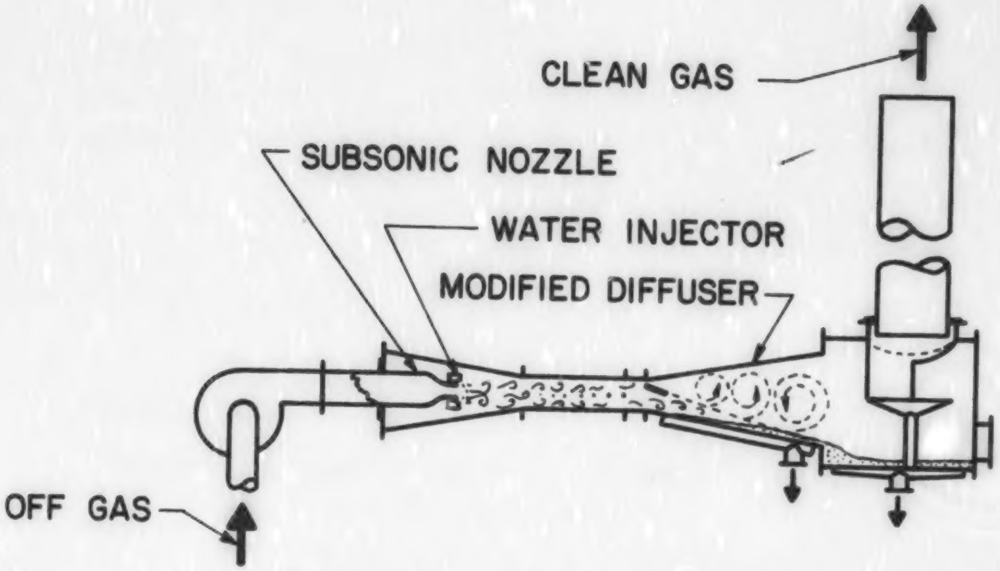
CLEAN GAS
SUBSONIC NOZZLE
WATER INJECTOR
MODIFIED DIFFUSER
OFF GAS

Figure 3. Fan coalescer.

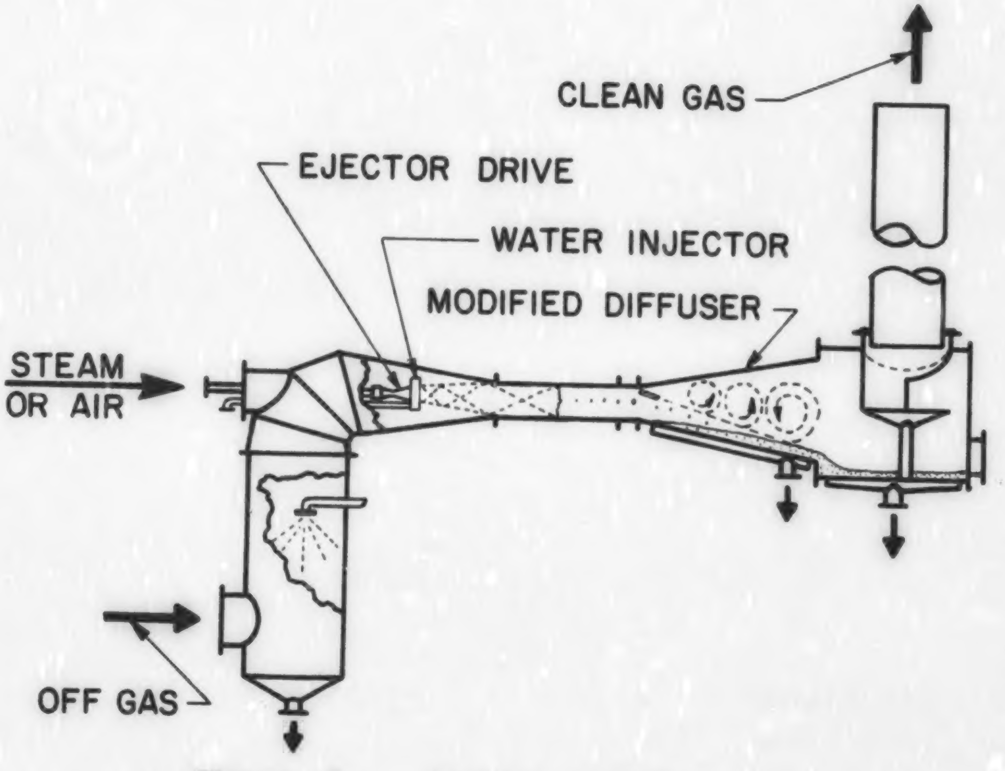
CLEAN GAS
EJECTOR DRIVE
WATER INJECTOR
MODIFIED DIFFUSER
STEAM OR AIR
OFF GAS

Figure 4. Ejector coalescer.

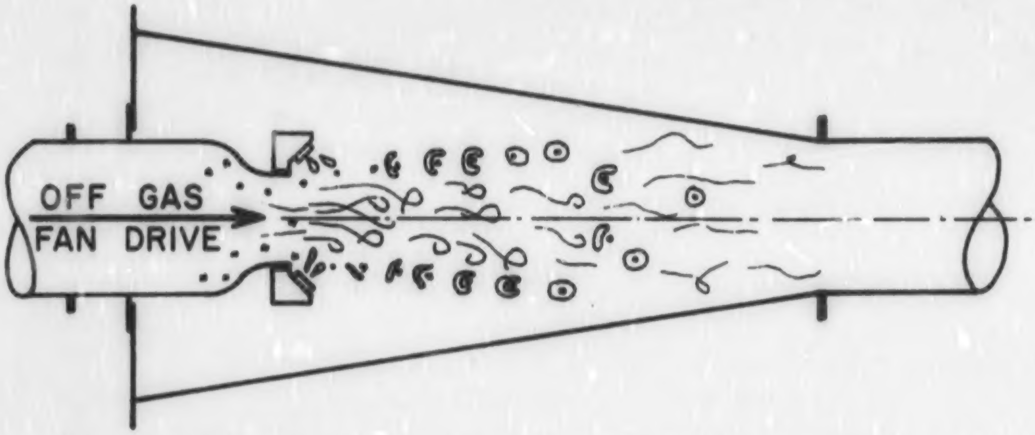
OFF GAS
FAN DRIVE

Figure 5. Shaped droplets - subsonic nozzle.

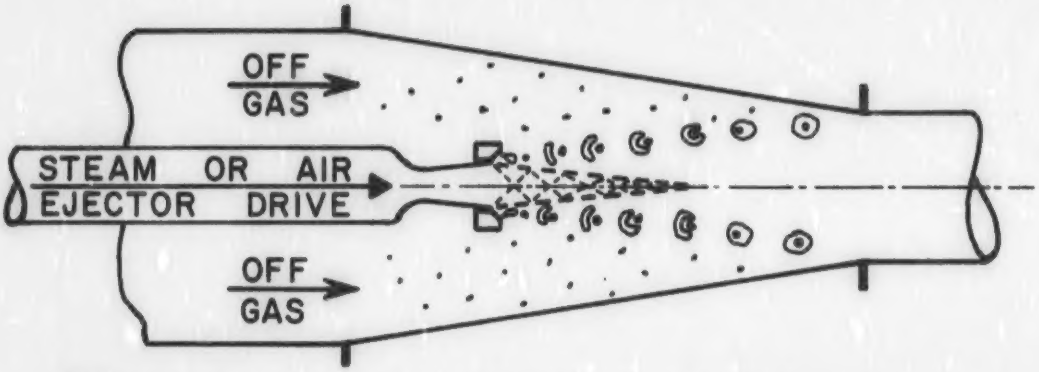
OFF GAS
STEAM OR AIR EJECTOR DRIVE
OFF GAS

Figure 6. Shaped droplets - supersonic nozzle.

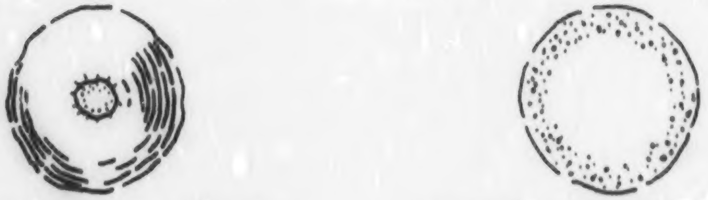
IMMEDIATELY AFTER CAPTURE
AFTER EVAPORATION

Figure 7. Droplet growth.

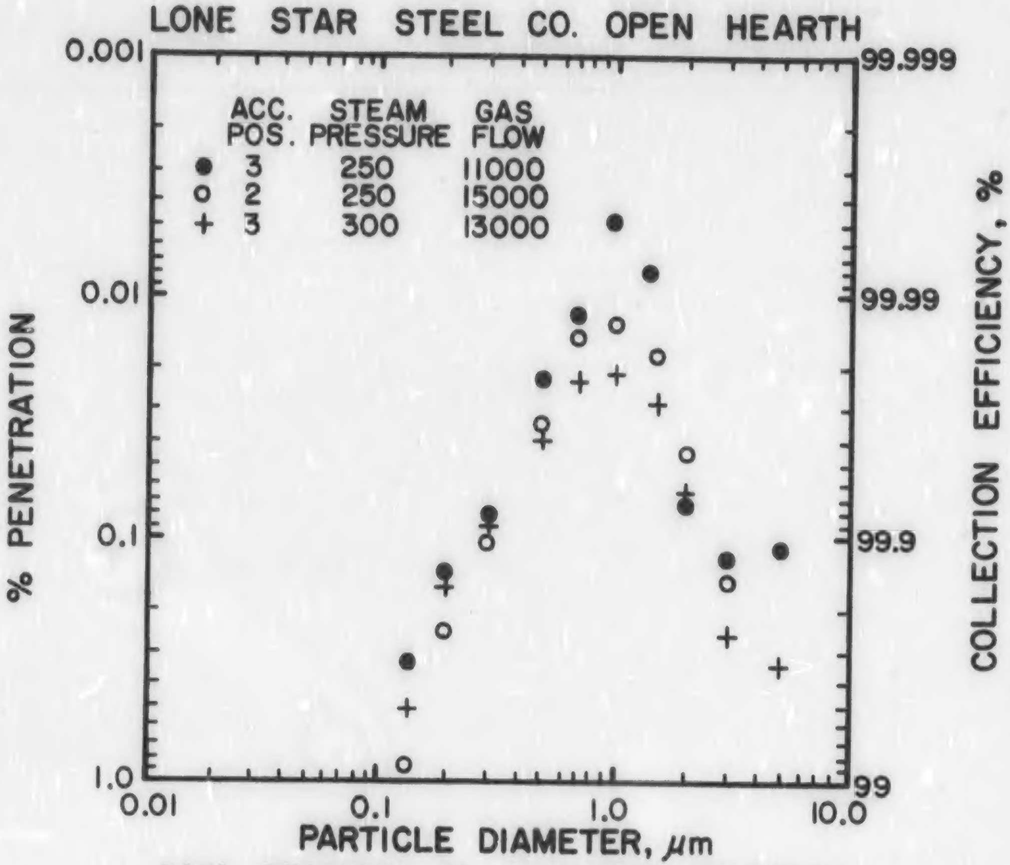

DATA RECORDED BY SOUTHERN RESEARCH INSTITUTE FOR E.P.A. — DEC., 1973

Figure 8. Supersonic ejector drive.

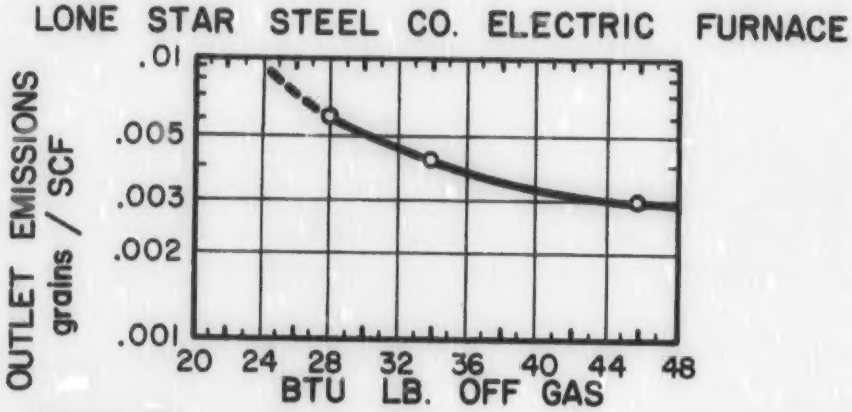

Figure 9. Coalescer - energy vs. cleaning.

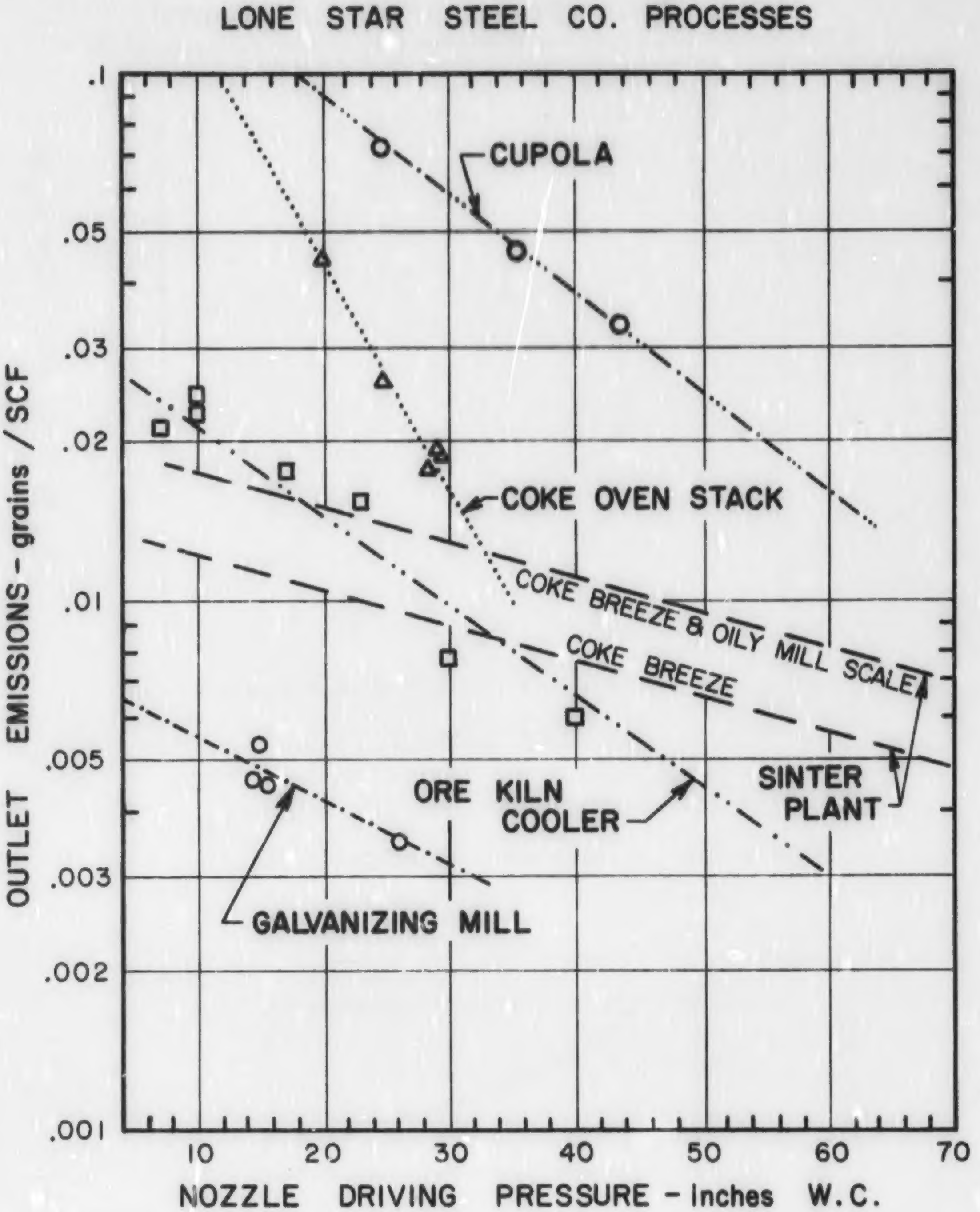

Figure 10. Fan coalescer - energy vs. outlet grain loading.

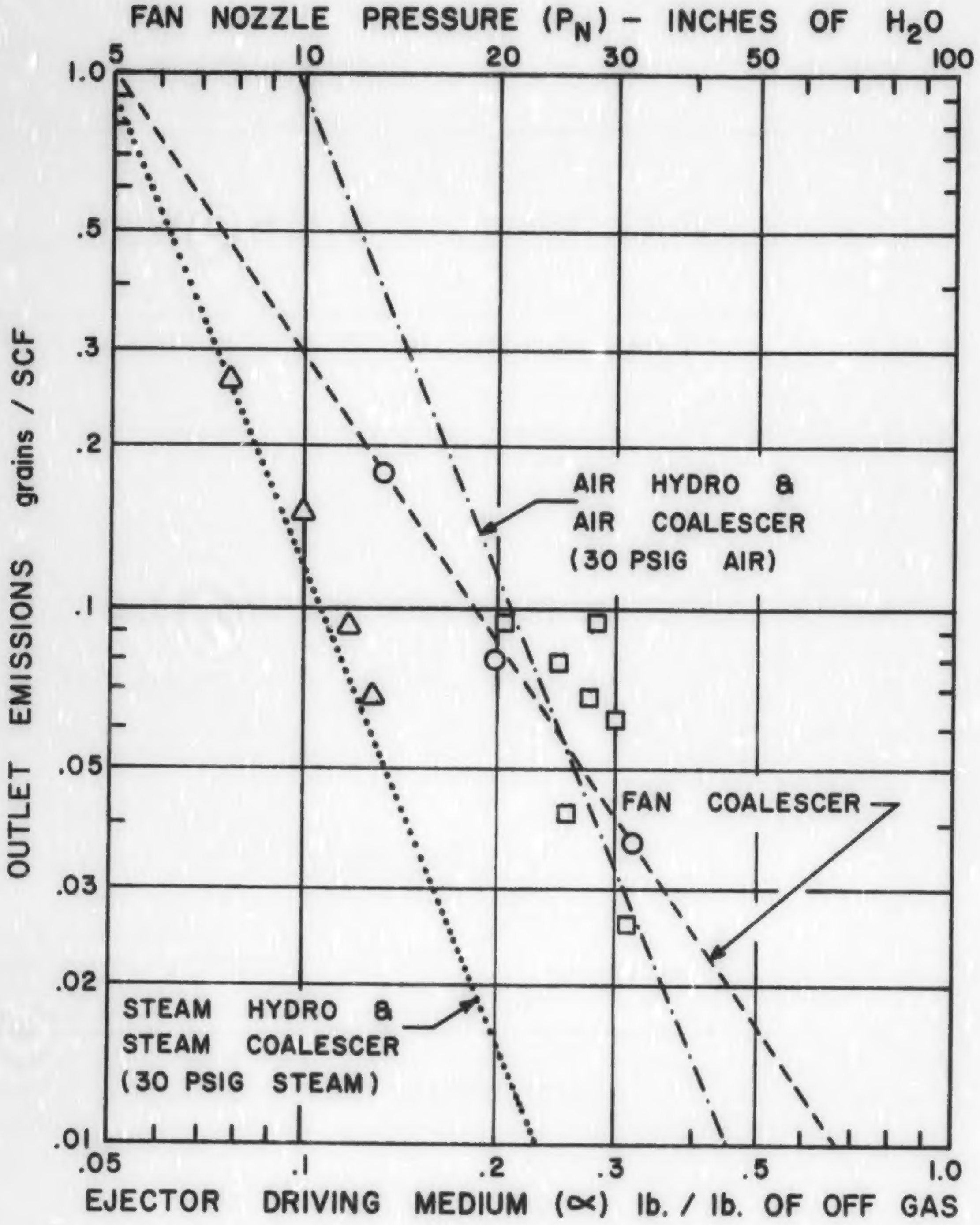

Figure 11. Paper recovery boiler

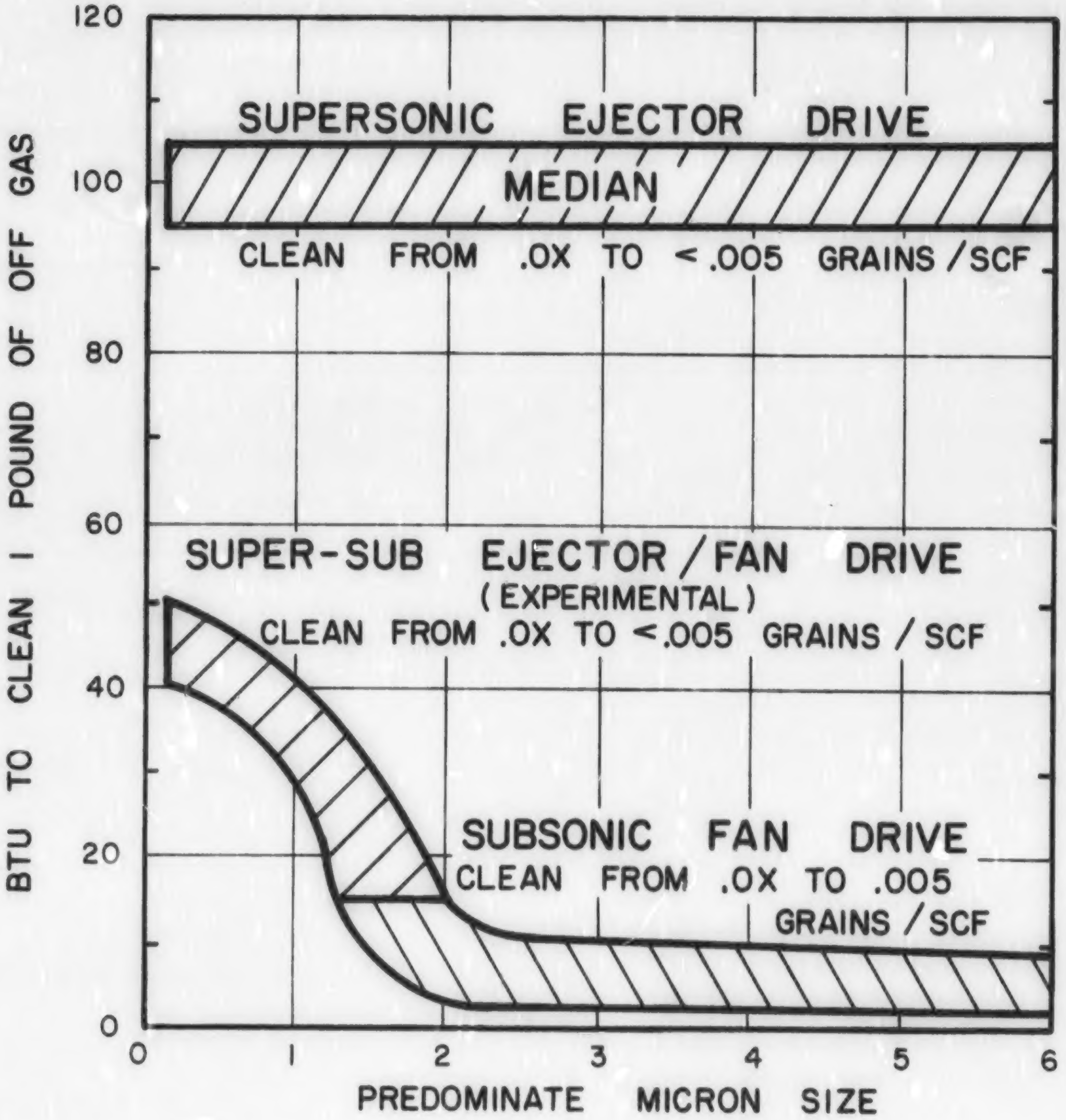

Figure 12. Energy vs. particle size.

REFERENCES

1. J. D. McCain and W. B. Smith, "Lone Star Steel Steam-Hydro Air Cleaning System Evaluation", Environmental Protection Technology Series, EPA-650/2-74-028 (April 1974).

2. L. J. Shannon, P. G. Gorman and M. Reichel, "Particulate Pollutant System Study Volume II - Fine Particle Emissions", National Technical Information Services Report, PB-203 521 (August 1971).

SYMPOSIUM ATTENDEES

J. ABBOTT
I.E.R.L. - MD-61
U.S. Environmental Protection Agency
Research Triangle Park, NC 2771

P.F. ADAMS
International Paper Company
P.O. Box 16807
Mobile, AL 36616

B. AGGARWAL
Ametek Process Systems
3427 Industrial Drive
Durham, NC 27704

F.J. ANDERSON
Carbon Products - Union Carbide
P.O. Box 6087
Cleveland, OH 44101

G. ANDES
AMAX Envir. Services Group
4704 Harlan Street
Denver, CO 80212

R. BACCAGLINI
ECAR Products Inc. (A-PAR)
436 W. Main Street
Wyckoff, NJ 07481

H. BARBARIKA
Air Pollution Technology, Inc.
4901 Morena Blvd., Suite 402
San Diego, CA 92117

E.T. BARROW
Ministry of Environment
880 Bay Street, 4th floor
Toronto, Ont, Canada M5S 1Z8

F. BASER
N.L. Industries
P.O. Box 1090
Hightstown, NJ 08520

R.A. BEANE
Air Pollution Control Commission
1558 Washington Street E.
Charleston, WV 25311

D.E. BECKNELL
Lear Siegler, Inc.
74 Inverness Drive, E.
Englewood, CO 80110

D. BERGQUIST
Carbon Products - Union Carbide
P.O. Box 6087
Cleveland, OH 44101

C. BILLINGS
Environmental Engineering Science
740 Boylston Street
Chestnut Hill, MA 02167

R.C. BINNING
Monsanto Research Corporation
P.O. Box 8, Station B
Dayton, OH 45407

S. BIONDO
Federal Power Commission
825 N. Capitol St. NE
Washington, D.C. 20426

R.H. BOLL
Babcock & Wilcox Co.
P.O. Box 835
Alliance, OH 44601

J.W. BRADLEY
Griffin Pipe Products
2000 Spring Road
Oak Brook, IL 60521

R.M. BRADWAY
GCA/Technology Division
Burlington Road
Bedford, MA 01730

I.L. BURGENER
Pfizer, Inc.
2001 Lynch Avenue
E. St. Louis, IL 62201

W.R. CADY
Allied Chemical Corp.
P.O. Box 1139R
Morristown, NJ 07960

S. CALVERT
Air Pollution Technology, Inc.
4901 Morena Blvd., Suite 402
San Diego, CA 92117

I.E. CAMPBELL
Smelter Control Research Assn, Inc.
150 E. Broad St., Suite 601
Columbus, OH 43221

Preceding page blank

P.R. CANDLER
Allied Chemical Corp.
P.O. Box 226
Geismar, LA 70734

K. CARLSSON
AB Svenska Flaktfabriken
Fack
S-35187 Vaxjo, Sweden

B. CARPENTER
Research Triangle Institute
Research Triangle Park, NC 27709

G.K.C. CHEN
Monsanto
800 N. Lindbergh Blvd.
St. Louis, MO 63166

G.H.S. CHENG
Environeering, Inc.
7401 N. Hamlin Avenue
Skokie, IL 60076

H.B. CHU
Department of Water & Power
111 N. Hope Street
Los Angeles, CA 90051

J. CLEMENTS
Standard Havens, Inc.
8800 E. 63rd
Kansas City, MO 64133

W. COLTHARP
Radian Corporation
8500 Shoal Creek Blvd.
Austin, TX 78766

F. CROWSON
Naval Surface Weapons Center
Code DG-31
Dahlgren. VA 22448

E.H. CUMPSTON
ECAR Products, Inc.
160 BenMont Avenue
Bennington, VT 05201

P.A. CZUCHRA
FMC Corporation
1800 FMC Drive West
Itasca, IL 60143

J.D'ANGELO
FMC Corporation
P.O. Box 4111
Pocatello, ID 83201

T. DEMBINSKY
C.A.P.C.C.
1 Penn Plaza
New York, NY 10001

D.C. DREHMEL
I.E.R.L. - MD-61
U.S. Environmental Protection Agency
Research Triangle Park, NC 27711

D.M. DUNKLE
Betz Laboratories, Inc.
Somerton Road
Trevose, PA 19047

G. DURFEE
Wyman-Gordon Company
244 Worcester St.
N. Grafton, MA 01536

L.A. DUVAL
Colerapa Industries, Inc.
4017 Hanway Blvd.
Ravenna, OH 44266

D.S. ENSOR
Meteorology Research, Inc.
464 W. Woodbury Road
Altadena, CA 91001

T.K. EWAN
Lone Star Steel Company
Highway 259 South
Lone Star, TX 75668

P.S. FARBER
Argonne National Laboratory
9700 S. Cass Avenue
Argonne, IL 60439

J.L. FASSO
St. Joe Minerals Corporation
Lead Smelting Division
Herculaneum, MO 63048

J.D. FERRELL
Stearns-Roger Inc.
Box 5888
Denver, CO 80217

T.A. FITZPATRICK
E.I. DuPont & Co., Inc.
1 Golden Acres Drive, No. 8
Wilmington, DE 19809

E.W. GAGAN
APC Directorate
Government of Canada
Ottawa, Ontario, Canada K1A 1C8

J. GALESKI
Midwest Research Institute
425 Volker Blvd.
Kansas City, MO 64110

S.A. GANDHI
Air Pollution Technology, Inc.
4901 Morena Blvd., Suite 402
San Diego, CA 92117

W.J. GILBERT, JR.
Croll-Reynolds Co. Inc.
751 Central Avenue
Westfield, NJ 07091

J.R. GOSNEY, JR.
Owens-Corning Fiberglas
Fiberglas Tower FF/7
Toledo, OH 43659

R. GRANT
Department of Commerce

E. GRASSEL
Donaldson Co., Inc.
1400 W. 94th St, P.O. Box 1299
Minneapolis, MN 55440

G.P. GRUBER
E.I. DuPont & Co., Inc.
P.O. Drawer 219
New Johnsonville, TN 37134

G.F. HAINES
Bethlehem Steel
Research Department
Bethlehem, PA 18016

D.L. HARMON
I.E.R.L. - MD-61
U.S. Environmental Protection Agency
Research Triangle Park, NC 27711

H.N. HEAD
Bechtel Corporation
P.O. Box 3965
San Francisco, CA 94119

R. HERBEST
Department of Commerce

P. HUBBARD
Ducon Company
147 E. 2nd Street
Mineola, NY 11501

R.B. IDA
U.S. Environmental Protection Agency
Bldg. 53, Box 25227
Denver Federal Center
Denver, CO 80225

R.J. JAWOROWSKI
Air Correction - U.O.P.
Tokeneke Road
Darien, CT 06820

H. N. JENKINS
Jenkins & Black, Inc.
P.O. Box 80609
Atlanta, GA 30366

R.H. JONES JR.
Ethyl Corporation
P.O. Box 341
Baton Rouge, LA 70821

A. KAPOOR
Buffalo Forge Company
490 Broadway
Buffalo, NY 14204

Y.G. KARDISH
Peabody Air Resources
P.O. Box 5202
Princeton, NJ 08540

R.A. KENT
Dart Industries Inc.
P.O. Box 37
Paramus, NJ 07652

D. KERIVAN
Cindaco Inc.
2673 South Dixie
Dayton, OH 45409

B.N. KHETANI
Monsanto Envirochem
800 N. Lindbergh
St. Louis, MO 63166

P.A. KITTLE
Apollo Chemical Corp.
35 S. Jefferson Road
Whippany, NJ 07981

H. KROCKTA
The Ducon Co., Inc.
147 E. 2nd Street
Mineola, NY 11501

W.F. LALOR
Cotton, Inc.
4505 Creedmoor Rd., Box 30067
Raleigh, NC 27612

R.E. LANGLOIS
Owens Corning Fiberglas
Technical Center
Granville, OH 43023

J.W. LEATHERDALE
J.W. Leatherdale, Inc.
382 Windsor Street
N. Plainfield, NJ 07060

F. LeBLANC
Department of Biology
University of Ottawa
Ottawa, Ontario, Canada K1N 6N5

D. LEITH
Harvard Univ., Dept. E.H.S.
665 Huntington Avenue
Boston, MA 02115

E.D. LEMON
U.S. Borax Corporation
3075 Wilshire Blvd.
Los Angeles, CA 90010

B. LINSKY
West Virginia University
Department of Civil Engineering
Morgantown, WV 26506

H.P. LIU
U.S. Borax Corporation
Boron, CA 93516

L.A. LOMBANA
BSP, Div. of Envirotech
One Davis Drive
Belmont, CA 94002

R.A. MACK
3M Company
P.O. Box 33331, Stop 71
St. Paul, MN 55133

V. MADDEN
Enviro-Test, Ltd.
8545 W. Colfax Avenue
Lakewood, CO 80215

J.D. McCAIN
Southern Research Institute
2000 9th Avenue South
Birmingham, AL 35205

R.W. McILVAINE
McIlvaine Company
2970 Maria Avenue
Northbrook, IL 60062

A. MEISEN
Dept. of Chemical Engineering
University of British Columbia
Vancouver, BC, Canada V6T 1W5

B. MENNINGA
Griffin Pipe Products
2000 Spring Road
Oak Brook, IL 60521

C. MENOHER
American Air Filter
215 Central Avenue
Louisville, KY 40201

T. MORTON
Babcock & Wilcox
609 N. Warren Avenue
Apollo, PA 15613

J.C. MYERS
Texas Air Control Board
8520 Shoal Creek
Austin, TX 78758

S.F. NEWTON
Tennessee Valley Authority
Wilhite Building
Muscle Shoals, AL 35660

P. J. NICOTRI
Environmental Elements Corporation
185 Arch Street
Ramsey, NJ 07446

G.M. OBELDOBEL
St. Joe Minerals Corp.
Route 18
Monaco, PA 15061

A.W. OBERHOFER
Nalco Chemical Company
6216 W. 66th Place
Chicago, IL 60638

R.G. OSTENDORF
Proctor & Gamble
7162 Reading Road
Cincinnati, OH 45222

J-L.PAQUET
Aluminum Co. of Canada
Arvida, Box 250
Quebec, Canada G7S 4K8

R.D. PARKER
Air Pollution Technology, Inc.
4901 Morena Blvd., Suite 402
San Diego, CA 92117

L. PATTON
Florida Sugar Cane League
115 S. Lopez
Clewiston, FL 33440

B.O. PAUL
Stauffer Chemical Company
P.O. Box 472
Mt. Pleasant, TN 38474

R.G. PETING
Griffin Pipe Products
2000 Spring Road
Oak Brook, IL 60521

M.A. PETRILLI
Monsanto Enviro-Chem
Box 14547 - Corp. Sq. Ofc. Park
St. Louis, MO 63178

M.J. PILAT
Dept. Civil Engineering
Univ. of Washington
Seattle, WA 98195

M.P. POLAKOVIC
Bureau of Air Pollution Control
P.O. Box 2807
Trenton, NJ 08625

S. POPKOFF
Research-Cottrell, Inc.
P.O. Box 750
Bound Brook, NJ 08805

N.E. PRANGE
Monsanto Enviro-Chem
Box 14547, Corp. Sq. Ofc. Park
St. Louis, MO 63178

D.A. PRICE
TRW - Energy Systems
One Space Park
Redondo Beach, CA 90278

B. RAGLAND
Schneible Company
714 N. Saginaw Street
Holly, MI 48033

A.C. REEVE
Amoco Chemicals Corp.
P.O. Box 400
Naperville, IL 60540

G. REY
U.S. Environmental Protection Agency-OEMI
Washington, D.C. 20460

S.R. REZNEK
U.S. Environmental Protection Agency
Washington, D.C. 20460

R. RHUDY
Bechtel Corporation
P.O. Box 3965
San Franciso, CA 94119

C.E. SCHAFER
Eastern Stainless Steel Co.
P.O. Box 1975
Baltimore, MD 21203

R.T. SCHNEIDER
Pridgen Engineering
P.O. Box 2008
Lakeland, FL 33803

G.C. SCHREIBER
Schneible Company
P.O. Box 100
Holly, MI 48442

G.L. SCHROEDER JR.
Albert Switzer & Assoc., Inc.
Suite 200, 3330 Lake Villa Dr.
Metairie, LA 70002

R.W. SCHUFF
Fluid-Ionic Systems
2525 E. Magnolia
Phoenix, AZ 85034

K.T. SEMRAU
Stanford Research Institute
333 Ravenswood Avenue
Menlo Park, CA 94025

S.V. SHEPPARD
Ceilcote Co., Inc.
140 Sheldon Road
Berea, OH 44130

S. SMALLWOOD
West Virginia APC Commission
1911 Warwood Avenue
Wheeling, WV 26003

D.L. SMITH
Conoco Coal Development
Research Division
Library, PA 15129

L.E. SPARKS
I.E.R.L. - MD-61
U.S. Environmental Protection Agency
Research Triangle Park, NC 27711

D.R. SPINK
Dept. Chemical Engineering
Univ. of Waterloo
Waterloo, Ont., Canada N2L 3G1

B.A. STEINER
Armco Steel Corporation
P.O. Box 600
Middletown, OH 45043

D. STELMAN
Atomics International
8900 DeSoto
Canoga Park, CA 91304

J.G. STITES
UOP Inc., Air Correction Division
10 UOP Plaza
Des Plaines, IL 60016

H. SURATI
Beltran Associates, Inc.
1133 E. 35th Street
Brooklyn, NY 11210

D.O. SWENSON
Black & Veatch Consulting Engr.
1500 Meadow Lake Pkwy.
Kansas City, MO 64114

M.F. SZABO
Pedco Environmental, Inc.
11499 Chester Rd.
Cincinnati, OH 45241

D.R. TALBOT
Martin Marietta Corporation
1450 S. Rolling Road
Baltimore, MD 21227

A.M. TELFORD
Illinois EPA
1309 Dial Court
Springfield, IL 62704

K. WALKER
Environmental Elements Corporation
185 Arch Street
Ramsey, NJ 07446

J.G. WEIS
Burns & McDonnell Eng. Co.
4600 E. 63rd St. Trafficway
P.O. Box 173
Kansas City, MO 64141

E.D. WESSMAN
Dept. of Mechanical Engineering
Univ. of Waterloo
Waterloo, Ontario, Canada N2L 3G1

L. WHITAKER
Harrington Industrial Plastics, Inc.
168 Freedom Avenue
Anaheim, CA 92801

F.A. WHITSON
TRW - Energy Systems
One Space Park
Redondo Beach, CA 90278

R. WIENER
Chemico Air Pollution Control
One Penn Plaza
New York NY 10001

D.A. WILSON
Aluminum Co. of Canada
Bldg. 270
Jonquieve, Quebec, Canada

G.J. WOFFINDEN
Meteorology Research, Inc.
464 W. Woodbury Road
Altadena, CA 91001

E.S. WYATT
Pridgen Engineering Co.
P.O. Box 2008
Lakeland, FL 33803

S. YUNG
Air Pollution Technology, Inc.
4901 Morena Blvd., Suite 402
San Diego, CA 92117

D.L. ZANDERS
Monsanto Research Corp.
123 Red Bud Court
Cary, NC 27511